
**TROPICAL POSITIVITY AND
SEMIALGEBRAIC SETS FROM POLYTOPES**
VOLUMES, DETERMINANTS AND MATROIDS

Der Fakultät für Mathematik und Informatik
der Universität Leipzig
eingereichte

DISSERTATION
zur Erlangung des akademischen Grades
DOKTOR RERUM NATURALIUM
(Dr. rer. nat.)
im Fachgebiet Mathematik

vorgelegt von
M.Sc. MARIE-CHARLOTTE BRANDENBURG
geboren am 23. Juni 1993 in Hamburg

Marie-Charlotte Brandenburg:
TROPICAL POSITIVITY AND SEMIALGEBRAIC SETS FROM POLYTOPES
VOLUMES, DETERMINANTS AND MATROIDS

BETREUER:
Prof. Dr. Rainer Sinn

To my father.

ABSTRACT

This dissertation presents recent contributions in tropical geometry with a view towards positivity, and on certain semialgebraic sets which are constructed from polytopes.

Tropical geometry is an emerging field in mathematics, combining elements of algebraic geometry and polyhedral geometry. A key in establishing this bridge is the concept of tropicalization, which is often described as mapping an algebraic variety to its “combinatorial shadow”. This shadow is a polyhedral complex and thus allows to study the algebraic variety by combinatorial means. Recently, the positive part, i.e. the intersection of the variety with the positive orthant, has enjoyed rising attention. A driving question in recent years is: *Can we characterize the tropicalization of the positive part?*

In this thesis we introduce the novel notion of positive-tropical generators, a concept which may serve as a tool for studying positive parts in tropical geometry in a combinatorial fashion. We initiate the study of these as positive analogues of tropical bases, and extend our theory to the notion of signed-tropical generators for more general signed tropicalizations. Applying this to the tropicalization of determinantal varieties, we develop criteria for characterizing their positive part. Motivated by questions from optimization, we focus on the study of low-rank matrices, in particular matrices of rank 2 and 3. We show that in rank 2 the minors form a set of positive-tropical generators, which fully classifies the positive part. In rank 3 we develop the starship criterion, a geometric criterion which certifies non-positivity. Moreover, in the case of square-matrices of corank 1, we fully classify the signed tropicalization of the determinantal variety, even beyond the positive part.

Afterwards, we turn to the study of polytropes, which are those polytopes that are both tropically and classically convex. In the literature they are also established as alcoved polytopes of type A . We describe methods from toric geometry for computing multivariate versions of volume, Ehrhart and h^* -polynomials of lattice polytropes. These algorithms are applied to all polytropes of dimensions 2, 3 and 4, yielding a large class of integer polynomials. We give a complete combinatorial description of the coefficients of volume polynomials of 3-dimensional polytropes in terms of regular central subdivisions of the fundamental polytope, which is the root polytope of type A . Finally, we provide a partial characterization of the analogous coefficients in dimension 4.

In the second half of the thesis, we shift the focus to study semialgebraic sets by combinatorial means. Intersection bodies are objects arising in geometric tomography and are known not to be semialgebraic in general. We study intersection bodies of polytopes and show that such an intersection body is always a semialgebraic set. Computing the

irreducible components of the algebraic boundary, we provide an upper bound for the degree of these components. Furthermore, we give a full classification for the convexity of intersection bodies of polytopes in the plane.

Towards the end of this thesis, we move to the study of a problem from game theory, considering the correlated equilibrium polytope P_G of a game G from a combinatorial point of view. We introduce the region of full-dimensionality for this class of polytopes, and prove that it is a semialgebraic set for any game. Through the use of oriented matroid strata, we propose a structured method for classifying the possible combinatorial types of P_G , and show that for $(2 \times n)$ -games, the algebraic boundary of each stratum is a union of coordinate hyperplanes and binomial hypersurfaces. Finally, we provide a computational proof that there exists a unique combinatorial type of maximal dimension for (2×3) -games.

AUTHORSHIP

Parts of this thesis resolve around results which arose from collaboration with other researchers.

[Chapter 1](#) is written by myself.

[Chapter 2](#) is based on the article [BLS22] which arose in collaboration with Georg Loho and Rainer Sinn. All authors of the article contributed to the results equally.

[Chapter 3](#) is based on [BEZ23], which is joint work with Sophia Elia and Leon Zhang. All results arose through equal contribution of all three authors, and the article is published in the *Journal of Symbolic Computation*.

[Chapter 4](#) is partly based on joint work with Katalin Berlow, Chiara Meroni and Isabelle Shankar, which was published in the article [BBMS22] in the Journal *Beiträge zur Algebra und Geometrie (Contributions to Algebra and Geometry)*. All authors contributed equally to the main results in [Sections 4.1](#) to [4.5](#), i.e. to [Theorems 4.1.8](#), [4.2.4](#) and [4.4.5](#). My personal contribution is mostly from the point of view of discrete and polyhedral geometry. I contributed with [Lemma 4.1.5](#), as well as [Algorithms 4.3.1](#) and [4.3.2](#). [Section 4.6.2](#) is based on discussions with Chiara Meroni. Again, we both contributed equally.

[Chapter 5](#) is based on the article [BHP22a], which arose in collaboration with Benjamin Hollering and Irem Portakal. My coauthors and I contributed equally to all mathematical expositions and results.

ACKNOWLEDGMENTS

First and foremost, I want to thank my family for their endless love and support.

I want to thank my advisor Rainer Sinn for his guidance, also during tumultuous times. Thank you for supporting me when I needed it, and for repeatedly reminding me not to take everything too seriously. I want to thank Christian Haase and Bernd Sturmfels for being as supporters and mentors by my side.

I want to thank Chiara Meroni, Claudia Fevola and Javier Sendra for making my transition to Leipzig feel so effortlessly. I am thankful for every paella and pizza along the way. I want to thank Lena Walter and Amy Wiebe for lively and shaking discussions, even in times of curfews. I am glad we always found all perfect matchings. Also, I thank Lena Walter for a productive collaboration during a "Qualitative und quantitative Faktorenanalyse", which we managed to establish over the years.

I am thankful for barbecues in the Villa garden, cooking sessions in the A3 kitchen, and every REWE salad that was eaten in the F3 section. There are many people who contributed to these memories, and I am thankful knowing every single one of you. I want to thank all of my office mates from over the years for discussions about beards and hugging trees, shooting targets on the blackboard with catapults, and, most recently, for not telling anyone where I am hiding while writing this thesis.

Looking back at the last three years, I thank all of my flatmates for being there in times when others could not. I am thankful for a warm home even in times without radiators, and Parmigianas and Mario Kart sessions during lockdowns and quarantines.

I want to thank all of my collaborators: Benjamin Hollering, Chiara Meroni, Georg Loho, Irem Portakal, Isabelle Shankar, Leon Zhang, Rainer Sinn and Sophia Elia. Without you, the last three years would certainly not have been nearly as rewarding. I thank everyone who supported me through lively or patient mathematical discussions, or by reading a part of this thesis, for their valuable comments.

Finally, I want to thank all members of the Nonlinear Algebra Group, Team Haase and the Villa and for making the experience of the last three years so special and unique. It is rare to be able to call so many places home.

CONTENTS

ABSTRACT	v
LIST OF SYMBOLS	xii
INTRODUCTION	1
1 BACKGROUND	5
1.1 Polyhedral Geometry	5
1.2 Matroids and Oriented Matroids	12
1.3 Tropical Combinatorics	14
1.4 Algebraic Varieties and Valuations	18
1.5 Gröbner Theory	20
1.6 Tropical Varieties	22
1.7 Toric Geometry	26
1.8 Semialgebraic Sets and Algebraic Boundaries	29
I TROPICAL POSITIVITY AND POLYTROPIES	33
2 TROPICAL POSITIVITY AND DETERMINANTAL VARIETIES	35
2.1 Positivity in Tropical Geometry	38
2.2 Determinantal Hypersurfaces	49
2.3 Determinantal Prevarieties and Bipartite Graphs	58
2.4 Rank 2	63
2.5 Rank 3	82
3 MULTIVARIATE VOLUME, EHRHART, AND h^*-POLYNOMIALS OF POLYTROPIES	91
3.1 Tropical Convexity and Polytropes	93
3.2 Multivariate Volume Polynomials	102
3.3 Multivariate Ehrhart and h^* -Polynomials	111
3.4 Computations and Observations	117
II SEMIALGEBRAIC SETS FROM POLYTOPES	125
4 INTERSECTION BODIES OF POLYTOPES	127
4.1 The Intersection Body of a Polytope is Semialgebraic	129
4.2 Non-Convex Intersection Bodies	136
4.3 The Algorithm	139
4.4 Algebraic Boundary and Degree Bound	141
4.5 The Cube	148
4.6 Convex Intersection Bodies of Polygons	151
5 COMBINATORICS OF CORRELATED EQUILIBRIA	165
5.1 The Correlated Equilibrium Polytope	167
5.2 The Correlated Equilibrium Cone	172
5.3 The Region of Full-Dimensionality	175
5.4 Combinatorial Types of Correlated Equilibrium Polytopes	177
BIBLIOGRAPHY	187
LIST OF FIGURES	198
LIST OF TABLES	199

LIST OF SYMBOLS

GENERAL NOTATION		SETS	
$\mathbf{1}$	all-ones vector	\sqcup	disjoint union
$\mathbf{0}$	origin	$ S $	size of finite set
e_i	standard basis vector in \mathbb{R}^d	int	interior
E_{ij}	standard basis vector in $\mathbb{R}^{d \times n}$	relint	relative interior
Id_n	identity matrix of size $(n \times n)$	$\text{cl}(S)$	Euclidean closure of S
$[n]$	$\{1, 2, \dots, n\}$	∂S	Euclidean boundary of S
$\binom{[n]}{k}$	subsets of $[n]$ of size k	\dim	dimension
$\langle x, y \rangle$	inner product of x and y	codim	codimension
A^t	transpose of matrix A	POLYTOPES	
FIELDS, RINGS AND VECTORSACES		P	polytope
\mathbb{N}	natural numbers	conv	convex hull
\mathbb{Z}	integers	aff	affine hull
\mathbb{Q}	rational numbers	vert	vertices
\mathbb{R}	real numbers	\mathcal{F}	collection of faces
\mathbb{C}	complex numbers	f_i	number of i -dimensional faces
\mathbb{T}	tropical semiring	P°, P^*	polar, dual
\mathbb{TP}^{d-1}	tropical projective torus	vol_k	$(k\text{-dim'l})$ Euclidean volume
K	field	Vol_k	$(k\text{-dim'l})$ normalized volume
$(K^d)^*$	dual vectorspace of K^d	SOME SPECIFIC POLYTOPES	
$(K^*)^d$	algebraic torus	Δ_d	d -dimensional simplex
$K[x_1, \dots, x_d]$	polynomial ring	$[0, 1]^d$	unit cube
$K[x_1, \dots, x_d]_{\leq k}$	polynomials of degree $\leq k$	$C^{(d)}$	centrally symmetric cube
$K[x_1^{\pm 1}, \dots, x_d^{\pm 1}]$	Laurent polynomial ring	$\Delta(d, k)$	hypersimplex
$K(x_1, \dots, x_d)$	Fraction field	B_n	Birkhoff polytope
$K\{\{t\}\}$	field of Puiseux series	P_M	Matroid bases polytope
\mathcal{R}	real Puiseux series	FP_n	Fundamental polytope
\mathcal{C}	complex Puiseux series	CONES AND FANS	
		C	cone
		cone	conical hull
		C^\vee	dual cone

\mathcal{L}	lineality space	GRÖBNER THEORY
Σ	polyhedral fan	
$\Sigma(P)$	normal fan of P	
EHRHART THEORY		
$\text{ehr}_P(t)$	univariate Ehrhart polynomial	TROPICAL GEOMETRY
$\text{ehr}_P(a)$	multivariate Ehrhart polynomial	
$\text{Ehr}_P(t)$	Ehrhart series	
$h^*(t)$	h^* -polynomial	
MATROIDS		
M	Matroid	
\mathcal{B}, E	bases, ground set	
P_M	Matroid bases polytope	
χ	Chirotope, oriented matroid	
\mathcal{H}	hyperplane arrangement	
s	signed covector	
GRAPHS		
$V(G)$	vertices	
$E(G)$	edges	
$\deg(v)$	degree of vertex v	
P_n	path graph	
K_n	complete graph	
$K_{m,n}$	complete bipartite graph	
Γ	bipartite graph	
Γ^c	bipartite complement	
\mathcal{G}_n	graph of Birkhoff polytope B_n	
VARIETIES AND VALUATIONS		
$\mathcal{V}(f_1, \dots, f_k)$	variety vanishing on f_1, \dots, f_k	
$\mathcal{V}(I)$	variety vanishing on I	
val	valuation	
lt	leading term	
lc	leading coefficient	
$\partial_a S$	algebraic boundary	
TROPICAL DETERMINANTAL VARIETIES		
\mathcal{C}_+	positive complex Puiseux series	
\mathcal{R}_+	positive real Puiseux series	
trop^{+c}	complex positive part	
$\text{trop}^{+\mathcal{R}}$	real positive part	
Trop^+	combinatorially positive part	
trop^+	(complex=real) positive part	
$\mathcal{C}^s, \mathcal{R}^s$	orthant of $\mathcal{C}^d, \mathcal{R}^d$	
trop^s	signed tropicalization	
I_r	determinantal ideal	

A^{IJ}	submatrix with rows I and columns J	u^\perp	Hyperplane orthogonal to u
f^{IJ}	minor of submatrix A^{IJ}	$\mathcal{H}(P)$	hyperplane arrangement of P
$T_{d,n}^r, (T_{d,n}^r)^+$	(positive) tropical determinantal variety	$Z(P)$	zonotope associated to P
$P_{d,n}^r, (P_{d,n}^r)^+$	(positive) tropical determinantal prevariety	∂_a	algebraic boundary
B_n	Birkhoff polytope	S^{d-1}	unit sphere
G_n	graph of Birkhoff polytope	S^{d-1}	unit sphere
$\sigma, \pi \in S_n$	permutations in the symmetric group	$C^{(d)}$	centrally symmetric cube
H_c	tropical hyperplane with apex c	H^+, H^-	positive / negative side of H
W_{kl}	wing of tropical hyperplane	$\mathcal{OT}(P)$	ordered type of \mathcal{HP}
$\Gamma(C)$	label (bipartite graph) of C	$s(C)$	cocircuit of chamber C
$\mathcal{BPT}_{d,n}$	space of bicolored phylogenetic trees	\mathcal{L}	affine line arrangement
$\text{trop}(\text{Gr}(2, d+n))$	tropical Grassmannian	n	number of players
$\mathcal{UPT}^{(R,G)}$	space of admissible uncolored phylogenetic trees	d_i	number of strategies of player i
$\Delta(d, 3)$	3rd hypersimplex	$s_{j_i}^{(i)}$	pure strategy j_i of player i
POLYTROPE			
c	weights of a complete digraph	$s_{j_1 \dots j_n}$	pure joint strategy
c^*	Kleene star	$X_{j_1 \dots j_n}^{(i)}$	payoff of player i at $s_{j_1 \dots j_n}$
$P(c^*)$	polytrope defined by Kleene star	$p^{(i)}$	mixed strategy of player i
$\Sigma(c^*)$	normal fan of $P(c^*)$	$p_{j_1 \dots j_n}$	mixed joint strategy
$P(a)$	indeterminate polytrope	G	game
\mathcal{R}_n	set of weights without negative cycles	$C_G, C(Y)$	correlated equilibrium cone
\mathcal{Pol}_n	polytrope region	$P_G, P(Y)$	correlated equilibrium polytope
I_n	toric ideal of all-pairs shortest path program	M	ambient dimension of \mathcal{S}
\mathcal{GF}_n	Gröbner fan of I_n	D	ambient dimension of P_G
FP_n	Fundamental polytope	N	number of incentive constraints
M	Stanley-Reisner ideal	\mathcal{S}	correlated equilibrium space
L	ideal of cuts in complete digraph	Y	point in \mathcal{S}
Todd	Todd operator	\mathcal{D}	region of full-dimensionality
B_k	Bernoulli numbers	\mathcal{R}_H°	open stratum in oriented matroid strata
$A(d, m), A_d$	Eulerian numbers, polynomials	$\partial_a \mathcal{R}$	algebraic boundary of oriented matroid strata

INTERSECTION BODIES

ρ	radial function
IP	intersection body of P
S^{d-1}	unit sphere
u	unit vector in S^{d-1}

INTRODUCTION

Polytopes are fundamental objects in geometry and mathematics as a whole. Dating back to Platon and Archimedes, it seems surprising that to this day they still prove to be rich objects of study. While some people argue that the golden times of the study of polytopes lies back in the 1990's, they still emerge in new mathematical contexts, such as physics, economics, statistics, and algorithmic game theory [Wei22; Voh11; Sul18; NRTV07]. From this point of view it might not be the objects themselves that are new, but the ever new arising questions as well as the interplay with other fields make them contemporary objects of study, while keeping their ancient Greek sublimity.

At the core of this dissertation lies the interplay between polyhedral geometry and semialgebraic structures. Connecting combinatorics and (real) algebraic geometry, we use tools from discrete geometry to study semialgebraic sets, and tools from algebraic geometry to understand discrete structures. Historically, these two fields have been proven to go well together: For instance, the classical question of realization spaces of polytopes establishes a natural bridge to semialgebraic sets. In this thesis we take a different route, adding tropical geometry to the mix.

The authors' intent is to showcase how combining methods and questions from different areas of mathematics establishes new connections, which enrich the modern mathematical field. Polyhedral structures lie at the heart of this thesis, and at the same time, working at the triple intersection between combinatorics, geometry and algebraic concepts, we are typically motivated by questions from other areas, such as optimization (Chapter 2), geometric tomography (Chapter 4) or game theory (Chapter 5) [Sch03; Gar06; AH02]. We work with methods from tropical geometry while borrowing tools from toric geometry, and we substantiate our results with explicit computations [BEZ20; BBMS21; BHP22b]. All results obtained in this thesis are concrete, and traceable through examples.

This dissertation consists of two main parts. The title of the first part is *Tropical Positivity and Polytopes*, and we study geometric objects from a tropical point of view. In the second part, *Semialgebraic Sets from Polytopes*, the central role is played by certain semialgebraic sets which are constructed from polytopes. As the subtitle of this thesis suggests, further main themes are *Volumes, Determinants and Matroids*. We now give a more thorough introduction to the two parts, emphasizing the common themes whenever possible and giving an outline of the main contributions of each chapter. Each of the chapters contains its own introduction, where we elaborate further on the context as well as the state of current research, and provide references to related work.

INTRODUCTION

Tropical Geometry is an emerging field in mathematics, living on the intersection between combinatorics and algebraic geometry. Tropicalization has been proven to be a powerful tool for studying algebraic varieties by combinatorial means: transforming an algebraic variety into a polyhedral complex while still preserving essential properties of the former has opened up possibilities to understand algebraic varieties from a combinatorial point of view. At the same time, many applications urge to add real aspects to the picture. As a starting point, understanding the signed tropicalization has developed into a fundamental question in tropical geometry in recent years. Interestingly, even understanding the intersection of an algebraic variety with the positive orthant is not well understood, and not even a uniform notion of *the positive part* has established in the most recent publications in the field.

[Chapter 2: Tropical Positivity and Determinantal Varieties](#) gives the first overview over all different notions of tropical positivity in the literature, and clarifies the distinction when working over the complex numbers or the reals. We introduce the novel notion of *positive tropical generators*, a concept which may serve as a tool for studying positive parts in tropical geometry in a combinatorial fashion. Afterwards, we initiate the study of the *positive tropical determinantal variety*. Motivated by questions from optimization, our main focus lies in the study of the positive part for low-rank matrices. We fully characterize the signed tropicalizations of determinantal hypersurfaces, and the positive part of the determinantal variety of rank 2. Introducing the novel notion of bicolored tree arrangements, we provide a partial characterization of the positive part of tropical determinantal varieties of rank 3.

The study of positive tropical geometry was pioneered by Speyer and Williams [SW05], who considered the positive part of the tropical Grassmannian. Any point in the Grassmannian gives rise to a realizable matroid, and points in the tropical Grassmannian correspond to valued matroids, i.e. lifting functions on matroid polytopes. Matroids in the (totally) positive Grassmannian are called positroids, and matroid polytopes of positroids are the intersection of the class of matroid polytopes with the class of polytopes which we consider in Chapter 3 [LP20].

[Chapter 3: Multivariate Volume, Ehrhart and \$h^*\$ -polynomials of polytropes](#) concerns the study of *polytropes*, a special class of polytopes which are both classically and tropically convex. In discrete geometry and algebraic combinatorics, they are established under the name of *alcoved polytopes of type A*, and the volume and univariate h^* -polynomials of these polytopes have enjoyed a lot of attention in recent years. In this chapter, we consider the associated toric variety, and, using methods from the intersection theory on this toric variety, we compute multivariate volume, Ehrhart and h^* -polynomials for all polytropes of dimension at most 4. This yields a total of 81 675 distinct multivariate polynomials, and the study of these allows for novel insights to a combinatorial interpretation of the coefficients of volume polynomials, establishing a remarkable connection to central triangulations of the *fundamental polytope*, the root polytope of type A.

The second part of this thesis concerns semialgebraic sets which arise from constructions involving polytopes. While in Chapter 3 a (multivariate) volume polynomial can be seen as a compact way to encode the Ehrhart and h^* -polynomial, in Chapter 4 the volume plays a central role in the construction of the main objects of study.

Chapter 4: *Intersection Bodies of Polytopes* considers *intersection bodies*, a class of convex bodies and star bodies arising in convex analysis and geometric tomography. We initiate the study of intersection bodies of polytopes from the point of view of real algebraic geometry, showing that these objects are indeed semialgebraic sets, and study the degrees of the algebraic boundary of these sets. We give an explicit semialgebraic description, which makes this class of intersection bodies computable. In the 2-dimensional case we obtain an unexpected result: the intersection body of a polygon is almost never convex. **Chapter 5: *Combinatorics of Correlated Equilibria*** concerns an equilibrium concept arising through a linear program in game theory. The set of correlated equilibria of a fixed game is a polytope, and the set of Nash equilibria is the intersection of this polytope with the Segre embedding of products of projective spaces. A driving question in the field is: When does the convex hull of the Nash equilibria greatly differ from the correlated equilibrium polytope? A key indicator for this is to understand when the polytope is of maximal dimension. We initiate the study of correlated equilibrium polytopes from a discrete geometric point of view, and introduce the notion of the *region of full-dimensionality* for any class of games. By studying the algebraic boundary of an oriented matroid strata for the class of (2×3) -games, we are able to fully classify all combinatorial types of correlated equilibrium polytopes of maximal dimension. Surprisingly, there exists only one unique such combinatorial type.

BACKGROUND

In this chapter we provide the background to the most prominent concepts in this thesis. The first half concerns the discrete and combinatorial notions. We begin by establishing common themes of polyhedral geometry, and introduce matroids and the main concepts from tropical combinatorics. In the second half of this chapter we turn to the background of the algebro-geometric aspect, such as the basic concept of algebraic varieties and fields with valuations. Afterwards we establish the main notions of Gröbner theory and discuss the Fundamental Theorem of tropical algebraic geometry. Finally, we give a brief introduction to toric varieties and the most important concepts concerning semialgebraic sets.

1.1 POLYHEDRAL GEOMETRY

Polyhedral structures lie at the heart of this dissertation. In this section we introduce these central objects and those constructions which will be recurrently used in the following chapters. We follow the conventions of [Zie95].

1.1.1 Polytopes

A *polyhedron* is the intersection of finitely many closed halfspaces and a *polytope* is a bounded polyhedron. Equivalently, a polytope $P \subseteq \mathbb{R}^d$ is the *convex hull* of finitely many points $v_1, \dots, v_n \in \mathbb{R}^d$ [Zie95, Theorem 1.1], i.e. $P = \text{conv}(v_1, \dots, v_n)$ where

$$\text{conv}(v_1, \dots, v_n) = \{\lambda_1 v_1 + \dots + \lambda_n v_n \mid \lambda_i \in [0, 1], \lambda_1 + \dots + \lambda_n = 1\}.$$

For notational convenience we write $\text{conv}(S)$ for the convex hull of the elements of a finite set S , and for a matrix $A \in \mathbb{R}^{d \times n}$ with columns v_1, \dots, v_n we use the convention $\text{conv}(A) = \text{conv}(v_1, \dots, v_n)$.

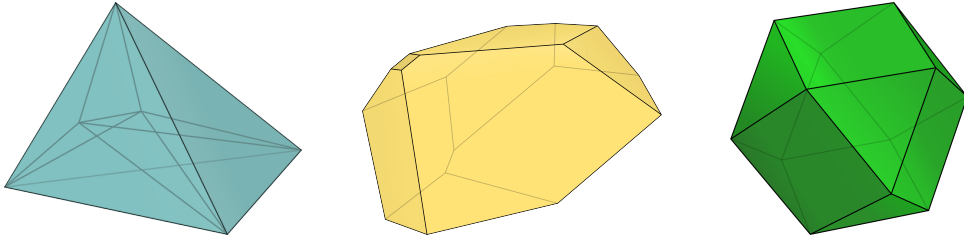


Figure 1.1: The Birkhoff polytope B_3 from Chapter 2, a polytrope from Chapter 3 and the polar of a zonotope from Chapter 4.

We denote by $\text{vert}(P)$ the set of vertices of a polytope $P \subseteq \mathbb{R}^d$. A polytope P is a *lattice polytope* if all of its vertices are contained in the integer lattice $\mathbb{Z}^d \subseteq \mathbb{R}^d$ and a *0/1-polytope* is a lattice polytope with $\text{vert}(P) \subseteq \{0, 1\}^d$.

The *normalized volume* or *lattice volume* of a lattice polytope is defined as $\text{Vol}(P) = \dim(P)! \text{vol}(P)$, where $\text{vol}(P)$ denotes the Euclidean volume of P . If $\dim(P) = k < d$, then we write $\text{Vol}_k(P)$ and $\text{vol}_k(P)$ for the respective volume inside the *affine span* $\text{aff}(P)$, which is the smallest affine space containing P . A polyhedron is *relatively open* if it is open inside its affine span. A k -dimensional *simplex* $\Delta_k \subseteq \mathbb{R}^d$ is the convex hull of $k+1$ affinely independent vectors and is *unimodular* if $\text{Vol}_k(\Delta_k) = 1$. The *standard simplex* $\Delta_{d-1} \subseteq \mathbb{R}^d$ is the convex hull of all standard unit vectors.

A hyperplane *supports* P if it bounds a closed halfspace containing P , and any intersection of P with such a supporting hyperplane yields a *face* F of P . A face is a *proper face* if $F \subsetneq P$ and inclusion-maximal proper faces are referred to as *facets*. Note that also the empty set is a face of P and by convention $\dim(\emptyset) = -1$. The numbers $f_i \in \mathbb{N}$ of i -dimensional faces of P form the *f-vector* $f = (f_{-1}, f_0, \dots, f_{\dim(P)})$. We denote by \mathcal{F} the collection of faces of P . These are partially ordered by inclusion and hence form a poset $(\mathcal{F}, \subsetneq)$, the *face lattice* of P . Two polytopes are *combinatorially equivalent* (or *combinatorially isomorphic*) if their face lattices are isomorphic, in which case we say that they have the same *combinatorial type*. The *polar* (or *polar dual*) of P is the polytope

$$P^\circ = \left\{ y \in (\mathbb{R}^d)^* \mid \langle x, y \rangle \leq 1 \text{ for all } x \in P \right\},$$

where $(\mathbb{R}^d)^*$ denotes the dual space of \mathbb{R}^d . A polytope is *simplicial* if all of its facets are simplices and *simple* if every vertex of P is contained in precisely $\dim(P)$ edges. Equivalently, P is simple if and only if P° is simplicial [Zie95, Proposition 2.16].

The *Minkowski sum* of polytopes $P_1, \dots, P_k \subseteq \mathbb{R}^d$ is

$$P_1 + \dots + P_k = \{x_1 + \dots + x_k \mid x_i \in P_i \text{ for } i \in [k]\}.$$

and a *zonotope* is a Minkowski sum of line segments.

A *polyhedral complex* \mathcal{P} is a finite collection of polyhedra such that

- (i) $\emptyset \in \mathcal{P}$,
- (ii) if $P \in \mathcal{P}$ then all faces of P are in \mathcal{P} ,
- (iii) if $P, P' \in \mathcal{P}$, then $P \cap P'$ is a face both of P and P' .

A polyhedral complex is *pure* of dimension k if $\dim(P) = k$ holds for every inclusion-maximal $P \in \mathcal{P}$. A pure k -dimensional polyhedral complex \mathcal{P} is *strongly connected* or *connected through codimension 1* if for every maximal $P, P' \in \mathcal{P}$ with $\dim(P) = \dim(P') = k$ there exists a sequence P_1, \dots, P_l such that $\dim(P_i) = k$ and $\dim(P \cap P_1) =$

$\dim(P_l \cap P') = \dim(P_{i-1} \cap P_i) = k - 1$ for every $i \in [l]$. The k -skeleton of a polyhedral complex is the collection of all faces of \mathcal{P} of dimension at most k . Similarly, the codimension 1-skeleton (or codim 1-skeleton) of a pure k -dimensional polyhedral complex is the collection of all faces of dimension at most $k - 1$.

1.1.2 Cones and Fans

A *polyhedral cone* $C \subseteq \mathbb{R}^d$ is a polyhedron such that $\lambda u + \mu v \in C$ for every $u, v \in C$ and $\lambda, \mu \in \mathbb{R}_{\geq 0}$. Equivalently, it is the *conical hull* of finitely many vectors $u_1, \dots, u_n \in \mathbb{R}^d$ [Zie95, Theorem 1.3], i.e.

$$C = \text{cone}(u_1, \dots, u_n) = \{\mu_1 u_1 + \dots + \mu_n u_n \mid \mu_1, \dots, \mu_n \geq 0\}.$$

As for the convex hull, we will use the notation $\text{cone}(S)$ for the conical hull of vectors in a finite set S . The *lineality space* of C is the linear space $\mathcal{L}(C) = C \cap (-C)$ and a cone is *pointed* if its lineality space is trivial. The *rays* of C are its 1-dimensional faces and a cone is *rational* if the slope of each ray is given by a rational vector. The *primitive ray generator* of a ray r with rational slope is the unique vector $u = (u_1, \dots, u_d) \in \mathbb{Z}^d$ such that $r = \{\lambda u \mid \lambda \geq 0\}$ and $\gcd(u_1, \dots, u_d) = 1$. The *dual cone* of C is

$$C^\vee = \left\{ y \in (\mathbb{R}^d)^* \mid \langle x, y \rangle \geq 0 \text{ for all } x \in C \right\}.$$

A *polyhedral fan* $\Sigma \subseteq \mathbb{R}^d$ is a finite family of nonempty polyhedral cones such that every nonempty face of a cone in Σ is also a cone in Σ , and the intersection of any two cones in Σ is a face of both. The fan Σ is *complete* if $\bigcup_{C \in \Sigma} C = \mathbb{R}^d$ and it is *pure* if all inclusion-maximal cones have the same dimension. A k -dimensional cone is a *simplicial cone* if it is generated by k rays and a *simplicial fan* is a fan in which every cone is simplicial. Similarly, a rational cone $C \subseteq \mathbb{R}^d$ is *smooth* if its primitive ray generators are contained in a lattice basis of \mathbb{Z}^d and a *smooth fan* is a fan in which every cone is smooth.

Let $P \subseteq \mathbb{R}^d$ be a polytope and let \mathcal{F} denote the collection of faces of P . For a fixed face $F \in \mathcal{F}$, the set of normal vectors of supporting hyperplanes form the (*inner*) *normal cone*

$$N_F = \left\{ u \in (\mathbb{R}^d)^* \mid F \subseteq \{x \in P \mid \langle x, u \rangle = \min(\langle y, u \rangle \mid y \in P)\} \right\}.$$

The collection $\Sigma(P)$ of normal cones of faces of P forms the (*inner*) *normal fan* of P .

1.1.3 Polyhedral Subdivisions

Regular subdivisions and triangulations of polytopes play a central role in polyhedral geometry. The Cayley trick establishes a connection between certain regular subdivisions and mixed subdivisions, and is the underlying reason for the identifications in Section 1.3, while matroid subdivisions play a central role in the description of tropical

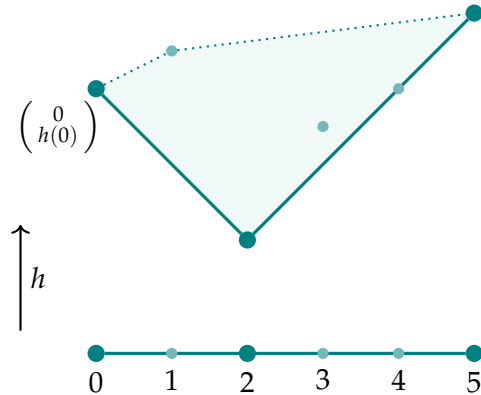


Figure 1.2: The regular subdivision of the interval from Example 1.1.1.

planes in Section 2.5. Central triangulations are a key concept for establishing one of the main results in Chapter 3 and are also an important construction in Chapter 4. We follow the exposition of [Zie95, Chapter 5.1] for general regular subdivisions, and [Jos21, Chapter 4.1] and [San05] for mixed subdivisions and the Cayley trick. [DLRS10, Chapters 2 and 9.2] may serve as further references.

A *polyhedral subdivision* \mathcal{S} of a polytope $P \subseteq \mathbb{R}^d$ is a polyhedral complex such that $\bigcup_{S \in \mathcal{S}} = P$. The subdivision is a *triangulation* if every polytope in \mathcal{S} is a simplex. Let $V \subseteq \mathbb{R}^d$ be a finite set of points such that $P = \text{conv}(V)$. We will typically consider the sets $V = \text{vert}(P)$ or $V = P \cap \mathbb{Z}^d$ in the case of lattice polytopes. A *regular subdivision* of P is a subdivision which is induced by a lifting function. More precisely, let $h : V \rightarrow \mathbb{R}$ and consider

$$\text{lift}(V) = \text{conv}\left(\begin{pmatrix} v \\ h(v) \end{pmatrix} \mid v \in V\right) \subseteq \mathbb{R}^{d+1}.$$

We sometimes refer to the value $h(v)$ as the *weight* of v . The *lower hull* of $\text{lift}(V)$ is the collection of faces of the polytope $\text{lift}(V)$ which have an inner normal vector whose last coordinate is positive (or equivalently an outer normal vector whose last coordinate is negative). We apply a coordinate projection to the lower hull of $\text{lift}(V)$ by projecting away the last coordinate. This yields a polyhedral complex which is a subdivision of $P = \text{conv}(V)$. Any subdivision of P which can be obtained by this procedure is called a *regular subdivision* P .

Example 1.1.1 (Regular subdivision). We consider the regular subdivision of the lattice points $V = P \cap \mathbb{Z}$ in the interval $P = \text{conv}(0, 5)$, which is induced by the lifting function

$$h(0) = 3, h(1) = 3 + \frac{1}{2}, h(2) = 1, h(3) = 2 + \frac{1}{2}, h(4) = 3, h(5) = 4,$$

as depicted in Figure 1.2. The regular subdivision consists of the maximal faces $\text{conv}(0, 2)$ and $\text{conv}(2, 5)$. \diamond

1.1 Polyhedral Geometry

Let $P_1, \dots, P_k \subseteq \mathbb{R}^d$ be polytopes such that their Minkowski sum $P = P_1 + \dots + P_k \subseteq \mathbb{R}^d$ is full-dimensional. A *Minkowski cell* is any d -dimensional polytope $B_1 + \dots + B_k$ such that the set B_i is the convex hull of some vertices of P_i for any $i \in [k]$. A *mixed subdivision* \mathcal{S} of P is a subdivision in which the inclusion-maximal polytopes are Minkowski cells and $B_i \cap B'_i$ is a face both of B_i and B'_i for any such cells $B = B_1 + \dots + B_k$, $B' = B'_1 + \dots + B'_k \in \mathcal{S}$ and any $i \in [k]$.

We now explain how mixed subdivisions of $P_1 + \dots + P_k$ are in bijection with subdivisions of the Cayley polytope $\mathcal{C}(P_1, \dots, P_k)$ via the *Cayley trick*. The *Cayley polytope* (or *Cayley embedding* of P_1, \dots, P_k) is defined as

$$\mathcal{C}(P_1, \dots, P_k) = \text{conv}(P_i \times \{e_i\} \mid i \in [k]) \subseteq \mathbb{R}^d \times \mathbb{R}^k.$$

We consider the affine subspace

$$H(\lambda_1, \dots, \lambda_k) = \left\{ (x, y) \in \mathbb{R}^d \times \mathbb{R}^k \mid y_i = \lambda_i \text{ for all } i \in [k] \right\}.$$

The intersection with the Cayley polytope yields the weighted Minkowski sum

$$\mathcal{C}(P_1, \dots, P_k) \cap H(\lambda_1, \dots, \lambda_k) = \sum_{i=1}^k \lambda_i P_i.$$

We obtain $P_1 + \dots + P_k$ up to a scaling factor $\frac{1}{k}$ by choosing the parameters $\lambda_i = \frac{1}{k}$ for all $i \in [k]$. The restriction of any polyhedral subdivision of $\mathcal{C}(P_1, \dots, P_k)$ to $H(\frac{1}{k}, \dots, \frac{1}{k})$ induces a mixed subdivision of $P_1 + \dots + P_k$. In fact, this procedure induces a bijection between subdivisions of $\mathcal{C}(P_1, \dots, P_k)$ and mixed subdivisions of $P_1 + \dots + P_k$ [HRSoo, Theorem 3.1 “Cayley Trick”]. A *coherent mixed subdivision* is a mixed subdivision of $P_1 + \dots + P_k$ which corresponds to a regular subdivision of the Cayley polytope. This is the class of subdivisions we will encounter in [Section 1.3](#) and can be seen for example in [Figure 1.5](#).

Example 1.1.2 (Cayley Trick). Let $P_1 = \text{conv}((0, 0), (1, 0))$ and $P_2 = \text{conv}((0, 0), (0, 2))$. The Cayley polytope is the 3-dimensional polytope with lattice points

$$\mathcal{C}(P_1, P_2) \cap \mathbb{Z}^4 = \left\{ \begin{pmatrix} 0 \\ 0 \\ 0 \\ 0 \end{pmatrix}, \begin{pmatrix} 1 \\ 0 \\ 0 \\ 0 \end{pmatrix}, \begin{pmatrix} 0 \\ 0 \\ 1 \\ 0 \end{pmatrix}, \begin{pmatrix} 0 \\ 1 \\ 0 \\ 0 \end{pmatrix}, \begin{pmatrix} 0 \\ 0 \\ 0 \\ 2 \end{pmatrix} \right\}.$$

As lifting function we choose $h : \mathcal{C}(P_1, P_2) \cap \mathbb{Z}^4 \rightarrow \mathbb{R}$ such that $h((0, 2, 0, 1)^t) = 1$ and weight 0 for all remaining lattice points. The intersection of the regular subdivision of $\mathcal{C}(P_1, P_2)$ with the 2-dimensional affine subspace $H(\frac{1}{2}, \frac{1}{2})$ is depicted in [Figure 1.3](#). By the discussion above, this is a coherent mixed subdivision of the rectangle $P = P_1 + P_2$. \diamond

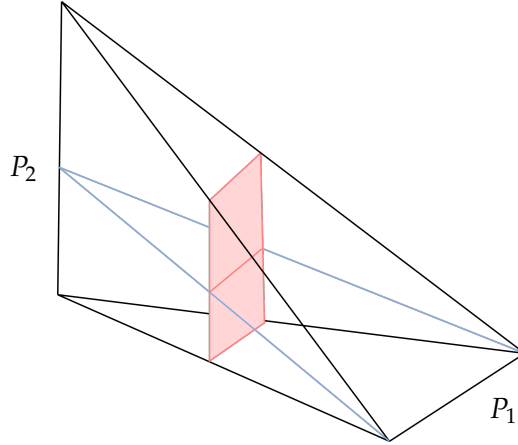


Figure 1.3: The regular subdivision of the Cayley polytope $\mathcal{C}(P_1, P_2)$ from Example 1.1.2. The blue edges indicate the regular subdivision of $\mathcal{C}(P_1, P_2)$, and the mixed subdivision of $\frac{1}{2}(P_1 + P_2)$ is shown in red.

1.1.4 Ehrhart Theory

Ehrhart theory concerns lattice point counting in lattice polytopes and is thus the theory of the discrete volume of polytopes. We will study multivariate Ehrhart and h^* -polynomials of polytopes in Chapter 3. In this section we follow the exposition in [BR15, Chapter 3].

The *Ehrhart counting function* $\text{ehr}_P(k)$ of $P \subseteq \mathbb{R}^d$ gives the number of lattice points in the k th dilate of P for $k \in \mathbb{Z}_{\geq 1}$, i.e. $\text{ehr}_P(k) = |kP \cap \mathbb{Z}^d|$.

THEOREM 1.1.3 (Ehrhart's Theorem [Ehr62]). The counting function $\text{ehr}_P(k)$ agrees with a polynomial in k for positive integers $k \in \mathbb{Z}_{\geq 1}$. The degree of this polynomial is equal to the dimension of P .

The constant term of this polynomial is equal to 1 and the leading coefficient equals the Euclidean volume of P within its affine span. In the 2-dimensional case, the Ehrhart polynomial recovers *Pick's formula*

$$|P \cap \mathbb{Z}^2| = \text{vol}(P) + \frac{|\partial P \cap \mathbb{Z}^2|}{2} + 1.$$

The *Ehrhart series* $\text{Ehr}_P(t)$ of a polytope P is the formal power series

$$\text{Ehr}_P(t) = 1 + \sum_{k \geq 1} \text{ehr}_P(k) t^k,$$

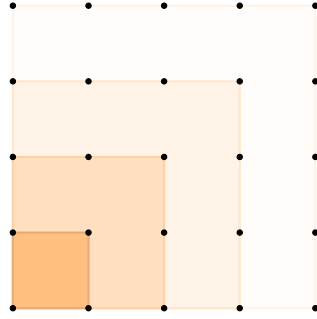


Figure 1.4: The Ehrhart polynomial of the unit square is $\text{ehr}(k) = (k + 1)^2$

which has the rational expression

$$\text{Ehr}_P(t) = \frac{h_P^*(t)}{(1-t)^{\dim(P)+1}},$$

where the h^* -polynomial $h_P^*(t) = \sum_{i=0}^{\dim(P)} h_i^* t^i$ has degree at most $\dim(P)$. The coefficients of the h^* -polynomial form the h^* -vector $h^* = (h_0^*, h_1^*, \dots, h_{\dim(P)}^*)$, where each h_i^* is a non-negative integer [Sta80] and their sum is equal to the normalized volume of P within its affine span. The Ehrhart polynomial may be recovered from the h^* -vector via

$$\text{ehr}_P(k) = \sum_{i=0}^d h_i^* \binom{k+d-i}{d}.$$

For a lattice polytope $P = \{x \in \mathbb{R}^d : Ax \leq b\}$ with $A \in \mathbb{Z}^{m \times d}$, $b \in \mathbb{Z}^m$, the *multivariate Ehrhart counting function* $\text{ehr}_P : \mathbb{Z}^m \rightarrow \mathbb{Z}$ gives the number of lattice points in the vector dilated polytope, i.e.

$$\text{ehr}_P(a) = |\{x \in \mathbb{Z}^d \mid Ax \leq a\}|.$$

This counting function is closely related to vector partition functions, which can be used to show that $\text{ehr}_P(a)$ is piecewise-polynomial [DM88].

Example 1.1.4 (Ehrhart polynomial). We consider the unit square

$$P = \left\{ x \in \mathbb{R}^2 \mid \begin{pmatrix} 1 & 0 \\ 0 & 1 \\ -1 & 0 \\ 0 & -1 \end{pmatrix} x \leq \begin{pmatrix} 1 \\ 1 \\ 0 \\ 0 \end{pmatrix} \right\}.$$

The Ehrhart polynomial of P is $\text{ehr}_P(k) = (k + 1)^2$ and the Ehrhart series is

$$\text{Ehr}_P(t) = 1 + \sum_{k \geq 1} (k + 1)^2 t^k = \frac{t^2 + 1}{(1-t)^3} = \frac{h^*(t)}{(1-t)^3}.$$

The h^* -vector is thus $h^* = (1, 1)$ and indeed the sum $h_0^* + h_1^* = 2$ is the normalized volume of P . The multivariate Ehrhart counting function counts the number of lattice

points in the parameterized polytope

$$\begin{aligned} P(a) &= \left\{ x \in \mathbb{R}^2 \mid \begin{pmatrix} 1 & 0 \\ 0 & 1 \\ -1 & 0 \\ 0 & -1 \end{pmatrix} x \leq \begin{pmatrix} a_1 \\ a_2 \\ a_3 \\ a_4 \end{pmatrix} \right\} \\ &= \{x \in \mathbb{R}^2 \mid -a_3 \leq x_1 \leq a_1, -a_4 \leq x_2 \leq a_2\}. \end{aligned}$$

for $a \in \mathbb{Z}^4$. If $-a_3 \leq a_1$ and $-a_4 \leq a_2$, then $P(a) \neq \emptyset$. For such $a \in \mathbb{Z}^4$, the multivariate Ehrhart counting function coincides with the polynomial

$$\text{ehr}_P(a) = (a_1 + a_3 + 1)(a_2 + a_4 + 1).$$

Note that $\text{ehr}(k(1, 1, 0, 0)^t) = (k+1)^2$ recovers the Ehrhart polynomial of the original square P . \diamond

1.2 MATROIDS AND ORIENTED MATROIDS

Matroids are axiomatic abstractions of linear spaces, which arise through the axiomatization of linear independence of columns of a matrix. Oriented matroids can be viewed as an abstraction of matroids representable over an ordered field. Matroids and matroid subdivisions of hypersimplices are a key concept in [Section 2.5](#) for the study of tropical determinantal varieties of rank 3. Oriented matroids serve as an inspiration for the ordered type of a hyperplane arrangement in [Section 4.6](#), and oriented matroid strata are central objects of study in [Chapter 5](#). We follow the exposition of [[Scho3](#), Chapters 39–40] and [[GOT17](#), Chapter 6.2.3].

Let E be a finite set. A *matroid* $M = (\mathcal{B}, E)$ on the *ground set* E is defined through a nonempty finite collection \mathcal{B} of subsets of E satisfying the *basis exchange axiom*

$$\forall X, Y \in \mathcal{B}, i \in X \setminus Y \exists j \in Y \setminus X: (X \setminus i) \cup j \in \mathcal{B} \text{ and } (Y \setminus j) \cup i \in \mathcal{B}.$$

A set $B \in \mathcal{B}$ is called a *basis* of M . The basis exchange axiom implies that bases of M have the same cardinality, and this cardinality is the *rank* of M . The rank of any subset $S \subseteq E$ is defined as $\text{rk}_M(S) = \max(|S \cap B| \mid B \in \mathcal{B})$ and a set $F \subseteq E$ is a *flat* if $\text{rk}(F \cup e) = \text{rk}(F) + 1$ for any $e \in E \setminus F$. Equivalently, F is a flat if it equals its span, where the *span* of a set $S \subseteq E$ is defined as

$$\text{span}(S) = \{e \in E \mid \text{rk}(S \cup e) = \text{rk}(S)\}.$$

Any $(r \times n)$ -matrix A of rank r with columns indexed by E induces a matroid M_A of rank r , where $B \subseteq E$ is a basis of M_A if and only if the determinant of the submatrix A_B with columns indexed by elements in B is nonzero. A matroid M is *realizable* if there exists a matrix A such that $M = M_A$.

The *matroid polytope* (or *matroid bases polytope*) is the convex hull

$$P_M = \text{conv} \left(\sum_{i \in B} e_i \mid B \in \mathcal{B} \right) \subseteq \mathbb{R}^E.$$

The vertices of P_M are in bijection with bases of M and the basis exchange axiom implies that a polytope matroid polytope is a 0/1-polytope with edges in direction $e_i - e_j$ for $i, j \in E$. Alternatively, we can characterize matroid polytopes as follows.

THEOREM 1.2.1 ([FS05, Proposition 2.3]). The matroid polytope P_M is given by the hyperplane description

$$\begin{aligned} P_M = \Big\{ x \in \mathbb{R}^E \mid & \forall e \in E \quad x_e \geq 0 \\ & \text{and } \sum_{e \in F} x_e \leq \text{rk}(F) \text{ for all flats } F \subseteq E \\ & \text{and } \sum_{e \in E} x_e = \text{rk}(M) \Big\} \end{aligned}$$

A *matroid subdivision* of a polytope P is a subdivision in which every face is a matroid polytope.

We now turn to chirotopes, which are maps encoding basis orientations of a matroid. Chirotopes are in bijection with *oriented matroids*, i.e. every chirotope gives rise to a unique oriented matroid and vice versa [BLVS+99, Theorem 3.5.5]. For the purposes of this thesis we thus use these terms interchangeably. A *chirotope* of rank r is a nontrivial alternating sign map $\chi : E^r \rightarrow \{-, 0, +\}$ such that

- (i) $\{\{\lambda_1, \dots, \lambda_r\}, \mid \lambda = (\lambda_1, \dots, \lambda_r) \in E^r, \chi(\lambda) \neq 0\}$ is the set of bases of a matroid,
- (ii) for all $\lambda = (\lambda_1, \dots, \lambda_{r-2}) \in E^{r-2}$ and $a, b, c, d \in E \setminus \{\lambda_1, \dots, \lambda_{r-2}\}$ the set

$$\{\chi(\lambda, a, b)\chi(\lambda, c, d), -\chi(\lambda, a, c)\chi(\lambda, b, d), \chi(\lambda, a, d)\chi(\lambda, b, c)\}$$

either contains $\{+, -\}$ or equals $\{0\}$.

Any $(r \times n)$ -matrix A of rank r with entries in an ordered field and columns indexed by E induces a chirotope χ_A , where $\chi_A(\lambda) = \text{sgn}(\det(A_\lambda))$ and A_λ denotes the submatrix of A with columns indexed by $\lambda_1, \dots, \lambda_r$ for $\lambda \in E^r$. A chirotope χ is *realizable* if $\chi = \chi_A$ for some matrix A .

A realizable oriented matroid can be viewed in terms of a *central hyperplane arrangement*, i.e. an arrangement of hyperplanes through the origin. Consider the arrangement \mathcal{H} of the n hyperplanes $A_e^\perp \subseteq \mathbb{R}^r$, $e \in E$, which are orthogonal to the n columns of A . The *chambers* of \mathcal{H} are the connected components of $\mathbb{R}^r \setminus \mathcal{H}$. To each such chamber C , we associate the *signed covector* $s \in \{-, +\}^E$, $s_e = \text{sgn}(\langle A_e, x \rangle)$ for any $x \in C$. The signed covector s describes for each hyperplane of \mathcal{H} on which side of the hyperplane

the chamber lies. These (maximal) signed covectors are also referred to as *topes* in the literature. Again, the collection of signed covectors uniquely describes the oriented matroid corresponding to the chirotope χ_A .

1.3 TROPICAL COMBINATORICS

The main theme of [Part I](#) of this dissertation is tropical geometry, i.e. geometry over the tropical semiring. In this section we establish the main combinatorial aspects of tropical geometry that we will encounter in this thesis – tropical convexity and tropical hypersurfaces. For this, we follow the conventions of [[Jos21](#), Chapter 1 and 5]. In [Section 1.6](#) we discuss the Fundamental Theorem of tropical geometry, expanding the tropical background towards a more algebraic direction. As is custom in tropical geometry, we identify $\mathbb{R}^d \cong (\mathbb{R}^d)^*$ with its dual space in this section.

The *min-plus tropical semiring* is defined as $\mathbb{T} = (\mathbb{R} \cup \{\infty\}, \oplus, \odot) = (\mathbb{R} \cup \{\infty\}, \min, +)$, where for elements $a, b \in \mathbb{T}$ we define the tropical addition $a \oplus b$ and tropical multiplication $a \odot b$ by

$$a \oplus b = \min(a, b), \quad a \odot b = a + b.$$

In this semiring, the additive neutral element is ∞ and the multiplicative neutral element is 0. We can extend the tropical operations to vector addition and scalar multiplication in the tropical semimodule \mathbb{T}^d by applying them coordinate-wise. More specifically, we define

$$\lambda \odot v \oplus \mu \odot w = (\min(\lambda + v_1, \mu + w_1), \dots, \min(\lambda + v_d, \mu + w_d)).$$

for any scalars $\lambda, \mu \in \mathbb{T}$ and vectors $v = (v_1, \dots, v_d)$, $w = (w_1, \dots, w_d) \in \mathbb{T}^d$. Analogously to the ordinary product of two matrices, the *tropical matrix product* $A \odot B \in \mathbb{T}^{d \times n}$ of $A \in \mathbb{T}^{d \times r}$, $B \in \mathbb{T}^{r \times n}$ is the matrix with entries

$$(A \odot B)_{ij} = \bigoplus_{k=1}^r A_{ik} \odot B_{kj} = \min(A_{ik} + B_{kj} \mid k \in [r]).$$

Since ∞ is the additive neutral element in the tropical semiring, the *tropical projective torus* is defined as $\mathbb{TP}^{d-1} = \mathbb{R}^d / (\mathbb{R} \odot \mathbf{1})$, in which points are considered modulo addition with the all-ones vector.

1.3.1 Tropical Convexity

We now introduce the tropical analogue of convexity, which gives rise to the notion of tropical polytopes. Polytopes are a special class of tropical polytopes, and will be the main object of study in [Chapter 3](#). They also serve as a tool for the proofs in [Section 2.5](#).

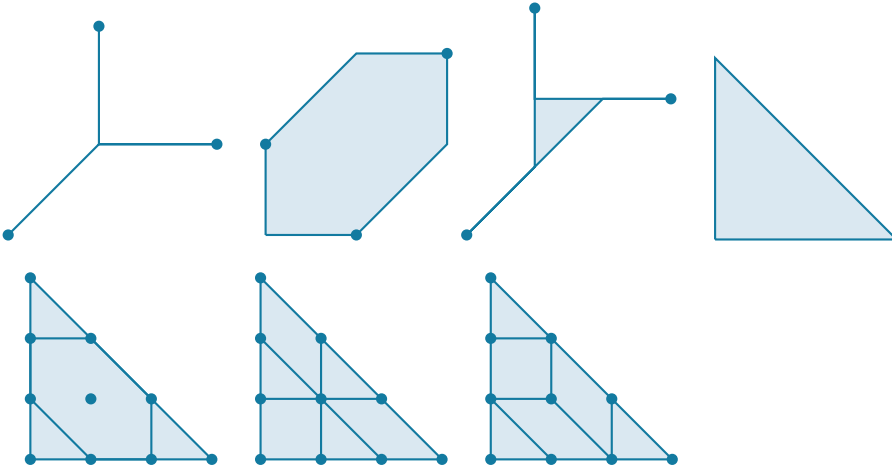


Figure 1.5: Left: The tropical polytopes P_1, P_2, P_3 from Example 1.3.1 in the chart where the last coordinate is 0, together with the dual mixed subdivision of $3\Delta_2$ from Example 1.3.3.
Right: The tropically convex set S that is not a tropical polytope.

Let $V = \{v_1, \dots, v_n\} \subseteq \mathbb{R}^d$ be a finite set of points. The *tropical convex hull* of V is given by the set of all tropical linear combinations

$$\text{tconv}(V) = \{\lambda_1 \odot v_1 \oplus \dots \oplus \lambda_n \odot v_n \mid \lambda_1, \dots, \lambda_n \in \mathbb{R}\}.$$

We write $\text{tconv}(A)$ for the tropical convex hull of the points which form the columns of a matrix $A \in \mathbb{R}^{d \times n}$. A set $S \subseteq \mathbb{R}^d$ is *tropically convex* if for any points $s, t \in S$ the set S contains the tropical line segment $\text{tconv}(s, t)$. Note that $\lambda \odot w = \lambda \mathbf{1} + w \in \text{tconv}(V)$ for any point $w \in \text{tconv}(V)$ and $\lambda \in \mathbb{R}$. Thus, we identify a tropically convex set with its image in the tropical projective torus $\mathbb{TP}^{d-1} = \mathbb{R}^d / (\mathbb{R} \odot \mathbf{1})$. A *tropical polytope* $P \subseteq \mathbb{TP}^{d-1}$ is the tropical convex hull of finitely many points.

Example 1.3.1 (Tropical convex hulls). Consider the tropical polytopes $P_i = \text{tconv}(A_i) \subseteq \mathbb{TP}^2$ with tropical vertices given as columns of the matrices

$$A_1 = \begin{pmatrix} 1 & 0 & -1 \\ 0 & 1 & -1 \\ 0 & 0 & 0 \end{pmatrix}, \quad A_2 = \begin{pmatrix} -1 & 0 & 1 \\ 0 & -1 & 1 \\ 0 & 0 & 0 \end{pmatrix}, \quad A_3 = \begin{pmatrix} 5 & -1 & -4 \\ -1 & 5 & -5 \\ 0 & 0 & 0 \end{pmatrix}.$$

The tropical polytopes P_1, P_2 and P_3 are depicted in Figure 1.5. Furthermore we note that $\text{tconv}(A_1) = \text{tconv}(A_1^t) - \left(\begin{smallmatrix} 1 \\ 1 \\ 0 \end{smallmatrix}\right)$. Indeed, viewing the columns of A_1^t as points in \mathbb{TP}^2 , we obtain

$$A_1^t = \begin{pmatrix} 1 & 0 & 0 \\ 0 & 1 & 0 \\ -1 & -1 & 0 \end{pmatrix} \cong \begin{pmatrix} 2 & 1 & 0 \\ 1 & 2 & 0 \\ 0 & 0 & 0 \end{pmatrix},$$

which can be obtained by adding the vector $\begin{pmatrix} 1 \\ 1 \\ 0 \end{pmatrix}$ to each column of A_1 . In the discussion below [Theorem 1.3.2](#) we will see that this isomorphism $\text{tconv}(A) \cong \text{tconv}(A^t)$ holds in more generality.

The triangle, which can be written as the ordinary convex hull $S = \text{conv}(\emptyset, e_1, e_2)$ is a tropically convex set, but not a tropical polytope. This can be seen from the fact that any point s in the interior of the edge $\text{conv}(e_1, e_2)$ cannot be written as the tropical convex hull of any finite subset of S that does not contain s itself. \diamond

The following theorem shows that any tropical polytope can be viewed as a polyhedral complex consisting of ordinary polytopes.

THEOREM 1.3.2 ([DS04, Theorem 1 and Lemma 7]). Let $V = \{v_1, \dots, v_n\} \subseteq \mathbb{TP}^{d-1}$ and let $v_{ij} = (v_j)_i$ denote the i th coordinate of v_j for $j \in [n]$. There is a piecewise-linear isomorphism between the tropical polytope $\text{tconv}(V)$ and the polyhedral complex of bounded faces of the unbounded polyhedron

$$\mathcal{P}_V = \{(y, z) \in \mathbb{R}^{d+n}/(1, \dots, 1, -1, \dots, -1) \mid y_i + z_j \leq v_{ij} \text{ for all } i \in [d], j \in [n]\}.$$

The boundary complex of \mathcal{P}_V is dual to the regular subdivision of the product of simplices $\Delta_{d-1} \times \Delta_{n-1}$ induced by the weights v_{ij} .

The bounded faces of \mathcal{P}_V are dual to the interior faces of the regular subdivision of $\Delta_{d-1} \times \Delta_{n-1}$, i.e. those faces which are not entirely contained in the boundary of $\Delta_{d-1} \times \Delta_{n-1}$. As a corollary of [Theorem 1.3.2](#) we obtain that the polyhedral complexes $\text{tconv}(A) \subseteq \mathbb{R}^d$ and $\text{tconv}(A^t) \subseteq \mathbb{R}^n$ are isomorphic for any matrix $A \in \mathbb{R}^{d \times n}$, since the regular subdivision of $\Delta_{d-1} \times \Delta_{n-1}$ induced by the weights v_{ij} is isomorphic to the regular subdivision of $\Delta_{n-1} \times \Delta_{d-1}$ induced by the weights v_{ji} . Furthermore, note that the product of simplices is a Cayley polytope

$$\Delta_{d-1} \times \Delta_{n-1} = \mathcal{C}(\underbrace{\Delta_{d-1}, \dots, \Delta_{d-1}}_{n \text{ times}}) \cong \mathcal{C}(\underbrace{\Delta_{n-1}, \dots, \Delta_{n-1}}_{d \text{ times}}) = \Delta_{n-1} \times \Delta_{d-1}. \quad (1.1)$$

By the Cayley trick (cf. [Section 1.1.3](#)), the regular subdivisions of $\Delta_{d-1} \times \Delta_{n-1}$ are thus in bijection with the coherent mixed subdivisions of $n\Delta_{d-1}$ and $d\Delta_{n-1}$.

Example 1.3.3. We continue with the three tropical polytopes from [Example 1.3.1](#). [Figure 1.5](#) shows the corresponding mixed subdivisions of $3\Delta_2$, which are in bijection with the regular subdivisions of $\Delta_2 \times \Delta_2$ that are dual to the tropical polytopes in the sense of [Theorem 1.3.2](#). \diamond

A tropical polytope P has a unique minimal set of points V such that $P = \text{tconv}(V)$, called *tropical vertices* [DS04, Proposition 21]. Considering P as a polyhedral complex in the sense of [Theorem 1.3.2](#), let $\text{pvert}(P)$ denote the set of those vertices of the polyhedral complex which are contained in the boundary of P . The set of tropical vertices of P is contained in $\text{pvert}(P)$. A point $p \in \text{pvert}(P)$ which is not a tropical vertex is called a

pseudovertex of P .

In [Chapter 2](#) we will encounter different notions of the rank of a matrix $A \in \mathbb{R}^{d \times n}$ in tropical geometry, which have interpretations in terms of the tropical polytope $P = \text{tconv}(A)$ [[DSS05](#)]. The *tropical rank* of A equals the dimension of P as a polyhedral complex, and the *Barvinok rank* of A is the number of tropical vertices of P . It is known that the tropical rank is bounded from above by the Barvinok rank. In between lies the *Kapranov rank*, which is the smallest dimension among all tropical linear spaces which contain P .

1.3.2 Tropical hypersurfaces and Newton polytopes

We now turn to the description of tropical hypersurfaces. These will be crucial in order to characterize tropical varieties and prevarieties. In [Chapter 2](#) we will consider tropical determinantal hypersurfaces, and introduce a notion of positivity for tropical prevarieties, i.e. for the intersection of finitely many tropical hypersurfaces.

A *tropical Laurent polynomial* is a finite sum of the form

$$f(x) = \bigoplus_{v \in S} c_v \odot x^{\odot v} = \min_{v \in S} (c_v + \langle x, v \rangle),$$

where $S \subseteq \mathbb{Z}^d$ and $c_v \neq \infty$ for all $v \in S$. We use the notation $x_i^{\odot 2}$ for $x_i \odot x_i$ for a single variable, and $x^{\odot v} = x_1^{\odot v_1} \odot \cdots \odot x_d^{\odot v_d}$ for a multivariate tropical Laurent monomial. For each subset $T \subseteq S$ we can consider the relatively open polyhedral regions

$$\begin{aligned} \mathcal{R}_T &= \left\{ x \in \mathbb{R}^d \mid f(x) = c_v + \langle x, v \rangle \text{ if and only if } v \in T \right\} \\ &= \left\{ x \in \mathbb{R}^d \mid -f(x) = \langle \left(\begin{smallmatrix} x \\ -1 \end{smallmatrix} \right), \left(\begin{smallmatrix} v \\ c_v \end{smallmatrix} \right) \rangle \text{ if and only if } v \in T \right\}. \end{aligned}$$

The nonempty regions form a disjoint, relatively open covering of \mathbb{R}^d . The *Newton polytope* of f is defined as

$$\mathcal{N}(f) = \text{conv}(v \mid v \in S) \subseteq \mathbb{R}^d.$$

The coefficients define the lifting function $h(v) = c_v$ on the set S , yielding the lifted Newton polytope $\text{lift}(S) = \text{conv}(\left(\begin{smallmatrix} v \\ c_v \end{smallmatrix} \right) \mid v \in S)$. Note that $x \in \mathcal{R}_T$ if and only if $\left(\begin{smallmatrix} x \\ -1 \end{smallmatrix} \right)$ is a linear functional minimizing the lower face $\text{lift}(T)$ of the lifted Newton polytope for some $T \subseteq S$. Hence, the nonempty regions $\mathcal{R}_T, T \subseteq S$ are dual to the regular subdivision of the Newton polytope with lifting function h . The *tropical hypersurface*

$\mathcal{T}(f)$ is the set

$$\begin{aligned}\mathcal{T}(f) &= \left\{ y \in \mathbb{R}^d \mid \text{the minimum of } \{c_v + \langle y, v \rangle \mid v \in S\} \text{ is attained at least twice} \right\} \\ &= \bigcup_{\substack{T \subseteq S \\ |T| \geq 2}} \mathcal{R}_T.\end{aligned}$$

Any such tropical hypersurface can be seen as a polyhedral complex, in which the polyhedra are the Euclidean closures of the regions \mathcal{R}_T in the above union. The previous observation yields the following duality statement.

THEOREM 1.3.4 ([Jos21, Theorem 1.13]). The tropical hypersurface $\mathcal{T}(f)$ is dual to the 1-skeleton of the regular subdivision of $\mathcal{N}(f)$, i.e. the collection of all faces of the subdivision of dimension at least 1.

If all $c_v, v \in S$ have the same value (i.e. f has *constant coefficients*), then the regular subdivision of $\mathcal{N}(f)$ is trivial, and so the tropical hypersurface $\mathcal{V}(f)$ coincides with the codimension-1 skeleton of the normal fan of the Newton polytope $\mathcal{N}(f)$.

Example 1.3.5 (Tropical hypersurfaces). [Figure 1.6](#) shows the tropical hypersurfaces $\mathcal{T}(f_1), \mathcal{T}(f_2) \subseteq \mathbb{R}^2$ and the dual regular subdivisions of $\mathcal{N}(f_1)$ and $\mathcal{N}(f_2)$ of the tropical polynomials

$$\begin{aligned}f_1 &= x_1 \oplus x_2 \oplus 1, \\ f_2 &= (1 \odot x_1^{\odot 2}) \oplus (x_1 \odot x_2) \oplus x \oplus y \oplus 1.\end{aligned}$$

◊

1.4 ALGEBRAIC VARIETIES AND VALUATIONS

We now turn to the background of the algebro-geometric aspects of this thesis. In this section we introduce the basic concept of algebraic varieties and fields with valuations.

1.4.1 Affine Algebraic Varieties

A (*complex, affine*) variety $\mathcal{V}(f_1, \dots, f_k) \subseteq \mathbb{C}^d$ is the vanishing set of finitely many polynomials $f_1, \dots, f_k \in \mathbb{C}[x_1, \dots, x_d]$, i.e.

$$\mathcal{V}(f_1, \dots, f_k) = \left\{ x \in \mathbb{C}^d \mid f_i(x) = 0 \text{ for all } i \in [k] \right\}.$$

If I is the ideal generated by polynomials f_1, \dots, f_k , then $\mathcal{V}(I) = \mathcal{V}(f_1, \dots, f_k)$. A *hypersurface* is a variety of the form $\mathcal{V}(f)$, i.e. the vanishing set of a single non-constant polynomial $f \neq 0$. A variety is *irreducible* if it cannot be written as the union of two

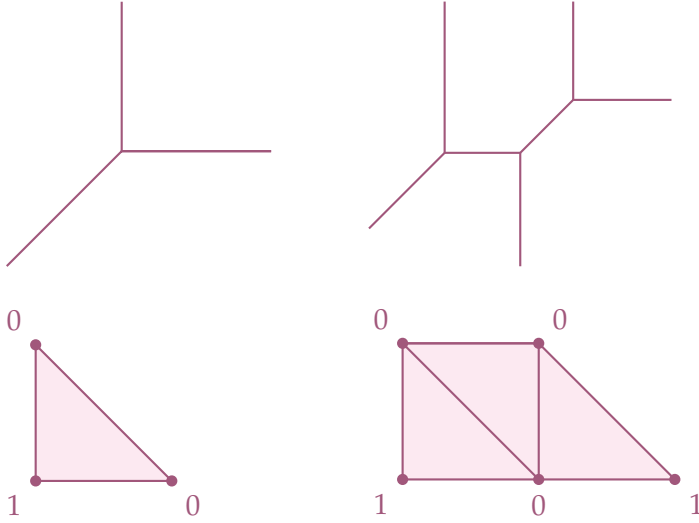


Figure 1.6: The tropical hypersurfaces and the dual subdivisions of the Newton polytopes of the tropical polynomials from Example 1.3.5. The labels of the lattice points of $\mathcal{N}(f)$ are the values of the respective coefficients of f , which induce the regular subdivision.

proper subvarieties, i.e.

$$\mathcal{V}(I) = \mathcal{V}(J) \cup \mathcal{V}(J') \implies \mathcal{V}(I) = \mathcal{V}(J) \text{ or } \mathcal{V}(I) = \mathcal{V}(J').$$

If $f, g \in \mathbb{C}[x_1, \dots, x_d]$ then $\mathcal{V}(fg) = \mathcal{V}(f) \cup \mathcal{V}(g)$ and hence a hypersurface $\mathcal{V}(f)$ is irreducible if and only if f cannot be factored into nonconstant polynomials $f = gg'$. The *Zariski topology* is the topology on \mathbb{C}^d in which varieties are the closed sets. The *Zariski closure* of a set $S \subseteq \mathbb{C}^d$ is the closure with respect to the Zariski topology, i.e. the smallest algebraic variety \mathcal{V} (with respect to inclusion) such that $S \subseteq \mathcal{V}$.

The complex algebraic torus is $(\mathbb{C}^*)^d = \{x \in \mathbb{C}^d \mid x_i \neq 0 \text{ for all } i \in [d]\}$. Similarly, we can define the algebraic torus over any field K as $(K^*)^d = \{x \in K^d \mid x_i \neq 0 \text{ for all } i \in [d]\}$.

1.4.2 Fields With Valuations

Valuations play a central role in the notion of tropicalization. Most importantly, in Chapter 2 we will consider the fields of real and complex Puiseux series, equipped with their canonical valuations induced by the degree map.

Let K be a field. A *valuation* on K is a function $\text{val} : K \rightarrow \mathbb{R} \cup \{\infty\}$ such that

- (i) $\text{val}(a) = \infty$ if and only if $a = 0$,
- (ii) $\text{val}(ab) = \text{val}(a) + \text{val}(b)$,
- (iii) $\text{val}(a + b) \geq \min(\text{val}(a), \text{val}(b))$

holds for all $a, b \in K$. These conditions imply that $\text{val}(a + b) = \min(\text{val}(a), \text{val}(b))$ if $\text{val}(a) \neq \text{val}(b)$. Every field has a *trivial valuation* in which $\text{val}(a) = 0$ for every nonzero $a \in K$. For a point $x = (x_1, \dots, x_d) \in K^d$ we write $\text{val}(x) = (\text{val}(x_1), \dots, \text{val}(x_d))$ for the coordinate-wise valuation.

Example 1.4.1 (Puiseux series). The field of Puiseux series $K\{\{t\}\}$ over a field K can be defined as the union of Laurent series $\bigcup_{N \geq 1} K((t^{1/N}))$ in the formal variable $t^{1/N}$. Nonzero elements in this field are of the form

$$x(t) = \sum_{k=k_0}^{\infty} c_k t^{k/N} \text{ for some } k_0 \in \mathbb{Z}, N \in \mathbb{N},$$

i.e. formal power sums with coefficients $c_k \in K$, rational exponents with a common denominator N , and a term with lowest exponent $\frac{k_0}{N}$ and nonzero coefficient c_{k_0} . We denote the leading term of $x(t)$ by $\text{lt}(x(t)) = c_{k_0} t^{k_0/N}$ and the leading coefficient by $\text{lc}(x(t)) = c_{k_0}$. The degree map $\deg : K\{\{t\}\} \rightarrow \mathbb{Q}$ maps a Puiseux series to its lowest non-zero exponent $\deg(x(t)) = \frac{k_0}{N}$. This induces the valuation $\text{val}(x) = \deg(x)$ for all nonzero $x \in K\{\{t\}\}$ and $\text{val}(0) = \infty$. \diamond

In the following sections, we denote the complex and real Puiseux series by $\mathcal{C} = \mathbb{C}\{\{t\}\}$ and $\mathcal{R} = \mathbb{R}\{\{t\}\}$ respectively. If K is an algebraically closed field of characteristic 0, then so is $K\{\{t\}\}$, and therefore \mathcal{C} is algebraically closed. In order to be able to define initial forms over fields with valuations, we consider the *valuation ring* $R = \{a \in K \mid \text{val}(a) \geq 0\} \cup \{0\}$. The unique maximal ideal of R is $\mathfrak{m} = \{a \in K \mid \text{val}(a) > 0\} \cup \{0\}$ and for $a \in K$ we denote by \bar{a} the image of a in the residue field R/\mathfrak{m} .

Example 1.4.2 (Images in the residue field). Let $x(t) = \sum_{k=k_0}^{\infty} c_k t^{k/N} \in K\{\{t\}\}$, so $\text{val}(x(t)) = \frac{k_0}{N}$. We compute the image $\overline{t^{-\text{val}(x(t))} x(t)}$ inside the residue field. Note that

$$\overline{t^{-\text{val}(x(t))} x(t)} = \sum_{k=k_0}^{\infty} c_k t^{(k-k_0)/N} = \sum_{k=0}^{\infty} c_{k+k_0} t^{k/N}$$

and the image inside the residue field is thus $\overline{t^{-\text{val}(x(t))} x(t)} = \text{lc}(x(t)) = c_{k_0}$. On the other hand, if K is a field with trivial valuation then $R/\mathfrak{m} = K$ and $\text{val}(x) = 0$ for any $x \in K \setminus \{0\}$. In this case $\overline{t^{-\text{val}(x)} x} = \bar{x} = x$. \diamond

1.5 GRÖBNER THEORY

Gröbner bases are a key concept in tropical geometry. The Fundamental Theorem of tropical algebraic geometry in [Section 1.6](#) establishes the connection between initial ideals and tropical varieties, and is the main tool to detect tropical positivity in [Chapter 2](#). In [Chapter 3](#) we study polytropes via the polytrope region, which is the intersection of

a polyhedral cone with certain Gröbner fan.

Let K be a field with valuation. In most of the literature on Gröbner theory, the valuation is assumed to be trivial and ideals are contained in the polynomial ring. This is the setup of [Chapter 3](#). However, for the purposes of tropical geometry as in [Section 1.6](#) it is important to allow non-trivial valuations and ideals in the Laurent polynomial ring. The material presented in this section reduces to the conventional exposition (as e.g. in [\[CLO15, Chapter 2\]](#)) in the case of trivial valuations. Here, the distinction between Laurent polynomial rings and polynomial rings does not make a significant difference. In order to avoid assumptions on the properties of the valuations for this thesis, we assume that (K, val) is either a field of complex or real Puiseux series $(\mathcal{C}, \text{val}) = (\mathbb{C}\{\{t\}\}, \text{val})$ or $(\mathcal{R}, \text{val}) = (\mathbb{R}\{\{t\}\}, \text{val})$ as described in [Example 1.4.1](#), or a field K with trivial valuation. We follow the exposition in [\[MS15, Chapter 2.4–2.5\]](#).

Given a vector $v = (v_1, \dots, v_d) \in \mathbb{Z}^d$, we write x^v for the Laurent monomial $\prod_{i=1}^d x_i^{v_i}$. Given a nonzero Laurent polynomial $f = \sum_{v \in S} c_v x^v$, $S \subseteq \mathbb{Z}^d$, the *weight* of a monomial term $c_v x^v$ with respect to w is $\text{val}(c_v) + \langle v, w \rangle$. The *initial form* $\text{in}_w(f)$ of f with respect to w is the sum of all terms of minimal weight. More precisely, let

$$m_w = \min(\text{val}(c_v) + \langle v, w \rangle \mid v \in S).$$

Then the initial form of f is defined as

$$\text{in}_w(f) = \sum_{\substack{v \in S: \\ \text{val}(c_v) + \langle v, w \rangle = m_w}} \overline{t^{-\text{val}(c_v)} c_v} x^v.$$

[Example 1.4.2](#) implies that if (K, val) equals $(\mathcal{C}, \text{val})$ or $(\mathcal{R}, \text{val})$ then

$$\text{in}_w(f) = \sum_{\substack{v \in S: \\ \text{val}(c_v) + \langle v, w \rangle = m_w}} \text{lc}(c_v) x^v$$

and if K has trivial valuation then

$$\text{in}_w(f) = \sum_{\substack{v \in S: \\ \langle v, w \rangle = m_w}} c_v x^v.$$

Let $I = \langle f_1, \dots, f_k \rangle \subseteq R$ be an ideal inside the polynomial ring $R = K[x_1, \dots, x_d]$ or inside the Laurent polynomial ring $R = K[x_1^{\pm 1}, \dots, x_d^{\pm 1}]$. The *initial ideal* $\text{in}_w(I) \subseteq R$ of I with respect to w is the ideal

$$\text{in}_w(I) = \langle \text{in}_w(f) \mid f \in I \rangle.$$

In general, the initial forms of the generators f_1, \dots, f_k do not generate the initial ideal $\text{in}_w(I)$. However, for any ideal $I \subseteq R$ there exists a *Gröbner basis* of I with respect to the

weight vector w , i.e. a finite set $\mathcal{G} \subseteq R$ such that $\text{in}_w(I) = \langle \text{in}_w(g) \mid g \in \mathcal{G} \rangle$. If R is the polynomial ring and K has trivial valuation, then every such Gröbner basis generates the ideal [CLO15, Corollary 2.5.6]. If R is the Laurent polynomial ring over a field with arbitrary valuation, then this is only the case if I is homogeneous [MS15, Remark 2.4.4]. In this case, we can choose \mathcal{G} to be a homogeneous Gröbner basis [MS15, Lemma 2.4.2].

Two distinct weight vectors $w, w' \in \mathbb{R}^d$ can induce the same initial ideal $\text{in}_w(I) = \text{in}_{w'}(I)$. The set of such weight vectors forms the (relatively open) polyhedron

$$\mathcal{C}_w(I) = \{w' \in \mathbb{R}^d \mid \text{in}_w(I) = \text{in}_{w'}(I)\}.$$

The collection of the Euclidean closures of all such polyhedra form the *Gröbner complex*, a polyhedral complex which covers the entire space \mathbb{R}^d . If K has trivial valuation, then each such polyhedron is a cone. The collection of all these cones forms the *Gröbner fan* \mathcal{GF} of the ideal I , which is a complete polyhedral fan.

Let K be a field with trivial valuation and $R = K[x_1, \dots, x_d]$. The initial ideal $\text{in}_w(I)$ is a monomial ideal for any fixed generic weight vector w . Let \mathcal{G} be a Gröbner basis of $\text{in}_w(I)$. A *standard monomial* with respect to \mathcal{G} is a monomial in $K[x_1, \dots, x_d]/\text{in}_w(I)$ and the standard monomials form a K -vectorspace basis for $K[x_1, \dots, x_n]/I$ [Stu96, Chapter 10]. Therefore, any polynomial p modulo I can be expressed in its *normal form* modulo \mathcal{G} , which is the unique representation of p modulo I as a K -linear combination of standard monomials [CLO15, Chapter 2 §6].

1.6 TROPICAL VARIETIES

In this section we discuss the Fundamental Theorem of tropical algebraic geometry, which characterizes three equivalent ways to describe tropical varieties. This will be particularly important in [Chapter 2](#), where we consider tropical determinantal varieties and point configurations on tropicalizations of linear spaces. We follow the conventions of [MS15, Chapter 3.2].

Let (K, val) be a field with valuation. As in [Section 1.5](#), we assume that (K, val) is either the field of complex or real Puiseux series, or a field with trivial valuation. Let $f = \sum_{v \in S} c_v x^v \in K[x_1^{\pm 1}, \dots, x_d^{\pm 1}]$ be a nonzero Laurent polynomial. The *tropicalization of the Laurent polynomial* f is the tropical Laurent polynomial

$$\text{trop}(f) = \bigoplus_{v \in S} \text{val}(c_v) \odot x^{\odot v}.$$

Recall from [Section 1.3.2](#) that $\mathcal{T}(\text{trop}(f))$ denotes the tropical hypersurface, i.e. a subcomplex of the dual complex of a regular subdivision of the Newton polytope $\mathcal{N}(f) = \mathcal{N}(\text{trop}(f))$. Kapranov's Theorem relates tropical hypersurfaces to valuations (cf. [Section 1.4.2](#)) and initial forms (cf. [Section 1.5](#)).

THEOREM 1.6.1 (Kapranov's Theorem, [MS15, Theorem 3.1.3]). Let K be an algebraically closed field with a nontrivial valuation, $f \in K[x_1^{\pm 1}, \dots, x_d^{\pm 1}]$ be a Laurent polynomial and $\mathcal{V}(f) \subseteq (K^*)^d$ be the defined hypersurface inside the algebraic torus. Then the following three subsets of \mathbb{R}^d coincide.

- (i) $\mathcal{T}(\text{trop}(f))$
- (ii) $\{w \in \mathbb{R}^d \mid \text{in}_w(f) \text{ is not a monomial}\}$
- (iii) $\text{cl}(\{\text{val}(x) \mid x \in \mathcal{V}(f)\})$

Example 1.6.2 (Tropical line). Let $f = x_1 - x_2 + t \in \mathcal{C}[x_1, x_2]$. Then the tropicalization of the Laurent polynomial is $\text{trop}(f) = x_1 \oplus x_2 \oplus 1$. The tropical hypersurface $\mathcal{T}(\text{trop}(f))$ is thus the tropical line from [Example 1.3.5](#) and is depicted in [Figure 1.6](#) on [page 19](#). This gives a description of $\text{trop}(\mathcal{V}(f))$ as in [Theorem 1.6.1\(i\)](#). In terms of initial forms we have

$$\text{in}_w(f) = \begin{cases} x_1 + t & \text{if } w = (1, w_2), w_2 > 1, \\ -x_2 + t & \text{if } w = (w_1, 1), w_1 > 1, \\ x_1 - x_2 & \text{if } w = (w_1, w_1), w_1 < 1, \\ x_1 - x_2 + t & \text{if } w = (1, 1), \\ \text{monomial} & \text{otherwise,} \end{cases}$$

and [Theorem 1.6.1\(ii\)](#) implies that the tropical line is the set of weight vectors w such that $\text{in}_w(f)$ is not a monomial. Finally, for a description as in [Theorem 1.6.1\(iii\)](#), note that

$$\mathcal{V}(f) = \left\{ \left(\begin{smallmatrix} x_1 \\ x_1+t \end{smallmatrix} \right) \mid x_1 \in \mathcal{C} \right\} = \left\{ \left(\begin{smallmatrix} x_2-t \\ x_2 \end{smallmatrix} \right) \mid x_2 \in \mathcal{C} \right\}$$

and we have

$$\begin{aligned} \text{val} \left(\left(\begin{smallmatrix} x_1 \\ x_1+t \end{smallmatrix} \right) \right) &= \begin{cases} \left(\begin{smallmatrix} \text{val}(x_1) \\ \text{val}(x_1) \end{smallmatrix} \right) & \text{if } \text{val}(x_1) < 1, \\ \left(\begin{smallmatrix} \text{val}(x_1) \\ 1 \end{smallmatrix} \right) & \text{if } \text{val}(x_1) \geq 1, \end{cases} \\ \text{val} \left(\left(\begin{smallmatrix} x_2-t \\ x_2 \end{smallmatrix} \right) \right) &= \begin{cases} \left(\begin{smallmatrix} \text{val}(x_2) \\ \text{val}(x_2) \end{smallmatrix} \right) & \text{if } \text{val}(x_2) < 1, \\ \left(\begin{smallmatrix} 1 \\ \text{val}(x_2) \end{smallmatrix} \right) & \text{if } \text{val}(x_2) \geq 1. \end{cases} \end{aligned}$$

As promised by [Theorem 1.6.1](#), all of these descriptions coincide. \diamond

The Fundamental Theorem of Tropical Algebraic Geometry extends Kapranov's Theorem to general algebraic varieties. Let $I \subseteq K[x_1^{\pm 1}, \dots, x_d^{\pm 1}]$ be an ideal and $\mathcal{V}(I) \subseteq (K^*)^d$ be the corresponding algebraic variety. The *tropicalization* $\text{trop}(\mathcal{V}(I))$ of the variety $\mathcal{V}(I)$ is the Euclidean closure of the set of valuations of points of $\mathcal{V}(I)$ inside the algebraic torus, i.e.

$$\text{trop}(\mathcal{V}(I)) = \text{cl}(\{\text{val}(x) \mid x \in \mathcal{V}(I)\}) \subseteq \mathbb{R}^d.$$

A *tropical variety* is any subset of \mathbb{R}^d that can be obtained as the tropicalization of some algebraic variety. Tropical varieties can be characterized as follows.

THEOREM 1.6.3 (Fundamental Theorem of Tropical Algebraic Geometry, [MS15, Theorem 3.2.3]). Let K be an algebraically closed field with a nontrivial valuation, $I \subseteq K[x_1^{\pm 1}, \dots, x_d^{\pm 1}]$ be an ideal and $\mathcal{V}(I) \subseteq (K^*)^d$ be the defined variety inside the algebraic torus. Then the following three subsets of \mathbb{R}^d coincide.

- (i) $\bigcap_{f \in I} \mathcal{T}(\text{trop}(f))$
- (ii) $\{w \in \mathbb{R}^d \mid \text{in}_w(I) \neq \langle 1 \rangle\}$
- (iii) $\text{cl}(\{\text{val}(x) \mid x \in \mathcal{V}(I)\})$

The tropicalization $\text{trop}(\mathcal{V}(I))$ is a pure, strongly connected (i.e. connected through codimension 1) polyhedral complex, whose dimension equals the dimension of $\mathcal{V}(I)$. The Fundamental Theorem implies that every tropical variety can be written as the intersection of infinitely many tropical hypersurfaces. In fact, any tropical variety is also a *tropical prevariety*, i.e. the intersection of finitely many hypersurfaces $\text{trop}(\mathcal{V}(I)) = \bigcap_{f \in \mathcal{B}} \text{trop}(\mathcal{V}(f))$ [MS15, Theorem 2.6.6]. The finite set $\mathcal{B} \subseteq I$ is a *tropical basis* of the ideal I .

We now discuss an analog to the “constant coefficient case” of tropical hypersurfaces from [Section 1.3.2](#) which we need for our purposes in [Chapter 2](#). In this case, a tropical variety turns out to be a polyhedral fan, i.e. a polyhedral complex without bounded faces. Let K be a field with trivial valuation and $K\{\{t\}\}$ be the field of Puiseux series over K . Take $f_1, \dots, f_k \in K[x_1^{\pm 1}, \dots, x_d^{\pm 1}]$ and consider the ideal $I = \langle f_1, \dots, f_k \rangle \subseteq K\{\{t\}\}[x_1^{\pm 1}, \dots, x_d^{\pm 1}]$ generated over the Laurent polynomial ring with coefficients in the Puiseux series. Then $\text{trop}(f_i)$ is a tropical polynomial with constant coefficients in the sense of [Section 1.3.2](#). Furthermore, the tropical variety $\text{trop}(\mathcal{V}(I))$ is a polyhedral fan [MS15, Lemma 2.6.5].

We close this section with a discussion on different versions of the Fundamental Theorem in the literature. Many older articles rely on a version of the Fundamental Theorem which is stated for ideals generated over the polynomial ring, and thus consider the variety $\mathcal{V}(I)$ inside K^d . The Fundamental Theorem over the polynomial ring states the following.

THEOREM 1.6.4 (Fundamental Theorem over the polynomial ring [SSo4, Theorem 2.1]). Let K be an algebraically closed field with a nontrivial valuation, $I \subseteq K[x_1, \dots, x_d]$ be an ideal and $\mathcal{V}(I) \subseteq K^d$ be the defined variety. Then the following three subsets of \mathbb{R}^d coincide.

- 1.) $\bigcap_{f \in I} \mathcal{T}(\text{trop}(f))$

- 2.) $\{w \in \mathbb{R}^d \mid \text{in}_w(I) \text{ does not contain a monomial}\}$
- 3.) $\text{cl}(\{\text{val}(x) \mid x \in \mathcal{V}(I) \cap (K^*)^d\})$

We now show that these two versions of the Fundamental Theorem agree. To make this statement more rigorous, we first collect some basic facts. For the remainder of this section, we denote by I the ideal generated by polynomials f_1, \dots, f_k over the polynomial ring and by I^\pm the ideal generated over the Laurent polynomial ring.

First note, that for any ideal $J \subseteq K[x_1^{\pm 1}, \dots, x_d^{\pm 1}]$ there exist polynomial generators $f_1, \dots, f_k \in K[x_1, \dots, x_d]$ such that $J = \langle f_1, \dots, f_k \rangle^\pm$. In other words, any such ideal J is of the form $J = I^\pm$ for some ideal $I \subseteq K[x_1, \dots, x_d]$. To see this, let g_1, \dots, g_k be Laurent polynomials which generate J . Then any element $h \in J$ is of the form $h = \sum_{i=1}^k c_i g_i$ for some Laurent polynomials $c_i, i \in [k]$. There exists some monomial $x^\alpha, \alpha \in \mathbb{Z}_{\geq 0}^d$ such that for all $i \in [k]$ the product $f_i = x^\alpha g_i$ is a polynomial. Thus,

$$h = \sum_{i=1}^k (x^{-\alpha} c_i)(x^\alpha g_i) = \sum_{i=1}^k (x^{-\alpha} c_i) f_i \in \langle f_1, \dots, f_k \rangle^\pm.$$

Second, note that we can write $I^\pm = I \cdot K[x_1^{\pm 1}, \dots, x_d^{\pm 1}]$, i.e. every element in I^\pm can be written as product fg , where $f \in I$ and $g \in K[x_1^{\pm 1}, \dots, x_d^{\pm 1}]$. To see this, let $I = \langle f_1, \dots, f_k \rangle$ and $h = \sum_{i=1}^k c_i f_i \in I^\pm$ with Laurent polynomials $c_i, i \in [k]$. Again, we can choose some monomial $x^\alpha, \alpha \in \mathbb{Z}_{\geq 0}^d$ such that for all $i \in [k]$ the product $x^\alpha c_i$ is a polynomial. This yields $h = \sum_{i=1}^k c_i f_i = x^{-\alpha} \sum_{i=1}^k x^\alpha c_i f_i$ and $\sum_{i=1}^k x^\alpha c_i f_i \in I$.

THEOREM 1.6.5. For any ideal, each of the three characterizations of the fundamental theorems over the polynomial ring (Theorem 1.6.4) and the Laurent polynomial ring (Theorem 1.6.3) are equivalent.

Proof. Let $f_1, \dots, f_k \in K[x_1, \dots, x_d] \subseteq K[x_1^{\pm 1}, \dots, x_d^{\pm 1}]$. Recall that we denote by I the ideal generated by polynomials f_1, \dots, f_k over the polynomial ring and by I^\pm the ideal generated over the Laurent polynomial ring. $\mathcal{V}(I) \subseteq K^d$ and $\mathcal{V}(I^\pm) \subseteq (K^*)^d$ denote the respective varieties. Furthermore, recall that any ideal over the Laurent polynomial ring has polynomial generators.

(i) \iff (1): We show that $\bigcap_{f \in I} \mathcal{T}(\text{trop}(f)) = \bigcap_{h \in I^\pm} \mathcal{T}(\text{trop}(h))$. **Kapranov's Theorem** (Theorem 1.6.1) implies that $\mathcal{T}(\text{trop}(f)) = \text{trop}(\mathcal{V}(f))$ for any Laurent polynomial. For the corresponding hypersurface inside the torus holds $\mathcal{V}(f) = \mathcal{V}(\langle f \rangle^\pm)$. We thus obtain

$$\begin{aligned} \bigcap_{f \in I} \mathcal{T}(\text{trop}(f)) &= \bigcap_{f \in I} \text{trop}(\mathcal{V}(\langle f \rangle^\pm)) \\ &= \bigcap_{f \in I} \bigcap_{g \in K[x_1^{\pm 1}, \dots, x_d^{\pm 1}]} \text{trop}(\mathcal{V}(\langle gf \rangle^\pm)) \end{aligned}$$

$$\begin{aligned}
&= \bigcap_{f \in I} \bigcap_{g \in K[x_1^{\pm 1}, \dots, x_d^{\pm 1}]} \mathcal{T}(\text{trop}(gf)) \\
&= \bigcap_{h \in I^\pm} \mathcal{T}(\text{trop}(h)).
\end{aligned}$$

(ii) \iff (2): We show that $\text{in}_w(I)$ contains a monomial if and only if $\text{in}_w(I^\pm) = \langle 1 \rangle$. First note that $\text{in}_w(fg) = \text{in}_w(f)\text{in}_w(g)$ holds in both rings [MS15, Lemma 2.6.2]. Let $w \in \mathbb{R}^d$ such that $\text{in}_w(I)$ contains a monomial. Then there exists some $f \in I$ such that $\text{in}_w(f) = x^\alpha$ for some $\alpha \in \mathbb{Z}_{\geq 0}^d$. Since $I \subseteq I^\pm$ we have that $f \in I^\pm$, and hence $x^{-\alpha}f \in I^\pm$. Furthermore, $\text{in}_w(x^{-\alpha}f) = x^{-\alpha}\text{in}_w(f) = x^{-\alpha}x^\alpha$ and thus $\text{in}_w(I^\pm) = \langle 1 \rangle$. Conversely, let $w \in \mathbb{R}^d$ such that $\text{in}_w(I^\pm) = \langle \text{in}_w(h) \mid h \in I^\pm \rangle = \langle 1 \rangle$. By [MS15, Lemma 2.6.2], for any $q \in \text{in}_w(I^\pm)$ there exists some $h \in I^\pm$ such that $q = \text{in}_w(h)$. Thus, $1 = \text{in}_w(h)$ for some $h \in I^\pm$. Since $I^\pm = I \cdot K[x_1^{\pm 1}, \dots, x_d^{\pm 1}]$ we can write $h = fg$ for some polynomial $f \in I$ and some Laurent polynomial g . Note that there exists a monomial $\alpha \in \mathbb{Z}_{\geq 0}^d$ such that $x^\alpha g \in K[x_1, \dots, x_d]$ and thus $x^\alpha fg \in I$. This yields

$$\text{in}_w(x^\alpha fg) = x^\alpha \text{in}_w(fg) = x^\alpha \in \text{in}_w(I).$$

(iii) \iff (3): Since the Laurent polynomial ring is the coordinate ring of the algebraic torus, by localization we obtain that $\mathcal{V}(I) \cap (K^*)^d = \mathcal{V}(I^\pm)$. Hence, we have equality of the sets $\{\text{val}(x) \mid x \in \mathcal{V}(I) \cap (K^*)^d\} = \{\text{val}(x) \mid x \in \mathcal{V}(I^\pm)\}$ and in particular their Euclidean closures agree. \square

1.7 TORIC GEOMETRY

In this section we give an introduction to toric varieties, divisors and toric intersection theory on smooth toric varieties. In Chapter 3 we will consider toric varieties defined by a certain class of smooth fans in order to compute volume polynomials of polytopes. We follow the exposition of [CLS11, Chapters 1, 3, 4, 12, 13].

1.7.1 Normal Toric Varieties

A *toric ideal* is a prime ideal that is generated by binomials which are differences of monomials. The lattice points $S = C^\vee \cap (\mathbb{Z}^d)^*$ in the dual cone of a rational polyhedral cone $C \subseteq \mathbb{R}^d$ form a (saturated) *semigroup*, i.e. $x + y \in C^\vee$ for all $x, y \in C^\vee$. If $\mathcal{A} = \{m_1, \dots, m_s\}$ is a finite generating set for S , we consider the matrix A with columns m_1, \dots, m_s . For each point $\alpha \in \ker A \cap \mathbb{Z}^s$ we write $\alpha = \alpha^+ - \alpha^-$, where $\alpha^+, \alpha^- \in \mathbb{Z}_{\geq 0}^s$. The (normal) *affine toric variety* $U_C \subseteq \mathbb{C}^s$ of the cone C is the variety defined by the toric ideal

$$I = \langle x^{\alpha^+} - x^{\alpha^-} \mid \alpha \in \ker A \cap \mathbb{Z}^s \rangle$$

[CLS11, Proposition 1.1.9]. We have that $\dim(U_C) = \dim(C)$. Since every proper face F of C is a cone of lower dimension, U_F is an affine open subset subset of U_C [CLS11, Proposition 1.3.16]. Each toric variety admits an action of a *torus* T , which is an algebraic variety isomorphic to the algebraic torus $(\mathbb{C}^*)^d$ that T inherits a group structure from this isomorphism.

Let Σ be a complete rational polyhedral fan, e.g. the normal fan of a polytope. The (normal) *toric variety* X_Σ associated to Σ consists of *affine pieces* U_C , $C \in \Sigma$, which are glued together along affine subvarieties corresponding to common faces [CLS11, Chapter 3.1]. We note that $\dim(X_\Sigma) = \dim(\Sigma)$ and that the variety is smooth if and only if the fan is smooth (in the sense of Section 1.1.2).

Example 1.7.1 (Affine toric varieties). Consider the cones

$$C = \text{cone}(e_1, e_2, e_1 + e_3, e_2 + e_3), \quad C^\vee = \text{cone}(e_1, e_2, e_3, e_1 + e_2 - e_3)$$

The four ray generators of C^\vee generate the semigroup $S = C^\vee \cap (\mathbb{Z}^3)^*$. Computing the kernel of the matrix whose columns are these four generators yields

$$A = \begin{pmatrix} 1 & 0 & 0 & 1 \\ 0 & 1 & 0 & 1 \\ 0 & 0 & 1 & -1 \end{pmatrix}, \quad \ker A = \text{span}(1 \ 1 \ -1 \ -1)$$

and so the toric ideal is by $I = \langle x_1x_2 - x_3x_4 \rangle$. This defines the toric variety U_C , which is a hypersurface in \mathbb{C}^4 . \diamond

Each affine piece can be written as union of “torus orbits” $U_C = \bigcup_{F \text{ is a face of } C} O(F)$. The Zariski closure of such a torus orbit is a (toric) subvariety of X_Σ of dimension $\text{codim}(C)$ [CLS11, Theorem 3.2.6]. Thus, each ray u of the fan Σ corresponds to a torus-invariant subvariety of codimension 1, called a *torus-invariant prime divisor*. From now on let X_Σ be a smooth variety. A *torus-invariant (Weil) divisor* on X_Σ is an integral combination

$$D = \sum_{\substack{u \in \Sigma \\ \dim(u)=1}} c_u D_u,$$

where the sum ranges over all 1-dimensional cones u of Σ , $c_u \in \mathbb{Z}$ and D_u is the torus-invariant prime divisor corresponding to the ray u . In principle, one has to distinguish between different classes of divisors, namely Weil divisors and Cartier divisors. However, on smooth varieties both classes coincide [CLS11, Theorem 4.0.22] and so we refer to them as divisors.

1.7.2 Volumes via Toric Intersection Theory

Let $P \subseteq \mathbb{R}^d$ be the simple lattice polytope

$$P = \left\{ x \in \mathbb{R}^d \mid \langle x, u_i \rangle + b_i \geq 0 \text{ for } i \in [m] \right\},$$

where u_i is the primitive (inner) facet normal of the facet

$$F_i = \{x \in P \mid \langle x, u_i \rangle + b_i = 0\}.$$

We denote by Σ the (inner) normal fan of P and by X_Σ the toric variety defined by the fan Σ . We assume that Σ is a smooth fan and thus X_Σ is a smooth variety of dimension $\dim(X_\Sigma) = \dim(P)$. As described in [Section 1.7.1](#), a fixed ray generator u_i of a ray in Σ corresponds to a torus-invariant prime divisor D_i of X_Σ . This is a subvariety of X_Σ of codimension 1 and as such gives rise to a cohomology class $[D_i] \in H^2(X, \mathbb{Q})$. We define the *divisor of the polytope P* as the linear combination $D_P = \sum_{i=1}^m b_i D_i$, which induces the cohomology class $[D_P] = [\sum_{i=1}^m b_i D_i] = \sum_{i=1}^m b_i [D_i]$.

Our main motivation for considering cohomology classes of divisors on toric varieties is to compute the volume of P . Inside the cohomology ring, the volume of P can be expressed the “integral” (or “intersection product”) as follows.

THEOREM 1.7.2 ([CLS11, Theorem 13.4.1]). The normalized volume of P is given by

$$\text{Vol}(P) = \int_X \left[\sum_{i=1}^m b_i D_i \right]^{\dim(X_\Sigma)}.$$

Instead of describing the intersection product inside the cohomology ring explicitly, we make use of an isomorphism between the cohomology ring and a quotient of a polynomial ring. We now explain this isomorphism and establish the analogous statement of [Theorem 1.7.2](#) under this isomorphism. The Stanley-Reisner ideal plays a central role in the statement of this isomorphism.

Let K be a field of characteristic 0. The boundary complex ∂P° of the polar polytope P° is a simplicial complex on m vertices, which allows us to consider the *Stanley-Reisner ideal* of ∂P° . This is the ideal M in the polynomial ring $R = K[x_1, \dots, x_m]$ which is generated by the (inclusion-minimal) non-faces of ∂P° , i.e.

$$M = \langle x_{i_1} \cdots x_{i_k} \mid \{i_1, \dots, i_k\} \text{ is not a face of } \partial P^\circ \rangle.$$

The cohomology ring $H^*(X, \mathbb{Q})$ is isomorphic to the graded ring $R/(L + M)$, where L is the ideal

$$L = \left\langle \sum_{i=1}^m \langle e, u_i \rangle x_i \mid e \in \mathcal{B} \right\rangle,$$

and \mathcal{B} be a basis of \mathbb{Z}^d . The variable x_i in $R/(L + M)$ corresponds to $[D_i]$, the cohomology class of a torus-invariant prime-divisor. Therefore, the expression $[\sum_{i=1}^m b_i D_i]^{\dim(X_\Sigma)}$ in [Theorem 1.7.2](#) translates to a polynomial

$$\left(\sum_{i=1}^m b_i x_i \right)^{\dim(P)} \in H^{2\dim(P)}(X, \mathbb{Q}) \otimes K = (R/(L + M))_{\dim(P)}.$$

The top cohomology group is a one-dimensional vector space. Let $\gamma \in K$ and γx^α be a basis of this vector space in normal form (in the sense of [Section 1.5](#)) modulo $L + M$ as a K -vectorspace. The expression $(\sum_{i=1}^m b_i x_i)^{\dim(P)} \in R/(L + M)$ has a normal form δx^α with coefficient $\delta \in K$. The volume of P is given by the constant $\frac{\delta}{\gamma}$ [[DLS03](#), Algorithm A]. In [Chapter 3](#) we explicitly compute these intersection products for polytropes of dimensions at most 4, i.e. polytopes with normal vectors $e_i - e_j, i, j \in [n - 1]$ and $\pm e_i$.

1.8 SEMIALGEBRAIC SETS AND ALGEBRAIC BOUNDARIES

In [Part II](#) of this thesis we make use of tools from real algebraic geometry to study sets defined by polynomial inequalities. In [Chapter 4](#) we show that the intersection body of a polytope is always a semialgebraic set and we give bounds on the degrees of the irreducible components of the algebraic boundary. In [Chapter 5](#) we study the possible combinatorial types of correlated equilibrium polytopes via oriented matroid strata, which are semialgebraic sets. We follow the conventions of [[BCRR98](#), Chapter 2].

A set $S \subseteq \mathbb{R}^d$ is a *basic closed semialgebraic set* if it can be written as the intersection of finitely many polynomial inequalities, i.e.

$$S = \left\{ x \in \mathbb{R}^d \mid f_1(x) \geq 0, \dots, f_k(x) \geq 0 \right\}$$

for polynomials $f_1, \dots, f_k \in \mathbb{R}[x_1, \dots, x_d]$. A set is a *basic open semialgebraic set* if it is of the form

$$S = \left\{ x \in \mathbb{R}^d \mid f_1(x) > 0, \dots, f_k(x) > 0 \right\}.$$

A *semialgebraic set* is a finite boolean combination (i.e. unions, intersections and complements) of basic (closed or open) semialgebraic sets.

Example 1.8.1 (Semialgebraic sets). Let $f_1 = x_1$, $f_2 = x_2$ and $f_3 = x_1^2 + x_2 - 1$. The set of points in \mathbb{R}^2 such that $f_3(x) \leq 0$ is the unit disk, and the set of points such that $f_1(x), f_2(x) \geq 0$ are the right and upper halfplane respectively. The basic closed semialgebraic sets

$$\begin{aligned} S_1 &= \left\{ x \in \mathbb{R}^2 \mid f_1 \geq 0, f_2 \geq 0, f_3 \leq 0 \right\}, \\ S_2 &= \left\{ x \in \mathbb{R}^2 \mid f_1 \leq 0, f_2 \leq 0, f_3 \leq 0 \right\} \end{aligned}$$

are shown in [Figure 1.7](#). ◇

Note that, in particular, every polytope is a basic semialgebraic set. Furthermore, any coordinate projection of a semialgebraic set is semialgebraic.

THEOREM 1.8.2 (Tarski-Seidenberg Theorem [[BCRR98](#), Theorem 2.2.1]).

Let $\pi : \mathbb{R}^{d+1} \rightarrow \mathbb{R}^d$, $(x_1, \dots, x_d, x_{d+1}) \mapsto (x_1, \dots, x_d)$ be the coordinate projection.

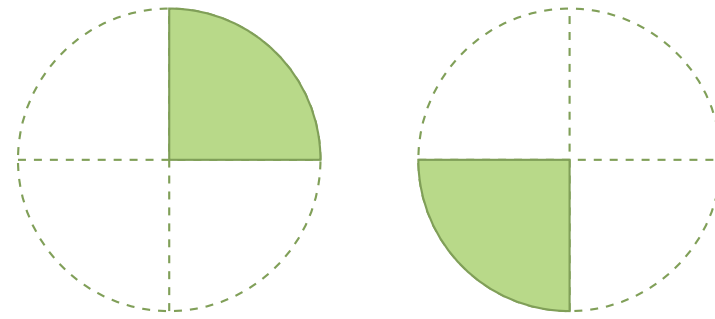


Figure 1.7: The semialgebraic sets S_1 (left) and S_2 (right) from Example 1.8.1.

However, this statement does not hold for basic semialgebraic sets: While the projection of a basic semialgebraic set is still semialgebraic, it is in general not basic.

In Chapters 4 and 5 we will study semialgebraic sets by algebraic means. The main tool for this is the *algebraic boundary* $\partial_a S \subseteq \mathbb{C}^d$ of such a set $S \subseteq \mathbb{R}^d$, which is the Zariski closure of the topological (Euclidean) boundary ∂S over \mathbb{C} . If a semialgebraic set is compact and convex, then its algebraic boundary is a hypersurface [Sin15, Proposition 2.9].

Example 1.8.3 (Algebraic boundary). The two sets S_1 and S_2 from Example 1.8.1 have a common algebraic boundary $\partial_a S_1 = \partial_a S_2$. It is the hypersurface defined by the polynomial

$$f_1 f_2 f_3 = x_1 x_2 (x_1^2 + x_2^2 - 1).$$

The irreducible components are thus the unit circle and the two coordinate hyperplanes, as shown in Figure 1.8. \diamond

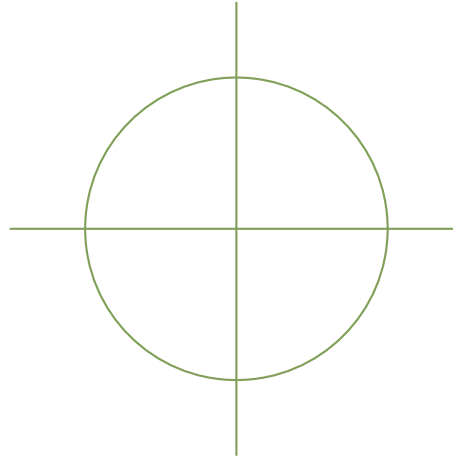


Figure 1.8: The real picture of the algebraic boundary of the semialgebraic sets S_1 and S_2 , as described in Example 1.8.3.

Part I

TROPICAL POSITIVITY AND POLYTROPES

TROPICAL POSITIVITY AND DETERMINANTAL VARIETIES

Tropicalization is a modern and powerful tool for understanding algebraic varieties via a polyhedral ‘shadow’, to which combinatorial tools can be applied (for instance to solve enumerative problems). We are particularly interested in identifying the tropicalization of semialgebraic subsets of algebraic varieties as a subset of the tropicalization of the whole (complex) variety. Specifically, we care about the *positive part* of an algebraic variety, which arises in various applications from combinatorial optimization [GMTW19] to physics [SW21; ALS21] and statistics [MSUZ16]. The tropicalizations of the positive parts of various classical varieties have been studied before. In this work, we focus on determinantal varieties inspired by applications to optimization.

A finite generating set of the vanishing ideal of a given variety (in other words, an algebraic description) can be tropicalized to define a polyhedral complex known as a tropical prevariety. If this happens to coincide with the tropicalization of the variety itself, the generating set is called a *tropical basis*. We coin the notion of *positive-tropical generators* as an analog of this property for the positive part. For determinantal varieties, all cases where the appropriate minors form a tropical basis have been classified in a series of works [DSS05; CJR11; Shi13]. We take the first steps towards a characterization when they are also positive-tropical generators.

This question has been studied before for other varieties: [SW21; ALS21] showed that the 3-term Plücker relations form a set of positive-tropical generators of the tropical Grassmannian (even though they are, in general, not a tropical basis). The main result of [Bor21] implies that the tropicalizations of the incidence Plücker relations form a set of positive-tropical generators of the tropical complete flag variety. For the tropical Pfaffian, [RS22, Corollary 4.5] implies that the polynomials defining the tropical Pfaffian prevariety, when restricting to a certain (Gröbner) cone, form a set of positive-tropical

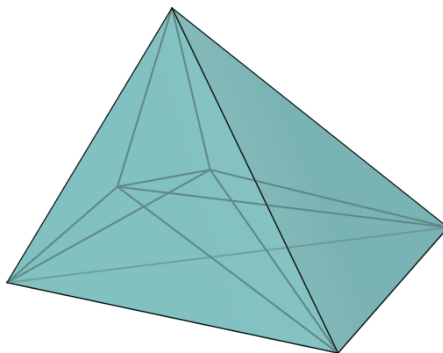


Figure 2.1: The Birkhoff polytope B_3 , which characterizes the tropical determinantal variety $T_{3,3}^2$.

generators of the restriction of the tropical Pfaffian to this cone. In the context of cluster varieties, the proof of [JLS21, Proposition 4.1] implies that the generators of the cluster variety form a positive-tropical generating set (although it is unknown whether they form a tropical basis).

The notions of positivity differ in the literature on positivity in tropical geometry, e.g. distinguishing between positive solutions over the complex Puiseux series and positive solutions that are fully real. We therefore also introduce the notion of *really positive-tropical generators*, which cut out the fully real, positive part. Inspired by Viro's patchworking [Vir83; Viro6] – a combinatorial tool to construct real algebraic curves with prescribed topology – we extend this idea of positive generators to arbitrary sign patterns, introducing the notion of (*really*) *signed-tropical generators*. Generating sets for signed tropicalizations have been studied in [Tab15] under the name 'real tropical bases'. Really signed-tropical generators turn out to allow for more flexibility and may exist even if real tropical bases do not.

Our main results are combinatorial criteria for the (signed) tropicalization of determinantal varieties, i.e. the set of matrices of bounded rank [MS05]. This variety is closely related to the Grassmannian. For this study, we introduce the *triangle criterion*, which is our main tool for identifying positivity. This criterion is purely combinatorial, and relies on the graph structure of the Birkhoff polytope. As a special case, we consider the determinantal varieties of low rank matrices, i.e. matrices of rank 2 and 3.

In rank 2, the (3×3) -minors form a tropical basis [DSS05]. We relate this to the novel notion of positive-tropical generators.

THEOREM 2.4.3. The (3×3) -minors form a set of positive-tropical generators the tropical determinantal variety of rank 2.

The points of the tropical variety (of matrices of Kapranov rank at most 2) are matrices, whose column span is contained in a tropical line and the columns can be interpreted as marked points on this line. This is how Devlin, and Markwig and Yu associate a bicolored phylogenetic tree to such a matrix [Devo5; MY09]. We show that this tree determines the positivity of the tropical matrix.

COROLLARY 2.4.6. A (tropical) matrix in the tropical determinantal variety of rank 2 lies in the tropicalization of the positive part if and only if the associated tree is a caterpillar tree.

This relies on the fact, that the nonnegative rank is equal to the rank for a real matrix of rank 2 (with nonnegative entries) and a result from [Ardo4], showing that the positive part consists precisely of those matrices with Barvinok rank 2 (Theorem 2.4.2). The construction of bicolored phylogenetic trees realizes the tropical determinantal variety combinatorially as a subfan of the tropical Grassmannian [MY09]. In the spirit of [MY09], we establish a bijection on the level of the corresponding matrices and tropical Plücker vectors, highlighting that this bijection is induced by a simple coordinate projection (Theorem 2.4.23).

In rank 3, the (4×4) -minors are in general not a tropical basis and we do not know if they are positive-tropical generators. For the combinatorial criterion, we thus only obtain a necessary condition for positivity – or, in other words, a combinatorial certificate of non-positivity, which we call Starship Criterion. In this case, the column span of a matrix in the tropicalization of the determinantal variety of rank 3 is contained in a tropical plane. The notion of a starship is inspired by the geometry of point configurations on a tropical plane, which certify non-positivity.

THEOREM 2.5.5 (STARSHIP CRITERION). A matrix in the tropical determinantal variety of rank 3 does not lie in the tropicalization of the positive part if the induced point configuration forms a starship.

By [HJJS09], a tropical plane is uniquely determined by its tree arrangement (namely the trees obtained by intersecting the plane with the hyperplanes at infinity). However, we show that the bicolored tree arrangement that we can derive from a tropical matrix (of Kapranov rank at most 3) does not contain sufficient information to determine positivity: The main issue is that some of the marked points (coming from the columns of the matrix) can be on bounded faces of the tropical plane, whereas the tree arrangement is unable to capture this information (Example 2.5.9). However, if the tropical matrix is positive, then the resulting arrangement of bicolored phylogenetic trees solely consists of caterpillar trees (Theorem 2.5.8).

THEOREM 2.5.8. If a matrix in the tropical determinantal variety of rank 3 lies in the tropicalization of the positive part, then the resulting bicolored phylogenetic tree arrangement solely consists of caterpillar trees.

In corank 1, we show that the characterization of positivity for the determinantal hypersurface extends nicely to the other orthants (Proposition 2.2.4). This heavily relies on the fact that in this case the tropical prevariety coincides with the tropical variety. This chapter is based on [BLS22], which is joint work with Georg Loho and Rainer Sinn.

Overview

In this chapter, we discuss different notions of tropical positivity, and characterize the positive part of determinantal varieties of low rank. The background is provided in Sections 1.1 to 1.6. In Section 2.1 we discuss the different notions of positivity in tropical geometry and generators of positivity. We extend this in Section 2.1.3 to arbitrary orthants and we introduce tropical determinantal varieties in Section 2.1.4. Section 2.2 covers determinantal hypersurfaces, whose Newton polytope is the Birkhoff polytope. In this section, we begin the combinatorial translation of positivity by introducing *cartoons*, which leads to the triangle criterion in terms of cartoons, followed by its geometric version. In Section 2.3, we explain how one can describe maximal cones of the determinantal prevariety by unions of perfect matchings, and obtain the triangle criterion in terms of bipartite graphs. In Section 2.4, we consider the special case of rank 2, and describe a bijection between a subfan of the Grassmannian and the

tropical determinantal variety. In [Section 2.5](#), we consider the rank 3 case. We obtain the starship criterion for positivity and consider bicolored tree arrangements.

2.1 POSITIVITY IN TROPICAL GEOMETRY

In this section, we describe different notions of positivity that can be found in the literature. Based on the differences of these notions, we introduce (*really*) *positive-tropical generating sets*, which characterize the (real) positive part of a tropical variety. We then generalize this to (*really*) *signed-tropical generating sets*, which describe the signed tropicalization of a variety with respect to a fixed orthant, and discuss the differences between these notions. Finally, we introduce *tropical determinantal varieties*, the main protagonists in this chapter.

2.1.1 Notions of Positivity

Let $\mathcal{C} = \bigcup_{n=1}^{\infty} \mathbb{C}((t^{1/n}))$ and $\mathcal{R} = \bigcup_{n=1}^{\infty} \mathbb{R}((t^{1/n}))$ be the fields of Puiseux series over \mathbb{C} and \mathbb{R} , respectively, as defined in [Section 1.4.2](#). Recall that we denote by $\text{lc}(x(t))$ the leading coefficient of a Puiseux series $x(t)$, i.e. the coefficient of the term of lowest exponent, and the leading term by $\text{lt}(x(t))$. The degree map $\text{val}(x(t))$ returns the degree of the leading term of a nonzero Puiseux series $x(t)$, and we consider the valuation map $\text{val}(x_1(t), \dots, x_d(t)) = (\text{val}(x_1(t)), \dots, \text{val}(x_d(t)))$. We define the *positive complex (and real respectively) Puiseux series* as

$$\begin{aligned}\mathcal{C}_+ &= \{x(t) \in \mathcal{C} \mid \text{lc}(x(t)) \in \mathbb{R}_{>0}\}, \\ \mathcal{R}_+ &= \{x(t) \in \mathcal{R} \mid \text{lc}(x(t)) \in \mathbb{R}_{>0}\},\end{aligned}$$

which are both convex cones (note that this notation differs e.g. from [[SW05](#)]).

Let $I \subseteq \mathcal{C}[x_1, \dots, x_d]$ be an ideal. The tropicalization $\text{trop}(\mathcal{V}(I))$ of the variety $\mathcal{V}(I) \subseteq \mathcal{C}^n$ is the Euclidean closure of the set $\{\text{val}(z) \mid z \in \mathcal{V}(I) \cap (\mathcal{C}^*)^d\}$. We consider $\text{trop}(\mathcal{V}(I))$ as a polyhedral complex, in which w, w' are contained in the relative interior of the same face if $\text{in}_w(I) = \text{in}_{w'}(I)$. A more detailed explanation of initial ideals and tropical varieties is given in [Sections 1.5](#) and [1.6](#).

Definition 2.1.1 (Positive parts). The *positive part* of $\text{trop}(\mathcal{V}(I))$ is $\text{trop}^{+c}(\mathcal{V}(I)) = \text{trop}(\mathcal{V}(I) \cap \mathcal{C}_+^d)$ and the *really positive part* is $\text{trop}^{+r}(\mathcal{V}(I)) = \text{trop}(\mathcal{V}(I) \cap \mathcal{R}_+^d)$. Similarly, a point $w \in \text{trop}(\mathcal{V}(I))$ is *positive* (respectively *really positive*) if it is contained in the positive part (respectively the really positive part) of $\text{trop}(\mathcal{V}(I))$.

For any set B of generators of an ideal I we have

$$\text{trop}(\mathcal{V}(I)) \subseteq \bigcap_{f \in B} \text{trop}(\mathcal{V}(f)),$$

and so also

$$\text{trop}^{+c}(\mathcal{V}(I)) \subseteq \bigcap_{f \in B} \text{trop}^{+c}(\mathcal{V}(f)). \tag{2.1}$$

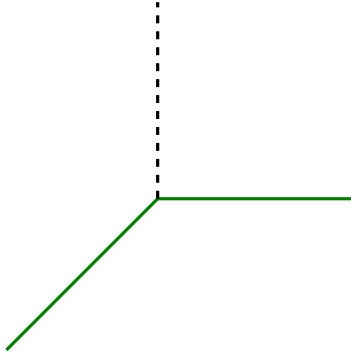


Figure 2.2: The positive part of the tropicalization of the line given by $f = x_1 - x_2 + t$ from Example 2.1.4.

We reserve the notation $\text{trop}^+(\mathcal{V}(I))$ for the case when $\text{trop}^{+c}(\mathcal{V}(I)) = \text{trop}^{+\mathcal{R}}(\mathcal{V}(I))$ holds, so that there can be no confusion about the notion of positivity. For ideals in the polynomial ring, the positive part of a tropical variety was characterized by Speyer and Williams as follows:

PROPOSITION 2.1.2 ([SW05, Proposition 2.2]). Let $I \subseteq \mathcal{C}[x_1, \dots, x_n]$ be an ideal. A point w lies in $\text{trop}^{+c}(\mathcal{V}(I))$ if and only if the initial ideal of I with respect to w does not contain any (non-zero) polynomial whose (non-zero) coefficients all have the same sign, i.e. if and only if

$$\text{in}_w(I) \cap \mathbb{R}_{\geq 0}[x_1, \dots, x_d] = \langle 0 \rangle.$$

Remark 2.1.3. In Section 1.6 we define tropical varieties primarily for ideals generated over the Laurent polynomial ring. However, Theorem 1.6.5 allows us to consider ideals over the polynomial ring instead. We make this choice in order to be able to apply Proposition 2.1.2, whose proof relies on the equivalence (2) \iff (3) of Theorem 1.6.4, the Fundamental Theorem over the polynomial ring.

Example 2.1.4 (Positive parts). We continue Example 1.6.2 of the tropical line and compute its positive part, as depicted in Figure 2.2. Let $f = x_1 - x_2 + t \in \mathcal{C}[x_1, x_2]$ and $I = \langle f \rangle$. Recall that

$$\mathcal{V}(f) = \left\{ \begin{pmatrix} x_1 \\ x_1 + t \end{pmatrix} \mid x_1 \in \mathcal{C} \right\} = \left\{ \begin{pmatrix} x_2 - t \\ x_2 \end{pmatrix} \mid x_2 \in \mathcal{C} \right\}.$$

Let $k \in \mathbb{Q}$, and consider the (positive) Puiseux series $x_1 = t^k$. Then

$$\text{val} \left(\begin{pmatrix} x_1 \\ x_1 + t \end{pmatrix} \right) = \text{val} \left(\begin{pmatrix} t^k \\ t^k + t \end{pmatrix} \right) = \begin{cases} \binom{k}{k} & \text{if } k < 1 \\ \binom{k}{1} & \text{if } k \geq 1 \end{cases}$$

and so these two rays of the tropical line are contained in the positive part. However, for any $x_2 \in \mathcal{C}$ with $\text{val}(x_2) \geq 1$ we have that $x_2 - t \notin \mathcal{C}_+$. Thus, the ray

$$\text{val} \left(\begin{pmatrix} x_2 - t \\ x_2 \end{pmatrix} \right) = \begin{pmatrix} 1 \\ \text{val}(x_2) \end{pmatrix}$$

is not contained in the positive part $\text{trop}^+(\mathcal{V}(f))$. This computation also reveals, that $\text{trop}^{+c}(\mathcal{V}(f)) = \text{trop}^{+\mathbb{R}}(\mathcal{V}(f))$ for the tropical line. In terms of initial forms, we have

$$\text{in}_w(f) = \begin{cases} x_1 + t & \text{if } w = (1, w_2), w_2 > 1 \\ -x_2 + t & \text{if } w = (w_1, 1), w_1 > 1 \\ x_1 - x_2 & \text{if } w = (w_1, w_1), w_1 < 1 \\ x_1 - x_2 + t & \text{if } w = (1, 1) \\ \text{monomial} & \text{otherwise.} \end{cases}$$

which, by [Proposition 2.1.2](#), implies that for any $w = (w_1, w_2) \in \text{trop}(\mathcal{V}(f))$ we have that w is positive if and only if $w \neq (1, w_2), w_2 > 1$. \diamond

[Proposition 2.1.2](#) implies that the positive part is closed. For certain ideals $I \subseteq \mathcal{C}[x_1, \dots, x_n]$ there is an equivalent definition of positivity in terms of the tropicalizations of the polynomials in the vanishing ideal of the variety.

Definition 2.1.5. Let $\mathcal{F} \subseteq \mathcal{C}_+[x_1, \dots, x_d]$ be a finite set of polynomials of the form

$$f = \sum_{e \in E^+} f_e x^e - \sum_{e \in E^-} f_e x^e,$$

such that $f_e \in \mathcal{C}_+$ for all $e \in E^+ \cup E^-$. In particular, the leading coefficient $\text{lc}(f_e)$ of every $f_e \in \mathcal{C}$ is real. The *combinatorially positive part* $\text{Trop}^+(f)$ of the tropical hypersurface $\text{trop}(\mathcal{V}(f))$ is the set of all points $w \in \text{trop}(\mathcal{V}(f))$ such that the minimum of

$$\{ \langle w, e \rangle + \text{val}(f_e) \mid e \in E^+ \cup E^- \}$$

is achieved at some $e \in E^+$ and at some $e \in E^-$. Let $\mathcal{P} = \bigcap_{f \in \mathcal{F}} \text{trop}(\mathcal{V}(f))$ be a tropical prevariety. The *combinatorially positive part* of \mathcal{P} with respect to \mathcal{F} is $\text{Trop}^+(\mathcal{P}) = \bigcap_{f \in \mathcal{F}} \text{Trop}^+(f)$.

In particular, the above definition can be made for every finite set of polynomials $\mathcal{F} \subseteq \mathcal{R}[x_1, \dots, x_d]$ with coefficients in the real Puiseux series. In [\[SSo4\]](#), the definition of the combinatorially positive part of tropical hypersurfaces is made for polynomials $f \in \mathbb{R}[x_1, \dots, x_n]$, in which case $\text{val}(f_e) = 0$ for all $e \in E^+ \cup E^-$.

If $I = \langle f \mid f \in \mathcal{F} \rangle$ and $\mathcal{P} = \text{trop}(\mathcal{V}(I))$ is also a tropical variety, then $\text{trop}^{+c}(\mathcal{V}(I)) = \bigcap_{f \in I} \text{Trop}^+(\mathcal{V}(f))$ by the following [Corollary 2.1.6](#). In this sense, the notions of positivity and combinatorial positivity agree for tropical varieties.

2.1 Positivity in Tropical Geometry

COROLLARY 2.1.6. For hypersurfaces the positive part coincides with the combinatorially positive part, i.e. $\text{Trop}^+(f) = \text{trop}^{+c}(\mathcal{V}(f))$ for any polynomial $f \in \mathcal{R}[x_1, \dots, x_d]$ (or more generally $f \in \mathcal{C}[x_1, \dots, x_d]$ such that its coefficients are in $(\mathcal{C}_+) \cup (-\mathcal{C}_+)$).

Proof. By definition, $w \in \text{Trop}^+(f)$ if and only if the minimum of

$$\{\langle w, e \rangle + \text{val}(f_e) \mid e \in E^+ \cup E^- \}$$

is achieved at some $e^+ \in E^+$ and at some $e^- \in E^-$. Equivalently, the initial form $\text{in}_w(f)$ contains the terms $f_{e^+}x^{e^+} - f_{e^-}x^{e^-}$, i.e. $\text{in}_w(\langle f \rangle) \cap \mathbb{R}_{\geq 0}[x_1, \dots, x_d] = \langle 0 \rangle$. By [Proposition 2.1.2](#), this is equivalent to $w \in \text{trop}^{+c}(\mathcal{V}(f))$. \square

2.1.2 Generators of Positivity

We make the following definitions.

Definition 2.1.7. Let $\mathcal{F} \subseteq \mathcal{R}[x_1, \dots, x_d]$ be a finite set of polynomials. Then \mathcal{F} is a set of *positive-tropical generators* (or is a *positive-tropical generating set*) if

$$\text{trop}(\mathcal{V}(I) \cap \mathcal{C}_+^d) = \bigcap_{f \in \mathcal{F}} \text{trop}(\mathcal{V}(f) \cap \mathcal{C}_+^d).$$

It is a set of *really positive-tropical generators* if

$$\text{trop}(\mathcal{V}(I) \cap \mathcal{R}_+^d) = \bigcap_{f \in \mathcal{F}} \text{trop}(\mathcal{V}(f) \cap \mathcal{R}_+^d).$$

The definition of a set of positive-tropical generators is reminiscent of the definition of a tropical basis in [Section 1.6](#). However, these notions are conceptually different and we now discuss the similarities and differences between them. We begin with similarities – under some circumstances, a tropical basis is guaranteed to be a set of positive-tropical generators.

THEOREM 2.1.8. If $\text{trop}(\mathcal{V}(f))$ is a tropical hypersurface, then f is a positive-tropical generator and a really positive-tropical generator for any $f \in \mathcal{R}[x_1, \dots, x_d]$.

Proof. This follows directly from the definition of (really) positive-tropical generators. \square

THEOREM 2.1.9. For a binomial ideal, every tropical basis containing a reduced Gröbner basis (with respect to any ordering) forms a set of positive-tropical generators.

Proof. Let I be a binomial ideal with tropical basis \mathcal{B} . By assumption, \mathcal{B} contains a reduced Gröbner basis \mathcal{G} . This Gröbner basis \mathcal{G} consists solely of binomials by [[ES96](#), Proposition 1.1]. Let $w \in \text{trop}(\mathcal{V}(I))$. Then $\text{in}_w(I) = \langle \text{in}_w(f) \mid f \in \mathcal{G} \rangle$ does not contain a monomial and so $\text{in}_w(f) = f$ for all $f \in \mathcal{G}$. Thus, $I = \text{in}_w(I)$ and \mathcal{G} is a reduced

Gröbner basis of $\text{in}_w(I)$. Now, [Proposition 2.1.2](#) together with [[BRS20](#), Lemma 5.6] implies that $w \in \text{trop}^{+c}(\mathcal{V}(I))$ if and only if $\text{in}_w(I) \cap \mathbb{R}_{\geq 0}[x_1, \dots, x_d] = \langle 0 \rangle$ if and only if $\mathcal{G} \cap \mathbb{R}_{\geq 0}[x_1, \dots, x_d] = \emptyset$. Therefore, $w \in \text{trop}^{+c}(\mathcal{V}(I)) = \bigcap_{f \in I} \text{trop}^{+c}(\mathcal{V}(f))$ if and only if $w \in \bigcap_{f \in \mathcal{G}} \text{trop}^{+c}(\mathcal{V}(f))$. Note that

$$\bigcap_{f \in I} \text{trop}^{+c}(\mathcal{V}(f)) \subseteq \bigcap_{f \in \mathcal{B}} \text{trop}^{+c}(\mathcal{V}(f)) \subseteq \bigcap_{f \in \mathcal{G}} \text{trop}^{+c}(\mathcal{V}(f)),$$

and so $w \in \text{trop}^{+c}(\mathcal{V}(I))$ if and only if $w \in \bigcap_{f \in \mathcal{B}} \text{trop}^{+c}(\mathcal{V}(f))$. \square

The following example illustrates, that not every set of positive-tropical generators forms a tropical basis.

Example 2.1.10 (The totally positive tropical Grassmannian). Positive-tropical generators have been studied in the case of the tropical Grassmannian. More precisely, it was shown that the 3-term Plücker relations are not a tropical basis, but they are indeed a positive-tropical generating set [[SW21](#); [ALS21](#)]. It is also known that the positive part and the really positive part agree [[SW05](#)]. Hence, the 3-term Plücker relations also form a really positive-tropical generating set. \diamond

If the positive part and the really positive part of a tropical variety coincide, then every set of positive-tropical generators is also a set of really positive-tropical generators, because

$$\begin{aligned} \text{trop}^{+c} \mathcal{V}(I) &= \bigcap_{f \in \mathcal{F}} \text{trop}^{+c}(\mathcal{V}(f)) \\ &\quad \| \\ \text{trop}^{+r} \mathcal{V}(I) &\subseteq \bigcap_{f \in \mathcal{F}} \text{trop}^{+r}(\mathcal{V}(f)). \end{aligned}$$

Remark 2.1.11. In [[Tab15](#)] the notion of a real tropical basis was introduced. This is a finite generating set, which cuts out the signed tropicalization of the real part of the variety. In particular, a real tropical basis is always a set of really positive-tropical generators. We elaborate on this further in [Remark 2.1.16](#).

For our notion of positive-tropical generators, [Example 2.1.10](#) and [Table 2.1](#) indicate that tropical bases and positive-tropical generators are distinct concepts of similar flavor. This motivates the following question.

Question 2.1.12. Is there a tropical variety where a tropical basis is not a set of positive-tropical generators?

In particular, we raise this question for tropical determinantal varieties, which will be the main object of study in the following sections. Given [Table 2.1](#), does this already fail for the minors?

2.1.3 Signed-Tropical Generators

We devote the remainder of this section to discuss how a description of a tropical hypersurface $\text{trop}(\mathcal{V}(f))$ for one orthant (the positive orthant) can be extended to all orthants by ‘flipping signs’. This goes back to the idea of Viro’s patchworking [Viro6]. It is crucial that for a hypersurface, the notions of positivity and combinatorial positivity coincide (cf. Corollary 2.1.6). More precisely, let $f = \sum_{\alpha} c_{\alpha} x^{\alpha}$ be a polynomial in d variables $x = (x_1, \dots, x_d)$ and $s \in \{-1, 1\}^d$ a sign vector. Analogously to the notions introduced in Section 2.1.1 we define

$$\mathcal{C}^s = \left\{ (\xi_1(t), \dots, \xi_n(t)) \in \mathcal{C}^d \mid \text{lc}(\xi_i) \in \mathbb{R} \text{ and } \text{sgn}(\text{lc}(\xi_i)) = s_i \text{ for all } i \in [d] \right\}$$

and $\text{trop}^s(\mathcal{V}(f)) = \text{trop}(\mathcal{V}(f) \cap \mathcal{C}^s)$. We consider the modified polynomial $f^s = \sum_{\alpha} s^{\alpha} c_{\alpha} x^{\alpha}$. By construction, for a point $\xi = (s_1 \xi_1, \dots, s_n \xi_n), \xi_i \in \mathcal{C}_+$ one obtains

$$f(\xi) = \sum_{\alpha} c_{\alpha} \xi^{\alpha} = \sum_{\alpha} s^{\alpha} c_{\alpha} (\xi_1, \dots, \xi_d)^{\alpha} = f^s(\xi_1, \dots, \xi_d).$$

In other words, $\xi \in \mathcal{V}(f) \cap \mathcal{C}^s$ if and only if $(\xi_1, \dots, \xi_d) \in \mathcal{V}(f^s) \cap (\mathcal{C}_+)^d$ and hence

$$\text{trop}^s(\mathcal{V}(f)) = \text{trop}^{+c}(\mathcal{V}(f^s)).$$

We can extend this idea to make the following definitions.

Definition 2.1.13. Let $\mathcal{V}(I) \subseteq \mathcal{C}^d$ be a variety and $\mathcal{F} \subseteq \mathcal{R}[x_1, \dots, x_d]$ be a finite set of polynomials. Let $s \in \{-1, 1\}^d$ be a fixed sign vector. The set \mathcal{F} is a set of *signed-tropical generators* of $\text{trop}(\mathcal{V}(I))$ with respect to s if

$$\text{trop}(\mathcal{V}(I) \cap \mathcal{C}^s) = \bigcap_{f \in \mathcal{F}} \text{trop}(\mathcal{V}(f) \cap \mathcal{C}^s) = \bigcap_{f \in \mathcal{F}} \text{trop}^s(\mathcal{V}(f)).$$

The finite set $\mathcal{F} \subseteq \mathcal{R}[x_1, \dots, x_d]$ is a set of *really signed-tropical generators* of $\text{trop}(\mathcal{V}(I))$ with respect to s if

$$\text{trop}(\mathcal{V}(I) \cap \mathcal{R}^s) = \bigcap_{f \in \mathcal{F}} \text{trop}(\mathcal{V}(f) \cap \mathcal{R}^s).$$

PROPOSITION 2.1.14. If $\text{trop}(\mathcal{V}(f))$ is a tropical hypersurface, then f is a (really) signed-tropical generator for $\text{trop}^s(\mathcal{V}(f))$ with respect to every sign vector $s \in \{-1, 1\}^d$ for any polynomial $f \in \mathcal{R}[x_1, \dots, x_d]$. Furthermore, if $f = \sum_{\alpha} c_{\alpha} x^{\alpha}$, then $\text{trop}^s(\mathcal{V}(f)) = \text{trop}^{+c}(\mathcal{V}(f^s))$, where $f^s = \sum_{\alpha} (\prod s_i^{\alpha_i}) c_{\alpha} x^{\alpha}$.

Proof. The first part of the statement follows directly from the definition of (really) signed-tropical generators. The second part is implied by the discussion above. \square

Let \mathcal{P} denote the tropical prevariety $\mathcal{P} = \bigcap_{f \in \mathcal{F}} \text{trop}(\mathcal{V}(f))$ with finite generating set \mathcal{F} . Note that, similarly to the positive part, also for the more general signed part we have

$$\text{trop}(\mathcal{V}(I) \cap \mathcal{C}^s) \subseteq \bigcap_{f \in \mathcal{F}} \text{trop}^s(\mathcal{V}(f)) \subseteq \mathcal{P}.$$

In this sense, one can interpret the “signed-tropical prevariety” $\bigcap_{f \in \mathcal{F}} \text{trop}^s(\mathcal{V}(f))$ as a combinatorial approximation of the signed tropicalization $\text{trop}(\mathcal{V}(I) \cap \mathcal{C}^s)$. Thus, when considering signed tropicalizations, a finite set \mathcal{F} that is a signed-tropical generating set with respect to every sign pattern $s \in \{-1, 1\}^d$ simultaneously might be a useful tool for understanding the different orthants $\text{trop}(\mathcal{V}(I) \cap \mathcal{C}^s)$ in a combinatorial fashion. Note that a set of positive-tropical generators is not necessarily a signed-tropical generating set for other orthants, as illustrated in the following example.

Example 2.1.15 (Positive generators do not generate all orthants). Consider the tropicalization of the linear space L that is the row span of M with Plücker vector p given by

$$M = \begin{pmatrix} 1 & 0 & -1 & 1 \\ 0 & 1 & -1 & -2 \end{pmatrix}, \quad p = \begin{pmatrix} 12 & 13 & 14 & 23 & 24 & 34 \\ 1 & -1 & -2 & 1 & -1 & 3 \end{pmatrix}.$$

A tropical basis of the tropicalized linear space $\text{trop}(L)$ is given by the polynomials

$$\begin{aligned} f_1 &= p_{12}x_3 - p_{13}x_2 + p_{23}x_1 = x_3 + x_2 + x_1 = 0 \\ f_2 &= p_{13}x_4 - p_{14}x_3 + p_{34}x_1 = -x_4 + 2x_3 + 3x_1 = 0 \\ f_3 &= p_{12}x_4 - p_{14}x_2 + p_{24}x_1 = x_4 + 2x_2 - x_1 = 0 \\ f_4 &= p_{23}x_4 - p_{24}x_3 + p_{34}x_2 = x_4 + x_3 + 3x_2 = 0 \end{aligned}$$

[MS15, Lemma 4.3.16], and $\text{trop}^{+c}(L) \subseteq \bigcap_{i=1}^4 \text{trop}^{+c}(\mathcal{V}(f_i))$. Note that $\text{trop}^{+c}(\mathcal{V}(f_1)) = \emptyset$, so $\text{trop}^{+c}(L) = \emptyset$ and $\{f_1\}$ is a positive-tropical generating set. Let $s = (-1, 1, 1, 1)$. Then $\text{trop}^s(L) \subseteq \bigcap_{i=1}^4 \text{trop}^s(\mathcal{V}(f_i))$. Since f_3^s has only positive coefficients, it follows that $\text{trop}^s(\mathcal{V}(f_3)) = \emptyset$, and so $\text{trop}^s(L) = \emptyset$. However, $\text{trop}^s(\mathcal{V}(f_1))$ is non-empty, so $\{f_1\}$ is not a signed-tropical generating set with respect to s . \diamond

Remark 2.1.16. As mentioned in Remark 2.1.11, a real tropical basis [Tab15] cuts out a signed version of the tropicalization of the real part of the variety. By definition, a real tropical basis is a set of really signed-tropical generators with respect to every sign pattern $s \in \{-1, 1\}^d$ simultaneously. We note however, that the converse is not true. For example, there are hypersurfaces for which there exists no real tropical basis [Tab15, Example 3.15]. On the other hand, by Proposition 2.1.14 the defining polynomial of a hypersurface is always a really signed-tropical generator for every orthant.

2.1.4 Determinantal Varieties

We set the stage for the following sections by introducing the determinantal varieties we will consider. Let $I_r \subseteq \mathcal{C}[x_{ij} \mid (i, j) \in [d] \times [n]]$ be the ideal generated by all $(r+1) \times$

2.1 Positivity in Tropical Geometry

$(r+1)$ -minors of a symbolic $(d \times n)$ -matrix. The determinantal variety $\mathcal{V}(I_r) \subseteq \mathcal{C}^{d \times n}$ consists of all $(d \times n)$ -matrices of rank at most r . As in the case of the Grassmannian [SW05], also for the tropicalization of determinantal varieties the positive part and the really positive part coincide.

PROPOSITION 2.1.17. Let $A \in \mathcal{C}^{d \times n}$ be a matrix such that the leading coefficient of every entry $A_{ij} \in \mathcal{C}$ is real. Then there exists a matrix $B \in \mathcal{R}^{d \times n}$ of real Puiseux series that has the same rank as A and the Puiseux series in every entry has the same leading term as in A , meaning that $\text{lt}(A_{ij}) = \text{lt}(B_{ij})$ holds for all $(i, j) \in [d] \times [n]$.

Proof. Without loss of generality, we assume $d \leq n$. We first show the claim for a matrix of full rank d . First set $B_{ij} = \text{lt}(A_{ij})$. If the rank of the resulting matrix B is less than d , then we can add terms of higher degree with generic real coefficients to the entries of B to obtain a matrix of full rank such that $\text{lt}(B_{ij}) = \text{lt}(A_{ij})$ for all $(i, j) \in [d] \times [n]$ as claimed.

Let now $\text{rk } A = r < d$. We can assume that the first r rows of A are linearly independent and write the remaining rows A_i for $r+1 \leq i \leq d$ as linear combinations of the first r , say

$$A_i = \sum_{k=1}^r c_k^i A_k$$

with $c_k^i \in \mathcal{C}$. We write $a_{kj}t^{\alpha_{kj}}$ for the leading term of A_{kj} (for $(k, j) \in [r] \times [n]$) and $b_k^i t^{\beta_k^i}$ for the leading term of c_k^i so that $a_{kj} \in \mathbb{R}$ and $b_k^i \in \mathbb{C}$. If the entry A_{ij} for $i \geq r+1$ is non-zero, then its leading coefficient is therefore of the form $\sum_{k \in S} a_{kj} b_k^i$ for some subset $S \subseteq [r]$. We thus know that $\sum_{k \in S} a_{kj} b_k^i \in \mathbb{R}$. Note that since $a_{kj} \in \mathbb{R}$ we have

$$\sum_{k \in S} a_{kj} b_k^i = \frac{1}{2} \left(\sum_{k \in S} a_{kj} b_k^i + \sum_{k \in S} \overline{a_{kj}} \overline{b_k^i} \right) = \frac{1}{2} \left(\sum_{k \in S} a_{kj} b_k^i + \sum_{k \in S} a_{kj} \overline{b_k^i} \right).$$

To get the matrix B as desired, we apply the first part of the proof to the first r rows of A so that we get rows B_1, \dots, B_r where each entry is a real Puiseux series. To fill in the last rows, we replace c_k^i by $(c_k^i + \overline{c_k^i})/2 \in \mathcal{R}$, where \bar{c} for a Puiseux series $c \in \mathcal{C}$ is defined as the series whose coefficients are the complex conjugates of the coefficients of c . Setting

$$B_i = \sum_{k=1}^r \frac{1}{2} (c_k^i + \overline{c_k^i}) A_k = \frac{1}{2} \left(\sum_{k=1}^r c_k^i A_k + \sum_{k=1}^r \overline{c_k^i} A_k \right)$$

for $i \geq r+1$ gives the leading term of B_{ij} as

$$\frac{1}{2} \left(\sum_{k \in S} a_{ik} b_k^i + \sum_{k \in S} a_{ik} \overline{b_k^i} \right) = \sum_{k \in S} a_{ik} b_k^i \in \mathbb{R}.$$

□

	$d = 3$	$d = 4$	$d = 5$	$d = 6$	$d = 7$
$r = 2$	YES Thm. 2.1.8 and 2.4.3	YES Thm. 2.4.3	YES Thm. 2.4.3	YES Thm. 2.4.3	YES Thm. 2.4.3
$r = 3$		YES Thm. 2.1.8	?	?	?
$r = 4$			YES Thm. 2.1.8	?	?
$r = 5$				YES Thm. 2.1.8	?
$r = 6$					YES Thm. 2.1.8

Table 2.1: When do the $(r+1) \times (r+1)$ -minors form a set of positive-tropical generators, i.e. when is $(T_{d,n}^r)^+ = (P_{d,n}^r)^+$ for $d \leq n$? A cell is colored in gray if the set of minors forms a tropical basis according to Theorem 2.1.19.

COROLLARY 2.1.18. The positive and the really positive part of the tropicalization of the variety $\mathcal{V}(I_r) \subseteq \mathcal{C}^{d \times n}$ of $(d \times n)$ -matrices of rank at most r coincide, i.e.

$$\text{trop}^{+c}(\mathcal{V}(I_r)) = \text{trop}^{+\mathcal{R}}(\mathcal{V}(I_r)).$$

In particular, every set of positive-tropical generators for the ideal I_r of $(r+1) \times (r+1)$ -minors is a set of really positive-tropical generators. \square

We denote by $T_{d,n}^r$ the tropicalization of the determinantal variety of $(d \times n)$ -matrices of rank at most r . Since the minors of a matrix are polynomials with constant coefficients, the tropical determinantal variety $T_{d,n}^r$ is a polyhedral fan (cf. Section 1.6), and its positive part is a closed subfan.

By Corollary 2.1.18 the positive part is independent of the choice between \mathcal{C} and \mathcal{R} , hence we denote it by $\text{trop}^+(\mathcal{V}(I_r)) = (T_{d,n}^r)^+$. While the ideal I_r is generated by the $(r+1) \times (r+1)$ -minors, this does not necessarily carry over to the tropical variety $T_{d,n}^r$. In a sequence of works it has been characterized when they actually form a tropical basis.

THEOREM 2.1.19 ([DSS05; CJR11; Shi12]). The $((r+1) \times (r+1))$ -minors of a $(d \times n)$ -matrix of variables form a tropical basis of the ideal I_r they generate if and only if $r \leq 2$, or $r = \min(d-1, n-1)$, or else $r = 3$ and $\min(d, n) \leq 6$.

2.1 Positivity in Tropical Geometry

It is thus worthwhile to define the *tropical determinantal prevariety*

$$P_{d,n}^r = \bigcap_{\substack{f \text{ is a} \\ ((r+1) \times (r+1))\text{-minor}}} \text{trop}(\mathcal{V}(f)) = \bigcap_{\substack{I \subseteq \binom{[d]}{r+1} \\ J \subseteq \binom{[n]}{r+1}}} \text{trop}(\mathcal{V}(f^{IJ})).$$

and the *positive tropical determinantal prevariety*

$$(P_{d,n}^r)^+ = \bigcap_{\substack{f \text{ is a} \\ ((r+1) \times (r+1))\text{-minor}}} \text{trop}^{+c}(\mathcal{V}(f)) = \bigcap_{\substack{I \subseteq \binom{[d]}{r+1} \\ J \subseteq \binom{[n]}{r+1}}} \text{trop}^{+c}(\mathcal{V}(f^{IJ})), \quad (2.2)$$

where f^{IJ} denotes the polynomial corresponding to the minor given by the rows indexed by I and columns indexed by J . As mentioned above, we have $T_{d,n}^r \subseteq P_{d,n}^r$ and $(T_{d,n}^r)^+ \subseteq (P_{d,n}^r)^+$. We emphasize again, that the notion of positivity for prevarieties is purely combinatorial, and the inclusion of a positive tropical variety and the corresponding positive tropical prevariety may be strict. We can interpret the matrices in the above sets in terms of the different notions of ranks for tropical matrices.

Definition 2.1.20 (Tropical notions of rank). A matrix $A \in \mathbb{R}^{d \times n}$ over the tropical semiring has rank 1 if it is the tropical matrix product of a $(d \times 1)$ -matrix and a $(1 \times n)$ -matrix. Let $A \in \mathbb{R}^{d \times n}$ be a tropical matrix and $M \in \mathbb{R}^{r \times r}$ a square submatrix. The submatrix M is *tropically singular* if the minimum in the evaluation of the tropical determinant

$$\bigoplus_{\sigma \in S_r} \left(\bigodot_{i=1}^r M_{i\sigma(i)} \right) = \min \left(\sum_{i=1}^r M_{i\sigma(i)} \mid \sigma \in S_r \right)$$

is attained at least twice, and non-singular otherwise. The *tropical rank* of A is the largest integer r such that A has a tropically non-singular submatrix. The *Kapranov rank* of A is the smallest integer r such that there exists a matrix $\tilde{A} \in \mathcal{C}^{d \times n}$ of rank r such that $A = \text{val}(\tilde{A})$. The *Barvinok rank* of A is the smallest integer r for which A can be written as the tropical sum of r rank-1 matrices. Equivalently, the Barvinok rank is the smallest integer r such that $A = X \odot Y$ for some matrices $X \in \mathbb{R}^{d \times r}$, $Y \in \mathbb{R}^{r \times d}$ (cf. [Proposition 2.4.1](#)).

It was shown in [\[DSS05\]](#) that

$$\text{tropical rank of } A \leq \text{Kapranov rank of } A \leq \text{Barvinok rank of } A \quad (2.3)$$

and that indeed all of these inequalities can be strict. In the light of these notions of rank, we can view the tropical determinantal variety $T_{d,n}^r$ and prevariety $P_{d,n}^r$ as sets as

$$\begin{aligned} T_{d,n}^r &= \left\{ A \in \mathbb{R}^{d \times n} \mid A \text{ has Kapranov rank } \leq r \right\}, \\ P_{d,n}^r &= \left\{ A \in \mathbb{R}^{d \times n} \mid A \text{ has tropical rank } \leq r \right\}. \end{aligned}$$

Note that the first inequality in (2.3) also implies the inclusion $T_{d,n}^r \subseteq P_{d,n}^r$. We now describe the geometric interpretations of these notions.

Throughout this chapter, we will only consider tropical linear spaces that arise as tropicalizations of classical linear spaces. The following is a well-known fact in tropical geometry. We provide a proof for completeness.

PROPOSITION 2.1.21. Let $A \in T_{d,n}^r$. Then the columns of A are n points in \mathbb{TP}^{d-1} lying on a tropical linear space of dimension at most $r - 1$.

Proof. Let $A \in T_{d,n}^r$. Then A has Kapranov rank $r' \leq r$, and there exists a matrix $\tilde{A} \in \mathcal{C}^{d \times n}$ of rank r' such that $A = \text{val}(\tilde{A})$. Hence, the columns of \tilde{A} are n points on a linear space $H \subseteq \mathcal{C}^d$ of dimension r' . Equivalently, we can view them as n points on a linear space in \mathcal{CP}^{d-1} of dimension $r' - 1$. The tropicalization of this linear subspace yields a linear space of the same dimension in \mathbb{TP}^{d-1} containing the columns of A . \square

2.1.5 The Lineality Space of Tropical Determinantal Varieties

As described above, a tropical determinantal varieties is a polyhedral fan. We now describe the lineality space of this fan, i.e. the common lineality space of all cones in $T_{d,n}^r$. By Proposition 2.1.21 we can consider matrices $A \in T_{d,n}^r$ as point configurations of n points on a common tropical linear space in \mathbb{TP}^{d-1} . We describe how the lineality space of $T_{d,n}^r$ can be interpreted in terms of these point configurations, and that matrices in $T_{d,n}^r$ modulo lineality space correspond to point configurations in \mathbb{TP}^{d-1} modulo translation.

The lineality space of $T_{d,n}^r$ is spanned by the vectors

$$\sum_{i=1}^d E_{ij} \text{ for } j \in [n] \text{ and } \sum_{j=1}^n E_{ij} \text{ for } i \in [d], \quad (2.4)$$

where E_{ij} denotes the standard basis matrix in $\mathbb{R}^{d \times n}$. Let $A \in T_{d,n}^r$ and consider the columns as a point configuration in \mathbb{TP}^{d-1} . Let H be an $(r - 1)$ -dimensional tropical linear space containing the columns of A . We now describe in which sense the combinatorics of the point configuration stays invariant modulo lineality space. We write $\mathbf{1}$ for the vector $(1, 1, \dots, 1)^t \in \mathbb{T}^d$. First, fix $j \in [n]$. Then

$$A' := A + \sum_{i=1}^d E_{ij} = (A_1, \dots, A_j + \mathbf{1}, \dots, A_n)$$

so A' is a matrix where for all columns holds $A'_k = A_k$, if $k \neq j$. However, as a point in \mathbb{TP}^{d-1} we have $A_j \cong A_j + \mathbf{1} = A'$. Therefore, as a point configuration inside \mathbb{TP}^{d-1} , we consider the point configurations given by the matrices A and A' to be the same.

2.2 Determinantal Hypersurfaces

Second, fix $i \in [d]$. Then

$$A'':=A+\sum_{j=1}^n E_{ij}=(A_1+e_i,\dots,A_n+e_i)$$

so A'' is a matrix where for all columns holds $A''_k = A_k + e_i$. Thus, the point configuration given by A'' is a translation by e_i of the point configuration defined by A . The points of A'' lie on the translated tropical linear space $H + e_i$. Hence, the points in $T_{d,n}^r$ modulo lineality space correspond to point configurations in \mathbb{TP}^{d-1} modulo translation.

2.2 DETERMINANTAL HYPERSURFACES

In this section, we seek to understand the positive part of the tropicalization of singular quadratic matrices. By definition of the Kapranov rank, the set $T_{n,n}^{n-1}$ is formed by all tropical $(n \times n)$ -matrices of Kapranov rank at most $n - 1$. Let $A \in \mathbb{T}^{n \times n}$ be such a matrix. We can interpret the columns of A as a point configuration of n labeled points on a tropical hyperplane in the tropical projective torus \mathbb{TP}^{n-1} . In this section, we characterize the *positive point configurations*, those given by matrices A in the positive part $(T_{n,n}^{n-1})^+$ of the tropical variety. We say that a cone $C \in T_{n,n}^{n-1}$ (or a point $A \in T_{n,n}^{n-1}$) is positive if it lies in the positive part.

2.2.1 Edges of the Birkhoff Polytope

We begin by investigating the maximal cones of $(T_{n,n}^{n-1})^+$ in the tropical hypersurface $T_{n,n}^{n-1} = \text{trop}(\mathcal{V}(\det))$, where we abbreviate

$$\det = \sum_{\sigma \in S_n} \left(\text{sgn}(\sigma) \prod_{i=1}^n x_{i\sigma(i)} \right) \in \mathbb{Z}[x_{ij} \mid i, j \in [n]].$$

As described in [Section 1.3.2](#), this entails that $T_{n,n}^{n-1}$ is the codim 1-skeleton of the normal fan of the Newton polytope of the polynomial \det . This Newton polytope is known as the *Birkhoff polytope* B_n (also called *perfect matching polytope* or *assignment polytope*) whose vertices are the $(n \times n)$ -permutation matrices.

For notational convenience we identify a permutation $\sigma \in S_n$ with the permutation matrix that represents it. Two vertices of B_n (corresponding to permutations $\sigma, \pi \in S_n$) are connected by an edge if and only if $\sigma\pi^{-1}$ is a cycle [[BS96](#)]. A maximal cone $C \in T_{n,n}^{n-1}$ is the normal cone of an edge $\text{conv}(\sigma, \pi)$ of B_n for $\sigma, \pi \in S_n$. For a weight vector w in the interior $\text{int}(C)$ of the cone, the initial ideal $\text{in}_w(I)$ of $I = \langle \det \rangle$ is generated by the binomial

$$\text{in}_w(\det) = \text{sgn}(\sigma) \prod_{i=1}^n x_{i\sigma(i)} + \text{sgn}(\pi) \prod_{i=1}^n x_{i\pi(i)}.$$

Applying [Proposition 2.1.2](#) to this polynomial yields a characterization of positive cones of $T_{n,n}^{n-1}$.

PROPOSITION 2.2.1. Let $C \in T_{n,n}^{n-1}$ be a cone which is dual to a face F_C of the Birkhoff polytope B_n . Then C is positive if and only if F_C contains an edge $\text{conv}(\sigma, \pi)$ such that $\text{sgn}(\sigma) \neq \text{sgn}(\pi)$.

Proof. If C is a maximal cone of $T_{n,n}^{n-1}$ then $F_C = \text{conv}(\sigma, \pi)$ is an edge, and [Proposition 2.1.2](#) implies that C is positive if and only if $\text{sgn}(\sigma) \neq \text{sgn}(\pi)$. Let C be a non-maximal cone. If F_C contains an edge $F_{C'} = \text{conv}(\sigma, \pi)$ such that $\text{sgn}(\sigma) \neq \text{sgn}(\pi)$, then the normal cone C' of this edge is positive. Since $C \subseteq C'$ and positivity is a closed property, it follows that C is positive.

Conversely, let C be positive. Then by [Proposition 2.1.2](#) for every $A \in \text{relint}(C)$ the initial form $\text{in}_A(\det)$ has terms of mixed signs. Since every monomial of the initial form corresponds to a vertex of B_n , and the edge graph of F_C is connected, this implies that there is an edge of F_C whose vertices correspond to monomials (i.e. permutations) of different signs. \square

Example 2.2.2 (The positive part of $T_{3,3}^2$). For $n = 3$ the Schlegel diagram of the 4-dimensional Birkhoff polytope B_3 is shown in [Figure 2.1](#). In this case, the graph of B_3 is the complete graph. [Figure 2.3](#) shows a coloring of the edges of B_3 with green edges corresponding to positive maximal cones of $T_{3,3}^2$ and red edges corresponding to non-positive maximal cones. The set of red edges has two connected components inducing a partition of the vertices of B_3 into even permutations and odd permutations, i.e. the alternating group A_3 and its complement $S_3 \setminus A_3$. The green edges form the cut $(A_n, S_n \setminus A_n)$ between these components. \diamond

2.2.2 Extension to All Orthants

In this section, we want to exploit the observation made in [Section 2.1.3](#) in order to understand the signed tropicalizations of the variety $T_{n,n}^{n-1}$ with respect to sign patterns beyond the positive orthant. Hence, we fix a sign matrix $s \in \{-1, 1\}^{n \times n}$. Recall from [Proposition 2.2.1](#) that a maximal cone of $T_{n,n}^{n-1} = \text{trop}(\mathcal{V}(\det))$ is positive if and only if the permutation $\sigma\pi^{-1}$ for the corresponding edge $\text{conv}(\sigma, \pi)$ is an even cycle. Therefore, we can interpret the partition of the maximal cones in positive and non-positive cones as a coloring of the edges of the graph \mathcal{G}_n of the Birkhoff polytope B_n , as in [Example 2.2.2](#). We color the edges dual to positive cones in green ("positive edges"), and the remaining ones in red ("non-positive edges").

The Newton polytopes of \det and \det^s agree. Hence, for each sign pattern s we obtain a 2-coloring of the edges of \mathcal{G}_n , corresponding to the (non-)positivity of the maximal cones of $\text{trop}(\mathcal{V}(\det^s))$. Then, the green edges correspond to maximal cones of $\text{trop}^s(\mathcal{V}(\det))$, i.e. the tropicalization of $(n \times n)$ -matrices of rank $n - 1$ in \mathcal{C}^s . We begin by investigating the 2-coloring for $s = 1$, i.e. the coloring given by $\text{trop}^{+c}(\mathcal{V}(\det))$.

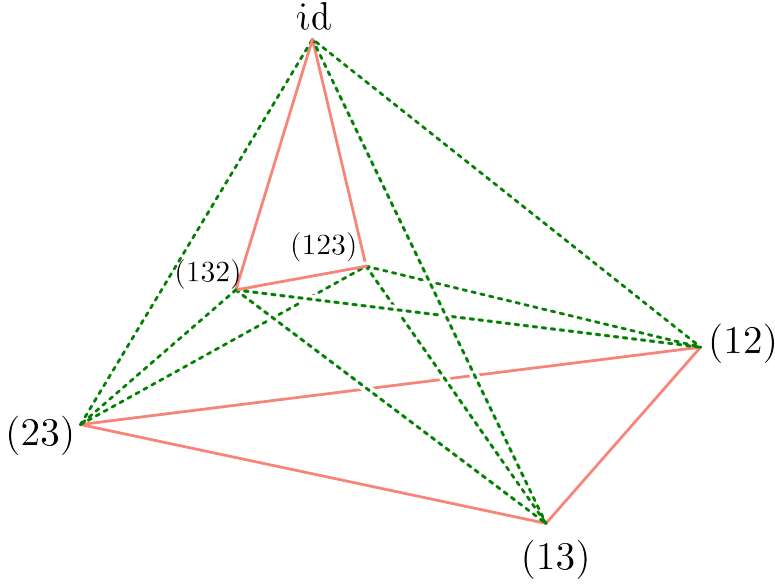


Figure 2.3: The graph of B_3 with edges colored according to the positivity of their dual cones in $T_{3,3}^2$, as explained in Example 2.2.2. The edges of the two triangles (12) , (13) , (23) and id , (123) , (132) are red, all remaining edges are green and dashed.

LEMMA 2.2.3. The 2-coloring of \mathcal{G}_n given by $\text{trop}^{+c}(\mathcal{V}(\det))$ has exactly 2 connected components formed by red edges. The vertices in one component correspond to the elements of the alternating group $A_n \subseteq S_n$, the even permutations of S_n . The vertices in the other component correspond to the odd permutations $S_n \setminus A_n$. Furthermore, the induced subgraphs on A_n and $S_n \setminus A_n$ only have red edges and the green edges are exactly the edges in the cut $(A_n, S_n \setminus A_n)$.

Proof. We identify the vertices in \mathcal{G}_n with the permutations in S_n so that the edge set is given by the pairs $\{(\sigma, \pi) \mid \sigma\pi^{-1} \text{ is a cycle}\}$. Let $\sigma \in A_n$, and $c \in A_n$ be a 3-cycle, and consider $\pi = \sigma c$. Then $\pi \in A_n$, and so π is a neighbor of σ in \mathcal{G}_n . The permutations σ and π have equal sign, so by Proposition 2.2.1 the edge (σ, π) is colored in red. Since the alternating group A_n is generated by 3-cycles, it follows that all permutations $\pi \in A_n$ are contained in one red connected component. All remaining vertices are in $S_n \setminus A_n$. Note that if τ is a transposition, then $S_n \setminus A_n = \tau A_n$, and that all edges inside τA_n are red. Finally, permutations in τA_n have negative sign, so all edges between A_n and τA_n are green. \square

PROPOSITION 2.2.4. Let $s \in \{-1, 1\}^{n \times n}$. The coloring of the graph \mathcal{G}_n induced by $\text{trop}^s(\mathcal{V}(\det))$ has 2 red connected components, which partition the vertices into 2 parts. Equivalently, the green edges are the edges of a cut.

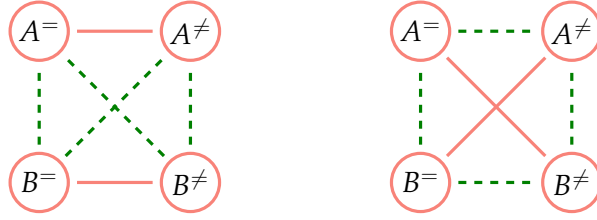


Figure 2.4: Auxiliary graphs for the 2-coloring for sign patterns s (left) and s' (right) after the sign flip of a single entry from the proof of [Proposition 2.2.4](#). Within the sets $A^=, A^\neq, B^=, B^\neq$ all edges are red. The color of the edge between two parts in the auxiliary graph represents the color of all edges in \mathcal{G}_n between the parts. Green edges are dashed.

Proof. By the discussion above, we are interested in the coloring of the graph \mathcal{G}_n given by the positive cones of $\text{trop}^{+c}(\mathcal{V}(\det^s))$. If $s = \mathbb{1}$, then the claim holds by [Lemma 2.2.3](#). Fix $(k, \ell) \in [n] \times [n]$. We show that if the claim holds for a fixed sign pattern $s \in \{-1, 1\}^{n \times n}$, then it also holds for the sign pattern s' , where $s'_{k\ell} = -s_{k\ell}$ and $s_{ij} = s'_{ij}$ for all other entries. That is, we show that the property is preserved under flipping the sign of the (k, ℓ) th entry. Let (A, B) be the partition of vertices of the coloring induced by \det^s . Note that

$$\det^s = \sum_{\sigma \in S_n} \left(\text{sgn}(\sigma) \prod_{i=1}^n s_{i\sigma(i)} x_{i\sigma(i)} \right),$$

so an edge (σ, π) is red if and only if

$$\text{sgn}(\sigma) \prod_{i=1}^n s_{i\sigma(i)} = \text{sgn}(\pi) \prod_{i=1}^n s_{i\pi(i)}.$$

Flipping the sign at (k, ℓ) thus switches the color of all edges $\text{conv}(\sigma, \pi)$ where there exists an $i' \in [n]$ such that $(i', \sigma(i')) = (k, \ell)$ and $(i, \pi(i)) \neq (k, \ell)$ for all $i \in [n]$ (or if there exists an $i'' \in [n]$ such that $(i'', \pi(i'')) = (k, \ell)$ and $(i, \sigma(i)) \neq (k, \ell)$ for all $i \in [n]$). Equivalently, flipping the sign at (k, ℓ) switches the color of all edges where $\sigma(k) = \ell$ and $\pi(k) \neq \ell$ (or $\sigma(k) \neq \ell$ and $\pi(k) = \ell$). Hence, we partition A into $A^= = \{\sigma \in A \mid \sigma(k) = \ell\}, A^\neq = A \setminus A^=$ and similarly $B = B^= \sqcup B^\neq$. We then flip the colors of all edges between $(A^=, A^\neq), (A^=, B^\neq), (B^=, A^\neq), (B^=, B^\neq)$, as shown in [Figure 2.4](#). The resulting graph has red components $A^= \sqcup B^\neq$ and $A^\neq \sqcup B^=$. \square

The above statement implies that the elements in the set $\{\text{trop}^s(f) \mid s \in \{-1, 1\}^{n \times n}\}$ correspond to certain cuts in the graph \mathcal{G}_n .

Question 2.2.5. Is there a group theoretical interpretation of the 2^{n^2} partitions given by the cuts for every sign pattern?

2.2.3 Triangle Criterion for Positivity

In this section, we identify the positive part of the tropical determinantal hypersurface $T_{n,n}^{n-1}$ from a different point of view. We make use of [Proposition 2.2.1](#) to obtain the *triangle criterion*, which will serve as a main tool to characterize positive parts of more general determinantal varieties and prevarieties for low-rank matrices in [Section 2.4](#) and [Section 2.5](#). It turns out that this works well for hypersurfaces of square matrices of size $n = 3, 4$ and corank 1, but there are examples for $n \geq 5$ where this fails.

[Proposition 2.2.1](#) implies that it suffices to consider maximal cones of $T_{n,n}^{n-1}$. The triangle criterion assigns a cartoon to each such maximal cone. We seek to determine the positivity of this cone from the respective cartoon. First, we give the construction of the cartoon and give the triangle criterion for detecting positivity for $n = 3, 4$. Afterwards, we describe its geometric interpretation in terms of tropical point configurations, and show that the triangle criterion does not hold for $n \geq 5$.

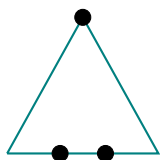
Construction 2.2.6 (Cartoons of maximal cones). Let $C \in T_{n,n}^{n-1}$ be a maximal cone. Then C is dual to an edge $\text{conv}(\sigma, \pi)$ of the Birkhoff polytope B_n , whose vertices correspond to permutations in S_n . Let K_n denote the complete graph on nodes $\{v_1, \dots, v_n\}$. To obtain the *cartoon* of C we decorate the complete graph with n points placed on edges and nodes of K_n as follows: for each $j \in [n]$, decorate the edge $v_{\sigma^{-1}(j)}v_{\pi^{-1}(j)}$ of K_n with a marking if $\sigma^{-1}(j) \neq \pi^{-1}(j)$. If $\sigma^{-1}(j) = \pi^{-1}(j)$, decorate the vertex $v_{\sigma^{-1}(j)}$.

Example 2.2.7 (Cartoons of maximal cones). Consider the cone

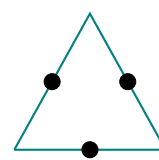
$$C = \text{cone}(E_{13}, E_{23}, E_{31}, E_{32}) \in T_{3,3}^2.$$

It is dual to the edge $\text{conv}(\sigma, \pi)$, where $\sigma = (1, 2)$ is a transposition and $\pi = \text{id}$. The cartoon is a decorated K_3 , with two markings on the edge v_1v_2 and a marking placed at the node v_3 . A cartoon of this type is shown in [Figure 2.5\(a\)](#). \diamond

PROPOSITION 2.2.8 (Triangle criterion for cartoons). Let $n = 3, 4$ and $C \in T_{n,n}^{n-1}$ be a maximal cone. C is positive if and only if its cartoon does not contain a marked triangle. A triangle is marked if every edge has at least one marking in its interior, and the markings of vertices are allowed to be moved to adjacent edges.

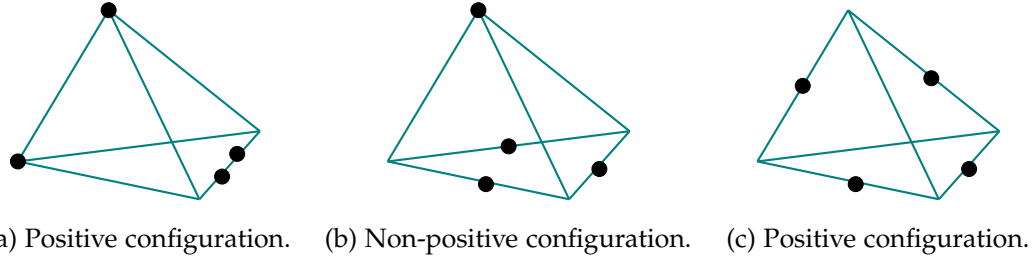


(a) Positive configuration.



(b) Non-positive configuration.

Figure 2.5: The possible cartoons of maximal cones in $T_{3,3}^2$.

Figure 2.6: The possible cartoons of maximal cones in $T_{4,4}^3$.

Proof. The cone C is dual to an edge $\text{conv}(\sigma, \pi)$. Two permutations form an edge of B_n if and only if $\sigma\pi^{-1}$ is a cycle. By Proposition 2.2.1 the cone C is positive if and only if $\sigma\pi^{-1}$ is a cycle of even length. Let $\sigma\pi^{-1}$ be a cycle of length ℓ , so it is of the form (i_1, \dots, i_ℓ) . Now, denote $I = \{i_1, \dots, i_\ell\}$ and $J = [n] \setminus I$. Then Construction 2.2.6 decorates each node $v_{\sigma^{-1}(j)}$ for $j \in J$ and decorates the cycle formed by the edges $(v_{\sigma^{-1}(i_{k+1})}, v_{\pi^{-1}(i_k)})$ (where $i_{\ell+1} = i_1$). Therefore, up to symmetry, it is enough to consider the potential cycle lengths to determine the configurations.

Figure 2.5 shows all possible cartoons for $n = 3$, up to permutation of the nodes of the graph. More precisely, Figure 2.5(a) shows the cartoon in the case that $\sigma\pi^{-1}$ is a transposition and Figure 2.5(b) shows the cartoon for when $\sigma\pi^{-1}$ is a 3-cycle. The possible cartoons for $n = 4$ are shown in Figure 2.6: Figure 2.6(a) shows the cartoon for when $\sigma\pi^{-1}$ is a transposition, Figure 2.6(b) the cartoon of a 3-cycle, and Figure 2.6(c) the cartoon of a 4-cycle. Summarizing, the configurations depicted in Figure 2.5(a), Figure 2.6(a) and Figure 2.6(c) are positive, while Figure 2.5(b) and Figure 2.6(b) are negative. \square

Example 2.2.9 (Triangle criterion fails for $n \geq 5$). Let $C \in T_{5,5}^4$ be the maximal cone that is dual to the edge $\text{conv}(\sigma, \pi)$ of B_5 , where $\sigma = (4, 5)$ is a transposition and $\pi = id$. Then, modulo the lineality space of $T_{5,5}^4$, every matrix $A \in \text{int}(C)$ satisfies the zero pattern

$$\begin{pmatrix} 0 & & & \\ & 0 & & \\ & & 0 & \\ & & & 0 & 0 \\ & & & 0 & 0 \end{pmatrix},$$

i.e. $A_{ij} = 0$ whenever $\sigma(i) = j$ or $\pi(i) = j$, and all other entries of A are nonnegative. The cone C has 18 rays, corresponding to the blank spaces in the zero pattern above. By Proposition 2.2.1 this cone is positive. However, the cartoon of C , as shown in Figure 2.7, contains a triangle in which each node is decorated with a marking. This example can be generalized to any $n \geq 5$. \diamond

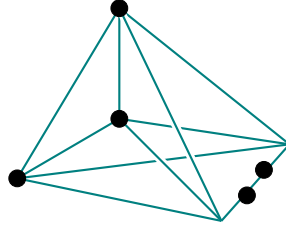


Figure 2.7: The cartoon of the cone in Example 2.2.9.

2.2.4 Geometric Triangle Criterion

As described in Proposition 2.1.21, the columns of $A \in T_{n,n}^{n-1}$ can be viewed as n points in \mathbb{TP}^{n-1} lying on a common tropical linear space of dimension $n - 2$. We now show how the cartoons describe the geometry of these point configurations. But first, we describe two different important kinds of cones. The Birkhoff polytope $B_n \subseteq \mathbb{R}^{n \times n}$ has vertices corresponding to permutations in S_n . Modulo lineality space of the normal fan of B_n , an edge $\text{conv}(\sigma, \pi)$ has normal cone

$$C = \text{cone}(E_{ij} \mid i, j \in [n], \sigma(i) \neq j, \pi(i) \neq j). \quad (2.5)$$

The standard simplex $\Delta_{n-1} \subseteq \mathbb{R}^n$ is the convex hull of the unit vectors e_1, \dots, e_n . Modulo lineality space of the normal fan of Δ_{n-1} , an edge $\text{conv}(e_k, e_l), k, l \in [n]$ has normal cone

$$W_{kl} = \text{cone}(e_i \mid i \in [n], i \neq k, i \neq l).$$

Up to translation, there is a unique tropical hyperplane H of dimension $n - 2$ in \mathbb{TP}^{n-1} . This hyperplane can be viewed as the codimension-1 skeleton of the normal fan of Δ_{n-1} . Equivalently, the tropical hyperplane $H = H_c$ is the set of points

$$H_c = \left\{ x \in \mathbb{TP}^{d-1} \mid \text{the minimum of } x_i + c_i, i \in [n] \text{ is attained at least twice} \right\} \quad (2.6)$$

and the point $-(c_1, \dots, c_d)$ is the *apex* of H . We call a cone W_{kl} of dimension $n - 2$ a *wing* of H .

Example 2.2.10 (A tropical point configuration). Let C be the cone from Example 2.2.7 and consider the matrix

$$A = \begin{pmatrix} 0 & 0 & 2 \\ 0 & 0 & 1 \\ 3 & 1 & 0 \end{pmatrix} \in \text{int}(C).$$

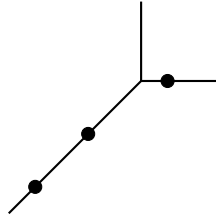


Figure 2.8: The point configuration from Example 2.2.10.

The point configuration in \mathbb{TP}^2 is displayed in Figure 2.8 in the chart where the last coordinate is 0, i.e.

$$A \sim \begin{pmatrix} -3 & -1 & 2 \\ -3 & -1 & 1 \\ 0 & 0 & 0 \end{pmatrix}.$$

The points lie on the common hyperplane with apex $(1, 1, 0)$. The first two columns lie on the wing $W_{1,2} = \text{cone}(e_3)$. The third column lies on the wing $W_{2,3} = \text{cone}(e_1)$. \diamond

The lineality space of $T_{n,n}^{n-1}$ is spanned by the vectors in (2.4) as shown in Section 2.1.5, and the lineality space of more general tropical determinantal varieties is given in Section 2.1.5.

LEMMA 2.2.11. Let $C \in T_{n,n}^{n-1}$ be a cone and $A \in C$. There exists a matrix $A' \in T_{n,n}^{n-1}$ such that $A \sim A'$ modulo lineality space of $T_{n,n}^{n-1}$ and $A'_{ij} \geq 0$ for all $i, j \in [n]$. Furthermore, the columns of A' are points on the tropical hyperplane H_0 with apex at the origin. If C is a maximal cone dual to the edge $\text{conv}(\sigma, \pi)$ of B_n , then $A'_{ij} = 0$ if $j \in \{\sigma(i), \pi(i)\}$.

Proof. Let $A \in C$. Then by (2.5) there is a matrix $A' \in C$ such that $A \sim A'$ modulo lineality space of $T_{n,n}^{n-1}$, and $A'_{ij} \geq 0$ for all $i, j \in [n]$ such that $j \notin \{\sigma(i), \pi(i)\}$ and $A'_{ij} = 0$ otherwise. For each column $j \in [n]$ this means that the minimum value is 0, and (2.6) implies that the columns of A lie on the tropical hyperplane H_0 . \square

Example 2.2.12 (A representation of A modulo lineality space). Consider the matrix from Example 2.2.10. We first subtract the apex $c = (1, 1, 0)$ of the tropical line from every column of the matrix. Then we add $m_j \mathbf{1}$ to every column, where m_j is the minimum entry of the j th column. This yields

$$\begin{pmatrix} 0 & 0 & 2 \\ 0 & 0 & 1 \\ 3 & 1 & 0 \end{pmatrix} \sim \begin{pmatrix} -1 & -1 & 1 \\ -1 & -1 & 0 \\ 3 & 1 & 0 \end{pmatrix} \sim \begin{pmatrix} 0 & 0 & 1 \\ 0 & 0 & 0 \\ 4 & 2 & 0 \end{pmatrix}.$$

\diamond

LEMMA 2.2.13. Let C be a maximal cone of $T_{n,n}^{n-1}$ and $\text{conv}(\sigma, \pi)$ be the dual edge of the Birkhoff polytope B_n . Let $A \in C$ and let H be a tropical hyperplane containing the columns of A . If the edge $v_{\sigma^{-1}(j)}v_{\pi^{-1}(j)}$ is decorated in the cartoon of C , then the j th column A_j of A lies on the wing $W_{\sigma^{-1}(j),\pi^{-1}(j)}$ of H . If the node $v_{\sigma^{-1}(j)}$ is decorated in the cartoon, then the column A_j lies on the wing $W_{k,\sigma^{-1}(j)}$ for some $k \in [n]$.

Proof. By [Lemma 2.2.11](#) we can assume that $A_{ij} = 0$ for all $i, j \in [n]$ such that $j \in \{\sigma(i), \pi(i)\}$, and $A_{ij} \geq 0$ otherwise, and that $H = H_0$ is the tropical hyperplane with apex at the origin. Equivalently, $A_{ij} = 0$ if $i \in \{\sigma^{-1}(j), \pi^{-1}(j)\}$. In particular $A_{\sigma^{-1}(j)j} = A_{\pi^{-1}(j)j} = 0$. The cartoon of C has a decorated edge $v_{\sigma^{-1}(j)}v_{\pi^{-1}(j)}$ if and only if $\sigma^{-1}(j) \neq \pi^{-1}(j)$. If $\sigma^{-1}(j) \neq \pi^{-1}(j)$, then the column A_j is contained in the wing $W_{\sigma^{-1}(j)\pi^{-1}(j)} = \text{cone}(e_i \mid i \neq \sigma^{-1}(j), i \neq \pi^{-1}(j))$. The cartoon has a decorated node $v_{\sigma^{-1}(j)}$ if and only if $\sigma^{-1}(j) = \pi^{-1}(j)$, and the column A_j may lie on any wing not containing the ray in direction $e_{\sigma^{-1}(j)}$. \square

Construction 2.2.14 (Cartoons of matrices). Let $C \in T_{n,n}^{n-1}$ be a maximal cone with dual edge $\text{conv}(\sigma, \pi)$ and $A \in \text{int}(C)$. Let H be a tropical hyperplane containing the columns of A . To obtain the *cartoon of A with respect to H* , we decorate the boundary complex of the $(n-1)$ -dimensional simplex Δ_{n-1} with n points placed on faces of Δ_{n-1} . More precisely, for each $j \in [n]$, decorate the face F of Δ_n with a marking if the column A_j lies in the interior of the cone of H that is dual to the face F .

LEMMA 2.2.15. Let $C \in T_{n,n}^{n-1}$ be a maximal cone. Let $A \in C$ and H be a tropical hyperplane such that each column of A lies in the interior of a wing of H . Then the cartoon of A with respect to H can be obtained from the cartoon of C by sliding markings from nodes of the edge graph \mathcal{G}_n of the Birkhoff polytope B_n to incident edges.

Proof. By assumption, each column lies in the interior of a wing of H , so the cartoon of A with respect to H has only markings on edges of Δ_{n-1} . If the cartoon of C has a marked edge $v_{\sigma^{-1}(j)}v_{\pi^{-1}(j)}$, then [Lemma 2.2.13](#) implies that the column A_j lies on the wing $W_{\sigma^{-1}(j),\pi^{-1}(j)}$ of H , and so the column A_j marks the same edge in the cartoon of A w.r.t. H . If the cartoon of C has a marked node $v_{\sigma^{-1}(j)}$, then [Lemma 2.2.13](#) implies that the column A_j lies on some wing $W_{k,\sigma^{-1}(j)}, k \in [n]$ of H , and so the column A_j marks the edge with vertices v_k and $v_{\sigma^{-1}(j)}$ in the cartoon of A w.r.t H . Thus, the cartoon of A w.r.t. H can be obtained from the cartoon of C by sliding the marking from the node $v_{\sigma^{-1}(j)}$ to the incident edge with vertex v_k . \square

THEOREM 2.2.16 (Geometric triangle criterion). Let $n = 3, 4$ and $C \in T_{n,n}^{n-1}$ be a maximal cone. Let $A \in C$ and H be a tropical hyperplane such that each column of A lies in the interior of a wing of H . Then the cartoon of A with respect to H has

markings only on edges of Δ_{n-1} , and C is positive if and only if the cartoon of A with respect to H does not contain a marked triangle.

Proof. By [Proposition 2.2.8 \(Triangle criterion for cartoons\)](#), C is positive if and only if the cartoon of C does not contain a marked triangle, i.e. a triangle with three distinct markings, where each edge contains at least one marking in its interior, or on an incident vertex. [Lemma 2.2.15](#) implies that the cartoon of A w.r.t H can be obtained from the cartoon of C by sliding the markings from nodes to edges. Hence, the set of marked triangles of the cartoon of A w.r.t H is a subset of the marked triangles of the cartoon of C . It thus remains to show that if the cartoon of C contains a marked triangle, then so does the cartoon of A w.r.t to H . For $n = 3$, there is a unique such configuration ([Figure 2.5\(b\)](#)) and all markings of the cartoon of C are already on edges. For $n = 4$, there is also a unique such configuration ([Figure 2.6\(b\)](#)), and the markings of the marked triangle are on edges. Hence, this is also a marked triangle in the cartoon of A w.r.t H . \square

Example 2.2.17 (Geometric triangle criterion fails for $n \geq 5$). Consider the (positive) cone from [Example 2.2.9](#). The cartoon of cone C , which is depicted in [Figure 2.7](#), has a marked triangle. However, sliding the markings from nodes to edges yields the cartoon in [Figure 2.9](#), which does not have a marked triangle. This example can be generalized to any $n \geq 5$. \diamond

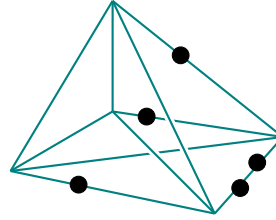


Figure 2.9: The cartoon from [Example 2.2.17](#).

2.3 DETERMINANTAL PREVARIETIES AND BIPARTITE GRAPHS

Let \det be the polynomial representing the determinant of a $(n \times n)$ -matrix. Recall from [Section 2.2.1](#) that $T_{n,n}^{n-1} = \text{trop}(\mathcal{V}(\det))$ is the codimension-1 skeleton of the normal fan of the Birkhoff polytope B_n . In [[Paf15](#)] the faces of B_n are identified with *face graphs*, which are unions of perfect matchings on the bipartite graph on vertices $[n] \sqcup [n]$.

Construction 2.3.1 (Face graphs [[Paf15](#)]). Let $C \in \text{trop}(\mathcal{V}(\det)) = T_{n,n}^{n-1}$ be a cone in the tropical hypersurface, and let $\Lambda \subseteq S_n$ such that $\text{conv}(\Lambda)$ is the face of B_n dual to C . We associate the bipartite graph $\Gamma(C)$ on vertices $V(\Gamma(C)) = R \sqcup G$, $R = \{r_1, \dots, r_n\}$, $G = \{g_1, \dots, g_n\}$ and edges

$$E(\Gamma(C)) = \{r_i g_j \mid \sigma(i) = j \text{ for some } \sigma \in \Lambda\}.$$

2.3 Determinantal Prevarieties and Bipartite Graphs

This extends to a labeling of the entire normal fan of B_n , where the label of the normal cone of a vertex σ is a perfect matching with edges $(r_i, g_{\sigma(i)}), i \in [n]$. The label of a cone dual to a face F is the union of all labels of normal cones of vertices contained in F . Thus, such a label is a union of perfect matchings.

PROPOSITION 2.3.2 (Triangle criterion for bipartite graphs). Let $C \in T_{n,n}^{n-1}$ be a maximal cone. Then $\Gamma(C)$ consists of a cycle of length $2l$, and a perfect matching of the remaining $2(n-l)$ vertices. C positive if and only if l is even.

Proof. Let C be a maximal cone and $\text{conv}(\sigma, \pi)$ be the edge of B_n dual to C . The bipartite graph $\Gamma(C)$ is a union of 2 perfect matchings, corresponding to σ and π . Since these permutations form an edge on B_n , we have that $\sigma\pi^{-1}$ is a cycle of length l , i.e. there are elements $i_1, \dots, i_l \in [n]$ such that $\sigma\pi^{-1}(i_k) = i_{k+1}$ (and $i_{l+1} = i_1$). Equivalently, $\sigma(i_k) = \pi(i_{k+1})$ and $\sigma(i_{k-1}) = \pi(i_k)$. For all other elements $i' \in [n]$ holds $\sigma(i') = \pi(i')$. Thus, $\Gamma(C)$ consists of isolated edges $(r_{i'}, g_{\sigma(i')})$ (forming a perfect matching) and a cycle $(r_{i_1}, g_{\sigma(i_1)}), (g_{\pi(i_2)}, r_{i_2}), (r_{i_2}, g_{\sigma(i_2)}), \dots, (g_{\pi(i_l)}, r_{i_l}), (r_{i_l}, g_{\sigma(i_l)}), (g_{\pi(i_{l+1})}, r_{i_1})$. Therefore, $\Gamma(C)$ consists of a cycle of length $2l$ and isolated edges. By [Proposition 2.2.1](#), the cone C is positive if and only if $\text{sgn}(\sigma\pi^{-1}) = -1$, and equivalently the length l of the cycle $\sigma\pi^{-1}$ is even. \square

We extend the idea of face graphs as labels of cones of $T_{r+1,r+1}^r = P_{r+1,r+1}^r$ by embedding these face graphs, for each I and J , in a bipartite graph $\Gamma(C)$ on vertices $[d] \sqcup [n]$. This yields a label $\Gamma(C)$ of cones in the tropical determinantal prevariety $P_{d,n}^r$.

Definition 2.3.3. Let $I = \{i_1, \dots, i_{r+1}\} \in \binom{[d]}{r+1}$, $J = \{j_1, \dots, j_{r+1}\} \in \binom{[n]}{r+1}$ where $i_k < i_{k+1}, j_k < j_{k+1}$, and let $\sigma \in S_{r+1}$ be a permutation $\sigma : [r+1] \rightarrow [r+1]$. In the following, sets I and J are always of this form. We define the *embedded permutation* to be the map

$$\begin{aligned} \sigma^{IJ} : I &\longrightarrow J \\ i_k &\longmapsto j_{\sigma(k)}. \end{aligned}$$

The *embedded Birkhoff polytope* $B_{r+1}^{IJ} \subseteq \mathbb{R}^{d \times n}$ is the convex hull of the permutation matrices of the embedded permutations $\sigma^{IJ}, \sigma \in S_{r+1}$, where in this embedding, for each $(i,j) \notin I \times J$ we set the ij th entry of each matrix in B_{r+1}^{IJ} to zero.

Recall from [Section 2.1.4](#) that $T_{d,n}^r \subseteq P_{d,n}^r = \bigcap_{f \in I_r} \text{trop}(\mathcal{V}(f))$, where $f \in I_r$ ranges over all $(r+1) \times (r+1)$ -minors of a $(d \times n)$ -matrix. More precisely, the ideal I_r is generated by polynomials

$$f^{IJ} = \sum_{\sigma \in S_{r+1}} \text{sgn}(\sigma) \prod_{k=1}^{r+1} x_{i_k j_{\sigma(k)}} = \sum_{\sigma \in S_{r+1}} \text{sgn}(\sigma) \prod_{k=1}^{r+1} x_{i_k \sigma^{IJ}(i_k)}.$$

Thus, a cone $C^{IJ} \in \text{trop}(\mathcal{V}(f^{IJ}))$ can be seen as cone in the normal fan of B_{r+1}^{IJ} .

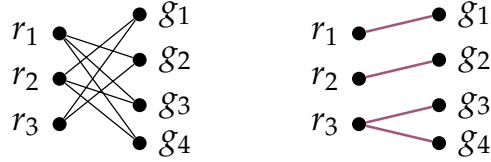


Figure 2.10: The label $\Gamma(C)$ of the cone in Example 2.3.6 (left) and the bipartite complement $\Gamma(C)^c$ (right).

Construction 2.3.4 (Labels of cones in $P_{d,n}^r$). Let $C \in P_{d,n}^r$ be a cone in the tropical determinantal prevariety. Then for each $I \subseteq [d], J \subseteq [n]$ of size $|I| = |J| = r + 1$ there exists a unique inclusion-minimal cone $C^{IJ} \in \text{trop}(\mathcal{V}(f^{IJ}))$ such that $C = \bigcap_{I,J} C^{IJ}$. Let $\Lambda(I, J) \subseteq \{\sigma^{IJ} \mid \sigma \in S_{r+1}\}$ such that $\text{conv}(\Lambda(I, J))$ is the face of B_{r+1}^{IJ} dual to C^{IJ} . Let $R = \{r_1, \dots, r_d\}$ and $G = \{g_1, \dots, g_n\}$. R corresponds to row indices of matrices in $P_{d,n}^r$, and G corresponds to column indices. To C we associate the bipartite graph $\Gamma(C)$ on vertices $V(\Gamma(C)) = R \sqcup G$ and edges

$$E(\Gamma(C)) = \bigcup_{I,J} \left\{ r_{i_k} g_{j_l} \mid \sigma^{IJ}(i_k) = j_l \text{ for some } \sigma^{IJ} \in \Lambda(I, J), l, k \in [r+1] \right\}.$$

Definition 2.3.5. Let Γ be a bipartite graph on vertices $V(\Gamma) = R \sqcup G$. The *bipartite complement* Γ^c is the bipartite graph on vertices $V(\Gamma) = V(\Gamma^c)$ and edges

$$E(\Gamma^c) = \{r_i g_j \mid r_i \in R, g_j \in G, r_i g_j \notin E(\Gamma)\}.$$

Example 2.3.6 (Label of a cone in $T_{3,4}^2$). Let $d = 3, n = 4$ and $r = 2$. Consider the cone $C \in P_{3,4}^2 = T_{3,4}^2$ with rays

$$C = \text{cone}(E_{11}, E_{22}, E_{33}, E_{34}).$$

Then $C = \bigcap_{I,J} C^{IJ}$, where $I = [3]$ and for $J_1 = \{1, 2, 3\}, J_2 = \{1, 2, 4\}$ the cone C^{IJ_k} is dual to the edge $\text{conv}(\sigma^{IJ_k}, \pi^{IJ_k})$ of $B_3^{IJ_k}$, where $\sigma = (1, 2, 3)$ and $\pi = (1, 3, 2)$. More precisely,

$$\begin{aligned} \sigma^{IJ_1}(1) &= 2, \quad \sigma^{IJ_1}(2) = 3, \quad \sigma^{IJ_1}(3) = 1, \quad \pi^{IJ_1}(1) = 3, \quad \pi^{IJ_1}(2) = 1, \quad \pi^{IJ_1}(3) = 2, \\ \sigma^{IJ_2}(1) &= 2, \quad \sigma^{IJ_2}(2) = 4, \quad \sigma^{IJ_2}(3) = 1, \quad \pi^{IJ_2}(1) = 4, \quad \pi^{IJ_2}(2) = 1, \quad \pi^{IJ_2}(3) = 2. \end{aligned}$$

For $J_3 = \{1, 3, 4\}, J_4 = \{2, 3, 4\}$ the cone C^{IJ_k} is dual to the edge $\text{conv}(\sigma^{IJ_k}, \pi^{IJ_k})$ with $\sigma = (1, 2, 3)$ and $\pi = (1, 3)$. Hence,

$$\begin{aligned} \sigma^{IJ_3}(1) &= 3, \quad \sigma^{IJ_3}(2) = 4, \quad \sigma^{IJ_3}(3) = 1, \quad \pi^{IJ_3}(1) = 4, \quad \pi^{IJ_3}(2) = 3, \quad \pi^{IJ_3}(3) = 1, \\ \sigma^{IJ_4}(1) &= 3, \quad \sigma^{IJ_4}(2) = 4, \quad \sigma^{IJ_4}(3) = 2, \quad \pi^{IJ_4}(1) = 4, \quad \pi^{IJ_4}(2) = 3, \quad \pi^{IJ_4}(3) = 2, \end{aligned}$$

Thus, the label $\Gamma(C)$ is the bipartite complement of the graph with edges $r_1 g_1, r_2 g_2, r_3 g_3$ and $r_3 g_4$, as shown in Figure 2.10. \diamond

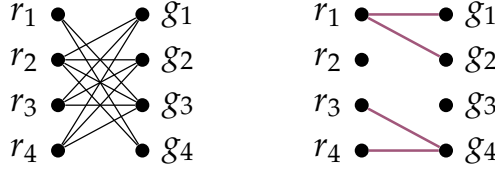


Figure 2.11: The label $\Gamma(C)$ of the two distinct cones in Example 2.3.7 (left) and the bipartite complement $\Gamma(C)^c$ (right).

Example 2.3.7 (Labels are not unique). Consider the two adjacent maximal cones

$$\begin{aligned} C_1 &= \text{cone}(E_{11}, E_{12}, E_{34}, E_{44}, E_{11} + E_{12} + E_{13}) \\ C_2 &= \text{cone}(E_{11}, E_{12}, E_{34}, E_{44}, E_{11} + E_{12} + E_{21} + E_{22}) \end{aligned}$$

of the tropical determinantal variety $T_{4,4}^2$ of rank 2. Both cones have the an identical label $\Gamma(C_1) = \Gamma(C_2)$, which is the bipartite complement of the bipartite graph on 4+4 vertices with the four edges $r_1g_1, r_1g_2, r_3g_4, r_4g_4$, as shown in Figure 2.11. Since $r = 2$, Theorem 2.4.15 will imply that both cones are positive. \diamond

THEOREM 2.3.8. If $C \in P_{d,n}^r$ is a cone, then each induced subgraph on vertices $I \subseteq \binom{[d]}{r+1}, J \subseteq \binom{[n]}{r+1}$ contains a subgraph consisting of a cycle of length $2l$, where $l = l(I, J) \in \mathbb{N}$ and a perfect matching of the remaining $2(r+1-l)$ vertices. If C is positive, then for each I, J the length of the cycle $l = l(I, J)$ is even.

Proof. Let C be a cone. Then there exist unique inclusion-minimal cones $C^{IJ} \in \text{trop}^{+c}(\mathcal{V}(f^{IJ}))$ such that $C = \bigcap_{I,J} C^{IJ}$, and $\Gamma(C)$ is the union of the labels $\Gamma(C^{IJ})$. By Proposition 2.3.2, every subgraph H on vertices $V(H) = I \sqcup J \subseteq R \sqcup G$, $|I| = |J| = r+1$ contains a subgraph consisting of a cycle of length $2l$, $l = l(I, J)$, and a perfect matching of the remaining vertices. If C is positive, then so is C^{IJ} for each I, J . In this case Proposition 2.3.2 implies that $l(I, J)$ is even. \square

We note that the converse of the statement above is not true. In fact, for most cones C that are not maximal (including non-positive cones), the label $\Gamma(C)$ is the complete bipartite graph $K_{n,d}$. We close this section with a property of the label $\Gamma(C)$.

PROPOSITION 2.3.9. Let $C \in P_{d,n}^r$ be a cone and $\Gamma(C)$ the label on vertices $V(\Gamma(C)) = R \sqcup G$. Each vertex $v \in R$ has degree at least $n - r$, and every vertex $g \in G$ has degree at least $d - r$.

Proof. By Theorem 2.3.8, each subgraph of $\Gamma(C)$ of size $(r+1) + (r+1)$ contains a union of perfect matchings. Let $v_1 \in R$ and assume for contradiction that $\deg(v_1) \leq |G| - (r+1) = n - (r+1)$. Then there are nodes $g_1, \dots, g_{r+1} \in G$ that are not adjacent to v_1 . Hence, for any $v_2, \dots, v_{r+1} \in R$, the vertex r_1 is isolated in the induced subgraph H on vertices $\{v_1, \dots, v_{r+1}\} \sqcup \{g_1, \dots, g_{r+1}\}$. However, by Theorem 2.3.8, the graph

H does not contain an isolated vertex, which yields the desired contradiction. An analogous argument implies that $\deg(g) \geq |R| - r = d - r$ for all $g \in G$. \square

We illustrate the difference between the applicability of the triangle criteria for cartoons ([Proposition 2.2.8](#)) and for bipartite graphs ([Proposition 2.3.2](#)). Indeed, for maximal cones of $T_{n,n}^{n-1}$ the description via cartoons and bipartite graphs are equivalent, as the proof of [Proposition 2.3.2](#) suggests. For arbitrary choices of d and n , there is a single bipartite graph describing a cone $C \in P_{d,n}^r$ as given in [Construction 2.3.4](#). We can describe C by a collection of cartoons as follows: for each $I \in \binom{[d]}{r+1}, J \in \binom{[n]}{r+1}$, detect all maximal cones $C^{IJ} \in \text{trop}(\mathcal{V}(f^{IJ}))$ such that $C \subseteq C^{IJ}$ and consider their cartoons. This describes the cone C by a collection of at least $\binom{d}{r+1} \binom{n}{r+1}$ cartoons (C might be contained in multiple maximal cones for fixed I, J). Each of the cartoons can be obtained from the graph $\Gamma(C^{IJ})$ and $\Gamma(C)$ as the union over all these graphs. In other words, a label can be seen as the union of the collection of cartoons. Therefore, the label $\Gamma(C)$ contains strictly less information. Still, [Theorem 2.3.8](#) gives a criterion to detect (combinatorial) non-positivity.

Example 2.3.10 (Detecting non-positivity from $\Gamma(C)$). Let $r = 2, d = 4, n = 3$, and consider the matrix

$$A = \begin{pmatrix} k_1 & 0 & 0 \\ 0 & k_2 & 0 \\ 0 & 0 & 1 + k_3 \\ 0 & 0 & 1 \end{pmatrix} \in T_{4,3}^2, k_1, k_2, k_3 > 0.$$

Let $C \in T_{4,3}^2$ be the maximal cone containing $A \in \text{int}(C)$, and let $J = [3]$. For each $I \in \binom{[4]}{3}$ there is a unique maximal cone C^{IJ} containing C . Their cartoons are displayed in [Figure 2.12](#) (left). The cone C is positive if and only if for each I (and J) there exists a positive cone $C^{IJ} \supseteq C$. C is not positive, which can be seen from the cartoons in [Figure 2.12](#) by the [Triangle criterion for cartoons](#) ([Proposition 2.2.8](#)). The label $\Gamma(C)$ can be seen in [Figure 2.12](#) (right). The induced subgraph H on vertices $\{r_1, r_2, r_3\} \sqcup \{g_1, g_2, g_3\}$ does not contain a cycle of length $2l$, l even. Hence, [Theorem 2.3.8](#) implies

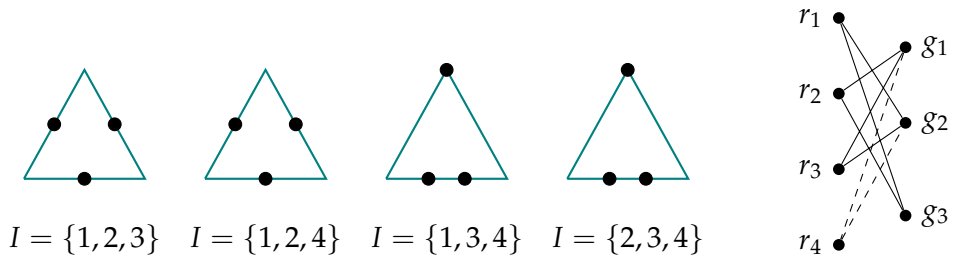


Figure 2.12: The cartoons of the maximal cones C^{IJ} in [Example 2.3.10](#) (left) and the label $\Gamma(C)$ (right). The edges outside the subgraph H are dashed.

that C is not positive, and there can be no positive cone with such a label. For $r = 2$, we present a full characterization of labels of maximal cones in terms of positivity in [Theorem 2.4.15](#). \diamond

2.4 RANK 2

In this section, we consider the tropicalization of the matrices of rank at most 2, that means the tropical determinantal variety $T_{d,n}^2$ of tropical matrices of (Kapranov) rank at most 2. It was shown in [\[DSS05\]](#) that the notions of tropical rank and Kapranov rank agree for rank 2.

We first give a characterization of the positive part of $T_{d,n}^2$ in terms of the Barvinok rank. In [Section 2.4.2](#), we consider a triangulation of the determinantal variety by the space of bicolored phylogenetic trees, and translate the characterization in terms of the Barvinok rank to its equivalent version in terms of bicolored phylogenetic trees. Using this language of phylogenetic trees, in [Section 2.4.3](#) we are able to give a full characterization of the positive cones of the tropical determinantal varieties in term of their bipartite labels (as defined in [Construction 2.3.4](#)). We note that this characterization is not equivalent to the previous ones, as the cones are not in bijection with their labels, but multiple cones can have the same label (cf. [Example 2.3.7](#)). Finally, in [Section 2.4.5](#) we explain the connection of bicolored phylogenetic trees with the tropical Grassmannian, which is the space of uncolored phylogenetic trees. Here, we give an explicit description of a projection map, which induces a bijection of the space of bicolored phylogenetic trees and those uncolored phylogenetic trees which allow a certain admissible coloring.

2.4.1 Positivity and Barvinok Rank

Ardila showed in [\[Ardo4\]](#) that a tropical matrix of tropical rank 2 is positive if and only if it has Barvinok rank 2. The proof reveals a crucial connection between the positivity of tropical matrices and the nonnegative rank of matrices with ordinary rank 2. We begin by reviewing different characterizations of the Barvinok rank.

PROPOSITION 2.4.1 ([\[DSS05, Proposition 2.1\]](#)). For a tropical matrix $A \in \mathbb{R}^{d \times n}$, the following are equivalent:

- (i) A has Barvinok rank at most r .
- (ii) The columns of A lie in the tropical convex hull of r points in \mathbb{TP}^{d-1} .
- (iii) There are matrices $X \in \mathbb{R}^{d \times r}, Y \in \mathbb{R}^{r \times d}$ such that $A = X \odot Y$.

Here, $X \odot Y$ denotes the tropical matrix multiplication, i.e. $(X \odot Y)_{ij} = \bigoplus_{k=1}^r X_{ik} \odot Y_{kj} = \min(X_{ik} + Y_{kj} \mid k \in [r])$. Tropical convex hulls are discussed in more detail in [Section 1.3.1](#). The equivalence of (i) and (iii) leads to the argument in [\[Ardo4\]](#), which we give for completeness.

THEOREM 2.4.2 ([Ardo4]). The positive part $(T_{d,n}^2)^+$ of the tropical determinantal variety $T_{d,n}^2$ coincides with the set of matrices of Barvinok rank 2.

Proof. Consider the map $f: \mathbb{R}^{d \times 2} \times \mathbb{R}^{2 \times n} \rightarrow \mathbb{R}^{d \times n}$, $(X, Y) \mapsto XY$. The image of this map is the determinantal variety $\mathcal{V}(I_2) \subseteq \mathbb{R}^{d \times n}$, i.e. the set of matrices of rank at most 2. We can write f as a polynomial map

$$f = (f_{11}, \dots, f_{dn}): \mathbb{R}^{2d+2n} \rightarrow \mathbb{R}^{dn} \quad \text{where} \quad f_{ij}(X, Y) = X_{i1}Y_{1j} + X_{i2}Y_{2j} .$$

Each f_{ij} has only positive coefficients, i.e. f is *positive*. By replacing ‘+’ with ‘min’ and replacing ‘.’ with ‘+’ in the definition of f , we obtain its tropicalization

$$\text{trop}(f) = g: \mathbb{R}^{d \times 2} \times \mathbb{R}^{2 \times n} \rightarrow \mathbb{R}^{d \times n}, \quad (X, Y) \mapsto X \odot Y .$$

Since f is positive, it follows that $\text{Im}(g) \subseteq \text{trop}^+(\mathcal{V}(I_2)) = (T_{d,n}^2)^+$ from [PS04, Theorem 2]. Furthermore, if $f(\mathbb{R}_{>0}^{2d+2n}) = \text{Im}(f) \cap \mathbb{R}_{>0}^{dn}$, then $\text{Im}(g) = (T_{d,n}^2)^+$. Indeed, this holds since every positive $(d \times n)$ -matrix of rank 2 can be written as the product of a positive $(d \times 2)$ -matrix and a positive $(2 \times n)$ -matrix [CR93, Theorem 4.1]. Finally, note that $\text{Im}(g)$ is precisely the set of matrices of Barvinok rank 2 by [Proposition 2.4.1](#). \square

Consider the columns of $A \in T_{d,n}^2$ as the coordinates of n points in \mathbb{TP}^{d-1} . [Proposition 2.1.21](#) implies that these are n points lying on a common tropical line L in \mathbb{TP}^{d-1} . A tropical line in \mathbb{TP}^{d-1} is a pure, connected 1-dimensional polyhedral complex not containing any cycles. This complex consists of d unbounded rays in direction of the standard basis $e_1, e_2, \dots, e_{d-1}, e_d \cong -(e_1 + \dots + e_{d-1})$. It has $k \leq d-3$ vertices, which are connected by $k-1$ bounded edges. It was shown in [SS04] that tropical lines are in bijection with phylogenetic trees on d leaves, and the space of tropical lines in \mathbb{TP}^{d-1} is the tropical Grassmannian $\text{trop}(\text{Gr}(2, d))$. We describe the tropical Grassmannian in more detail in [Section 2.4.4](#). On the other hand, since in the case of rank 2 the Kapranov and the tropical rank coincide, the tropical convex hull of the n columns of A is a 1-dimensional polyhedral complex that only consists of bounded line segments. Recall from [Section 1.3.1](#) that this complex has two different kinds of vertices, called tropical vertices (which is a subset of the n columns of A) and pseudovertices. As a set, the tropical convex hull is strictly contained in the tropical line L .

[Proposition 2.4.1](#) and [Theorem 2.4.2](#) together characterize the possible “positive” point configurations of n points on a tropical line: Such a tropical point configuration is positive if and only if its tropical convex hull has (at most) 2 tropical vertices. This means that the columns lie on a tropical line segment, which is a concatenation of classical line segments [DS04, Proposition 3]. Based on this connection with the Barvinok rank, we obtain a stronger result about the representation by (3×3) -minors.

THEOREM 2.4.3. The (3×3) -minors form a set of positive-tropical generators for the positive tropical determinantal variety $(T_{d,n}^2)^+$ of rank 2.

Proof. By [Theorem 2.4.2](#) and [\(2.1\)](#) (in [Section 2.1.1](#)), we have that

$$\left\{ A \in \mathbb{R}^{d \times n} \mid A \text{ has Barvinok rank } \leq 2 \right\} = (T_{d,n}^2)^+ \subseteq \bigcap_{\substack{f \text{ is a} \\ (3 \times 3)\text{-minor}}} \text{trop}^{+c}(\mathcal{V}(f)).$$

It thus remains to show the reverse inclusion. Let $A \in \text{trop}^{+c}(\mathcal{V}(f))$ for every (3×3) -minor f . Let $I = \{i_1, i_2, i_3\} \in [d]$, $J = \{j_1, j_2, j_3\} \subseteq [d]$ and consider the minor

$$f^{IJ}(x_{i_1 j_1}, x_{i_1 j_2}, x_{i_1 j_3}, x_{i_2 j_1}, x_{i_2 j_2}, x_{i_2 j_3}, x_{i_3 j_1}, x_{i_3 j_2}, x_{i_3 j_3}) = \sum_{\sigma \in S_3} \text{sgn}(\sigma) \prod_{k=1}^3 x_{i_k j_{\sigma(k)}}.$$

By assumption, $A \in \text{trop}^{+c}(\mathcal{V}(f^{IJ}))$. In other words, there exists some matrix $\tilde{A}^{IJ} \in \mathcal{V}(f^{IJ}) \cap (\mathcal{C}_+)^{d \times n}$ such that $A = \text{val}(\tilde{A}^{IJ})$ and

$$f^{IJ}(\tilde{A}_{i_1 j_1}^{IJ}, \tilde{A}_{i_1 j_2}^{IJ}, \tilde{A}_{i_1 j_3}^{IJ}, \tilde{A}_{i_2 j_1}^{IJ}, \tilde{A}_{i_2 j_2}^{IJ}, \tilde{A}_{i_2 j_3}^{IJ}, \tilde{A}_{i_3 j_1}^{IJ}, \tilde{A}_{i_3 j_2}^{IJ}, \tilde{A}_{i_3 j_3}^{IJ}) = 0.$$

Note that \tilde{A}^{IJ} might differ for different choices of I, J . Recall that, by assumption, $A \in (P_{d,n}^2)^+ \subseteq P_{d,n}^2 = T_{d,n}^2$ by [\(2.2\)](#) (in [Section 2.1.4](#)) and [Theorem 2.1.19](#), and so A (and each submatrix) has Kapranov rank ≤ 2 . Hence, the columns of A lie on a tropical line L , and the convex hull of its columns is a 1-dimensional polyhedral complex supported by L . We want to show that A has Barvinok rank ≤ 2 , i.e. that the tropical convex hull of the columns of A has at most 2 tropical vertices. Let M be the $(3 \times n)$ -submatrix of A with rows $i_1, i_2, i_3 \in [d]$. We view the columns of M as n points in \mathbb{TP}^2 and consider the tropical convex hull of these points as polyhedral complex of ordinary line segments. First, we show that the tropical convex hull of the n columns of M does not contain a pseudovertex that is incident to more than 2 edges. Assume for contradiction that there is such a pseudovertex p incident to 3 line segments l_1, l_2, l_3 . Then there must be 3 columns j_1, j_2, j_3 of M whose tropical convex hull contains p and the three line segments l_1, l_2, l_3 . Consider the (3×3) -submatrix N with rows $I = \{i_1, i_2, i_3\}$ and columns $J = \{j_1, j_2, j_3\}$. Note that N is the valuation of the submatrix $\tilde{N} \in (\mathcal{C}_+)^{3 \times 3}$ of the matrix \tilde{A}^{IJ} . By assumption, the matrix \tilde{N} is positive and has rank ≤ 2 . Thus, N has Kapranov rank ≤ 2 , i.e. $N \in (T_{3,3}^2)^+$. Therefore, [Theorem 2.2.16 \(Geometric triangle criterion\)](#) implies that the tropical convex hull of columns of N cannot contain a pseudovertex incident to 3 line segments. Hence, M does not contain such a subconfiguration. We have thus shown that A does not contain a $(3 \times n)$ -submatrix where the convex hull of the columns contain a pseudovertex that is incident to (at least) 3 line segments. Note that the tropical convex hull of the columns of a matrix is isomorphic to the tropical convex hull of its rows. We can thus apply the same argument to A^t to obtain that A also does not contain a $(d \times 3)$ -submatrix with this property either.

We have shown that the tropical convex hull of the columns of any $(3 \times n)$ - or $(d \times 3)$ -submatrix of A has at most 2 tropical vertices. We now show the same statement for the entire $(d \times n)$ -matrix A . Assume for contradiction that the convex hull of the n columns in \mathbb{TP}^{d-1} contains a pseudovertex p of that is incident to line segments l_1, l_2, l_3 . Then again there must be 3 columns j_1, j_2, j_3 of A such that their tropical convex hull contains p and l_1, l_2, l_3 . However, these columns form a $(3 \times d)$ -submatrix of A , which yields a contradiction to the argument above. \square

2.4.2 Bicolored Phylogenetic Trees

It was shown in [Devo05; MY09] that $T_{d,n}^2$ is a shellable complex of dimension $d + n - 4$. Furthermore, it admits a triangulation by the space of *bicolored phylogenetic trees* $\mathcal{BPT}_{d,n}$. That is, $\mathcal{BPT}_{d,n}$ is a simplicial fan, whose cones are in correspondence with the combinatorial types of bicolored phylogenetic trees. The identification of matrices in $T_{d,n}^2$ with bicolored trees is as follows.

Construction 2.4.4 (Bicolored phylogenetic trees [MY09]). Let A_1, \dots, A_n be tropically collinear points in \mathbb{TP}^{d-1} and L be a tropical line through these points. The tropical convex hull $\text{tconv}(A_1, \dots, A_n)$ is a connected 1-dimensional polyhedral complex supported on a subset of L . First, for each $j \in [n]$ attach a green leaf with label j at the point A_j . Note that the line L has an unbounded ray in each coordinate direction e_1, \dots, e_d . Shorten such an unbounded ray in direction e_i to obtain a red leaf with label i . This procedure results in a tree on d red and n green leaves. We refer to these color classes as $R = \{r_1, \dots, r_d\}$ (for “red” or “rows of A ”) and $G = \{g_1, \dots, g_n\}$ (for “green”, corresponds to columns of A). An example of this construction is shown in Figure 2.13.

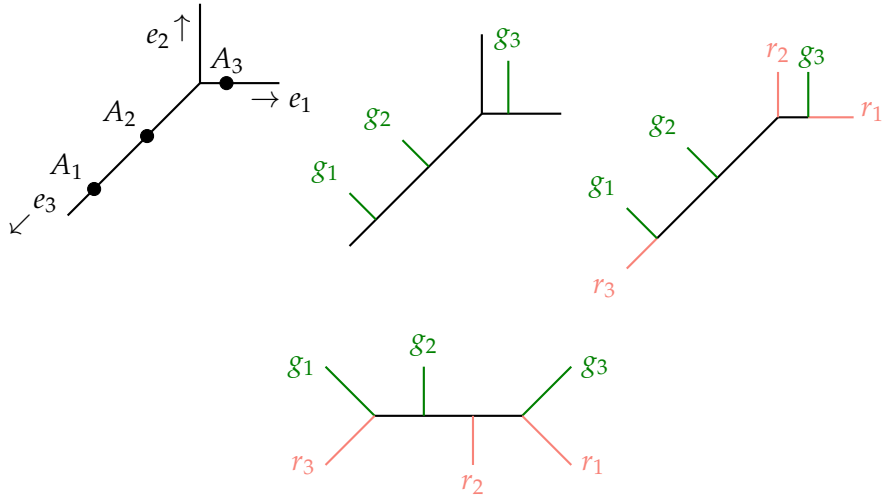


Figure 2.13: The construction of the bicolored phylogenetic tree for the matrix from Example 2.2.10, from left to right.

Definition 2.4.5. An *internal edge* of a bicolored tree is an edge between two vertices that are not leaves. A vertex of a bicolored tree is an *internal vertex* if it is adjacent to at least 2 internal edges. A tree is a *caterpillar tree* if every vertex is incident to at most two internal edges.

We refer to a bicolored phylogenetic tree as *positive* if it can be obtained by applying [Construction 2.4.4](#) to a positive matrix $A \in (T_{d,n}^2)^+$. The geometric interpretation ([Proposition 2.4.1 \(ii\)](#)) of (positive) matrices of Barvinok rank 2 implies the following for bicolored trees.

COROLLARY 2.4.6. A bicolored phylogenetic tree is positive if and only if it is a caterpillar tree.

Proof. Let P be a bicolored phylogenetic tree. Then the tree corresponds to a cone in the triangulation $\mathcal{BPT}_{d,n}$ of $T_{d,n}^2$ in which for every matrix A , [Construction 2.4.4](#) yields P . Note that, by construction, the set of bounded edges of P coincides with the tropical convex hull of the columns of A . By [Theorem 2.4.2](#), A is positive if and only if A has Barvinok rank 2, i.e. the tropical convex hull of the columns of A is the concatenation of ordinary line segments ([Proposition 2.4.1](#)). Equivalently, the tropical convex hull (and the resulting phylogenetic tree) does not contain a vertex that is incident to 3 internal edges or more. \square

We now describe the fan structure of $\mathcal{BPT}_{d,n}$. Understanding the structure of this fan will be crucial for the arguments made in [Sections 2.4.3](#) and [2.4.5](#).

Definition 2.4.7. Let $P \in \mathcal{BPT}_{d,n}$ be a phylogenetic tree. The removal of an internal edge splits the tree into two connected components, inducing a partition of the set of leaves of P . These partitions $(S, ([d] \sqcup [n]) \setminus S)$ are the *bicolored splits* of the tree. A bicolored split is *elementary* if one of the two parts has only 2 elements.

The construction of bicolored phylogenetic trees implies that each of the two parts of a bicolored split contains leaves of both colors.

The lineality space of the space $\mathcal{BPT}_{d,n}$ of bicolored phylogenetic trees coincides with the lineality space of $T_{d,n}^2$ as described in [Section 2.1.5](#). By construction, two collinear point configurations that are equal up translation induce the same bicolored phylogenetic trees. Modulo this lineality space, the fan $\mathcal{BPT}_{d,n}$ is a simplicial fan in which every cone is generated by $d+n-3$ rays. The rays of a cone in $\mathcal{BPT}_{d,n}$ correspond to the bicolored splits of the trees in the cone. More precisely, if $r = \{\lambda A \mid \lambda \geq 0\}$ is a ray of the fan $\mathcal{BPT}_{d,n}$, then for each $\lambda > 0$ [Construction 2.4.4](#) produces the same tree. This tree has a single internal edge, separating the leaves S and $([d] \sqcup [n]) \setminus S$, and both S and $([d] \sqcup [n]) \setminus S$ contain leaves of both color classes.

Two (bicolored) splits $(S_1, ([d] \sqcup [n]) \setminus S_1) = (S_1, S_1^c), (S_2, ([d] \sqcup [n]) \setminus S_2) = (S_2, S_2^c)$ are *compatible* if

$$S_1 \subseteq S_2 \text{ or } S_1 \subseteq S_2^c \text{ or } S_2 \subseteq S_1^c \text{ or } S_1^c \subseteq S_2^c.$$

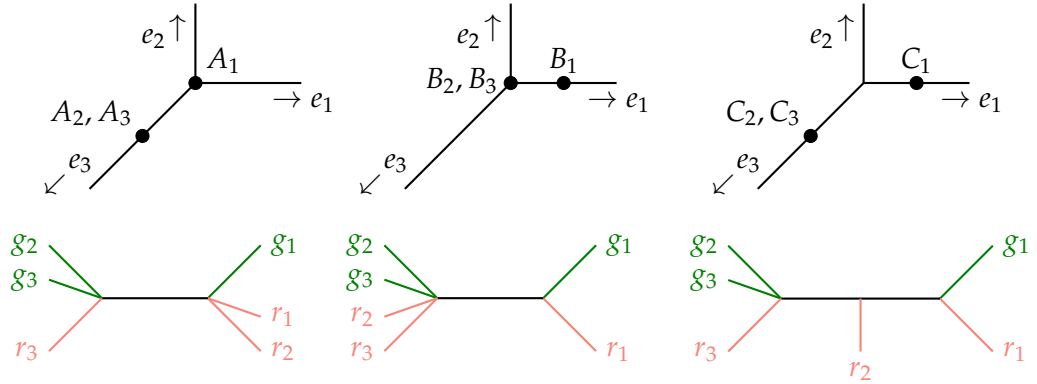


Figure 2.14: The point configurations \$A, B\$ and \$C = A + B\$ from Example 2.4.9 and the respective bicolored phylogenetic trees.

A set of bicolored splits form a cone \$C\$ in \$\mathcal{BPT}_{d,n}\$ if and only if they are pairwise compatible. If a bicolored tree \$P\$ is contained in the relative interior of the cone \$C\$, then the rays of \$C\$ are thus in correspondence with the internal edges of \$P\$.

Definition 2.4.8. A tree is *maximal* if it is contained in the interior of a maximal cone of \$\mathcal{BPT}_{d,n}\$. Equivalently, a tree is maximal if it has \$d+n-3\$ internal edges.

Example 2.4.9 (Compatible bicolored splits). Consider the matrices

$$A = \begin{pmatrix} 0 & 0 & 0 \\ 0 & 0 & 0 \\ 0 & 1 & 1 \end{pmatrix}, \quad B = \begin{pmatrix} 1 & 0 & 0 \\ 0 & 0 & 0 \\ 0 & 0 & 0 \end{pmatrix}$$

Both \$A\$ and \$B\$ span rays in \$\mathcal{BPT}_{3,3}\$, as the corresponding phylogenetic trees are the bicolored splits \$(r_1r_2g_1, r_3g_2g_3)\$ and \$(r_1g_1, r_2r_3g_2g_3)\$ respectively, as shown in Figure 2.14. Note that the bicolored splits are compatible (\$r_1g_1 \subseteq r_1r_2g_1\$), so they span a 2-dimensional cone. The sum \$C = A + B\$ is a point in the interior of this cone, and corresponds to the tree with exactly these two bicolored splits. Hence, the rays \$A, B\$ correspond to the bounded edges of the tree \$A + B\$. \diamond

Remark 2.4.10. The fan structure of the triangulation \$\mathcal{BPT}_{d,n}\$ together with Corollary 2.4.6 implies that every positive cone of \$T_{d,n}^2\$ is contained in a positive maximal cone, as every (non-maximal) caterpillar tree can be obtained by contracting internal edges of a maximal caterpillar tree, and maximal phylogenetic trees correspond to maximal cones in \$\mathcal{BPT}_{d,n}\$.

We present one result regarding the triangulation, that will be useful for characterizing the positive labels of cones of \$T_{d,n}^2\$ in terms of bipartite graphs. This proof uses the *balancing condition* of tropical lines. A first introduction to tropical lines was given in Section 2.4.1, describing a tropical line as a pure, embedded 1-dimensional polyhedral

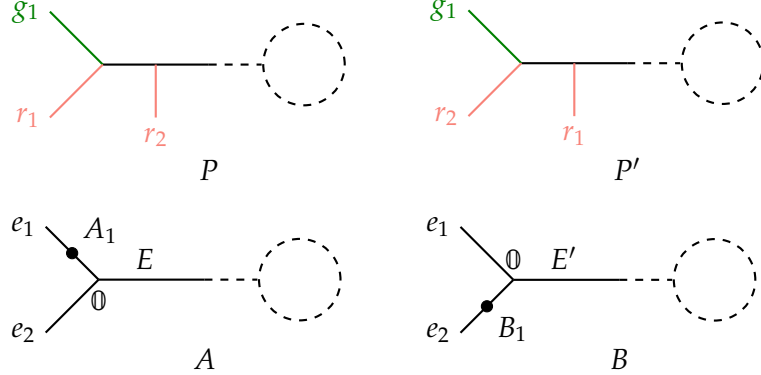


Figure 2.15: The trees P and P' from Lemma 2.4.11 and the corresponding point configurations A and B .

complex. Let v be a vertex of this polyhedral complex. If the tropical line in \mathbb{TP}^{d-1} is non-degenerate (i.e. has $d - 3$ bounded edges), then the balancing condition implies that the slopes of all edges incident to v sum to the zero vector.

LEMMA 2.4.11. Let P be a fixed maximal bicolored phylogenetic tree and let \mathcal{S} be the set of bicolored splits of P , such that \mathcal{S} contains the splits

$$S_{r_1,g_1,r_2} = (\{r_1, g_1, r_2\}, (R \sqcup G) \setminus \{r_1, g_1, r_2\}) \text{ and } S_{r_1,g_1} = (\{r_1, g_1\}, (R \sqcup G) \setminus \{r_1, g_1\}),$$

as depicted in Figure 2.15 on the left. Let $\mathcal{C}_P \in \mathcal{BPT}_{d,n}$ be the maximal cone in the space of bicolored phylogenetic trees, so that all matrices in the interior of \mathcal{C}_P correspond to P , and $C \in T^2_{d,n}$ be the unique maximal cone of the tropical determinantal variety containing \mathcal{C}_P . Then C also contains the maximal cone $\mathcal{C}_{P'} \in \mathcal{BPT}_{d,n}$, where all matrices correspond to trees P' of fixed combinatorial type, and the set of bicolored splits of P' is $\mathcal{S}' = (\mathcal{S} \setminus S_{r_1,g_1}) \cup S_{r_2,g_1}$, where $S_{r_2,g_1} = (\{r_2, g_1\}, (R \sqcup G) \setminus \{r_2, g_1\})$ (Figure 2.15 on the right).

Proof. We reverse Construction 2.4.4 to obtain a point configuration of points $A_1, \dots, A_n \in \mathbb{TP}^{d-1}$ forming a matrix $A \in \mathcal{C}_P$. Let A_1, \dots, A_n be such points and L a tropical line containing them. The line L is a 1-dimensional polyhedral complex consisting of bounded edges and d unbounded rays in directions $e_1, \dots, e_d = -(e_1 + \dots + e_{d-1})$. Since P is maximal the line L is non-degenerate, i.e. has $d - 3$ bounded segments. We now construct explicit matrices A, B , realizing P and P' respectively.

The bicolored split S_{r_1,g_1} of P implies that the point A_1 lies on the ray of L in direction e_1 , and the bicolored split S_{r_1,g_1,r_2} implies that the rays e_1 and e_2 meet in a common vertex v , and that there is a bounded edge E of L separating the rays in directions e_1, e_2 from the rays in directions e_3, \dots, e_d (cf. Figure 2.15). Similarly, if B is a matrix realizing P' , and L' is the line through columns of B , then the bicolored split S_{r_2,g_1} of P' implies that the point B_1 lies on the ray direction e_2 , and the bicolored split S_{r_1,g_1,r_2} implies that

the rays e_1 and e_2 meet in a common vertex v' , and that there is an internal edge E' of L' separating the rays in directions e_1, e_2 from the rays in directions e_3, \dots, e_d . Since all remaining bicolored splits of P and P' are the same, we can assume that all columns $A_k = B_k$ coincide for $k \geq 2$. Therefore, $L = L'$ and the point configurations only differ in the position of the points A_1, B_1 respectively, as depicted in Figure 2.15 (bottom). After translation of the point configurations, we can assume that both for L and L' the vertices v, v' are the origin $\mathbb{0}$. The points A_1 and B_1 can be realized by the first two unit vectors respectively. Since L and L' satisfy the balancing condition, the internal edges E, E' have slope $-e_1 - e_2 = e_3 + \dots + e_d$, and so all remaining points in the two point configurations can be realized as points $M_j = (M_{1j}, \dots, M_{dj})$, where $M_{1j} = M_{2j} = 0$ and $M_{kj} > 0$ for all $3 \leq k \leq d$ and $j = 2, \dots, n$. Therefore, the tree P can be realized as the matrix A , and P' is induced by the matrix B as follows:

$$A = \left(\begin{array}{c|cccc} 1 & 0 & 0 & \dots & 0 \\ 0 & 0 & 0 & \dots & 0 \\ \hline 0 & & & & \\ \vdots & & M & & \\ 0 & & & & \end{array} \right) \quad B = \left(\begin{array}{c|cccc} 0 & 0 & 0 & \dots & 0 \\ 1 & 0 & 0 & \dots & 0 \\ \hline 0 & & & & \\ \vdots & & M & & \\ 0 & & & & \end{array} \right),$$

where M is some $(d-2) \times (n-1)$ -matrix such that $M_{ij} > 0 \quad \forall i \in [d-2], j \in [n-1]$. We need to show that, for a fixed (3×3) -minor f^{IJ} , the initial forms selected by the weights in A and in B , respectively, are the same. So let $i_1 < i_2 < i_3, j_1 < j_2 < j_3$ be the indices of three rows and three columns, respectively. They define the polynomial f^{IJ} corresponding to the (3×3) -minor

$$\begin{aligned} f^{IJ} = & x_{i_1 j_1} x_{i_2 j_2} x_{i_3 j_3} + x_{i_1 j_2} x_{i_2 j_3} x_{i_3 j_1} + x_{i_1 j_3} x_{i_2 j_1} x_{i_3 j_2} \\ & - x_{i_1 j_1} x_{i_2 j_3} x_{i_3 j_2} - x_{i_1 j_3} x_{i_2 j_2} x_{i_3 j_1} - x_{i_1 j_2} x_{i_2 j_1} x_{i_3 j_3} \end{aligned}$$

and (3×3) -submatrices A^{IJ}, B^{IJ} of A, B . With this notation, we need to prove the equality $\text{in}_{A^{IJ}}(f^{IJ}) = \text{in}_{B^{IJ}}(f^{IJ})$, where $\text{in}_{A^{IJ}}(f^{IJ})$ is the polynomial consisting of those terms with minimal A^{IJ} -weight.

If $1 \notin \{j_1, j_2, j_3\}$ or $1, 2 \notin \{i_1, i_2, i_3\}$ them $A^{IJ} = B^{IJ}$ and the claim holds. For $j_1 = 1$ and $i_1 = 1, i_2 = 2$ the submatrices are

$$A^{IJ} = \begin{pmatrix} 1 & 0 & 0 \\ 0 & 0 & 0 \\ 0 & M_{i_3 j_2} & M_{i_3 j_3} \end{pmatrix} \quad \text{and} \quad B^{IJ} = \begin{pmatrix} 0 & 0 & 0 \\ 1 & 0 & 0 \\ 0 & M_{i_3 j_2} & M_{i_3 j_3} \end{pmatrix}.$$

The choice $M_{ij} > 0$ implies that $\text{in}_{A^{IJ}}(f) = \text{in}_{B^{IJ}}(f) = x_{i_1j_2}x_{i_2j_3}x_{i_3j_1} - x_{i_1j_3}x_{i_2j_2}x_{i_3j_1}$, where in each case both terms have weight 0. If $j_1 = 1, i_1 = 1, i_2 \neq 2$ the submatrices are

$$A^{IJ} = \begin{pmatrix} 1 & 0 & 0 \\ 0 & M_{i_2j_2} & M_{i_3j_2} \\ 0 & M_{i_3j_2} & M_{i_3j_3} \end{pmatrix} \quad \text{and} \quad B^{IJ} = \begin{pmatrix} 0 & 0 & 0 \\ 0 & M_{i_3j_2} & M_{i_3j_2} \\ 0 & M_{i_3j_2} & M_{i_3j_3} \end{pmatrix}.$$

The initial form with respect to these matrices can only differ if $M_{i_2j_2} + M_{i_3j_3}$ or $M_{i_3j_2} + M_{i_2j_3}$ are the terms with minimal B^{IJ} -weight. However, e.g. $M_{i_2j_2}$ appears as weight of the term $x_{i_1j_3}x_{i_2j_2}x_{i_3j_1}$, and since $M_{ij} > 0$, the weight $M_{i_2j_2}$ is strictly smaller. Finally, if $j_1 = 1, i_1 = 2$ then the argument is analogous to the above case $j_1 = 1, i_1 = 1, i_2 \neq 2$. \square

The roles of R and G can be exchanged in the above statement. Thus, if $d, n \geq 3$, then every maximal bicolored caterpillar tree has exactly 2 such pairs of bicolored splits. This implies the following result on the number of triangulating cones for positive cones in $T_{d,n}^2$.

COROLLARY 2.4.12. Let $C \in T_{d,n}^2$ be a maximal cone and $P \in C$ a bicolored caterpillar tree. Then the triangulation of C by the space of bicolored phylogenetic trees subdivides C into at least 4 parts.

2.4.3 Positivity and Bipartite Graphs

We now describe the labels of $P_{d,n}^2 = T_{d,n}^2$, which were introduced in [Section 2.3](#). In particular, we show that for $r = 2$, even though different cones might have the same label, the labels detect positivity. In other words, a label fully characterizes when a maximal cone lies in $(P_{d,n}^2)^+$. Recall from [Theorem 2.4.3](#) that $(P_{d,n}^2)^+ = (T_{d,n}^2)^+$, so this criterion also applies to positive cones of the tropical determinantal variety of rank 2. By [Remark 2.4.10](#), it suffices to consider maximal cones.

LEMMA 2.4.13. Let $C \in T_{d,n}^2$ be a maximal cone and $\mathcal{C}_1, \dots, \mathcal{C}_m \in \mathcal{BPT}_{d,n}$ be maximal cones of the space of bicolored phylogenetic trees triangulating C . Let P_k be the combinatorially unique (maximal) bicolored phylogenetic tree corresponding to \mathcal{C}_k . Then

$$E(\Gamma(C)^c) \supseteq \{r_i g_j \mid \{i, j\} \text{ is an elementary bicolored split of } P_k \text{ for some } k \in [m]\}.$$

Proof. The rays of the space of bicolored phylogenetic trees are in bijection with bicolored splits (A, B) , i.e. trees with one internal edge partitioning the set of leaves into two parts A and B , such that both parts contain leaves of both colors (cf. [Section 2.4.2](#)). As a matrix in $\mathbb{R}^{d \times n}$, a ray generator (modulo lineality space) can be given as $\sum_{i,j \in A} E_{ij}, |A| \leq |B|$. If $A = \{i, j\}$ is an elementary bicolored split, then E_{ij} spans a ray of some \mathcal{C}_k , so $\text{cone}(E_{ij})$ is contained in C . Any point except the rays of C are

nontrivial nonnegative combinations of rays of C . Thus, $\text{cone}(E_{ij})$ is also an extremal ray of C . It follows that

$$\begin{aligned} \{r_i g_j \mid E_{ij} \text{ spans a ray of } C\} &\supseteq \{r_i g_j \mid \{i, j\} \text{ is an elementary bicolored split} \\ &\quad \text{of } P_k \text{ for some } k \in [m]\}. \end{aligned}$$

Let $C^{IJ} \in \text{trop}(\mathcal{V}(f^{IJ}))$ be the inclusion-minimal cone containing C . Then $\text{cone}(E_{ij}) \subseteq C^{IJ}$. Since C^{IJ} is a cone in the normal fan of B_3^{IJ} , all rays of C^{IJ} are of the form $\text{cone}(E_{kl})$. Hence, $\text{cone}(E_{ij})$ cannot be written as a nontrivial nonnegative combination of rays of C^{IJ} , and so $\text{cone}(E_{ij})$ is a ray of C^{IJ} . By [Construction 2.3.4](#) and [\(2.5\)](#) (in [Section 2.2.4](#)) , for the cone C^{IJ} holds

$$E(\Gamma(C^{IJ})^c) = \left\{ r_i g_j \mid E_{ij} \text{ spans a ray of } C^{IJ} \right\},$$

and $r_i g_j$ is an edge in $\Gamma(C)^c$ if and only if it is contained in $\Gamma(C^{IJ})^c$ for all I, J such that $i \in I$ and $j \in J$. Thus,

$$E(\Gamma(C)^c) \supseteq \{r_i g_j \mid E_{ij} \text{ spans a ray of } C\}.$$

□

Example 2.4.14 (Incompatible bicolored elementary bicolored splits). Consider the maximal cone C from [Example 2.3.6](#). The edges in $\Gamma(C)^c$ are $r_1 g_1, r_2 g_2, r_3 g_3$ and $r_3 g_4$. Let $A \in C$ and P be the bicolored phylogenetic tree corresponding to A . [Lemma 2.4.13](#) implies that these are all the possible candidates for elementary bicolored splits of bicolored phylogenetic trees in C . Note that the bicolored splits corresponding to the edges $r_3 g_3$ and $r_3 g_4$ are not compatible. Thus, there exists no phylogenetic tree having both as elementary bicolored splits simultaneously. ◇

THEOREM 2.4.15. Let $\Gamma(C)$ be the label of a maximal cone $C \in T_{d,n}^2$. Then C is positive if and only if the bipartite complement of $\Gamma(C)$ consists of 4 edges which form two disjoint paths of length 2 (as shown in [Figure 2.16](#)), and isolated vertices.

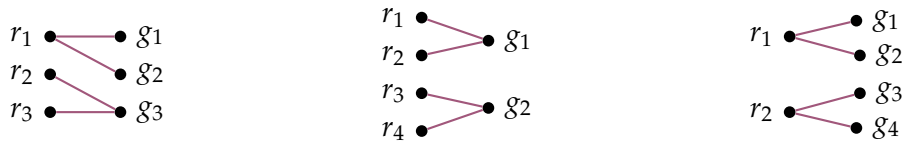


Figure 2.16: The possible complements $\Gamma(C)^c$ of positive labels (up to relabeling of the vertices within the parts, and without isolated vertices).

Proof. Let $\Gamma(C)^c$ be a graph consisting of 4 edges which form two disjoint paths p^1, p^2 . As first case, consider $p^1 = g_1 r_1 g_2$ and $p^2 = r_2 g_3 r_3$. [Lemma 2.4.13](#) implies that the union

of elementary bicolored splits of all bicolored phylogenetic trees in C is contained in

$$S = \{\{r_1, g_1\}, \{r_1, g_2\}, \{r_2, g_3\}, \{r_3, g_3\}\}.$$

Any subset of S of size 3 contains two bicolored splits that are not compatible (cf. [Section 2.4.2](#)). Hence, every maximal phylogenetic tree P in C has at most 2 elementary bicolored splits. At the same time, every maximal phylogenetic tree contains at least 2 elementary bicolored splits, and this number is 2 if and only if P is a caterpillar tree. Thus, each maximal phylogenetic tree in C is a caterpillar tree. The argument is similar for $p^1 = r_1g_1r_2, p^2 = r_3g_2r_4$ and for the case $p^1 = g_1r_1g_2, p^2 = g_3r_2g_4$. In all of these cases, [Corollary 2.4.6](#) implies that C is positive.

Suppose C is a positive cone. By [Theorem 2.3.8](#), every induced subgraph H on $3+3$ vertices contains a subgraph \mathcal{G}_{pos} consisting of a 4-cycle and a disjoint edge. For the remainder of this proof, we consider the bipartite complement H^c . By [Proposition 2.3.9](#), every vertex in H^c has degree at most 2. Note that H^c cannot have a P_4 ([Figure 2.17\(a\)](#)) as a subgraph, since its complement ([Figure 2.17\(b\)](#)) does not contain a graph isomorphic to \mathcal{G}_{pos} . Hence, H^c (and therefore $\Gamma(C)^c$) consists of disjoint paths of length 3 and isolated edges.



Figure 2.17

Similarly, H^c cannot contain a perfect matching (3 isolated edges as shown in [Figure 2.18\(a\)](#)), since the complement ([Figure 2.18\(b\)](#)) does not contain a graph isomorphic to \mathcal{G}_{pos} .



Figure 2.18

Thus, $\Gamma(C)^c$ has at most 4 edges which form two disjoint paths of length 2. However, by [Lemma 2.4.13](#) the edges of $\Gamma(C)^c$ contain the union of all elementary bicolored splits of trees in C . [Corollary 2.4.12](#) implies that there are at least 4 distinct such trees and hence at least 4 distinct elementary bicolored splits. Therefore, the number of edges of $\Gamma(C)^c$ is 4. \square

2.4.4 Bicoloring Trees and the Tropical Grassmannian $\text{trop}(\text{Gr}(2, d+n))$

We now investigate the striking resemblance between $T_{d,n}^2$, (its triangulation given by) the moduli space $\mathcal{BPT}_{d,n}$ of bicolored phylogenetic trees on $d+n$ leaves, and the tropical Grassmannian $\text{trop}(\text{Gr}(2, d+n))$, the moduli space of ordinary phylogenetic trees. It was shown in [SSo4] that a tropical Plücker vector $p \in \text{trop}(\text{Gr}(2, d+n))$ gives a tree metric by

$$-p_{ij} = \text{length of the path between leaves } i \text{ and } j, \quad (2.7)$$

where the length of a path is the sum of the lengths of all edges of the path and the length of the leaves i, j . Thus, each point $p \in \text{trop}(\text{Gr}(2, d+n))$ corresponds to a metric tree on $d+n$ leaves. A point $p \in \mathbb{TP}^{\binom{d+n}{2}}$ is a tropical Plücker vector (i.e. is contained in the tropical Grassmannian) if and only if it satisfies the 3-term Plücker relation (or *4-point condition*)

$$\min(p_{ij} + p_{kl}, p_{il} + p_{jk}, p_{ik} + p_{jl}) \text{ is attained at least twice}$$

for all distinct $i, j, k, l \in [d+n]$. As in the case of $\mathcal{BPT}_{d,n}$, the tropical Grassmannian $\text{trop}(\text{Gr}(2, d+n))$ is a polyhedral fan. We now describe the fan structure of $\text{trop}(\text{Gr}(2, d+n))$, which will play an important role in the proofs in [Section 2.4.5](#). The lineality space of the tropical Grassmannian $\text{trop}(\text{Gr}(2, d+n))$ is spanned by the vectors

$$\sum_{\substack{i \in [d+n] \\ i \neq k}} \tilde{e}_{ik}, \quad k \in [d+n]$$

where the vectors $\tilde{e}_{ij} = \tilde{e}_{ji} \in \mathbb{TP}^{\binom{d+n}{2}-1}$ are the standard basis vectors. We now explain how points in $\text{trop}(\text{Gr}(2, d+n))$ behave modulo this lineality space. Let $p \in \text{trop}(\text{Gr}(2, d+n))$ and fix $k \in [d+n]$. Then

$$p' := (p + \sum_{\substack{i \in [d+n] \\ i \neq k}} \tilde{e}_{ik})_{st} = \begin{cases} p_{st} & \text{if } s, t \neq k \\ p_{st} + 1 & \text{if } s = k \text{ or } t = k. \end{cases} \quad (2.8)$$

Recall that $-p_{ij}$ is the length of the path between leaves i and j of an (uncolored) phylogenetic tree P . That is, the tree P has internal edges of certain lengths, and each leaf i has a length ℓ_i . The vector p' is the tree metric of the tree P' of the same combinatorial type, where all lengths of internal edges coincide with the lengths of internal edges of P . Furthermore, the leaf i of P' has length ℓ'_i , and (2.8) implies that $\ell_i = \ell'_i$ for $i \neq k$ and $\ell_k = \ell'_k - 1$. Therefore, the points in $\text{trop}(\text{Gr}(2, d+n))$ modulo lineality space correspond to metric phylogenetic trees modulo leaf lengths.

Definition 2.4.16. Let P be a phylogenetic tree on $d+n$ leaves. A *split* of P is a partition of the leaves into two parts induced by the deletion of an internal edge of P . A split is *elementary* if one of the two parts has only 2 elements.

The fan trop($\text{Gr}(2, d+n)$) is, modulo its lineality space, a simplicial fan in which every cone is generated by $d+n-3$ rays. The rays of trop($\text{Gr}(2, d+n)$) (modulo lineality space) correspond to splits, i.e. partitions of the leaves $[d+n]$ into two parts $(S, ([d+n]) \setminus S)$. As trees, these are phylogenetic trees with a unique internal edge separating the leaves in S and $([d+n]) \setminus S$. Similarly to their bicolored counterparts in [Section 2.4.2](#), two (uncolored) splits $(S_1, S_1^c), (S_2, S_2^c)$ are *compatible* if

$$S_1 \subseteq S_2 \text{ or } S_1 \subseteq S_2^c \text{ or } S_2 \subseteq S_1^c \text{ or } S_1^c \subseteq S_2.$$

A set of splits forms a cone C in trop($\text{Gr}(2, d+n)$) if and only if they are pairwise compatible. If a tree P is contained in the interior of C , then the rays of C are in correspondence to the bounded edges of P . The maximal cones of the tropical Grassmannian trop($\text{Gr}(2, d+n)$) correspond to phylogenetic trees with $d+n-3$ internal edges.

Example 2.4.17 (Compatible uncolored splits). Let $d+n=5$ and consider the tropical Plücker vectors

$$\begin{aligned} p &= (12 \quad 13 \quad 14 \quad 15 \quad 23 \quad 24 \quad 25 \quad 34 \quad 35 \quad 45 \\ &\quad 0 \quad -1 \quad -1 \quad -1 \quad -1 \quad -1 \quad -1 \quad 0 \quad 0 \quad 0) \\ q &= (0 \quad 0 \quad -1 \quad -1 \quad 0 \quad -1 \quad -1 \quad -1 \quad -1 \quad 0) \end{aligned}$$

Both p and q span rays in trop($\text{Gr}(2, d+n)$), as the corresponding phylogenetic trees are split trees with splits $(12, 345)$ and $(123, 45)$ respectively, and in both cases the unique internal edge has length 1 and all leaves have length 0. Note that the splits are compatible ($12 \subseteq 123$), so they span a 2-dimensional cone. The sum $p+q$ is a point in the interior of the cone, and corresponds to the tree with exactly these two splits. Moreover, the length of each internal edge is 1 and all leaf lengths are 0. \diamond

LEMMA 2.4.18. If $d+n \geq 5$, then a maximal phylogenetic tree on $d+n$ leaves has at most $\frac{d+n}{2}$ elementary splits.

Proof. By definition, an elementary split arises through the removal of an internal edge which separates 2 leaves from all others. Within this proof, we call such an edge an “outer edge”. Let k be the number of outer edges. We double count the number of leaf-edge-incidences for outer edges (i.e. the pairs (leaf, outer edge) such that the leaf is adjacent to the outer edge). A single outer edge is adjacent to precisely 2 leaves. Thus, the number of such pairs is $2k$. On the other hand, a single leaf is adjacent to at most one outer edge. The tree has $d+n$ leaves, and hence the number of pairs is at most $d+n$. Combining both counts yields $2k \leq d+n$ or equivalently $k \leq \frac{d+n}{2}$. \square

Remark 2.4.19. The number of elementary splits is minimized by caterpillar trees (which have precisely 2 elementary splits) and the bound in [Lemma 2.4.18](#) is attained by snowflake trees, which are trees with a unique internal vertex incident to all internal edges. If $d+n=4$, then there exists a unique tree, which has precisely one elementary

split. If the tree admits a (d, n) -coloring (as defined below), then $d = n = 2$, since every split cannot have a monochromatic part. If $d + n \leq 3$, then there exists no elementary split.

Definition 2.4.20. A (d, n) -bicoloring of P is a 2-coloring of the leaves into d red and n green leaves such that no split of P has a monochromatic part.

There is a simple characterization of the existence of a bicoloring in terms of the number of leaves and elementary splits.

PROPOSITION 2.4.21. Let P be a maximal phylogenetic tree on $d + n$ leaves for some fixed $d, n \in \mathbb{N}$ and let k be the number of elementary splits of P . Then P has a (d, n) -bicoloring if and only if $k \leq \min(d, n)$. In this case, the number of possible (d, n) -bicolorings is $2^k \binom{d+n-2k}{d-k}$.

In particular, for any phylogenetic tree P on m leaves, there exist $d, n \in \mathbb{N}$ such that $d + n = m$ and P has a (d, n) -bicoloring.

Proof. Let P be a phylogenetic tree on $d + n$ leaves, and suppose P has a (d, n) -bicoloring. Since every elementary split contains exactly one leaf of each color in the part with 2 elements, it follows directly that there are at least k leaves of each color, and thus $k \leq d$ and $k \leq n$.

Conversely, let k be the number of elementary splits of P and $k \leq \min(d, n)$. For each of these k elementary splits there are exactly 2 possible colorings of the part with two elements. Thus, there are exactly 2^k possible colorings of the sets of size 2 of the elementary splits.

Since P has $d + n$ leaves in total, there are $d + n - 2k$ remaining leaves to color: $d - k$ in one color and $n - k$ in the other color. Note that for any such coloring, the removal of any internal edge will split the colored tree into 2 parts, with leaves of both colors in both parts. Thus, any such coloring is a bicoloring. In total there are hence

$$2^k \binom{d+n-2k}{n-k} = 2^k \binom{d+n-2k}{d-k}$$

(d, n) -bicolorings of a maximal tree with k elementary splits. Finally, by Lemma 2.4.18 a maximal phylogenetic tree on m leaves has at most $k \leq \frac{m}{2}$ elementary splits. Thus, choosing values for $d, n \in \mathbb{N}$ such that $d + n = m$ and $k \leq \min(d, n)$ is always possible. For non-maximal trees this is a lower bound: Let (A, B) be an inclusion-minimal split, i.e. a split such that $|A| \leq |B|$ and there exists no split (C, D) such that $C \subseteq A$ or $D \subseteq A$. Then A contains at least 2 leaves and we can apply the same argument as above to inclusion-minimal splits instead of elementary splits. \square

Example 2.4.22 (Admissible bicolorings). Consider the maximal tree on 5 leaves as shown in Figure 2.19, with elementary splits $(12, 345)$ and $(123, 45)$. We choose the partition $d + n = 2 + 3$, i.e. we want to color 2 leaves in red and 3 leaves in green. In order to obtain a bicoloring, we need to color one of the leaves in $\{1, 2\}$ in red, and

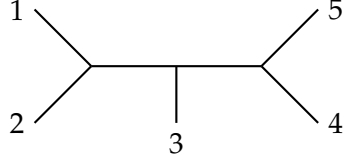


Figure 2.19: The tree from Example 2.4.22

one of the leaves in $\{4, 5\}$ in red, and color the remaining 3 leaves in green. For the partition $1 + 4$, there is no $(1, 4)$ -bicoloring of this tree, as every such 2-coloring has at least one monochromatic elementary split. \diamond

2.4.5 Bicoloring Trees and Back

We now show that the combinatorial idea of “bicoloring a tree” can be made precise also on the algebraic level. In this section we describe a map which, for each (d, n) -bicoloring of leaves $[d + n]$, establishes a bijection between the polyhedral fan $\mathcal{BPT}_{d,n}$ and a suitable subfan of $\text{trop}(\text{Gr}(2, d + n))$. On the level of trees, the map correspond to “coloring a tree” and its inverse to “forgetting the colors”. A similar result was established in [MY09, Lemma 2.10]. Theorem 2.4.23 reveals that this map can be seen as a coordinate projection.

We first describe the subfan of $\text{trop}(\text{Gr}(2, d + n))$, and the map from this subfan to $\mathcal{BPT}_{d,n}$. Fix $d, n \in \mathbb{N}$ and let $R \sqcup G = [d + n]$ be a 2-coloring of the leaves in color classes (R, G) such that $|R| = d, |G| = n$. We say that the coloring (R, G) of the leaves is *admissible* for P if it is a (d, n) -bicoloring (as defined in Definition 2.4.20), i.e. if for every split of P both parts contain leaves of both colors. Let now $\mathcal{UPT}^{(R,G)}$ be the collection of cones in $\text{trop}(\text{Gr}(2, d + n))$ corresponding to (uncolored) phylogenetic trees such that the coloring (R, G) is admissible. Consider the coordinate projection

$$\begin{aligned} \pi^{(R,G)} : \mathcal{UPT}^{(R,G)} &\longrightarrow \mathcal{BPT}_{d,n} \\ (p_{ij})_{ij \in \binom{[d+n]}{2}} &\longmapsto (p_{ij})_{i \in R, j \in G}. \end{aligned} \tag{2.9}$$

We will show that the image of this map is indeed $\mathcal{BPT}_{d,n}$. Let $p \in \mathcal{UPT}^{(R,G)}$, and denote by P the uncolored, metric phylogenetic tree defined by p . For such a fixed uncolored tree P and coloring (R, G) , let $P^{(R,G)}$ denote the coloring of P with respect to (R, G) . Let $\pi^{(R,G)}(p) = A \in \mathcal{BPT}_{d,n}$. We say that $\pi^{(R,G)}$ *preserves the combinatorial type* of P if the bicolored phylogenetic tree defined by A has the same combinatorial type (sometimes also called *tree topology*) as P . A tree is called a *split tree* if it has exactly one internal edge.

THEOREM 2.4.23. The map $\pi^{(R,S)}$ induces a bijection of fans $\mathcal{BPT}_{d,n}$ and $\mathcal{UPT}^{(R,G)}$, which preserves the combinatorial types of trees.

The proof of this theorem is deferred to the end of this section. The structure of the proof is as follows. We first describe a “nice” representation (modulo linearity spaces of $\mathcal{UPT}^{(R,G)}$ and $\mathcal{BPT}_{d,n}$) of p and A (Lemma 2.4.27). We then establish the result for the linearity spaces of the fans (Lemma 2.4.28) and the rays (Proposition 2.4.29). Since both fans are simplicial, the bijection then follows from the linearity of the map.

By Proposition 2.4.21, for each cone $C \in \text{trop}(\text{Gr}(2, d+n))$ there exists at least one choice of $R \sqcup G = [d+n]$ such that the projection of $p \in \text{relint}(C)$ gives the respective bicoloring of the tree corresponding to C . However, this choice of $R \sqcup G$ cannot be made globally, as the following example shows.

Example 2.4.24 (A global bicoloring is impossible). Consider any uncolored phylogenetic tree P with labeled leaves $1, \dots, d+n$ and splits $(\{1, 2\}, [d+n] \setminus \{1, 2\})$ and $(\{1, 2, 3\}, [d+n] \setminus \{1, 2, 3\})$, as shown in Figure 2.20. We can choose a coloring such that $1 \in R$ and $2, 3 \in G$. The cone in $\mathcal{BPT}_{d,n}$ containing P is adjacent to the cone containing P' , where P' is defined by the same set of splits as P , except that the first split $(\{1, 2\}, [d+n] \setminus \{1, 2\})$ is replaced by the split $(\{2, 3\}, [d+n] \setminus \{2, 3\})$. However, the coloring with $1 \in R$ and $2, 3 \in G$ is not an admissible bicoloring of P' , since the split $(\{2, 3\}, [d+n] \setminus \{2, 3\})$ has a part that does not contain leaves of both color classes. A similar argument can be made for the coloring $2 \in R$, $1, 3 \in G$. \diamond

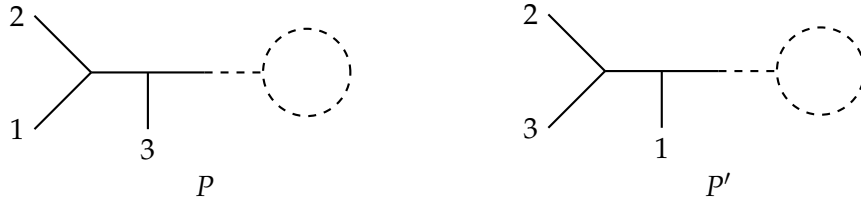


Figure 2.20: The trees from Example 2.4.24.

Remark 2.4.25. In Theorem 2.4.23 we show that $\pi^{(R,G)}$ is a bijective map, and hence an inverse exists. The inverse map $(\pi^{(R,G)})^{-1}$ can be interpreted as “forgetting the colors” of a bicoloored tree. Given a bicoloored phylogenetic tree P , we forget the colors relabeling the leaves with $[d+n]$. The relabeling is not canonical. For example, we can assign to the red leaves the labels in $[d]$ and assign the labels $d+j, j \in [n]$ to the green leaves.

Furthermore note that the map $\pi^{(R,G)}$ does not preserve positivity. The cones in the totally positive Grassmannian correspond to trees with clockwise ordered labels [SW05]. There are examples of caterpillar trees with a labeling of the leaves that is not in clockwise order. On the other hand, there are trees with clockwise ordered labels that are not caterpillar trees.

It was described in [FR15, Example 3.10] that a 1-dimensional tropical linear space is a Stiefel tropical linear space if and only if it is a caterpillar tree. This gives us a characterization of the preimage of the fan of positive bicolored phylogenetic trees under $\pi^{(R,G)}$.

PROPOSITION 2.4.26. Fix (R, G) such that $R \sqcup G = [d+n]$ and let $\Sigma^{(R,G)}$ be the subfan of $\mathcal{UPT}^{(R,G)} \subseteq \text{trop}(\text{Gr}(2, d+n))$ consisting of all Stiefel tropical linear spaces for which (R, G) is an admissible (d, n) -bicoloring. Let $(\mathcal{BPT}_{d,n})^+ = \mathcal{BPT}_{d,n} \cap (T_{d,n}^2)^+$ denote the restriction of $\mathcal{BPT}_{d,n}$ to the positive part. Then $\pi^{(R,G)}(\Sigma^{(R,G)}) = (\mathcal{BPT}_{d,n})^+$ induces a bijection of fans.

Proof. A 1-dimensional tropical linear space is a Stiefel tropical linear space if and only if it is a caterpillar tree [FR15, Example 3.10]. Thus, Corollary 2.4.6 implies that every admissible (d, n) -bicoloring of a tree associated to a Stiefel tropical linear space belongs to the tropicalization of a nonnegative matrix and vice versa. By Theorem 2.4.23, $\pi^{(R,G)}$ is a bijection of fans $\mathcal{UPT}^{(R,G)}$ and $\mathcal{BPT}_{d,n}$ that preserves combinatorial types. Restricting $\pi^{(R,G)}$ therefore induces a bijection of $\Sigma^{(R,G)}$ and $(\mathcal{BPT}_{d,n})^+$. \square

We devote the remainder of this section to the proof of Theorem 2.4.23. To this end, fix a partition (R, G) of $[d+n]$ such that $|R| = d$ and $|G| = n$.

LEMMA 2.4.27. Let P be a (uncolored) phylogenetic split tree with one internal edge of length λ , and $m = d+n$ leaves, where the removal of the internal edge splits the leaves into two parts \mathcal{S}_1 and \mathcal{S}_2 . Let $P^{(R,G)}$ be the bicolored split tree $(R_1 \sqcup G_1, R_2 \sqcup G_2)$, i.e. a tree with one internal edge of positive length, red leaves $R = \{r_1, \dots, r_d\}$, and green leaves $G = \{g_1, \dots, g_n\}$, where the removal of the internal edge splits the leaves into two parts $R_1 \sqcup G_1$ and $R_2 \sqcup G_2$, and additionally $R_1 \sqcup R_2 = R, G_1 \sqcup G_2 = G$.

- 1.) Let $p \in \text{trop}(\text{Gr}(2, d+n))$ be the tropical Plücker vector corresponding to P . Then $p \sim p^\lambda$ modulo the lineality space of $\text{trop}(\text{Gr}(2, d+n))$, where

$$p_{ij}^\lambda = \begin{cases} -\lambda & \text{if } i \in \mathcal{S}_1 \text{ and } j \in \mathcal{S}_2 \\ 0 & \text{if } i, j \in \mathcal{S}_1 \text{ or } i, j \in \mathcal{S}_2. \end{cases}$$

- 2.) Let $A \in \mathcal{BPT}_{d,n}$ be a matrix corresponding to $P^{(R,G)}$. Then there exists a unique $\mu > 0$ such that $A \sim A^\mu$ modulo the lineality space of $\mathcal{BPT}_{d,n}$, where A^μ is the matrix with columns

$$A_j^\mu = \begin{cases} -\mu \sum_{i \in R_2} e_i & \text{if } j \in G_1 \\ -\mu \sum_{i \in R_1} e_i & \text{if } j \in G_2. \end{cases}$$

Proof. We begin by showing (1). Let ℓ_1, \dots, ℓ_m denote the lengths of the leaves $1, \dots, m$ of P . By (2.7) (in [Section 2.4.4](#)), the Plücker vector p corresponding to P is

$$\begin{aligned} p_{ij} &= \begin{cases} -\lambda - \ell_i - \ell_j & \text{if } i \in \mathcal{S}_1 \text{ and } j \in \mathcal{S}_2 \\ -\ell_i - \ell_j & \text{if } i, j \in \mathcal{S}_1 \text{ or } i, j \in \mathcal{S}_2 \end{cases} \\ &= p_{ij}^\lambda + p_{ij}^\ell, \end{aligned}$$

where we define $p_{ij}^\ell = -\ell_i - \ell_j$. Note that p^ℓ lies in the lineality space of the tropical Grassmannian $\text{trop}(\text{Gr}(2, d+n))$, and so $p \sim p^\ell$.

For (2), note that the bicolored split tree $P^{(R,G)}$ is also generated by the matrix A^μ for any $\mu > 0$. Since A and A^μ generate the same tree, they are both contained in the interior of the same cone of $\mathcal{BPT}_{d,n}$. Since $P^{(R,G)}$ is a split tree, modulo lineality space of $\mathcal{BPT}_{d,n}$, this cone is 1-dimensional. We choose $\mu = 1$ and consider the matrix A^1 as generator for this ray. Then for every point $A' \in \text{cone}(A^1)$ there exists a unique $\mu \geq 0$ such that $A' = \mu A^1 = A^\mu$. Hence, this also holds for the original matrix A , i.e. there exists a unique $\mu > 0$ such that $A \sim A^\mu$ modulo lineality space of $\mathcal{BPT}_{d,n}$. \square

LEMMA 2.4.28. $\pi^{(R,G)}$ induces a bijection of lineality spaces of the tropical determinantal variety $T_{d,n}^2$ and the tropical Grassmannian $\text{trop}(\text{Gr}(2, d+n))$. Thus, if $p \sim p'$ then $\pi^{(R,G)}(p) \sim \pi^{(R,G)}(p')$.

Proof. The fan $\mathcal{UPT}^{(R,G)}$ is a subfan of $\text{trop}(\text{Gr}(2, d+n))$. Since the lineality space of a fan is the intersection of the lineality spaces of all cones it contains, the lineality space of $\text{trop}(\text{Gr}(2, d+n))$ is thus contained in the lineality space of $\mathcal{UPT}^{(R,G)}$. We first show that the images of the $d+n$ generators of the lineality space of $\text{trop}(\text{Gr}(2, d+n))$ (as described in [Section 2.4.4](#)) span the lineality space of $\mathcal{BPT}_{d,n}$. This implies that $\pi^{(R,G)}$ induces a bijection of lineality spaces. Let $p = \sum_{\substack{i \in [d+n] \\ i \neq k}} \tilde{e}_{ik}$, $k \in [d+n]$. Since $R \sqcup G = [d+n]$, either $k \in R$ or $k \in G$. If $k \in R$, then for $i \in R, j \in G$ we have

$$p_{ij} = \begin{cases} 0 & \text{if } i = k \\ 1 & \text{otherwise.} \end{cases}$$

Thus, $\pi^{(R,G)}(p)$ is the matrix $\pi^{(R,G)}(p) = \sum_{\substack{i=1 \\ i \neq k}}^d \sum_{j=1}^n E_{ij}$. On the other hand, if $k \in G$, then $\pi^{(R,G)}(p) = \sum_{i=1}^d \sum_{\substack{j=1 \\ j \neq k}}^n E_{ij}$. Indeed, these vectors span the same vector space as

the vectors given in (2.4) in [Section 2.1.5](#). Hence, $\pi^{(R,G)}$ induces a bijection of lineality spaces of $\text{trop}(\text{Gr}(2, d+n))$ and $\mathcal{BPT}_{d,n}$.

Let $p, p' \in \text{trop}(\text{Gr}(2, d+n))$ arbitrary, such that $p \sim p'$ modulo lineality space \mathcal{L} of $\text{trop}(\text{Gr}(2, d+n))$. Then $p \in p' + \mathcal{L}$, and since $\pi^{(R,G)}$ is linear, it follows that

$\pi^{(R,G)}(p + \mathcal{L}) = \pi^{(R,G)}(p) + \pi^{(R,G)}(\mathcal{L})$, where $\pi^{(R,G)}(\mathcal{L})$ is the lineality space of $\mathcal{BPT}_{d,n}$ by the above. Hence, $\pi^{(R,G)}(p) \sim \pi^{(R,G)}(p')$. \square

PROPOSITION 2.4.29. The map $\pi^{(R,G)}$ induces a bijection of rays of the fans $\mathcal{UPT}^{(R,G)}$ and $\mathcal{BPT}_{d,n}$ and preserves the combinatorial types of split trees.

Proof. Let $p \in \mathcal{UPT}^{(R,G)} \subseteq \text{trop}(\text{Gr}(2, d+n))$ be a ray generator. Then p corresponds to a split tree P with two parts S_1, S_2 of leaves. By [Lemma 2.4.27](#) we have that $p \sim p^\lambda$ modulo the lineality space of $\text{trop}(\text{Gr}(2, d+n))$. By construction, $\pi^{(R,S)}(p^\lambda) = A^\lambda$, so by [Lemma 2.4.28](#) $p \sim p^\lambda$ implies $\pi^{(R,G)}(p) \sim A^\lambda$. Note that A^λ is the matrix representing the (R, G) -bicoloring $P^{(R,G)}$ of P . Hence, $\pi^{(R,G)}$ sends rays of $\mathcal{UPT}^{(R,G)}$ onto rays of $\mathcal{BPT}_{d,n}$, preserving the combinatorial type of split trees. Note that this implies injectivity: Let r, r' be distinct rays of $\mathcal{UPT}^{(R,G)}$ with respective ray generators p, p' . Then p, p' correspond to phylogenetic split trees P, P' of distinct combinatorial types. Since the (R, G) -bicoloring is admissible for both P and P' , the matrices $\pi^{(R,G)}(p)$ and $\pi^{(R,G)}(p')$ correspond to bicolored trees of distinct combinatorial types. Hence, $\pi^{(R,G)}(r)$ and $\pi^{(R,G)}(r')$ are distinct rays of $\mathcal{BPT}_{d,n}$.

For surjectivity, let $r = \text{cone}(A)$ be a ray of $\mathcal{BPT}_{d,n}$. Then there is a unique $\lambda > 0$ such that $A \sim A^\lambda$. Let A^ℓ be a matrix in the lineality space of $\mathcal{BPT}_{d,n}$ such that $A = A^\lambda + A^\ell$. By construction $\pi^{(R,G)}(p^\lambda) = A^\lambda$ and since $\pi^{(R,G)}$ is a bijection on the lineality spaces, there is a unique p^ℓ in the lineality space of $\text{trop}(\text{Gr}(2, d+n))$ such that $A^\ell = \pi^{(R,G)}(p^\ell)$. Again, since $\pi^{(R,G)}$ is linear, it follows for $p := p^\lambda + p^\ell$ that

$$\pi^{(R,G)}(p) = \pi^{(R,G)}(p^\lambda) + \pi^{(R,G)}(p^\ell) = A^\lambda + A^\ell = A.$$

\square

Proof of [Theorem 2.4.23](#). [Proposition 2.4.29](#) establishes the statement for rays. Let $p \in \mathcal{UPT}^{(R,G)}$ be an arbitrary Plücker vector and P be the corresponding uncolored phylogenetic tree with splits. Modulo lineality space of $\text{trop}(\text{Gr}(2, d+n))$, we can assume that P has all leaf lengths 0. Let S_1, \dots, S_k be the compatible splits of P with internal edge lengths $\lambda_1, \dots, \lambda_k$, and p^{S_1}, \dots, p^{S_k} be the Plücker vectors of the corresponding split trees P_1, \dots, P_k . Since the S_i are the splits of P , it follows that $p^{S_1} + \dots + p^{S_k} = p$ and p^{S_1}, \dots, p^{S_k} are ray generators for the rays of the cone C such that $p \in \text{relint}(C)$. Since C is simplicial, this sum is unique. By above, $\pi^{(R,G)}$ is a bijection on the level of rays, so equivalently $\pi^{(R,G)}(p^{S_1}), \dots, \pi^{(R,G)}(p^{S_k})$ is a set of rays in $\mathcal{BPT}_{d,n}$, corresponding to the bicolored split trees $P_1^{(R,S)}, \dots, P_k^{(R,S)}$. Since the definition of compatibility is independent of the coloring, these bicolored splits are compatible and hence form a cone C' in $\mathcal{BPT}_{d,n}$. Again, $\mathcal{BPT}_{d,n}$ is a simplicial fan, and so any point C' has a unique representation as sum of ray generators of C' . Consider $A = \pi^{(R,G)}(p^{S_1}) + \dots + \pi^{(R,G)}(p^{S_k})$. Then by construction, this matrix corresponds to a tree with bicolored splits $P_1^{(R,S)}, \dots, P_k^{(R,S)}$,

i.e. the tree $P^{(R,G)}$. Finally, since $\pi^{(R,G)}$ is a coordinate projection, if $i \in R, j \in G$, then

$$p_{ij} = \pi^{(R,G)}(p^{S_1} + \cdots + p^{S_k})_{ij} = \pi^{(R,G)}(p^{S_1})_{ij} + \cdots + \pi^{(R,G)}(p^{S_k})_{ij} = A_{ij}$$

and so $\pi^{(R,G)}(p) = A$. Since $\pi^{(R,G)}$ is a bijection of the rays, and all sums are unique, this extends to a bijection to the entire fan. \square

2.5 RANK 3

In this section, we show the extensions and limitations of the techniques for certifying positivity for $T_{d,n}^3$. The main idea is to identify a criterion for a matrix A not to be contained in the positive determinantal prevariety $(P_{d,n}^3)^+$ by identifying a (4×4) -minor, such that A is not contained in the respective positive tropical hypersurface. As $(T_{d,n}^3)^+ \subseteq (P_{d,n}^3)^+$, we thereby also obtain a condition for A not to be contained in $(T_{d,n}^3)^+$. As before, we consider the columns of a matrix $A \in T_{d,n}^3$ as a point configuration of n points in \mathbb{TP}^{d-1} . Due to the rank condition (Proposition 2.1.21), these points lie on a common tropical plane. We view a tropical plane as an embedded pure 2-dimensional polyhedral complex in \mathbb{TP}^{d-1} . It has d unbounded rays r_1, \dots, r_d , where the slope of r_i is in standard unit direction e_i . Furthermore it has bounded edges with edge directions $\sum_{i \in I} e_i$ for $I \subseteq [d], |I| \geq 2$. More precisely, a tropical plane is a subcomplex of the polyhedral complex that is dual to a regular matroid subdivision of the hypersimplex

$$\Delta(d, 3) = [0, 1]^d \cap \left\{ x \in \mathbb{R}^d \mid \sum_{i=1}^d x_i = 3 \right\}$$

where in this subdivision of $\Delta(d, 3)$ each maximal cell corresponds to a matroid of rank 3. Regular subdivisions are defined in Section 1.1.3, and an exposition on matroids and matroid polytopes is given in Section 1.2. We describe this subcomplex of $\Delta(d, 3)$ in more detail in Section 2.5.2.

Definition 2.5.1. Let $A \in T_{d,n}^3$ and consider the induced point configuration. The matrix $A \in T_{d,n}^3$ (or equivalently the corresponding point configuration) is *generic* with respect to a tropical plane E if every point A_j lies on the interior of a 2-dimensional face of E . We call a 2-dimensional face of the plane E a *marked face* if it contains a point of the point configuration in its interior.

Recall from Section 2.2.4 that we call the 2-dimensional faces of a tropical plane in \mathbb{TP}^3 the wings of the plane.

2.5.1 Starship Criterion for Positivity

We establish a condition on the local properties of a tropical plane based on Theorem 2.2.16 (Geometric triangle criterion). The idea is as follows: Let $A \in T_{d,n}^3$ and E be a tropical plane containing the columns of A . The matrix A is non-positive if there

exists a non-positive (4×4) -submatrix. The [geometric triangle criterion](#) describes the associated point configuration of 4 points in \mathbb{TP}^3 . We identify a projection of E which selects such a (4×4) -submatrix to certify non-positivity. The condition to identify the correct submatrix solely depends on the collection of marked faces, i.e. a local structure of the underlying tropical plane. Since a tropical plane is dual to a matroid subdivision of $\Delta(d, 3)$, we thus argue via normal cones of faces of matroid polytopes, reducing this problem to a question about flags of flats of the respective matroids. Recall from [Section 1.2](#) that all facets of a matroid polytope are given by an inequality defined by some flat of the corresponding matroid.

LEMMA 2.5.2. Let M be a matroid of rank 3 on n elements, and H_1, H_2, H_3 be distinct flats of rank 2. If $H_1 \cap H_2 \cap H_3 = G$ is a flat of rank 1, then $H_3 \not\subseteq H_1 \cup H_2$.

Proof. Assume for contradiction that $H_3 \subseteq H_1 \cup H_2$. Let $h \in H_3 \setminus G$. Then $h \in H_1$ or $h \in H_2$, and without loss of generality we can assume $h \in H_1$. Since G is a flat, and $h \notin G$ we get that $\text{rk}(G \cup \{h\}) = 2 = \text{rk}(H_1)$. Hence, $G \cup \{h\} \subseteq H_1$ implies that $\text{span}(G \cup \{h\}) = H_1$. However, at the same time, since $\text{rk}(G \cup \{h\}) = 2 = \text{rk}(H_3)$ and $G \cup \{h\} \in H_3$, we have that $\text{span}(G \cup \{h\}) = H_3$. Thus, $H_1 = \text{span}(G \cup \{h\}) = H_3$, contradicting the assumption that H_1, H_2, H_3 are distinct. \square

LEMMA 2.5.3. Let $E \subseteq \mathbb{TP}^{d-1}$ be a realizable tropical plane, i.e. a tropical plane that arises as the tropicalization of a plane in \mathcal{CP}^{d-1} . Let F_1, F_2, F_3 be distinct 2-dimensional faces of E , intersecting in a common unbounded 1-dimensional face r . Then there is an index set $I \subseteq [d]$ with $|I| = 4$ such that for the coordinate projection $\pi_I : \mathbb{TP}^{d-1} \rightarrow \mathbb{TP}^3$ onto these coordinates the following holds: $\pi_I(E) \subseteq \mathbb{TP}^3$ is a tropical plane with wings $\pi_I(F_1), \pi_I(F_2), \pi_I(F_3)$ intersecting in the common unbounded 1-dimensional $\pi_I(r)$.

Proof. Let $E \subseteq \mathbb{TP}^{d-1}$ be a realizable tropical plane. Then E is a subcomplex of a polyhedral complex that is dual to a matroid subdivision of $\Delta(d, 3)$, where each maximal matroid polytope corresponds to a matroid of rank 3. Let v be the vertex of the ray $r = F_1 \cap F_2 \cap F_3$, and P be the matroid polytope dual to v . Let M be the corresponding matroid of rank 3 on ground set $[n]$. Each 2-dimensional face F_k spans the normal cone of a face of P . The 1-dimensional faces of F_k that are incident to v have slopes $\sum_{i \in G_k} e_i$ and $\sum_{i \in H_k} e_i$ respectively. Here, for each $k = 1, 2, 3$, we have that $\emptyset \subsetneq G_k \subsetneq H_k \subsetneq [n]$ is a chain of flats of M [[MS15](#), Theorem 4.2.6]. Thus, G_k is a flat of rank 1, and H_k is a flat of rank 2. By assumption, F_1, F_2, F_3 intersect in an unbounded 1-dimensional face r . Hence, there exists an element $g \in [n]$ such that $G_1 = G_2 = G_3 = \{g\}$. Therefore, H_1, H_2, H_3 intersect in a flat of rank 1. By assumption, H_1, H_2, H_3 are distinct, and so by [Lemma 2.5.2](#) we can choose distinct $h_1 \in H_1 \setminus (H_2 \cup H_3)$, $h_2 \in H_2 \setminus (H_1 \cup H_3)$ and $h_3 \in H_3 \setminus (H_1 \cup H_2)$. Let $I = \{h_1, h_2, h_3, g\}$. Then $\pi_I(r) \subseteq \mathbb{TP}^3$ is the ray spanned by e_g , and $\pi_I(F_k) = \text{cone}(e_g, e_{h_k})$.

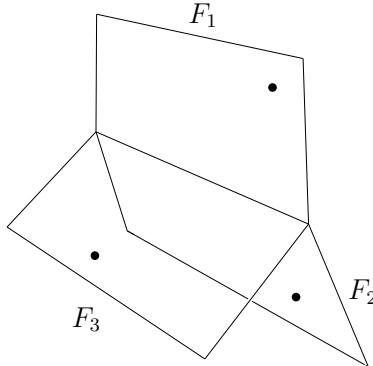


Figure 2.21: A configuration of three marked 2-faces forming a starship.

Finally, we show that $\pi_I(E)$ is tropical plane. Since E is realizable, E is the tropicalization of a 2-dimensional plane \mathcal{E} in \mathcal{CP}^{d-1} . We can first apply the coordinate projection to obtain a linear space $\pi_I(\mathcal{E}) \subseteq \mathcal{CP}^3$ of dimension at most 2. Note that $\pi_I(E)$ is the tropicalization of $\pi_I(\mathcal{E})$, and is thus a tropical linear space of dimension at most 2. But since $\pi_I(F_k) \subseteq \pi_I(E)$ and $\pi_I(F_k)$ is a 2-dimensional cone, $\pi_I(E)$ has dimension 2 and is a tropical plane. \square

Definition 2.5.4 (Starship). Let $A \in T_{d,n}^3$ be a matrix and let E be a tropical plane containing the points given by the columns of A . If E has 3 marked 2-faces F_1, F_2, F_3 that intersect in an unbounded 1-dimensional face, then we say that E contains the *starship*¹ formed by the marked faces F_1, F_2, F_3 . Such a configuration can be seen in Figure 2.21.

THEOREM 2.5.5 (Starship criterion). Let $A \in T_{d,n}^3$ be a matrix in the relative interior of a cone $C \in T_{d,n}^3$ and let E be a tropical plane containing the points given by the columns of A . If E has 3 marked 2-faces that intersect in an unbounded 1-dimensional face, then C is not positive. In other words, C is not positive if E contains a starship.

Proof. Let A_1, A_2, A_3 be the points lying on 2-faces F_1, F_2, F_3 respectively, and let $j \in [n] \setminus \{1, 2, 3\}$. By Lemma 2.5.3 there exists a coordinate projection onto coordinates $I = \{i_1, \dots, i_4\}$ such that $\pi_I(F_1), \pi_I(F_2), \pi_I(F_3)$ are 2-dimensional faces of the tropical plane $\pi_I(E) \subseteq \mathbb{TP}^3$, which intersect in a common unbounded ray in direction e_{i_4} . Note that the projection of the point $\pi_I(A_k)$ marks the 2-face $\pi_I(F_k)$ for $k = 1, 2, 3$, and $\pi_I(A_4) \in \pi_I(E)$. This point configuration of 4 points in \mathbb{TP}^3 is also represented by the (4×4) -submatrix of A with rows $I = \{i_1, i_2, i_3, i_4\}$ and columns $J = \{1, 2, 3, j\}$. Dually, this corresponds to 3 marked edges of the simplex Δ_3 incident to the triangle that is dual to the ray e_{i_4} . By the Geometric triangle criterion (Theorem 2.2.16) this

¹more precisely, a starship of type “Lambda-class T-4a shuttle”

(4×4) -matrix is not positive. Thus, if $\{j_1, j_2, j_3, j_4\} = \{1, 2, 3, j\}$, then for the minor

$$f^{IJ} = \sum_{\sigma \in S_4} \operatorname{sgn} \sigma \prod_{k=1}^4 x_{i_k \sigma(j_k)}$$

holds that $A \notin \operatorname{trop}^{+c}(\mathcal{V}(f^{IJ}))$. It follows that A is not contained in the positive tropical determinantal prevariety (as defined in (2.2) in [Section 2.1.4](#)), i.e.

$$A \notin \bigcap_{\substack{f^{IJ} \text{ is a} \\ (4 \times 4)\text{-minor}}} \operatorname{trop}^{+c}(\mathcal{V}(f^{IJ})) = (P_{d,n}^3)^+$$

and in particular

$$A \notin \bigcap_{f \in I_r} \operatorname{trop}^{+c}(\mathcal{V}(f)) = (T_{d,n}^3)^+.$$

□

We give an example of a matrix $A \in T_{d,n}^3$, in which the point configuration in \mathbb{TP}^{d-1} does not contain a starship, but an appropriate coordinate projection does.

Example 2.5.6 (The converse of the [Starship criterion](#) does not hold). Consider the matrix

$$A = \begin{pmatrix} k & k & 0 & 0 & 0 \\ 0 & k & k & 0 & 1 \\ 0 & 0 & k & k & 0 \\ 0 & 0 & 0 & k & k \\ k & 0 & 0 & 0 & k \end{pmatrix}$$

for any $k > 1$. This is a point configuration where

$$A_1 \in W_1 = \operatorname{cone}(e_1, e_5), \quad A_2 \in W_2 = \operatorname{cone}(e_1, e_2), \quad A_3 \in W_3 = \operatorname{cone}(e_2, e_3),$$

$$A_4 \in W_4 = \operatorname{cone}(e_3, e_4), \quad A_5 \in W_5 = e_2 + \operatorname{cone}(e_4, e_5),$$

which are 2-dimensional wings of a tropical plane $E \subseteq \mathbb{TP}^4$. Hence, this point configuration does not satisfy the assumptions of the [Starship criterion](#) ([Theorem 2.5.5](#)) – it does not contain a starship. We project the marked wings W_1, W_2, W_3, W_5 onto the first 4 coordinates. Then $\pi(W_1) = \operatorname{cone}(e_1)$, $\pi(W_2) = \operatorname{cone}(e_1, e_2)$, $\pi(W_3) = \operatorname{cone}(e_2, e_3)$, $\pi(W_5) = e_2 + \operatorname{cone}(e_4)$. The projections $\pi(W_1), \pi(W_2), \pi(W_3)$ are cones of the (unique) tropical plane E' in \mathbb{TP}^3 with apex at the origin, and the projection $\pi(W_5)$

is a ray in the wing cone (e_2, e_4) of E' . Thus, the submatrix

$$\begin{array}{cccc} & A_1 & A_2 & A_3 & A_5 \\ \begin{matrix} 1 \\ 2 \\ 3 \\ 4 \end{matrix} & \left(\begin{array}{cccc} k & k & 0 & 0 \\ 0 & k & k & 1 \\ 0 & 0 & k & 0 \\ 0 & 0 & 0 & k \end{array} \right) \end{array}$$

constitutes a starship (with unbounded ray in direction e_2) with respect to E' , where the projections of A_1, A_3 and A_5 are the marking points. If $i_1 = 1, i_2 = 2, i_3 = 3, i_4 = 5$ and

$$f^{IJ} = \sum_{\sigma \in S_4} \operatorname{sgn} \sigma \prod_{k=1}^4 x_{i_k \sigma(k)}$$

then the [Geometric triangle criterion \(Theorem 2.2.16\)](#) implies that we have that $A \notin \operatorname{trop}^{+c}(\mathcal{V}(f^{IJ}))$ and hence $A \notin (P_{d,n}^3)^+$ (so in particular $A \notin (T_{d,n}^3)^+$) for arbitrary matrices $A \in P_{d,n}^3$. If C is a cone containing A in its relative interior, then this implies that C is not positive. Hence, the converse of [Theorem 2.5.5](#) does not hold for the matrix $A \in P_{d,n}^3$. We continue with this in [Example 2.5.9](#). \diamond

2.5.2 Bicolored Tree Arrangements

Tree arrangements were introduced in [\[HJJSo9\]](#) for studying the Dressian $Dr(d, 3)$. It was shown that tree arrangements encode matroid subdivisions of the hypersimplex $\Delta(d, 3)$ by looking at the induced subdivision on the boundary. In particular, this implies that we can associate a tree arrangement to every tropical plane. In this section, we extend this idea and introduce *bicolored tree arrangements*, which correspond to a tropical plane with a configuration of points on it. However, we will see in [Example 2.5.9](#) that this is not a one-to-one correspondence.

We first describe the established bijection between tropical planes and (uncolored) tree arrangements, following [\[HJJSo9\]](#). As introduced at the beginning of this section, a tropical plane is a subcomplex of the polyhedral complex that is dual to a regular matroid subdivision of the hypersimplex $\Delta(d, 3)$. Inside the affine space $\{x \in \mathbb{R}^d \mid \sum_{i=1}^d x_i = 3\}$, the facets of $\Delta(d, 3)$ are given by $x_i = 0$ and $x_i = 1$. A tropical plane is the polyhedral complex dual to the subcomplex of a matroid subdivision of $\Delta(d, 3)$ consisting of the faces which are not contained in $\{x_i = 0\}$. Every matroid subdivision of $\Delta(d, 3)$ is uniquely determined by the restriction of the subdivision to the n facets of $\Delta(d, 3)$ defined by $\{x_i = 1\}$ [\[HJJSo9, Section 4\]](#). We restrict this matroid subdivision to the remaining facets given by $\{x_i = 1\}$. These facets are isomorphic to a hypersimplex $\Delta(d, 2)$, so the restricted subdivisions are dual to a tropical line in \mathbb{TP}^{d-2} . This tropical line has rays in directions $e_1, \dots, e_{i-1}, e_{i+1}, \dots, e_d$. As these tropical lines are in bijection

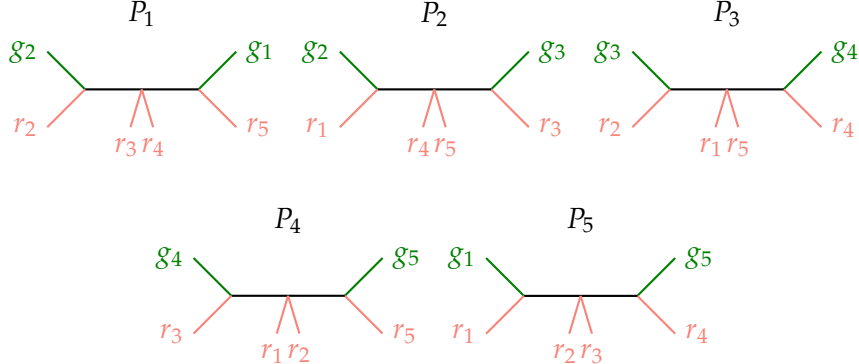


Figure 2.22: The bicolored tree arrangement of the non-positive matrix in Example 2.5.6.

with (uncolored) phylogenetic trees, this yields a *tree arrangement*. We extend this idea as follows.

Construction 2.5.7 (Bicolored tree arrangements). Let $A \in T_{d,n}^3$ be the matrix giving n points A_1, \dots, A_n on a tropical plane E in \mathbb{TP}^{d-1} . If A is generic with respect to E , then every point $A_j, j \in [n]$ lies in the interior of a 2-face $F \subseteq E$, where each 1-dimensional face of F has slope $\sum_{i \in I} e_i$. When restricting to a facet $\{x_{i'} = 1\}$ of $\Delta(d, 3)$, then the subdivision of this facet is dual to the collection of faces of E that contain the unbounded ray in direction $e_{i'}$. We denote the collection of these unbounded faces by $\mathcal{F}_{i'}$.

Let $J_{i'} \subseteq [n]$ be the set of points lying on a face in $\mathcal{F}_{i'}$. To obtain a bicolored tree arrangement, project all of these 2-dimensional faces of E and the points in $J_{i'}$ onto the coordinates $1, \dots, i' - 1, i' + 1, \dots, d$. The projection of the 2-faces in $\mathcal{F}_{i'}$ form tropical line $L_{i'}$, and the projection of the points are points on $L_{i'}$. Hence, applying Construction 2.4.4 induces a bicolored phylogenetic tree $P_{i'}$. We call the collection of these bicolored trees P_1, \dots, P_d a *bicolored tree arrangement*.

THEOREM 2.5.8. Let $A \in T_{d,n}^3$ be generic with respect to the tropical plane E . If A is positive, then every tree in the induced bicolored tree arrangement is a caterpillar tree.

Proof. Let P be a tree in the bicolored tree arrangement that is not a caterpillar tree. We show that A is not positive. After relabeling we can assume that $P = P_d$, i.e. P is the tree on the d th facet. Since P is not a caterpillar tree, it has an internal vertex that is incident to at least 3 internal edges. Thus, P corresponds to a tropically collinear point configuration, on which there are points with labels 1, 2, 3 on a tropical line $L \in \mathbb{TP}^{d-2}$ whose tropical convex hull in \mathbb{TP}^{d-2} contains the 3 internal edges. Consider the $((d-1) \times 3)$ -matrix $\overline{A}^{\{1,2,3\}}$ consisting of the respective columns A_1, A_2, A_3 . This matrix $\overline{A}^{\{1,2,3\}}$ has Kapranov rank 2. By Corollary 2.4.6, it has no positive lift of rank 2. Thus, $\overline{A}^{\{1,2,3\}}$ has a (3×3) -submatrix B with row indices i_1, i_2, i_3 , such that (possibly

after relabeling) the column B_k lies on the ray of a tropical line in \mathbb{TP}^2 with slope e_k for $k = 1, 2, 3$.

Pick any additional column j , and consider the (4×4) -submatrix D with row indices i_1, i_2, i_3, d and column indices $1, 2, 3, j$. Then the points given by the columns D_k , $k \in [3]$, and D_j lie on a common tropical plane $E \subseteq \mathbb{TP}^3$. By genericity of A w.r.t. E , the points D_k , $k \in [3]$ lie in the interior of the faces of E that are (up to translation) the cones spanned by the rays e_k and e_d , respectively. Dually, this corresponds to 3 marked edges of the simplex Δ_3 incident to the triangle that is dual to the ray e_d . By the [Geometric triangle criterion \(Theorem 2.2.16\)](#) this (4×4) -matrix is not positive. As in the proof of [Theorem 2.5.5](#), this implies that A is not positive. \square

Example 2.5.9 (The converse of [Theorem 2.5.8](#) does not hold). Consider the matrix from [Example 2.5.6](#). This matrix is not positive. However, the bicolored trees in this arrangement are all caterpillar trees, as depicted in [Figure 2.22](#). Thus, the converse of [Theorem 2.5.8](#) does not hold. \diamond

Remark 2.5.10. The Starship criterion can be obtained as a corollary of [Theorem 2.5.8](#) in the special case that A is generic w.r.t to the tropical plane E . Indeed, if A is positive, then every tree in the bicolored tree arrangement is a caterpillar tree. However, a starship with unbounded ray in direction $e_{i'}$ yields a tree $P_{i'}$ that is not a caterpillar tree. Thus, A is not positive. We note that however, that a tree which is not a caterpillar tree does not necessarily arise from a point configuration containing a starship, so in the general setup none of the two statements implies the other.

In both statements of [Theorem 2.5.5](#) and [Theorem 2.5.8](#), the converse fails to be true. A main problem lies in the fact that both the tree arrangement and the Starship criterion are only able to capture the geometry of the unbounded faces of the tropical plane. While this information is enough to reconstruct the entire plane [[HJJSo9](#)], this does not suffice to capture information about the point configuration on bounded faces of the tropical plane.

3

MULTIVARIATE VOLUME, EHRHART, AND h^* -POLYNOMIALS OF POLYTROPES

Polytropes are a fundamental class of polytopes, which masquerade in the literature as alcoved polytopes of type A [LP07; LP18]. Among many others, they include order polytopes, some associahedra and matroid polytopes, hypersimplices, and Lipschitz polytopes. They are tropical polytopes which are classically convex [JK10] and are closely related to the notion of Kleene stars and the problem of finding shortest paths in weighted graphs [Tra17; JS19]. Polytropes also arise in a range of algorithmic applications to other fields, including phylogenetics [YZZ19], mechanism design [CT18], and building theory [JSYo7].

It is well known that computing the volume of a polytope is hard, and already approximating the volumes of convex bodies is “difficult” [BF87]. For an exact computation, computing the volume of a polytope is #P-hard (and thus at least NP-hard), even when restricting to the class of polytopes defined by a totally unimodular matrix [DF88]. However, viewing polytropes as the “building blocks” of tropical polytopes, understanding their volumes provides insight into the volume of tropical polytopes. Determining whether the volume of such a tropical polytope is zero is equivalent to deciding whether a mean payoff game is winning [AGG12]. The volume of a tropical polytope can hence serve as a measurement of how far a game is from being winning [GM19].

Unimodular triangulations of polytropes were studied in the language of affine Coxeter arrangements in [LP07], producing a volume formula and non-negativity of the h -vector corresponding to the triangulation. Motivated by a novel possibility for combining algebraic methods with enumerative results from tropical geometry, we continue to study the volume of polytropes, both continuously and discretely. The Ehrhart counting

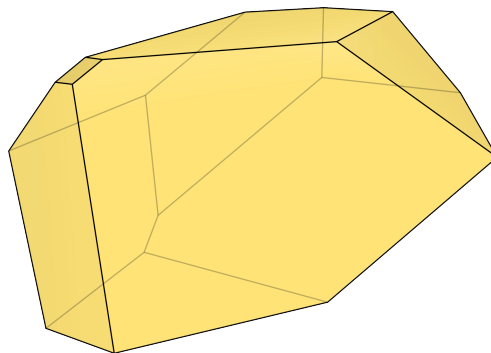


Figure 3.1: A 3-dimensional polytrope.

function encodes the discrete volume by counting the number of lattice points in any positive integral dilate of a polytope. For lattice polytopes, this counting function is given by a univariate polynomial, the Ehrhart polynomial, with leading term equal to the Euclidean volume of the polytope. Rewriting the Ehrhart polynomial in the basis of binomial coefficients determines the h^* -polynomial and reveals additional beautiful connections between the coefficients and the geometry of the polytope. It is an area of active research to determine the relations between the h^* -coefficients of alcoved polytopes [SVL13, Question 1]; for example, it is conjectured that the h^* -vectors of alcoved polytopes of type A are unimodal.

In recent work, Loho and Schymura [LS20] developed a separate notion of volume for tropical polytopes driven by a tropical version of dilation, which yields an Ehrhart theory for a new class of tropical lattices. This notion of volume is intrinsically tropical and exhibits many natural properties of a volume measure, such as being monotonic and rotation-invariant. Nevertheless, the discrete and classical volume can be more relevant for certain applications; for example, the irreducible components of a Mustafin variety correspond to the lattice points of a certain tropical polytope [CHSW11; Zha21], which can thus be counted by an Ehrhart polynomial.

We pass from univariate polynomials to multivariate polynomials to push the connections between the combinatorics of the polynomials and the geometry even further. Combinatorial types of polytropes have been classified up to dimension 4 [Tra17; JS19]. Each polytrope of the same type has the same normal fan. Given a normal fan, we create multivariate polynomial functions in terms of the rays that yield the (discrete) volume and h^* -polynomials for any polytrope of that type. We first use algebraic methods to compute the multivariate volume polynomials, following the algorithm in [DLS03]. We then transform these polynomials into multivariate Ehrhart polynomials, which are highly related to vector partition functions, using the Todd operator. Finally we perform the change of basis to recover the h^* -polynomials.

RESULT 3.4.1. We compute the multivariate volume, Ehrhart, and h^* -polynomials for all types of polytropes of dimension ≤ 4 .

Each combinatorial type of polytropes of dimension $n - 1$ corresponds to a certain triangulation of the fundamental polytope FP_n , the polytope with vertices $e_i - e_j$ for $i, j \in [n]$ [JS19]. Our computations show that the volume polynomials of polytropes of dimension 3 have integer coefficients with a strong combinatorial meaning:

THEOREM 3.4.3. The coefficients of the volume polynomials of maximal 3-dimensional polytropes reflect the combinatorics of the corresponding regular central subdivision of FP_3 .

For example, each coefficient of a monomial of the form $a_{ij}a_{kl}a_{st}$ is either 6 or 0. This reflects whether the vertices $e_i - e_j, e_k - e_l$ and $e_s - e_t$ form a face in the triangulation of FP_4 or not. Similarly, the coefficient of the monomial $a_{ij}^2a_{kl}$ is -3 if the vertex $e_k - e_l$ is incident to a triangulating edge of a square facet of FP_3 and 0 otherwise. These intriguing observations naturally lead to a question of generalization.

Question 3.4.6. How do the coefficients of the volume polynomials of maximal $(n - 1)$ -dimensional polytropes reflect the combinatorics of the corresponding regular central subdivision of FP_n ?

To emphasize this question, we show that our data of volume polynomials of dimension 4 is highly structured:

THEOREM 3.4.5. In the 8855-dimensional space of homogeneous polynomials of degree 4, the 27 248 normalized volume polynomials of 4-dimensional polytropes span a 70-dimensional affine subspace.

We note that these polynomials have integer coefficients, and the possible non-zero coefficients are $\pm 1, \pm 2, \pm 3, \pm 4, -6, 8, \pm 12, 24$. Similar to the three-dimensional case, each coefficient of a monomial of the form $a_{ij}a_{kl}a_{st}a_{uv}$ is either 24 or 0, which reflects whether the vertices $e_i - e_j, e_k - e_l, e_s - e_t$ and $e_u - e_v$ form a face in the triangulation of FP_5 . We present a partial characterization of these coefficients in [Table 3.1](#).

This chapter is based on [\[BEZ23\]](#), which is joint work with Sophia Elia and Leon Zhang. Our code and the resulting polynomials are publicly available on a GitHub repository [\[BEZ20\]](#).

Overview

In this chapter we describe methods for computing the multivariate volume, Ehrhart, and h^* -polynomials for all polytropes. The necessary background is given in [Sections 1.1](#) to [1.3](#), [1.5](#) and [1.7](#). We begin in [Section 3.1](#) by extending the exposition on tropical convexity from [Section 1.3.1](#), and introduce the class of polytropes. We describe our methods to compute multivariate volume polynomials in [Section 3.2](#), and extend to multivariate Ehrhart and h^* -polynomials in [Section 3.3](#). In [Section 3.4](#), we apply these methods to compute the volume, Ehrhart, and h^* -polynomials of polytropes of dimension 2, 3 and 4. We give a complete description of the coefficients of volume polynomials of 3-dimensional polytropes in terms of regular central subdivisions of the fundamental polytope, and give a partial characterization of these coefficients in dimension 4.

3.1 TROPICAL CONVEXITY AND POLYTROPES

The class of polytropes is a subclass of tropical polytopes, namely the class tropical polytopes which are also classically convex. In this section we describe how polytropes can be seen as “building blocks” of tropical polytopes [\[DS04\]](#) and outline the connection to Kleene stars [\[Tra17; JS19\]](#).

Let $V = \{v_1, \dots, v_n\} \subseteq \mathbb{R}^d$ be a finite set of points. Recall from [Section 1.3](#) that the tropical convex hull of V is given by the set of all tropical linear combinations

$$\text{tconv}(V) = \{\lambda_1 \odot v_1 \oplus \dots \oplus \lambda_n \odot v_n \mid \lambda_1, \dots, \lambda_n \in \mathbb{R}\}.$$

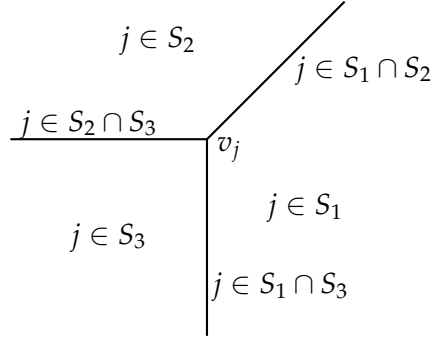


Figure 3.2: The max-tropical hyperplane $H_{v_j}^{\max} \subseteq \mathbb{TP}^2$ in the chart where the third coordinate is 0, with faces labeled for type identification.

and we identify a tropically convex set $\text{tconv}(V) \subseteq \mathbb{R}^d$ with its image in the tropical projective torus $\mathbb{TP}^{d-1} = \mathbb{R}^d / (\mathbb{R} \odot \mathbf{1})$. Let $P = \text{tconv}(V) \subseteq \mathbb{TP}^{d-1}$ be a tropical polytope, i.e. the tropical convex hull of finitely many points. We denote by v_{ij} the i th coordinate of v_j , $j \in [n]$, i.e. the ij th entry of the $(d \times n)$ -matrix with columns v_1, \dots, v_n . The (*tropical*) *type* of a point $x \in \mathbb{TP}^{d-1}$ with respect to V is the collection of sets $S(x) = (S_1, \dots, S_d)$, where an index $j \in [n]$ is contained in S_i if

$$v_{ij} - x_i = \min(v_{1j} - x_1, \dots, v_{dj} - x_d).$$

Geometrically, we can view the type of x as follows. The *max-tropical hyperplane* $H_{v_j}^{\max} \subseteq \mathbb{TP}^{d-1}$ with apex at $v_j \in \mathbb{TP}^{d-1}$ is

$$H_{v_j}^{\max} = \left\{ y \in \mathbb{TP}^{d-1} \mid \text{the maximum of } \{y_i - v_{ij} \mid i \in [d]\} \text{ is attained at least twice} \right\}.$$

Each such hyperplane $H_{v_j}^{\max}$ induces a complete polyhedral fan \mathcal{F}_{v_j} in \mathbb{TP}^{d-1} . Two points $x, y \in \mathbb{TP}^{d-1}$ lie in the same relatively open cone of \mathcal{F}_{v_j} if and only if $v_j - x$ and $v_j - y$ achieve their minima in the same set of coordinates. For a point $x \in \mathbb{TP}^{d-1}$ with type $S(x) = (S_1, \dots, S_d)$, the set S_i records for which hyperplanes $H_{v_j}^{\max}$ the point x lies in a face of \mathcal{F}_{v_j} such that $v_j - x$ is minimal in coordinate i . [Figure 3.2](#) shows the regions in which $j \in [n]$ is contained in S_i for $i \in [3]$, based on the position of x in \mathbb{TP}^2 .

Each collection of points with the same type is called a *cell* of the tropical hyperplane arrangement $H_{v_1}^{\max}, \dots, H_{v_n}^{\max}$. Due to the resemblance to ordinary hyperplane arrangements, in which the cells correspond to signed covectors of an oriented matroid, this is also known as the *covector decomposition* [[Jos21](#), Chapter 6.3], and this construction also gives rise to the notion of tropical oriented matroids [[AD09](#)].

A cell of type $S = (S_1, \dots, S_d)$ is bounded if and only if $S_i \neq \emptyset$ for each $i \in [d]$. Such a bounded cell is a *polytrope*, i.e. a tropical polytope that is classically convex [[JK10](#)]. The tropical polytope $P = \text{tconv}(V)$ is the union of all bounded cells in the tropical hyperplane arrangement.

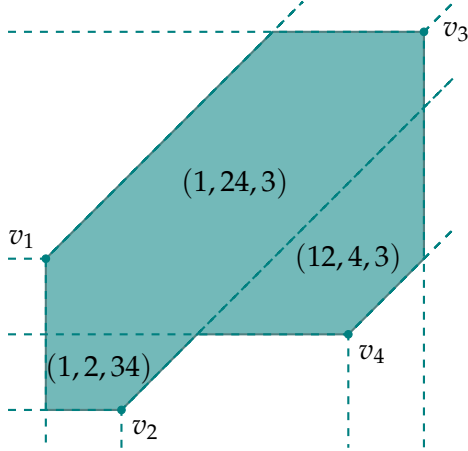


Figure 3.3: The tropical polytope in \mathbb{TP}^2 as given in [Example 3.1.1](#), pictured in the chart where the last coordinate is 0. It is canonically decomposed into three polytopes, labeled with their respective types $S = (S_1, S_2, S_3)$.

Example 3.1.1 (The cells of a tropical polytope). Consider the tropical polytope $P = \text{tconv}(V)$, $V = (v_1, v_2, v_3, v_4)$ with tropical vertices

$$v_1 = \begin{pmatrix} 0 \\ 1 \\ 0 \end{pmatrix}, \quad v_2 = \begin{pmatrix} 1 \\ -1 \\ 0 \end{pmatrix}, \quad v_3 = \begin{pmatrix} 5 \\ 4 \\ 0 \end{pmatrix}, \quad v_4 = \begin{pmatrix} 4 \\ 0 \\ 0 \end{pmatrix}.$$

The max-tropical hyperplanes $H_{v_j}^{\max}$ with apex $v_j, j \in [4]$ induce a subdivision of \mathbb{TP}^2 , and the tropical polytope P is the union of the three maximal cells of this subdivision. The types of the bounded cells are $S = (S_1, S_2, S_3) \in \{(1, 2, 34), (1, 24, 3), (12, 4, 3)\}$, as illustrated in [Figure 3.3](#). We use the shorthand notation $S_j = 12$ for $S_j = \{1, 2\}$. Each of the maximal cells is both classically and tropically convex. Thus, this gives the canonical decomposition of P into polytrope cells. \diamond

The tropical type of a cell depends both on the choice of generators v_1, \dots, v_n as well as on their ordering. However, the tropical vertices, as described in [Section 1.3.1](#), serve as unique minimal set of generators for every tropical polytope [[DS04](#), Proposition 21]. We will see in [Proposition 3.1.5](#) that a polytrope is a tropical simplex, i.e. the number of tropical vertices of a polytrope in \mathbb{TP}^{n-1} is n . Let P be a polytrope and let $v_1, \dots, v_n \in \mathbb{R}^n$ be affine representatives of the tropical vertices of P such that $v_{ii} = 0$ for all $i \in [n]$, and v_1, \dots, v_n are ordered lexicographically. Following [[Tra17](#), Section 4], we define the *lex-type* of P as the tropical type of the unique maximal bounded cell of $\text{tconv}(v_1, \dots, v_n)$. Note that the tropical type is a labeled refinement of the combinatorial type [[DS04](#), Corollary 13]. The combinatorial type is independent of the ordering of the vertices, and thus also the combinatorial type two polytopes of the same lex-type agrees.

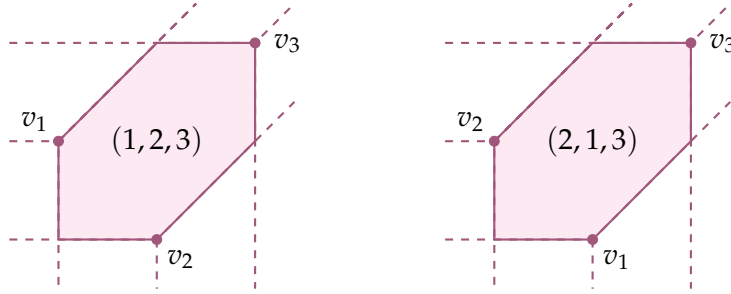


Figure 3.4: The two hexagonal cells with distinct tropical types from Example 3.1.2.

Example 3.1.2 (Two hexagonal cells with distinct tropical types). Consider the tropical convex hulls of the columns of

$$c = \begin{pmatrix} 0 & 1 & 2 \\ 1 & 0 & 2 \\ 0 & 0 & 0 \end{pmatrix} \text{ and } d = \begin{pmatrix} 1 & 0 & 2 \\ 0 & 1 & 2 \\ 0 & 0 & 0 \end{pmatrix},$$

as depicted in Figure 3.4. In both cases the tropical hyperplane arrangement has a unique 2-dimensional bounded cell, which is a hexagon. In the case of c the tropical type of this cell is $(1, 2, 3)$, while for d the type of this cell is $(2, 1, 3)$. Viewed as a polytrope, the lex-type of the bounded cell is $(1, 2, 3)$, since the columns of c are ordered lexicographically. \diamond

Remark 3.1.3. The notion of lex-type follows the definition of tropical type in [Tra17]. This differs from the original definition of the type of a tropical polytope from [DS04], where the ordering of v_1, \dots, v_n is taken into account. Applying the original definition, the two hexagonal cells in Example 3.1.2 are thus considered as tropical polytopes of distinct types, and every permutation of the ordering of v_1, \dots, v_n yields a different type. Choosing a lexicographic order v_1, \dots, v_n , as in [Tra17], the lex-type of P is a representative of the set of all distinct tropical types (in the sense of [DS04]) of polytropes with n tropical vertices up to the action of the symmetric group S_n . The existence of such a representative follows from [Tra17, Section 4]. All cited results in this chapter which concern a count of types refer to the number of lex-types, i.e. modulo the action of the symmetric group. In all other context in this chapter this distinction is irrelevant.

We now describe the connection between polytropes and Kleene stars, which arise in optimization when minimizing the lengths of paths in a weighted directed graph [JS19]. Let $c \in \mathbb{R}^{n^2-n}$. We can identify c with an $(n \times n)$ -matrix having zeros along the diagonal. Under this identification, c describes weights on the edges of a complete directed graph with n vertices, where the entry c_{ij} represents the weight of the edge going from node i to node j . A digraph has a *negative cycle* if there exists a directed cycle whose edge weights sum to a negative number.

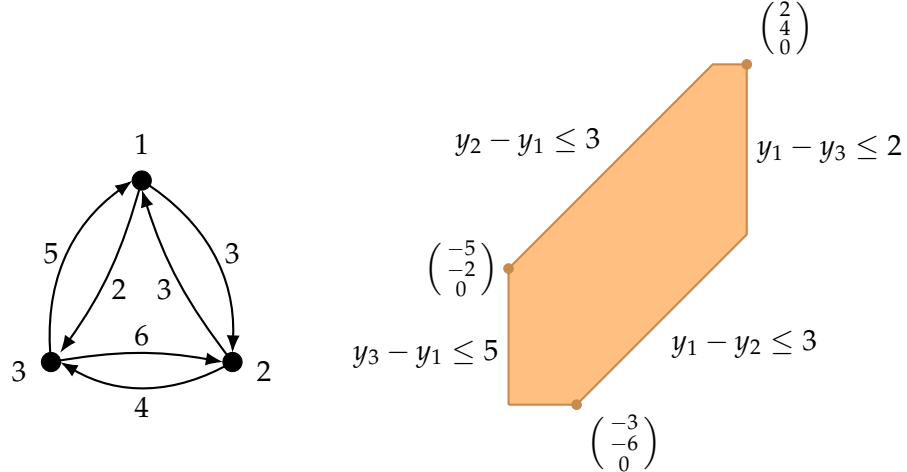


Figure 3.5: The complete directed graph from Example 3.1.4 and polytrope P from Example 3.1.6, both corresponding to the Kleene star $c = (3, 2, 3, 4, 5, 6)$. The polytrope P is pictured in the chart where the last coordinate is zero.

Example 3.1.4 (Weights on digraphs and Kleene stars). Let $n = 3$ and consider the vector $c = (3, 2, 3, 4, 5, 6) \in \mathbb{R}^6$. We view c as the (3×3) -matrix

$$c = \begin{pmatrix} 0 & 3 & 2 \\ 3 & 0 & 4 \\ 5 & 6 & 0 \end{pmatrix},$$

where each off-diagonal entry represents the weight of an edge in a complete directed graph on 3 vertices, as depicted in Figure 3.5. Furthermore, note that in this example the weighted digraph has no negative cycles, and that the coordinate c_{ij} records the weight of the lowest-weight path from node i to node j . We continue with this in Example 3.1.6. \diamond

We define $\mathcal{R}_n \subseteq \mathbb{R}^{n^2-n}$ to be the set of all vectors c with no negative cycles in the corresponding weighted graph. The *Kleene star* $c^* \in \mathbb{R}^{n \times n}$ of c is the $(n \times n)$ -matrix such that c_{ij}^* is the weight of the lowest-weight path from i to j . If c has no negative cycles, then it can be computed as the $(n-1)$ th tropical power $c^* = c^{\odot(n-1)}$ [JS19, Section 2]. In this case, the shortest path from node i to itself is the trivial path, which has length 0. Thus, for any $c \in \mathcal{R}_n$ the Kleene star c^* is zero along the diagonal, and we can again identify c^* with a vector in \mathbb{R}^{n^2-n} . Following [Tra17, Section 2.3.2] the *polytrope region* $\mathcal{P}ol_n \subseteq \mathcal{R}_n \subseteq \mathbb{R}^{n^2-n}$ is the closed polyhedral cone given by

$$\begin{aligned} \mathcal{P}ol_n &= \{c \in \mathcal{R}_n \mid c = c^*\} \\ &= \{c \in \mathbb{R}^{n \times n} \mid c_{ii} = 0, c_{ij} \leq c_{ik} + c_{kj} \text{ for all pairwise distinct } i, j, k \in [n]\}. \end{aligned}$$

Thus, points in the polytrope region correspond to weighted graphs whose edges satisfy the triangle inequality. As the name suggests, the polytrope region parameterizes the set of all polytropes.

PROPOSITION 3.1.5 ([Pue13, Theorem 1], [Tra17, Proposition 12]). Let $P \subseteq \mathbb{TP}^{n-1}$ be a non-empty set. The following statements are equivalent:

- (i) P is a polytrope.
- (ii) There is a matrix $c \in \mathcal{P}ol_n$ such that $P = \text{tconv}(c)$, where the columns of the matrix c are taken as a set of n points in \mathbb{TP}^{n-1} .
- (iii) There is a matrix $c \in \mathcal{P}ol_n$ such that

$$P = \{y \in \mathbb{R}^n \mid y_i - y_j \leq c_{ij}, y_n = 0\}.$$

Furthermore, the matrix c in the last two statements are equal, and uniquely determined by P .

Example 3.1.6 (Polytropes from Kleene stars). The Kleene star c from [Example 3.1.4](#) defines the polytrope $P = \{y \in \mathbb{R}^3 \mid y_i - y_j \leq c_{ij}, y_3 = 0\}$, as depicted in [Figure 3.5](#). Considering the columns of c as points in \mathbb{TP}^2 , the matrix c is equivalent to

$$c = \begin{pmatrix} 0 & 3 & 2 \\ 3 & 0 & 4 \\ 5 & 6 & 0 \end{pmatrix} \sim \begin{pmatrix} -5 & -3 & 2 \\ -2 & -6 & 4 \\ 0 & 0 & 0 \end{pmatrix}.$$

As promised by [Proposition 3.1.5 \(ii\)](#), these are the coordinates of the three tropical vertices of P , i.e. $P = \text{tconv}(c)$. \diamond

Example 3.1.7 (Not all tropical vertices are Kleene stars). There are matrices $d \in \mathbb{R}^{n \times n}$ such that $P = \text{tconv}(d)$, as in condition (ii) from [Proposition 3.1.5](#), but $d \notin \mathcal{P}ol_n$. Indeed, consider the matrix d from [Example 3.1.2](#). Then $P = \text{tconv}(d)$. Viewing the columns of d as points in \mathbb{TP}^2 we obtain

$$d = \begin{pmatrix} 1 & 0 & 2 \\ 0 & 1 & 2 \\ 0 & 0 & 0 \end{pmatrix} \sim \begin{pmatrix} 0 & -1 & 2 \\ -1 & 0 & 2 \\ -1 & -1 & 0 \end{pmatrix}.$$

However, $d_{13} = 2 > 1 = -1 + 2 = d_{12} + d_{23}$ and so $d \notin \mathcal{P}ol_3$. Furthermore, the set $\{y \in \mathbb{R}^3 \mid y_i - y_j \leq d_{ij}, y_3 = 0\}$ is empty. Ordering the columns of the matrix on the right hand side lexicographically yields a matrix which is equivalent to the matrix the matrix c from [Example 3.1.2](#). This is the Kleene star such that $P = \text{tconv}(c) = \{y \in \mathbb{R}^3 \mid y_i - y_j \leq c_{ij}, y_3 = 0\}$. \diamond

The statement from [Proposition 3.1.5](#) implies that polytopes in \mathbb{TP}^{n-1} are tropical simplices, i.e. the tropical convex hull of exactly n points. A polytope of dimension $n - 1$ is *maximal* if it has $\binom{2n-2}{n-1}$ vertices as an ordinary polytope. To see why this is indeed the maximal number of classical vertices, recall from [Theorem 1.3.2](#) that a polytope is dual to a regular subdivision of the product of simplices $\Delta_{n-1} \times \Delta_{n-1}$. The normalized volume of this polytope is $\binom{2n-2}{n-1}$, bounding the number of maximal cells in the regular subdivision and hence the number of vertices of the polytope. This bound is attained in every dimension [[DS04](#), Proposition 19]. Any maximal polytope P is a smooth polytope [[GOT17](#), Chapter 7.3], i.e. a simple polytope whose normal fan is a smooth fan in the sense of [Section 1.1.2](#). Furthermore, if P is maximal, then every inequality $y_i - y_j \leq c_{ij}$ is facet-defining. Thus, the rays of the normal fan are (coordinate projections of) the vectors in direction $e_i - e_j$, $i, j \in [n]$, i.e. the roots in the root system A_n . As a consequence, two maximal polytopes of the same tropical type have the same normal fan.

In the following, we describe how maximal polytopes can be classified through algebraic methods. Let R be the polynomial ring $R = K[x_{ij} \mid (i, j) \in [n]^2, i \neq j]$, where K is a field containing the rational numbers. In [Section 3.2](#) we will choose K to be the fraction field $K = \mathbb{Q}(a_{ij} \mid (i, j) \in [n]^2, i \neq j)$, where the variables a_{ij} define the “indeterminate polytope” $P(a) = \{y \in \mathbb{R}^n \mid y_i - y_j \leq a_{ij}, y_n = 0\}$. We consider the toric ideal

$$I_n = \langle x_{ij}x_{ji} - 1, x_{ij}x_{jk} - x_{ik} \mid i, j, k \in [n] \text{ pairwise distinct} \rangle, \quad (3.1)$$

which appears in [[Tra17](#)] as the toric ideal associated with the all-pairs shortest path program. In the language of [Section 1.7.1](#), this is the toric ideal associated to the matrix A with columns of the form $e_i - e_j$. Let \mathcal{GF}_n be the Gröbner fan of I_n , as described in [Section 1.5](#). The matrix A is known to be (totally) unimodular (cf. [Section 3.2.2](#)), and hence \mathcal{GF}_n is the *chamber complex* of all polytopes with inner facet normals in directions $e_i - e_j$, where $i, j \in [n]$ ([[Stu96](#), Proposition 8.15], [[DLRS10](#), Chapter 5.4]). This means that the normal fan of the polytope

$$P(c) = \{y \in \mathbb{R}^n \mid y_i - y_j \leq c_{ij}, y_n = 0\}$$

is fixed for each relatively open cone (also called *chamber*) C in the chamber complex \mathcal{GF}_n and every point $c \in C$. In other words, the the combinatorial type of $P(c)$ is fixed along an open chamber of \mathcal{GF}_n . Let $\mathcal{GF}_n|_{\mathcal{P}ol_n}$ be the restriction of the Gröbner fan of I_n to the polytope region $\mathcal{P}ol_n$. This polyhedral fan captures the tropical types of polytopes.

THEOREM 3.1.8 ([[Tra17](#), Theorems 17 - 18]). Relatively open cones of $\mathcal{GF}_n|_{\mathcal{P}ol_n}$ are in bijection with lex-types of polytopes in \mathbb{TP}^{n-1} . Maximal open cones of $\mathcal{GF}_n|_{\mathcal{P}ol_n}$ are in bijection with lex-types of maximal polytopes in \mathbb{TP}^{n-1} .

We now illustrate how this result can be used to show that there is a unique lex-type of maximal polytopes in dimension 2.

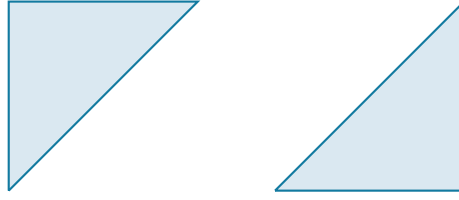


Figure 3.6: The two different types of alcoved triangles.

Example 3.1.9 (The Gröbner fan \mathcal{GF}_3). The toric ideal $I_3 \subseteq K[x_{12}, x_{13}, x_{21}, x_{23}, x_{31}, x_{32}]$ from (3.1) is given by

$$I_3 = \langle x_{12}x_{23}x_{31} - 1, x_{13}x_{31} - 1, x_{21}x_{13}x_{32} - 1, x_{23}x_{32} - 1 \rangle.$$

Using Macaulay2 [GS22] we compute that the Gröbner fan \mathcal{GF}_3 is a complete polyhedral fan in \mathbb{R}^6 , and the lineality space \mathcal{L} of \mathcal{GF}_3 is 2-dimensional. With indexing $w = (w_{12}, w_{13}, w_{21}, w_{23}, w_{31}, w_{32})$ the space \mathcal{L} is spanned by the vectors $(1, 0, -1, -1, 0, 1)$ and $(0, 1, 0, 1, -1, -1)$. Modulo \mathcal{L} , the primitive ray generators of \mathcal{GF}_3 the standard unit vectors e_1, \dots, e_6 , together with the ray generators

$$(1, 0, 0, 0, 0, 1), (0, 0, 1, 0, 1, 0), (0, 0, 0, 0, 1, 1), (0, 0, 1, 1, 1, 0), (0, 0, 1, 0, 1, 1).$$

The fan \mathcal{GF}_3 consists of 18 maximal cones. Restricting to the polytrope region \mathcal{Pol}_3 , the fan $\mathcal{GF}_3|_{\mathcal{Pol}_3}$ consists of a single maximal cone, which corresponds to the unique maximal lex-type in dimension 2. The remaining 17 maximal cones of \mathcal{GF}_3 restrict to proper faces of this cone. 6 of these lower-dimensional cones correspond to pentagons, 9 cones correspond to rectangles and 2 cones to triangles. These triangles are the two different types of alcoved triangles, which are depicted in Figure 3.6. ◇

Recall from Theorem 1.3.2 that a tropical polytope $\text{tconv}(V) \subseteq \mathbb{TP}^{n-1}$ can be described as the polyhedral complex of bounded faces of an unbounded polyhedron \mathcal{P}_V , and is dual to a regular subdivision of the product of simplices $\Delta_{|V|-1} \times \Delta_{n-1}$. If $\text{tconv}(V)$ is a polytrope, then Proposition 3.1.5 implies that $|V| = n$. Even more, $\text{tconv}(V)$ is a polytrope if and only if the bounded region of \mathcal{P}_V consists of a single bounded face [DS04, Theorem 15], and hence all maximal cells in the dual subdivision of $\Delta_{n-1} \times \Delta_{n-1}$ share some vertex. Thus, the types of polytropes are dual to “central subdivisions” of $\Delta_{n-1} \times \Delta_{n-1}$. By (1.1) (on page 16) and the Cayley trick (Section 1.1.3), this is identical to studying coherent mixed subdivisions of the dilated simplex $n\Delta_{n-1}$. Regular subdivisions of products of simplices can hence be related to certain regular subdivisions of the *fundamental polytope* FP_n , a subpolytope of $n\Delta_{n-1}$ (up to translation), introduced by Vershik [Ver15] and further studied by Delucchi and Hoessly [DH20]. The fundamental polytope FP_n (or *root polytope of type A*) is defined as

$$FP_n = \text{conv}(e_i - e_j \mid i \neq j \in [n]).$$

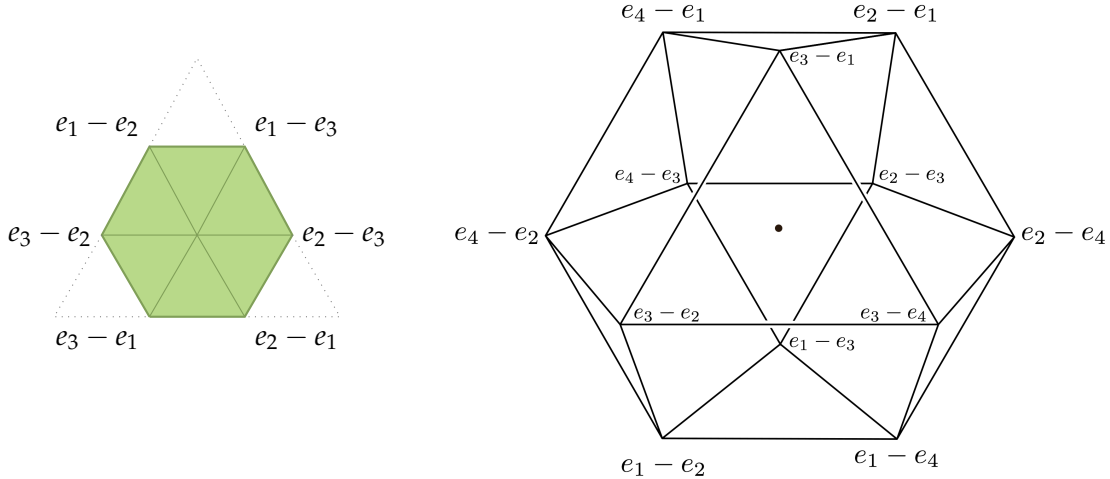


Figure 3.7: The fundamental polytopes from Example 3.1.10. Left: The fundamental polytope FP_3 with its unique central subdivision. Right: The fundamental polytope FP_4 with unique interior lattice point $\mathbb{0}$.

The fundamental polytopes FP_3 and FP_4 are pictured in Figure 3.7. A *regular central subdivision* of FP_n is a regular subdivision in which the unique relative interior lattice point $\mathbb{0}$ of FP_n is a vertex of each maximal cell. These central subdivisions were studied in [ABH+11] as subdivisions of the boundary of the root polytope of type A .

Example 3.1.10 (The fundamental root polytopes FP_3 and FP_4). If $n = 2$, then the fundamental polytope FP_3 coincides with the permutohedron Π_3 (up to translation by the vector $(2, 2, 2)^t$). This is a 2-dimensional polytope with 6 vertices, containing the origin as its only interior lattice point. It has a single regular central triangulation, which is in bijection with the unique lex-type of maximal polytopes in TP^2 . Figure 3.7 shows FP_3 as a subpolytope of the dilated and translated simplex $3\Delta_2 - (1, 1, 1)^t$, and the fundamental polytope FP_4 . \diamond

The number of lex-types of polytopes can be enumerated using the following theorem.

THEOREM 3.1.11 ([JS19, Theorem 22]). The types of full-dimensional polytopes in TP^{n-1} are in bijection with regular central subdivisions of FP_n .

In dimension 2, the hexagon is the unique lex-type of maximal polytopes, as can be seen in Example 3.1.9. In dimension 3 there are 6 distinct maximal types [JK10; JP12]. Using Theorem 3.1.8, [Tra17] showed that in dimension 4 there are 27 248 distinct types. In higher dimensions, this number is unknown. These type counts were independently confirmed in [JS19] using the identification in Theorem 3.1.11. We relate our computational results to regular central subdivisions of the fundamental polytope in Sections 3.4.3 and 3.4.4.

3.2 MULTIVARIATE VOLUME POLYNOMIALS

We seek to compute a *multivariate volume polynomial* for each tropical type of polytropes. That is, for each fixed tropical type we compute a polynomial $\hat{q}(a)$ in variables a_{ij} , where $i, j \in [n], i \neq j$ such that, when c^* is a Kleene star defining a polytrope $P = P(c^*)$ of the respective tropical type, the polynomial \hat{q} evaluates to the normalized volume of the polytrope $\hat{q}(c^*) = \text{Vol}(P(c^*))$. For each maximal tropical type, our computation of such a polynomial will depend on a fixed Kleene star c^* of the appropriate type. In this and the following sections we introduce the multivariate polynomials of interest and describe methods for computing these functions for polytropes, motivated by the methods in [Tra17] and [DLS03]. Throughout this chapter, we assume that $P(c^*)$ is a lattice polytope unless stated otherwise, i.e. that c^* is an integer vector. Furthermore, we will always measure the volume of a polytope P inside its affine span. For simplicity we abbreviate the Euclidean volume by $\text{vol}(P) = \text{vol}_{\dim(P)}(P)$ and the discrete volume by $\text{Vol}(P) = \text{Vol}_{\dim(P)}(P)$ throughout this chapter.

3.2.1 The Toric Variety of a Polytrope

In order to compute multivariate volume polynomials of polytropes we use methods from toric geometry as described in [Section 1.7](#). Let P be a maximal polytrope, i.e. $P = P(c^*)$ with

$$P(c^*) = \left\{ y \in \mathbb{R}^{n-1} \mid y_i - y_j \leq c^*, y_n = 0 \right\}$$

for some Kleene star $c^* \in \mathcal{P}ol_n$ inside a maximal open region of $\mathcal{P}ol_n$. Let u_{ij} denote the primitive ray generators of the (inner) normal fan $\Sigma(c^*)$ of $P(c^*)$, i.e. $u_{ij} = -(e_i - e_j)$ for $(i, j) \in [n-1]^2, i \neq j$ and $u_{in} = -e_i, u_{ni} = e_i$ for $i \in [n-1]$. Recall that if P is maximal, then all these $n^2 - n$ vectors indeed span rays of the fan $\Sigma(c^*)$. Let $X_{\Sigma(c^*)}$ be the normal toric variety defined by the fan $\Sigma(c^*)$. Since the normal fan of $P(c^*)$ is a smooth fan (as defined in [Section 1.1.2](#)) the variety $X_{\Sigma(c^*)}$ is smooth. We denote by D_{ij} the torus-invariant prime divisor corresponding to the ray u_{ij} . Then the polytope $P(c^*)$ corresponds to the divisor

$$D_{P(c^*)} = \sum_{\substack{ij \in [n] \times [n] \\ i \neq j}} c_{ij}^* D_{ij}.$$

Let K be a field of characteristic 0 and $R = K[x_{ij} \mid (i, j) \in [n]^2, i \neq j]$. At the end of this section we will make the choice $K = \mathbb{Q}(a_{ij} \mid (i, j) \in [n]^2, i \neq j)$ for indeterminates a_{ij} . Recall from [Section 1.7.1](#) that the variable x_{ij} corresponds to the ray u_{ij} and thus the facet of $P(c^*)$ that lies in the hyperplane $\langle y, u_{ij} \rangle = c_{ij}^*$. As described in [Section 1.7.2](#), the normalized volume of $P(c^*)$ can be computed via the toric variety $X_{\Sigma(c^*)}$ from the coefficient δ , where δx^α is the normal form of

$$\sum_{\substack{i,j \in [n] \\ i \neq j}} c_{ij}^* x_{ij}$$

inside the quotient ring $R/(L + M)$, and x^α corresponds to a choice of a basis of the top cohomology group. Here, M is the Stanley-Reisner ideal of the boundary complex of $\partial P(c^*)^\circ$ and L is the ideal

$$L = \left\langle \sum_{\substack{ij \in [n] \times [n] \\ i \neq j}} \langle b, u_{ij} \rangle x_{ij} \mid b \in \mathcal{B} \right\rangle,$$

where \mathcal{B} is any basis for \mathbb{Z}^n . Choosing \mathcal{B} to be the standard basis for \mathbb{Z}^n , for a given vector $b = e_k$ we get

$$\sum_{\substack{ij \in [n] \times [n] \\ i \neq j}} \langle e_k, u_{ij} \rangle x_{ij} = \sum_{j \in [n]} x_{kj} - \sum_{j \in [n]} x_{jk}$$

and so the ideal is equal to

$$L = \left\langle \sum_{j \in [n]} x_{kj} - \sum_{j \in [n]} x_{jk} \mid k \in [n] \right\rangle.$$

Considering the complete directed graph K_n on n vertices, this ideal can be viewed as generated by the cuts of K_n that isolate a single vertex.

The main idea of this section is the following. We consider the “indeterminate polytrope”

$$P(a) = \{y \in \mathbb{R}^n \mid y_i - y_j \leq a_{ij}, y_n = 0\},$$

defined by indeterminates a_{ij} . When evaluated at a Kleene star $c^* \in \mathcal{P}ol_n$, the polytope $P(c^*)$ is a polytrope, and for any maximal open region $C \in \mathcal{GF}|_{\mathcal{P}ol_n}$ the tropical type of the maximal polytrope is fixed. Inside this region, all polytropes have the same normal fan $\Sigma = \Sigma(c^*)$. Restricted to such a chamber, the coordinates of each vertex are linear functionals in variables a_{ij} . Thus, inside a chamber the volume is a polynomial in variables a_{ij} .

Formally, let $K = \mathbb{Q}(a_{ij} \mid (i, j) \in [n]^2, i \neq j)$ and $C \in \mathcal{GF}|_{\mathcal{P}ol_n}$ a maximal open chamber in the polytrope region. Then there is a polynomial $q = q_C$ such that for each $c^* \in C$ holds

$$q(c^*) = \text{Vol}(P(c^*)).$$

We refer to this polynomial as the *volume polynomial*, which is, up to a correcting factor $\gamma \in K$, given by the leading coefficient δ of the normal form

$$\delta x^\alpha = \sum_{\substack{i,j \in [n] \\ i \neq j}} a_{ij} x_{ij}$$

inside the ring $R/(L + M)$. In the following section, we determine the ideal M and the correcting factor of δ by combining results from [DLS03; BY06; Tra17].

3.2.2 Computing Multivariate Volume Polynomials

We continue the discussion from [Section 3.2.1](#) in order to compute multivariate volume polynomials of polytropes. It remains to determine the ideal M and the correcting factor of δ . For both of these purposes we first show that polytropes fit into the framework of [DLS03], i.e. that there exists a nonnegative unimodular matrix A such that $P(a) = \{y \in \mathbb{R}_{\geq 0}^{n^2-n} \mid Ay = Aa, x \geq 0\}$ and $\ker(A) \cap \mathbb{R}_{>0}^n = \emptyset$, and all column sums are positive. Recall that a matrix is *totally unimodular* if every minor equals $-1, 0$, or 1 . We note that every nonnegative totally unimodular matrix is unimodular in the sense of [DLS03].

PROPOSITION 3.2.1. Let $P(a)$ be the indeterminate polytope. Then there exists a nonnegative totally unimodular matrix A such that $P(a) = \{y \in \mathbb{R}_{\geq 0}^{n^2-n} \mid Ay = Aa, x \geq 0\}$ and $\ker(A) \cap \mathbb{R}_{>0}^n = \emptyset$, and all column sums are positive.

Proof. Consider $P(a) = \{y \in \mathbb{R}^n \mid y_i - y_j \leq a_{ij}, y_n = 0\}$. As $P(a)$ is contained in the linear space given by $y_n = 0$, we can project onto the first $n - 1$ coordinates, which yields

$$P(a) = \{y \in \mathbb{R}^{n-1} \mid By \leq a\}$$

for a suitable matrix $B \in \mathbb{Z}^{(n^2-n) \times (n-1)}$ with rows B_{ij} indexed by $(i, j) \in [n]^2, i \neq j$. More precisely, if $i, j \in [n - 1]$ then $B_{ij} = e_i - e_j$, and $B_{in} = e_i, B_{nj} = -e_j$.

For each inequality $y_i - y_j \leq a_{ij}$ we introduce a nonnegative slack variable $y_{ij} \geq 0$ and replace the inequality by the equation $y_i - y_j + y_{ij} = a_{ij}$. Furthermore, we replace the inequalities $y_i \leq a_{in}, -y_j \leq a_{nj}$ by equations $y_i + y_{in} = a_{in}, -y_j + y_{nj} = a_{nj}$. This gives a representation as $(B \mid Id_n) y = a$ with $y = (y_1, \dots, y_{n-1}, y_{12}, \dots, y_{n-1,n})$.

In particular, we have the equation $-y_j + y_{nj} = a_{nj}$. We can thus substitute the variable y_j by $y_{nj} - a_{nj}$, which leaves us with a system of equations of the form

$$y_{ij} + y_{ni} - y_{nj} = a_{ij} + a_{ni} - a_{nj} \tag{3.2}$$

$$y_{jn} + y_{nj} = a_{jn} + a_{nj}. \tag{3.3}$$

This system of equations only involves the nonnegative variables $y_{ij}, i, j \in [n], i \neq j$. Adding these equations gives

$$y_{ij} + y_{ni} + y_{jn} = a_{ij} + a_{ni} + a_{jn}. \tag{3.2'}$$

The set of solutions to the system with equations (3.2) and (3.3) is equal to the set of solutions to the system with (3.2') and (3.3), yielding a nonnegative matrix A with

positive column sums, such that

$$P(a) = \left\{ y \in \mathbb{R}_{\geq 0}^{n^2-n} \mid Ay = Aa \right\}$$

and $\ker(A) \cap \mathbb{R}_{\geq 0}^{n^2-n} = \emptyset$. It is well-known that the constraint matrix B is totally unimodular [Tra17, Section 2.3.3]. This property is preserved under the operations we applied to obtain the matrix A , and hence A is totally unimodular. \square

Remark 3.2.2. The expressions $a_{ij} + a_{ni} + a_{jn}$ and $a_{in} + a_{ni}$ can be interpreted in terms shortest paths of the complete digraph. These are the weights of the shortest cycle passing through i and n and the shortest directed cycle passing through i, j and n respectively.

Example 3.2.3 (The matrix A in dimension 2). Any 2-dimensional polytrope $P(a)$ has a description in terms of inequalities as

$$P(a) = \left\{ \begin{pmatrix} y_1 \\ y_2 \end{pmatrix} \in \mathbb{R}^2 \mid \begin{array}{l} y_1 - y_2 \leq a_{12}, y_2 - y_1 \leq a_{21} \\ y_1 \leq a_{13}, y_2 \leq a_{23} \\ y_1 \geq -a_{31}, y_2 \geq -a_{32} \end{array} \right\},$$

when a is contained in the polytrope region $\mathcal{P}ol_3$. We want to compute the constraint matrix A by turning the above description of a polytrope into one involving only equalities, mimicking the proof of [Proposition 3.2.1](#). We begin by translating the above to a matrix description of $P(a)$:

$$\begin{pmatrix} 1 & -1 \\ 1 & 0 \\ -1 & 1 \\ 0 & 1 \\ -1 & 0 \\ 0 & -1 \end{pmatrix} \begin{pmatrix} y_1 \\ y_2 \end{pmatrix} \leq \begin{pmatrix} a_{12} \\ a_{13} \\ a_{21} \\ a_{23} \\ a_{31} \\ a_{32} \end{pmatrix}$$

Introducing slack variables y_{ij} , we get the representation

$$\begin{pmatrix} 1 & -1 & 1 & 0 & 0 & 0 & 0 & 0 \\ 1 & 0 & 0 & 1 & 0 & 0 & 0 & 0 \\ -1 & 1 & 0 & 0 & 1 & 0 & 0 & 0 \\ 0 & 1 & 0 & 0 & 0 & 1 & 0 & 0 \\ -1 & 0 & 0 & 0 & 0 & 0 & 1 & 0 \\ 0 & -1 & 0 & 0 & 0 & 0 & 0 & 1 \end{pmatrix} \begin{pmatrix} y_1 \\ y_2 \\ y_{12} \\ y_{13} \\ y_{21} \\ y_{23} \\ y_{31} \\ y_{32} \end{pmatrix} = \begin{pmatrix} a_{12} \\ a_{13} \\ a_{21} \\ a_{23} \\ a_{31} \\ a_{32} \end{pmatrix}.$$

Substituting $y_1 = y_{31} - a_{31}$, $y_2 = y_{32} - a_{32}$ and deleting zero-columns and zero-rows gives us

$$\begin{pmatrix} 1 & 0 & 0 & 0 & 1 & -1 \\ 0 & 1 & 0 & 0 & 1 & 0 \\ 0 & 0 & 1 & 0 & -1 & 1 \\ 0 & 0 & 0 & 1 & 0 & 1 \end{pmatrix} \begin{pmatrix} y_{12} \\ y_{13} \\ y_{21} \\ y_{23} \\ y_{31} \\ y_{32} \end{pmatrix} = \begin{pmatrix} a_{12} + a_{31} - a_{32} \\ a_{13} + a_{31} \\ a_{21} - a_{31} + a_{32} \\ a_{23} + a_{32} \end{pmatrix}.$$

This is a system of equations of the form (3.2) and (3.3). Replacing them by the system of equations as given in (3.2') and (3.3') yields

$$Ay = \begin{pmatrix} 1 & 0 & 0 & 1 & 1 & 0 \\ 0 & 1 & 0 & 0 & 1 & 0 \\ 0 & 1 & 1 & 0 & 0 & 1 \\ 0 & 0 & 0 & 1 & 0 & 1 \end{pmatrix} \begin{pmatrix} y_{12} \\ y_{13} \\ y_{21} \\ y_{23} \\ y_{31} \\ y_{32} \end{pmatrix} = \begin{pmatrix} a_{12} + a_{23} + a_{31} \\ a_{13} + a_{31} \\ a_{21} + a_{13} + a_{32} \\ a_{23} + a_{32} \end{pmatrix} = Aa.$$

This gives us the desired representation $P(a) = \{y \in \mathbb{R}_{\geq 0}^{n^2-n} \mid Ay = Aa\}$. \diamond

Let $K = \mathbb{Q}(a_{ij} \mid (i, j) \in [n]^2, i \neq j)$, for indeterminate variables a_{ij} , and consider the polynomial ring $R = K[x_{ij} \mid (i, j) \in [n]^2, i \neq j]$. Following [DLS03], we consider the toric ideal $I \subseteq R$ seen previously in Section 3.1:

$$I_n = \langle x^r - 1 \mid r \text{ is a row of } A \rangle = \langle x_{in}x_{ni} - 1, x_{ij}x_{jn}x_{ni} - 1 \rangle = \langle x_{ij}x_{ji} - 1, x_{ij}x_{jk} - x_{ik} \rangle,$$

where $(i, j, k) \in [n]^3$ are pairwise distinct. For our purposes, i.e. for $n \leq 5$, the equality of these ideals can be verified computationally e.g. with Macaulay2 [GS22].

Fix a maximal tropical type and a Kleene star c^* corresponding to a polytrope $P(c^*)$ of that type. We write $M = \text{in}_{c^*}(I_n)$ for the initial ideal of I_n with respect to the weight vector c^* .

PROPOSITION 3.2.4 ([DLS03, Corollary 2.2]). The initial ideal M is the Stanley-Reisner ideal of the normal fan $\Sigma(c^*)$ of the simple polytope $P(c^*)$.

In order to compute the volume polynomial, we would like to apply Algorithm 3.2.6. For this, we need to know the minimal prime ideals of M . A prime ideal is a *minimal prime ideal* over I_n (or a *minimal prime of I_n*) if it is minimal (with respect to inclusion) among all prime ideals containing I_n .

PROPOSITION 3.2.5 ([BY06, Lemmas 5 and 6], [DLS03]). The facets of $P(c^*)$ are in bijection with variables x_{ij} of $R/(L + M)$. The vertices of $P(c^*)$ are in bijection with minimal primes of M .

In the above bijection, the facet F_{ij} given by the inequality $y_i - y_j = c_{ij}^*$ is identified with the variable x_{ij} . A vertex v of the polytrope can be identified with the minimal prime $\langle x_{ij} \mid ij \notin \mathcal{I}_v \rangle$, where $\mathcal{I}_v = \{ij \mid F_{ij} \text{ contains } v\}$. Thus, a minimal prime is generated by variables which correspond to facets that do not contain a given vertex v .

We fix a maximal open cone $C \in \mathcal{GF}|_{\mathcal{P}ol_n}$ and a Kleene star $c^* \in C$. Recall that $X_{\Sigma(c^*)}$ is the smooth toric variety defined by the normal fan $\Sigma(c^*)$ of the maximal polytrope $P(c^*)$, and that we consider $X_{\Sigma(c^*)}$ as a variety defined over $K = \mathbb{Q}(a_{ij} \mid (i,j) \in [n]^2, i \neq j)$. Let D be the divisor on $X_{\Sigma(c^*)}$ corresponding to the polytrope $P(a)$ given by the indeterminates a_{ij} , i.e. $P(a) = \{y \in \mathbb{R}^n \mid y_i - y_j \leq a_{ij}, y_n = 0\}$. We can write D as

$$D = \sum_{\substack{ij \in [n] \times [n] \\ i \neq j}} a_{ij} D_{ij},$$

where D_{ij} is the prime divisor corresponding to the ray of $\Sigma(c^*)$ spanned by $u_{ij} = e_j - e_i$. Recall from [Section 1.7.2](#) that (the cohomology class of) the divisor D_{ij} corresponds to the variable x_{ij} in $R/(L + M)$. Let

$$q = \sum_{\substack{ij \in [n] \times [n] \\ i \neq j}} a_{ij} x_{ij}$$

be the polynomial in $R/(L + M)$ representing the cohomology class $[D]$ of the divisor D . Since the dimension of any polytrope is $n - 1$ when being defined by a Kleene star in $\mathcal{GF}|_{\mathcal{P}ol_n}$, we can compute the volume polynomial restricted to the open maximal cone $C \in \mathcal{GF}|_{\mathcal{P}ol_n}$ by

$$\text{Vol}(P(a)) = \int_{X_{\Sigma(c^*)}} [D]^{n-1}.$$

The intersection number $\int_{X_{\Sigma(c^*)}} [D]^{n-1}$ is a constant in $R/(L + M)$ and thus a rational function with variables a_{ij} . In the following we present an algorithm to compute the integral of a cohomology class of $X_{\Sigma(c^*)}$ inside $R/(L + M)$, which we can apply to q^{n-1} , i.e. the polynomial representing $[D]^{n-1}$. In other words, if the input of [Algorithm 3.2.6](#) is given by the polynomial $p = q^{n-1}$, the output is a multivariate volume polynomial which is valid for every $d^* \in C$.

Algorithm 3.2.6 (Computing the integral of a cohomology class of a toric variety X).

- INPUT:** A polynomial $p(x)$ with coefficients in a field $K \supset \mathbb{Q}$.
OUTPUT: The integral $\int_X p$ of the corresponding cohomology class on X .
- 1: Compute a Gröbner basis \mathcal{G} for the ideal $L + M$.
 - 2: Find a minimal prime $\langle x_j \mid x_j \notin \mathcal{I}_v \rangle$ of M , and compute the normal form of $\prod_{i \in \mathcal{I}_v} x_i$ modulo the Gröbner basis \mathcal{G} . It looks like $\gamma \cdot x^\alpha$, where γ is a non-zero element of K and x^α is the unique standard monomial of degree $n - 1$.
 - 3: Compute the normal form of p modulo \mathcal{G} and let $\delta \in k$ be the coefficient of x^α in that normal form.
 - 4: Output the scalar $\delta/\gamma \in K$.

This algorithm appeared as [DLS03, Algorithm A] and the correctness of the algorithm follows from [DLS03, Sections 2–3]. Note that γ is independent of the choice of the minimal prime $\langle x_j \mid x_j \notin \mathcal{I}_v \rangle$ in (2). This can be seen from the fact that $X_{\Sigma(c^*)}$ is smooth, and hence any two monomials $\prod_{i \in \mathcal{I}_v} x_i$ are congruent to each other modulo $L + M$. The entire discussion above implies the following theorem.

THEOREM 3.2.7. Let $C \in \mathcal{GF}_n|_{\mathcal{P}ol_n}$ be a maximal open cone, fix $c^* \in C$ and consider the “indeterminate polytrope”

$$P(a) = \{y \in \mathbb{R}^n \mid y_i - y_j \leq a_{ij}, y_n = 0\},$$

with fixed normal fan $\Sigma(c^*)$. Let $K = \mathbb{Q}(a_{ij} \mid (i, j) \in [n]^2, i \neq j)$, let R denote the polynomial ring with coefficients in K and

$$q = \sum_{\substack{ij \in [n] \times [n] \\ i \neq j}} a_{ij} x_{ij}$$

be the polynomial in $R/(L + M)$ in variables x_{ij} and indeterminates $a_{ij} \in K$. Using $p = q^{n-1}$ as the input of [Algorithm 3.2.6](#), the output $\frac{\delta}{\gamma} \in K$ is a multivariate volume polynomial in variables a_{ij} , i.e.

$$\text{Vol}_C(a) = \frac{\delta}{\gamma},$$

such that for every $d^* \in C$ the normalized volume of $P(d^*)$ is $\text{Vol}(P(d^*)) = \text{Vol}_C(d^*)$.

Remark 3.2.8. Recall that $\mathcal{GF}_n|_{\mathcal{P}ol_n}$ is the restriction of the Gröbner fan of I_n to the polytrope region $\mathcal{P}ol_n$. By [Theorem 3.1.8](#), maximal open cones of $\mathcal{GF}_n|_{\mathcal{P}ol_n}$ are in bijection with types of maximal polytropes. Since [Algorithm 3.2.6](#) only depends on $\text{in}_{c^*}(I_n)$ and not on the choice of c^* itself, the multivariate volume polynomial is constant along an open cone of $\mathcal{GF}_n|_{\mathcal{P}ol_n}$. This reflects the fact that polytropes of the same tropical type have the same normal fan. Therefore, maximal polytropes of the same type have the same multivariate volume polynomial, and it suffices to compute

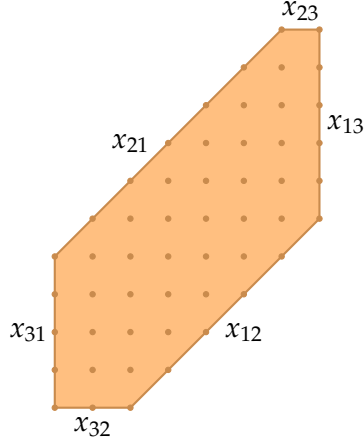


Figure 3.8: The polytrope $P(c^*)$ corresponding to $c^* = (3, 2, 3, 4, 5, 6)$. The facets are in bijection with variables in R and vertices are in bijection with minimal primes of I_3 .

the polynomial for only one representative c^* for each maximal cone. Furthermore, the polynomials agree on the intersection of the closure of two of these cones [Stu95]. Thus, given a Kleene star c^* corresponding to a non-maximal polytrope $P(c^*)$, we can choose any of the maximal closed cones that contain c^* and evaluate the corresponding multivariate volume polynomial at c^* to compute the volume of $P(c^*)$.

Example 3.2.9 (The volume polynomial in dimension 2). We apply the above discussion to compute the multivariate volume polynomial for 2-dimensional polytropes. Note that the volume, Ehrhart- and h^* -polynomial of the hexagon can be derived by more elementary methods as, for example, counting unimodular simplices in an alcoved triangulation and Pick's formula. However, as the presentation is less instructive in dimensions 3 and 4, we showcase the algebraic machinery on this example. As in Example 3.1.9, the toric ideal I_3 is

$$I_3 = \langle x_{12}x_{23}x_{31} - 1, x_{13}x_{31} - 1, x_{21}x_{13}x_{32} - 1, x_{23}x_{32} - 1 \rangle.$$

We also have L as

$$L = \langle x_{12} + x_{13} - x_{21} - x_{31}, x_{21} + x_{23} - x_{12} - x_{32}, x_{31} + x_{32} - x_{13} - x_{23} \rangle.$$

Let $c^* = (3, 2, 3, 4, 5, 6)$ as in Examples 3.1.4 and 3.3.4. By Example 3.1.9 the restriction $\mathcal{GF}_3|_{\mathcal{P}_{ol_3}}$ consists of a single open maximal cone containing c^* . The corresponding polytrope $P(c^*)$ is the hexagon displayed in Figure 3.8, with facets labeled according to Proposition 3.2.5.

Using Macaulay2, we compute that the initial ideal M of I_3 with respect to the weight vector c^* is

$$M = \langle x_{12}x_{21}, x_{13}x_{21}, x_{12}x_{23}, x_{12}x_{31}, x_{13}x_{31}, x_{23}x_{31}, x_{13}x_{32}, x_{21}x_{32}, x_{23}x_{32} \rangle.$$

A Gröbner basis for $L + M$ is given by

$$\mathcal{G} = \langle x_{31} - x_{12} + x_{21} - x_{13}, x_{13}x_{21}, x_{12}x_{13} + x_{13}^2, x_{32} - x_{23} + x_{12} - x_{21}, x_{13}x_{23} + x_{13}^2, \\ x_{21}^2 - x_{13}^2, x_{12}x_{21}, x_{12}^2 - x_{13}^2, x_{13}^3, x_{21}x_{23} + x_{13}^2, x_{12}x_{23}, x_{23}^2 - x_{13}^2 \rangle.$$

Any vertex gives us a minimal prime. We choose the vertex v incident to the facets labeled by x_{31} and x_{32} , giving us the minimal prime $\langle x_{ij} \mid ij \notin \mathcal{I}_v \rangle = \langle x_{12}, x_{13}, x_{21}, x_{23} \rangle$ and the monomial $\prod_{ij \in \mathcal{I}_v} x_{ij} = x_{31}x_{32}$. Modulo the Gröbner basis \mathcal{G} , this has normal form $\gamma \cdot x^\alpha = (-1)x_{13}^2$, so $\gamma = -1$ and $x^\alpha = x_{13}^2$.

Let $q = \sum_{\substack{ij \in [3]^2 \\ i \neq j}} a_{ij}x_{ij}$. This is the polynomial in $R/(L + M)$ corresponding to the divisor described in [Section 3.2](#). We want to compute the volume of the polytrope $P(c^*)$ by applying [Algorithm 3.2.6](#) to $p = q^2$. The normal form of the polynomial q^2 modulo \mathcal{G} is

$$(a_{12}^2 - 2a_{12}a_{13} + a_{13}^2 + a_{21}^2 - 2a_{13}a_{23} - 2a_{21}a_{23} \\ + a_{23}^2 - 2a_{21}a_{31} + a_{31}^2 - 2a_{12}a_{32} - 2a_{31}a_{32} + a_{32}^2)x_{13}^2,$$

so the coefficient δ of x^α gives us the volume polynomial for the normalized volume

$$\text{Vol}(a) = \frac{\delta}{\gamma} = -(a_{12}^2 - 2a_{12}a_{13} + a_{13}^2 + a_{21}^2 - 2a_{13}a_{23} - 2a_{21}a_{23} \\ + a_{23}^2 - 2a_{21}a_{31} + a_{31}^2 - 2a_{12}a_{32} - 2a_{31}a_{32} + a_{32}^2).$$

Evaluating at the original vector c^* gives 79, which is the normalized volume of the original polytope. The volume polynomial $\text{vol}(a)$ for the Euclidean volume of $P(a)$ is given as

$$\text{vol}(a) = \frac{1}{2} \text{Vol}(a).$$

The fact that $\mathcal{GF}_3|_{\mathcal{P}_{ol_3}}$ consists of a single maximal cone, together with [Remark 3.2.8](#) implies that this polynomial is a universal volume polynomial, which computes the volume of every 2-dimensional polytrope. \diamond

Remark 3.2.10. The volumes of polytropes were studied in the language of alcoved polytopes of type A in [[LP07](#), Theorem 3.2], and this theory was extended to general root systems in [[LP18](#), Theorem 8.2]. The normalized volume of an alcoved polytope is described as a sum of discrete volumes of alcoved simplices. More specifically, given a fixed alcoved polytope of type A , the normalized volume of the respective polytope P can be computed as

$$\text{Vol}(P) = \sum_{\sigma \in S_{n-1}} |P_\sigma \cap \mathbb{Z}^{n-1}|,$$

where $P_\sigma = \{x \in \mathbb{R}^{n-1} \mid x + \Delta_\sigma \subseteq P\}$ and

$$\Delta_\sigma = \left\{ y \in \mathbb{R}^{n-1} \mid 0 \leq y_{\sigma(1)} \leq \dots \leq y_{\sigma(n-1)} \leq 1 \right\}.$$

This is a formula yields a value for the normalized volume for polytropes of any dimension. At the same time, as the expression $x + \Delta_\sigma \subseteq P$ in the definition of P_σ is of semialgebraic nature, it does seem clear how to utilize this approach to obtain multivariate polynomials using algebraic methods.

3.3 MULTIVARIATE EHRHART AND h^* -POLYNOMIALS

In this section we describe how to compute the multivariate analogues of the Ehrhart and the h^* -polynomial for polytropes. An introduction to Ehrhart polynomials and h^* -polynomials is given in [Section 1.1.4](#). In order to obtain such a multivariate Ehrhart polynomial, we fix a tropical type of polytropes and apply the Todd operator to the respective multivariate volume polynomial. We then extend to multivariate h^* -polynomials by applying a change of basis to the Ehrhart polynomial, which involves the use of Eulerian polynomials.

3.3.1 Computing multivariate Ehrhart polynomials

As in the previous section, let $C \in \mathcal{GF}|_{\mathcal{P}ol_n}$ be a maximal open cone, $c^* \in C$ and $P(c^*)$ be a lattice polytope given by inequalities

$$P(c^*) = \left\{ x \in \mathbb{R}^{n-1} \mid x_i - x_j \leq c_{ij}^*, -c_{ni}^* \leq x_i \leq c_{in}^* \right\}.$$

Recall from [Section 1.1.4](#) that the Ehrhart polynomial $\text{ehr} : \mathbb{Z} \rightarrow \mathbb{Z}$ counts the number of lattice points in an integer dilate of a lattice polytope when evaluated at a positive integer, i.e.

$$\text{ehr}_{P(c^*)}(k) = \left| kP(c^*) \cap \mathbb{Z}^{n-1} \right| = \left| \left\{ x \in \mathbb{R}^{n-1} \mid x_i - x_j \leq kc_{ij}^*, -kc_{ni}^* \leq x_i \leq kc_{in}^* \right\} \right|.$$

Thus, the Ehrhart polynomial of $P(c^*)$ counts lattice points in the class of lattice polytopes that can be obtained by uniformly translating the all facet-defining hyperplanes of $P(c^*)$ simultaneously. The multivariate lattice point counting function $\text{ehr}_C(a) : \mathbb{Z}^{n^2-n} \rightarrow \mathbb{Z}$ is given by

$$\text{ehr}_C(a) = \left| \left\{ x \in \mathbb{R}^{n-1} \mid x_i - x_j \leq a_{ij}, -a_{ni} \leq x_i \leq a_{in} \right\} \right|,$$

where we allow the facet-defining hyperplanes to translate independently from each other, preserving (or possibly coarsening) the normal fan $\Sigma(c^*)$. As we will see, the restriction of the lattice point counting function $\text{ehr}_C(a)|_C : C \cap \mathbb{Z}^{n^2-n} \rightarrow \mathbb{Z}$ is a polynomial in variables a_{ij} . We use the Todd operator to pass from multivariate volume polynomials to these multivariate Ehrhart polynomials of polytropes. We begin by defining single and multivariate versions of the Todd operator, following [\[BR15, Chapter 12\]](#) and [\[CLS11, Chapter 13.5\]](#), and then explain the method we used for computations. Finally, we illustrate these methods by computing the multivariate and univariate

Ehrhart polynomials of the hexagon from [Example 3.2.9](#).

The Todd operator is related to the Bernoulli numbers, a sequence of rational numbers B_k for $k \in \mathbb{Z}_{\geq 0}$ whose first few terms are $1, -\frac{1}{2}, \frac{1}{6}, 0, -\frac{1}{30}, 0$. They are defined through the generating function

$$\frac{z}{\exp(z) - 1} = \sum_{k \geq 0} \frac{B_k}{k!} z^k.$$

Definition 3.3.1. The *Todd operator* is the differential operator

$$\text{Todd}_h = 1 + \sum_{k \geq 1} (-1)^k \frac{B_k}{k!} \left(\frac{d}{dh} \right)^k.$$

Note that for a univariate polynomial $f(h)$ of degree d we have $(\frac{df}{dh})^k = 0$ for any $k > d$. Thus, restricting to polynomials of degree at most d yields $\text{Todd}_h : K[x]_{\leq d} \rightarrow K[x]_{\leq d}$, where we obtain the finite expression

$$\text{Todd}_h(f) = 1 + \sum_{k=1}^d (-1)^k \frac{B_k}{k!} \left(\frac{df}{dh} \right)^k,$$

i.e. $\text{Todd}_h(f)$ is a polynomial. The Todd operator can be succinctly expressed in shorthand as

$$\text{Todd}_h = \frac{\frac{d}{dh}}{1 - \exp\left(-\frac{d}{dh}\right)}.$$

In order to compute the multivariate Ehrhart polynomials, we use a multivariate version of the Todd operator. For $h = (h_1, h_2, \dots, h_m)$, we write

$$\text{Todd}_h = \prod_{j=1}^m \left(\frac{\frac{\partial}{\partial h_j}}{1 - \exp(-\frac{\partial}{\partial h_j})} \right).$$

The Todd operator allows one to pass from a continuous measure of volume on a polytope to a discrete measure: a lattice point count. Let

$$P = \left\{ x \in \mathbb{R}^d \mid Ax \leq b \right\}$$

for some $A \in \mathbb{R}^{m \times d}, b \in \mathbb{R}^m$. For $h \in \mathbb{R}^m$, the *shifted polytope* P_h is defined as

$$P_h = \left\{ x \in \mathbb{R}^d \mid Ax \leq b + h \right\}.$$

THEOREM 3.3.2 (Khovanskii-Pukhlikov, [BR15, Chapter 12.4]). Let $P \subseteq \mathbb{R}^d$ be a full-dimensional smooth polytope. Then

$$|P \cap \mathbb{Z}^d| = \text{Todd}_h \text{vol}(P_h)|_{h=0}.$$

In words, the number of lattice points of P equals the evaluation of the Todd operator at $h = 0$ on the relative Euclidean volume of the shifted polytope P_h .

In [Theorem 3.3.2](#), one applies the Todd operator to the volume of a shifted version P_h of the polytope P . In our setting of multivariate volume polynomials that are constant on fixed cones of the polytrope region in the Gröbner fan, a nice simplification occurs that allows us to ignore this shift. As above, let $C \in \mathcal{GF}|_{\mathcal{P}_{\text{ol},n}}$ be a maximal open cone. By [Section 3.2](#), there is a multivariate volume polynomial $\text{Vol}_C(a)$ which evaluates to the normalized volume of $P(c^*)$ for any $c^* \in C$. The polynomial $\text{vol}_C(a) = \frac{1}{(n-1)!} \text{Vol}_C(a)$ thus evaluates to the Euclidean volume.

The shifted polytrope $P(c^*)_h$ has the description

$$P(c^*)_h = \left\{ x \in \mathbb{R}^{n-1} \mid x_i - x_j \leq c_{ij}^* + h_{ij}, -(c_{ni}^* + h_{ni}) \leq x_i \leq c_{in}^* + h_{in} \right\} = P(c^* + h)$$

for any $h \in \mathbb{R}^{n^2-n}$. As long as h is small enough, the shifted polytrope remains in the same cone, i.e. $c^* + h \in C$, and its Euclidean volume is given by evaluating the multivariate volume polynomial $\text{vol}_C(a + h)$ at c^* . As $\text{vol}_C(a)$ is a polynomial, we have

$$\left(\prod_{\substack{i,j \in [n] \\ i \neq j}} \frac{\partial}{\partial h_{ij}} \right) \text{vol}_C(a + h)|_{h=0} = \left(\prod_{\substack{i,j \in [n] \\ i \neq j}} \frac{\partial}{\partial a_{ij}} \right) \text{vol}_C(a).$$

Hence, we obtain that

$$\text{ehr}_C(a) = \text{Todd}_h \text{vol}_C(a + h)|_{h=0} = \text{Todd}_a \text{vol}_C(a).$$

Example 3.3.3 (The Ehrhart polynomial in dimension 2). We now apply the Todd operator to the multivariate volume polynomial of the hexagon from [Example 3.2.9](#). As in the before, this 2-dimensional example can be computed with more elementary methods, such as Pick's formula. However, this example generalizes to higher dimensions, and we use it to present our methods in a manageable size. Recall that in dimension 2 the volume polynomial is

$$\text{vol}(a) = \sum_{\substack{i,j \in [3] \\ i \neq j}} -\frac{1}{2} a_{ij}^2 + \sum_{\substack{i,j,k \in [3] \\ i,j,k \text{ distinct}}} (a_{ij}a_{ik} + a_{ji}a_{ki}).$$

Applying the multivariate Todd operator to this volume polynomial, we obtain

$$\begin{aligned}
 & \left. \text{Todd}_h \text{vol}(a + h) \right|_{h=0} \\
 &= \left(\frac{\frac{\partial}{\partial h_{32}}}{1 - \exp(-\frac{\partial}{\partial h_{32}})} \right) \cdots \left(\frac{\frac{\partial}{\partial h_{13}}}{1 - \exp(-\frac{\partial}{\partial h_{13}})} \right) \left[\left(\frac{\frac{\partial}{\partial h_{12}}}{1 - \exp(-\frac{\partial}{\partial h_{12}})} \right) \text{vol}(a + h) \right] \Big|_{h=0} \\
 &= \left(\frac{\frac{\partial}{\partial h_{32}}}{1 - \exp(-\frac{\partial}{\partial h_{32}})} \right) \cdots \left(\frac{\frac{\partial}{\partial h_{13}}}{1 - \exp(-\frac{\partial}{\partial h_{13}})} \right) \left[\left(1 + \sum_{k=1}^2 (-1)^k \frac{B_k}{k!} \left(\frac{\partial}{\partial h_{12}} \right)^k \right) \text{vol}(a + h) \right] \Big|_{h=0} \\
 &= \left(\frac{\frac{\partial}{\partial a_{32}}}{1 - \exp(-\frac{\partial}{\partial a_{32}})} \right) \cdots \left(\frac{\frac{\partial}{\partial a_{13}}}{1 - \exp(-\frac{\partial}{\partial a_{13}})} \right) \left[\left(1 + \sum_{k=1}^2 (-1)^k \frac{B_k}{k!} \left(\frac{\partial}{\partial a_{12}} \right)^k \right) \text{vol}(a) \right] \\
 &= \left(\frac{\frac{\partial}{\partial a_{32}}}{1 - \exp(-\frac{\partial}{\partial a_{32}})} \right) \cdots \left(\frac{\frac{\partial}{\partial a_{13}}}{1 - \exp(-\frac{\partial}{\partial a_{13}})} \right) \left[\text{vol}(a) + \frac{1}{2} (-a_{12} + a_{13} + a_{32}) - \frac{1}{12} \right] \\
 &\quad \vdots \\
 &= -\frac{1}{2} a_{12}^2 + a_{12}a_{13} - \frac{1}{2} a_{13}^2 - \frac{1}{2} a_{21}^2 + a_{13}a_{23} + a_{21}a_{23} - \frac{1}{2} a_{23}^2 + a_{21}a_{31} - \frac{1}{2} a_{31}^2 \\
 &\quad + a_{12}a_{32} + a_{31}a_{32} - \frac{1}{2} a_{32}^2 + \frac{1}{2} a_{12} + \frac{1}{2} a_{13} + \frac{1}{2} a_{21} + \frac{1}{2} a_{23} + \frac{1}{2} a_{31} + \frac{1}{2} a_{32} + 1 \\
 &= \text{vol}(a) + \sum_{\substack{i,j \in [3] \\ i \neq j}} \frac{a_{ij}}{2} + 1.
 \end{aligned}$$

Hence, for integral Kleene stars $c^* \in \mathbb{Z}^6$, i.e. whenever $P(c^*)$ is a smooth maximal lattice polytrope, we get that

$$|P(c^*) \cap \mathbb{Z}^2| = \text{vol}(c^*) + \sum_{\substack{i,j \in [3] \\ i \neq j}} \frac{c_{ij}^*}{2} + 1.$$

Pick's formula implies that $\sum_{\substack{i,j \in [3] \\ i \neq j}} c_{ij}^*$ is the number of lattice points on the boundary of $P(c^*)$. Evaluating this polynomial at $c^* = (3, 2, 3, 4, 5, 6)$ gives 52, the number of lattice points in the polytrope. Evaluating at $tc^* = (3t, 2t, 3t, 4t, 5t, 6t)$ recovers the univariate Ehrhart polynomial of the polytrope $P(c^*)$

$$\text{ehr}_{P(c^*)}(t) = \frac{79}{2}t^2 + \frac{23}{2}t + 1.$$

◇

3.3.2 Computing multivariate h^* -polynomials

We now describe how to compute a multivariate h^* -polynomial from a multivariate Ehrhart polynomial corresponding to each tropical type. As discussed in [Section 1.1.4](#),

3.3 Multivariate Ehrhart and h^* -Polynomials

the coefficients of the h^* -polynomial $h^*(t) = h_0 + h_1 t + \cdots + h_d t^d$ are the coefficients of the Ehrhart polynomial expressed in the basis

$$\left\{ \binom{t+d-i}{d} \mid i \in \{0, 1, \dots, d\} \right\}$$

of the vector space of polynomials in t of degree at most d . To transform the Ehrhart polynomial to the h^* -polynomial, we perform a change of basis, in which the Eulerian polynomials play a central role. We first explain this transformation in the univariate case, following [BR15, Chapter 2].

The Eulerian polynomial $A_d(t)$ is defined through the generating function

$$\sum_{j \geq 0} j^d t^j = \frac{A_d(t)}{(1-t)^{d+1}}.$$

Explicitly, we can write the Eulerian polynomial as

$$A_d(t) = \sum_{m=1}^d A(d, m-1) t^m,$$

where $A(d, m)$ is the Eulerian number that counts the number of permutations of $[d]$ with exactly m ascents. The first few Eulerian polynomials are $A_0(t) = 1$, $A_1(t) = t$, and $A_2(t) = t^2 + t$. Recall from [Section 1.1.4](#) that the Ehrhart series of a d -dimensional polytope P is

$$\text{Ehr}_P(t) = \sum_{k \geq 0} \text{ehr}_P(k) t^k = \sum_{k \geq 0} (\lambda_0 + \lambda_1 k + \cdots + \lambda_d k^d) t^k = \sum_{i=0}^d \frac{\lambda_i A_i(t)}{(1-t)^{i+1}}.$$

On the other hand, we have

$$\text{Ehr}_P(t) = \frac{h_P^*(t)}{(1-t)^{d+1}}.$$

This yields an expression for the h^* -polynomial in terms of the coefficients of the Ehrhart polynomial as

$$h_P^*(t) = \sum_{i=0}^d \lambda_i A_i(t) (1-t)^{d-i}.$$

Let $\text{ehr}_C(a)$ be a multivariate Ehrhart polynomial defined on a fixed open maximal cone C of $\mathcal{GF}|_{\mathcal{P}ol}$, as in [Section 3.3.1](#). Since C is a cone, we have $kc^* \in C \cap \mathbb{Z}^{n^2-n}$ for

every $k \in \mathbb{Z}_{>0}$, $c^* \in C \cap \mathbb{Z}^{n^2-n}$, and so we similarly obtain

$$\begin{aligned}\text{Ehr}(t) &= \sum_{k \geq 0} \text{ehr}_C(ka)t^k \\ &= \sum_{k \geq 0} (\lambda_0(a) + \lambda_1(a)k + \cdots + \lambda_d(a)k^d)t^k \\ &= \sum_{i=0}^d \frac{\lambda_i(a)A_i(t)}{(1-t)^{i+1}} \\ &= \frac{h^*(a, t)}{(1-t)^{d+1}}.\end{aligned}$$

where $\lambda_s(a)$ is a homogeneous polynomial of degree s in variables a_{ij} . To compute the coefficient of the multivariate h^* -polynomial, we thus collect the terms of each degree in the above expression.

Example 3.3.4 (The h^* -polynomial in dimension 2). We compute the multivariate h^* -polynomial of the hexagon as discussed above. Recall from [Example 3.3.3](#) that

$$\begin{aligned}\text{ehr}(ta) &= \lambda_2(a)t^2 + \lambda_1(a)t + 1 \\ &= \left(\sum_{\substack{i,j \in [3] \\ i \neq j}} -\frac{1}{2}a_{ij}^2 + \sum_{\substack{i,j,k \in [3] \\ i,j,k \text{ distinct}}} (a_{ij}a_{ik} + a_{ji}a_{ki}) \right) t^2 + \left(\sum_{\substack{i,j \in [3] \\ i \neq j}} \frac{a_{ij}}{2} \right) t + 1.\end{aligned}$$

With these coefficients we can compute

$$\begin{aligned}\lambda_2(a)A_2(t)(1-t)^0 &= \left(\sum_{\substack{i,j \in [3] \\ i \neq j}} -\frac{1}{2}a_{ij}^2 + \sum_{\substack{i,j,k \in [3] \\ i,j,k \text{ distinct}}} (a_{ij}a_{ik} + a_{ji}a_{ki}) \right) (t^2 + t), \\ \lambda_1(a)A_1(t)(1-t)^1 &= \left(\sum_{\substack{i,j \in [3] \\ i \neq j}} \frac{1}{2}a_{ij} \right) (-t^2 + t), \\ \lambda_0(a)A_0(t)(1-t)^2 &= t^2 - 2t + 1.\end{aligned}$$

The sum of these three polynomials gives the multivariate h^* -polynomial of the hexagon:

$$\begin{aligned}h^*(a, t) &= \left(\sum_{\substack{i,j \in [3] \\ i \neq j}} -\frac{1}{2}(a_{ij}^2 + a_{ij}) + \sum_{\substack{i,j,k \in [3] \\ i,j,k \text{ distinct}}} (a_{ij}a_{ik} + a_{ji}a_{ki}) + 1 \right) t^2 \\ &\quad + \left(\sum_{\substack{i,j \in [3] \\ i \neq j}} \frac{1}{2}(a_{ij} - a_{ij}^2) + \sum_{\substack{i,j,k \in [3] \\ i,j,k \text{ distinct}}} (a_{ij}a_{ik} + a_{ji}a_{ki}) - 2 \right) t + 1.\end{aligned}$$

Evaluating $h^*(a, t)$ at $(c, t) = (3, 2, 3, 4, 5, 6, t)$ yields

$$h^*(c^*, t) = 29t^2 + 49t + 1,$$

which is the univariate h^* -polynomial of the hexagon $P(c^*)$ from Examples 3.3.3 and 3.2.9. The coefficients of $h^*(c^*, t)$ sum to 79, which equals the normalized volume of $P(c^*)$, as observed previously in Example 3.2.9. \diamond

3.4 COMPUTATIONS AND OBSERVATIONS

In this section we describe the results of our application of the methods described in Sections 3.2 and 3.3 to maximal polytropes of dimension at most 4. All scripts and results of our computations can be found in a GitHub Repository [BEZ20]. We summarize our computational results as follows.

RESULT 3.4.1. We compute the multivariate volume, Ehrhart and h^* -polynomials for all tropical types of polytropes of dimension ≤ 4 .

Since the Ehrhart polynomials and h^* -polynomials solely depend on the volume polynomials, we focus on studying the coefficients of the latter. For 3-dimensional polytropes we establish a connection of these coefficients with central subdivisions of the fundamental polytope FP_3 . We first discuss the computational details.

3.4.1 Data and computation

We applied the methods described in Sections 3.2 and 3.3 to a dataset which was obtained in the work of [JS19]. The dataset contains the vertices of one polytrope for each maximal lex-type of dimension 3 and 4. The vertices of each polytrope were arranged to form a Kleene star and corresponding weight vector c^* . The aforementioned methods were then applied to obtain multivariate volume, Ehrhart and h^* -polynomials for the corresponding tropical type, using SageMath (version 9.0) [Sag], with an interface to Macaulay2 (version 1.15) [GS22]. The GitHub repository [BEZ20] contains the input data and the output of every step as a text file, and all scripts we used for the computations. Furthermore, it contains scripts for tests, with which we verified the correctness of our computations, and the respective output files of these tests.

Our computations were performed on a desktop computer with a 3.6 GHz quad-core processor. On average, the running time was about 5 minutes for each 4-dimensional volume polynomial, 0.15 seconds for each Ehrhart polynomial and 0.73 seconds for each h^* -polynomial. Parallelization is possible as the computations are independent for each tropical type.

In order to verify our computational results, we independently computed the univariate volume and Ehrhart polynomials with respect to our input data and compared them with our multivariate results, as explained in Examples 3.3.3, 3.3.4 and 3.2.9. To check

the h^* -polynomial of a representative polytrope, we attempted to compute its h^* -polynomial by computing its Ehrhart series with `Normaliz` [BISO] and compared this with our multivariate h^* -polynomial evaluated at the corresponding weight vector. We attempted to perform this check on a cluster, interrupting the `Normaliz` computation of each polytrope's Ehrhart series after 10 minutes. We ran this computation for 1459 (of 27 248) polytropes of dimension 4. For 670 (of 1459), the `Normaliz` computation finished in under 10 minutes and the respective h^* -polynomials matched. Investigating further on a small sample of cases in which the `Normaliz` computation did not finish within 10 minutes revealed that the Ehrhart series computation could take as long as 12 hours, in comparison to the 5 minutes required by our methods.

3.4.2 2-dimensional polytropes

First, we consider 2-dimensional polytropes. As noted in [Section 3.1](#), there is a unique lex-type of maximal polytropes, as the polytrope region contains only a single maximal cone ([Example 3.1.9](#)). We computed the multivariate volume polynomial by applying [Algorithm 3.2.6](#), where we use a fixed representative c^* from the interior of the polytrope region to compute the initial ideal $M = \text{in}_{c^*}(I_3)$ of the toric ideal I_3 ([Example 3.2.9](#)). Applying the Todd operator to the normalized volume polynomial yields the multivariate Ehrhart polynomial ([Example 3.3.3](#)), and the use of Eulerian polynomials allows us to compute the multivariate h^* -polynomial ([Example 3.3.4](#)). We note that the volume, Ehrhart and h^* -polynomials are all symmetric with respect to the S_3 -action.

3.4.3 3-dimensional polytropes

In the case of maximal 3-dimensional polytropes there are 6 types of maximal polytropes [JK10; JP12]. We applied the algorithms in [Sections 3.2](#) and [3.3](#) to Kleene stars corresponding to polytropes representing these 6 types, yielding the volume, Ehrhart, and h^* -polynomials of their respective tropical types.

Example 3.4.2 (A volume polynomial of a 3-polytrope). One of the six normalized volume polynomials is

$$\begin{aligned}
& 2a_{12}^3 - 3a_{12}^2a_{13} + a_{13}^3 - 3a_{12}^2a_{14} + 6a_{12}a_{13}a_{14} - 3a_{13}^2a_{14} + a_{21}^3 - 3a_{13}^2a_{23} + 6a_{13}a_{14}a_{23} - 3a_{14}^2a_{23} \\
& - 3a_{14}a_{23}^2 - 3a_{21}a_{23}^2 + a_{23}^3 - 3a_{21}^2a_{24} + 6a_{14}a_{23}a_{24} + 6a_{21}a_{23}a_{24} - 3a_{14}a_{24}^2 - 3a_{23}a_{24}^2 + a_{24}^3 - 3a_{21}^2a_{31} \\
& + 6a_{21}a_{24}a_{31} - 3a_{24}^2a_{31} - 3a_{24}a_{31}^2 + a_{31}^3 - 3a_{12}^2a_{32} + 6a_{12}a_{14}a_{32} - 3a_{14}^2a_{32} - 3a_{31}^2a_{32} - 3a_{14}a_{32}^2 \\
& + 6a_{14}a_{24}a_{34} + 6a_{24}a_{31}a_{34} + 6a_{14}a_{32}a_{34} + 6a_{31}a_{32}a_{34} - 3a_{14}a_{34}^2 - 3a_{24}a_{34}^2 - 3a_{31}a_{34}^2 - 3a_{32}a_{34}^2 + 2a_{34}^3 \\
& + 6a_{21}a_{31}a_{41} - 3a_{31}^2a_{41} + 6a_{31}a_{32}a_{41} - 3a_{32}^2a_{41} - 3a_{21}a_{41}^2 - 3a_{32}a_{41}^2 + a_{41}^3 - 3a_{12}^2a_{42} + 6a_{12}a_{13}a_{42} \\
& - 3a_{13}^2a_{42} + 6a_{12}a_{32}a_{42} + 6a_{32}a_{41}a_{42} - 3a_{13}a_{42}^2 - 3a_{32}a_{42}^2 - 3a_{41}a_{42}^2 + a_{42}^3 - 3a_{21}^2a_{43} + 6a_{13}a_{23}a_{43} \\
& + 6a_{21}a_{23}a_{43} - 3a_{23}^2a_{43} + 6a_{21}a_{41}a_{43} - 3a_{41}^2a_{43} + 6a_{13}a_{42}a_{43} + 6a_{41}a_{42}a_{43} - 3a_{13}a_{43}^2 - 3a_{21}a_{43}^2 \\
& - 3a_{42}a_{43}^2 + a_{43}^3.
\end{aligned}$$

◇

3.4 Computations and Observations

We devote the remainder of this subsection to an analysis of the coefficients of the normalized volume polynomials. Recall from [Section 3.1](#) that the 6 tropical types of maximal 3-dimensional polytropes correspond to different regular central triangulations of the fundamental polytope FP_4 .

THEOREM 3.4.3. The coefficients of the volume polynomials of maximal 3-dimensional polytropes reflect the combinatorics of the corresponding regular central triangulation of FP_3 . More precisely, the coefficient of a monomial of the form $a_{ij}a_{kl}a_{st}$ describes the triangles on the boundary of FP_3 , the coefficient of a monomial $a_{ij}^2a_{kl}$ describes triangulating edges, and the coefficient of a_{ij}^3 relates to the degree of the vertex $e_i - e_j$ of FP_3 .

Proof. Consider the normalized volume polynomials

$$\text{Vol} \left(\left\{ x \in \mathbb{R}^4 \mid x_i - x_j \leq a_{ij}, x_4 = 0 \right\} \right) = \sum_{v \in \mathbb{N}^{12}} \alpha_v a^v,$$

of degree 3, where

$$a^v = \prod_{\substack{i,j \in [4] \\ i \neq j}} a_{ij}^{v_{ij}} \quad \text{and} \quad \sum_{\substack{i,j \in [4] \\ i \neq j}} v_{ij} = 3.$$

Thus, there is a natural decomposition of the set of all possible exponent vectors v into three different disjoint subsets T_{111} , T_{21} , and T_3 , one for each partition of $[3]$.

$$\begin{aligned} T_{111} &= \{v \in \mathbb{N}^{12} \mid v_{ij} = v_{kl} = v_{st} = 1 \text{ for some } i \neq j, k \neq l, s \neq t \text{ and} \\ &\quad (i,j), (k,l), (s,t) \text{ are pairwise distinct}\}, \\ T_{21} &= \{v \in \mathbb{N}^{12} \mid v_{ij} = 2, v_{kl} = 1 \text{ for some } i \neq j, k \neq l \text{ and } (i,j) \neq (k,l)\}, \\ T_3 &= \{v \in \mathbb{N}^{12} \mid v_{ij} = 3 \text{ for some } i \neq j\}. \end{aligned}$$

The 6 tropical types of maximal 3-dimensional polytropes correspond to different regular central triangulations of the fundamental polytope FP_4 . A regular central triangulation is determined by a choice of a triangulating edge in each of the six square facets of FP_4 . The coefficients of the volume polynomials encode the data of these six facet triangulations as follows.

- 1.) Let $v \in T_{111}$, so that the monomial a^v is $a_{ij}a_{kl}a_{st}$ for some $i \neq j, k \neq l, s \neq t$ and $(i,j), (k,l), (s,t)$ are pairwise distinct. The coefficients α_v are directly determined by the corresponding triangulation of FP_4 :

$$\alpha_v = \begin{cases} 6 & \text{if } \text{conv}(e_i - e_j, e_k - e_l, e_s - e_t) \text{ is a triangle in the} \\ & \text{corresponding regular central triangulation of } FP_4, \\ 0 & \text{otherwise.} \end{cases}$$

- 2.) Let $v \in T_{21}$, so that the monomial a^v is $a_{ij}^2 a_{kl}$ for some $i \neq j, k \neq l$ and $(i, j) \neq (k, l)$.

The coefficient α_v is nonzero only if $e_i - e_j$ and $e_k - e_l$ are adjacent vertices of FP_4 . Every edge of FP_4 is contained in a unique square facet. The coefficient α_v is determined by the unique square facet S of FP_4 containing the edge $\text{conv}(e_i - e_j, e_k - e_l)$ as

$$\alpha_v = \begin{cases} -3 & \text{if } e_k - e_l \text{ incident to triangulating edge of } S \\ 0 & \text{otherwise.} \end{cases}$$

- 3.) Let $v \in T_3$, so that the monomial a^v is a_{ij}^3 for some $i \neq j$. The coefficient α_v is given by

$$\alpha_v = 7 - \deg(e_i - e_j),$$

where $\deg(e_i - e_j)$ is the number of edges incident to the vertex $e_i - e_j$ in the regular central subdivision of FP_4 . Note that every vertex in such a triangulation has degree 4, 5, 6 or 7, and so the coefficient α_v has value 0, 1, 2 or 3 for every $v \in T_3$.

□

We note that the above descriptions of the coefficients of the volume polynomial imply that the sums of coefficients corresponding to each partition of 3 are the same for all six volume polynomials:

$$\sum_{v \in T_3} \alpha_v = 12, \quad \sum_{v \in T_{21}} \alpha_v = -108, \quad \sum_{v \in T_{111}} \alpha_v = 120.$$

Example 3.4.4 (A regular central triangulation of FP_4). Consider the polytrope $P(c^*)$ defined by the Kleene star

$$c^* = \begin{pmatrix} 0 & 11 & 20 & 29 \\ 21 & 0 & 19 & 20 \\ 20 & 29 & 0 & 11 \\ 19 & 20 & 21 & 0 \end{pmatrix}.$$

This polytrope is depicted in [Figure 3.1](#). Assigning the height c_{ij}^* to the vertex $e_i - e_j$ of the fundamental polytope FP_4 and height 0 to the central lattice point at the origin, yields the regular central triangulation in [Figure 3.9](#). The coordinates of the vertices of FP_4 are shown in [Figure 3.7](#) and the volume polynomial corresponding to this polytrope is the polynomial displayed in [Example 3.4.2](#). In this subdivision the vertex $e_1 - e_2$ has degree $\deg(e_1 - e_2) = 5$, and so the coefficient of $a_{12}^3 = 7 - 5 = 2$. The vertices $e_1 - e_2$ and $e_1 - e_4$ are adjacent vertices in FP_4 , and $e_1 - e_4$ is incident to the unique triangulating edge of the square facet of FP_4 containing both vertices. Thus, the coefficient of $a_{12}^2 a_{14}$ is -3 . On the other hand, the vertices $e_3 - e_2$ and $e_4 - e_2$ are adjacent in FP_4 , but the vertex $e_3 - e_2$ is not contained in such a triangulating edge, and

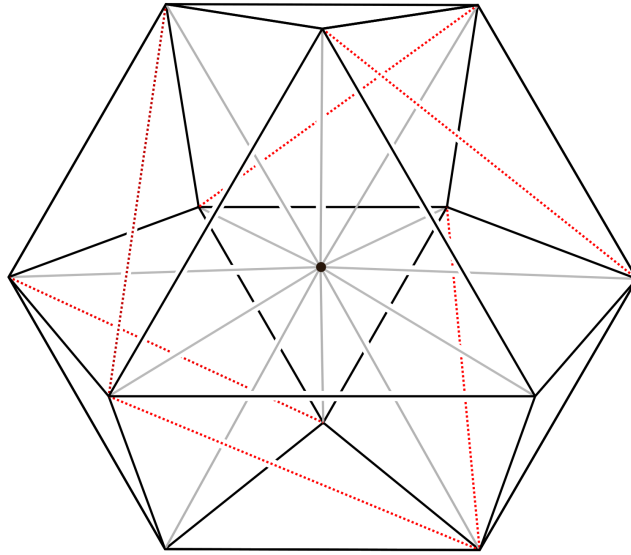


Figure 3.9: The regular central triangulation of FP_4 corresponding to the polytrope in [Example 3.4.4](#), with triangulating edges of square facets of FP_4 colored red.

so the coefficient of $a_{32}^2 a_{42}$ is 0. Finally, the vertices $e_3 - e_1, e_3 - e_2, e_3 - e_4$ form a face in the triangulation, and so the coefficient of $a_{31} a_{32} a_{41}$ is 6. \diamond

3.4.4 4-dimensional polytropes

Finally we consider 4-dimensional polytropes. In this case there are 27 248 tropical types of maximal polytropes. As before, we applied the methods of [Sections 3.2](#) and [3.3](#) to obtain multivariate volume, Ehrhart, and h^* -polynomials for these polytropes.

We embed the 27 248 normalized volume polynomials in the vector space of homogeneous polynomials of degree 4 using the canonical basis. This vector space has dimension $\binom{23}{4} = 8855$. This yields the following result.

THEOREM 3.4.5. In the 8855-dimensional space of homogeneous polynomials of degree 4, the 27 248 normalized volume polynomials of 4-dimensional polytropes span a 70-dimensional affine subspace.

The affine span of these volume polynomials has dimension 70, implying that there is much structure in their coefficients. We note that this equals the number of facets in a regular central triangulation of FP_5 .

We were able to computationally verify the relations collected in [Table 3.1](#). For example, all coefficients for monomials corresponding to the partition $2 + 2 = 4$ lie in the set $\{0, 6\}$, and the sum of all such coefficients is 300. Furthermore, the S_5 -orbit of the monomials $a_{12} a_{13} a_{14} a_{15}$ and $a_{21} a_{31} a_{41} a_{51}$ always appears in the volume polynomial with

coefficient 24. Finally, the coefficient -4 always appears exactly twice as often as the coefficient 12.

Partition	Example monomial	Possible coefficients	Coefficient sum
4	a_{12}^4	$-6, -3, -2, -1, 0, 1, 2, 3$	-20
$3 + 1$	$a_{12}^3 a_{13}$	$-4, 0, 4, 8$	320
$2 + 2$	$a_{12}^2 a_{13}^2$	$0, 6$	300
$2 + 1 + 1$	$a_{12} a_{13} a_{14}^2$	$-12, 0, 12$	-2160
$1 + 1 + 1 + 1$	$a_{12} a_{13} a_{14} a_{15}$	$0, 24$	1680

Table 3.1: Relations of some coefficients of volume polynomials of 4-dimensional polytropes.

As in the 3-dimensional case, a monomial corresponding to the partition $1 + 1 + 1 + 1 = 4$ has coefficient 24 if and only if it appears as a face in the corresponding triangulation. Beyond these observations, we were unable to detail the exact relationship between the volume polynomials and their corresponding regular central triangulations.

Question 3.4.6. How do the coefficients of the volume polynomials of maximal $(n - 1)$ -dimensional polytropes reflect the combinatorics of the corresponding regular central subdivision of FP_n ?

A natural first step would be to prove that, for v with partition $1 + 1 + \cdots + 1 = n - 1$, the coefficient α_v is nonzero if and only if it corresponds to a face in the regular central triangulation. For $n = 3, 4$ we verified that this is indeed the case.

Part II

SEMIALGEBRAIC SETS FROM POLYTOPES

4

INTERSECTION BODIES OF POLYTOPES

In this chapter we study intersection bodies of polytopes from the perspective of discrete and real algebraic geometry. Originally, intersection bodies were defined by Lutwak [Lut88] in the context of convex geometry. In view of the notion of $(d - 1)$ -dimensional cross-section measures and the related concepts of associated bodies (such as intersection bodies, cross-section bodies, and projection bodies), intersection bodies play an essential role in geometric tomography (see [Gar06, Chapter 8] and [Mar94, Section 2.3]), which is, in the words of Gardner, the “area of mathematics dealing with the retrieval of information about a geometric object from data about its sections, or projections, or both” [Gar06, Preface]. In particular, we mention here the Busemann-Petty problem which asks if one can compare the volumes of two convex bodies by comparing the volumes of their sections [Gar94a; Gar94b; Kol98; GKS99; Zha99a]. Moreover, Ludwig showed that the unique non-trivial $\mathrm{GL}(d)$ -covariant star-body-valued valuation on convex polytopes corresponds to taking the intersection body of the dual polytope [Ludo6]. Due to such results, the knowledge on properties of intersection bodies interestingly contributes also to the (still not systematized) theory of starshaped sets [HHMM20, Section 17].

Recently, there is increased interest in investigating convex geometry from an algebraic point of view [BPT13; Sin15; RS10; RS11]. In this chapter, we will focus on the intersection bodies of polytopes from this perspective. It is known that in \mathbb{R}^2 , the intersection body of a polytope which is centered at the origin (i.e. centrally symmetric and the center of symmetry is the origin) is the same polytope rotated by $\pi/2$ and dilated by a factor of 2 (see e.g. [Gar06, Theorem 8.1.4]). Moreover, if K is a full-dimensional convex body in \mathbb{R}^d centered at the origin, then so is its intersection body [Gar06, Chapter 8.1]. But what do these objects look like in general? In \mathbb{R}^d , with $d \geq 3$,

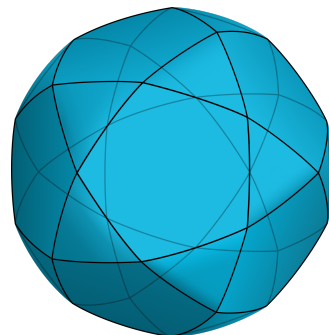


Figure 4.1: The intersection body of the icosahedron.

they cannot be polytopes [Cam99; Zha99b] and they may not even be convex. In fact, for every convex body K , there exists a translate of K such that its intersection body is not convex. This happens because of the important role played by the origin in the construction of the intersection body. However, we show that intersection bodies of polytopes behave well in regards of semialgebraicity.

THEOREM 4.2.4. The intersection body of a polytope is a semialgebraic set.

This result relies on the fact that the combinatorial type of the intersection of a polytope with a hyperplane is fixed for each region of a certain central hyperplane arrangement. The proof is constructive, and hence reveals an algorithm to explicitly compute the intersection body of a polytope (Algorithm 4.3.2). Furthermore, this allows us to approximate the intersection body by the dual polytope of a certain zonotope. We consider the algebraic boundary of an intersection body and give a bound on the possible degrees.

THEOREM 4.4.5. Let $P \subseteq \mathbb{R}^d$ be a full-dimensional polytope containing the origin, and let $f_1(P)$ be the number of edges of P . Then the degrees of the irreducible components of the algebraic boundary of IP are bounded from above by

$$f_1(P) - (d - 1).$$

Although the intersection body of a polytope is always semialgebraic, in many cases it is not a convex body. We give a full characterization of convex intersection bodies of polytopes in dimension 2.

THEOREM 4.6.14. Let $P \subseteq \mathbb{R}^2$ be a polygon. Then IP is a convex body if and only if

- (i) $P = -P$, or
- (ii) the origin is the midpoint of an edge of P and $P \cup -P$ is convex.

Sections 4.1 to 4.5 of this chapter are based on [BBMS22], which is joint work with Katalin Berlow, Chiara Meroni and Isabelle Shankar. All supplementary material, including implementations of Algorithm 4.3.2 in SageMath [Sag] and OSCAR [Osc], as well as an interactive case study of the intersection bodies of translates of the 3-dimensional cube are publicly available on a MathRepo page [BBMS21].

Overview

We study intersection bodies of polytopes from a point of view of discrete and real algebraic geometry. The background is provided in Sections 1.1, 1.2, 1.4 and 1.8. In Section 4.1, we prove semialgebraicity for the intersection body of polytopes containing the origin, and we generalize the result to arbitrary polytopes in Section 4.2. In Section 4.3, we present an algorithm to compute the radial function of the intersection body of a polytope. An implementation is available at [BBMS21]. In Section 4.4,

we describe the algebraic boundary of the intersection body, which is a hypersurface consisting of several irreducible components, each corresponding to a region of a certain hyperplane arrangement. [Theorem 4.4.5](#) gives a bound on the degree of the irreducible components. [Section 4.5](#) focuses on the intersection body of the d -cube centered at the origin ([Figure 4.6\(a\)](#)). In the final [Section 4.6.2](#) we give a classification of convex intersection bodies of 2-dimensional polytopes.

4.1 THE INTERSECTION BODY OF A POLYTOPE IS SEMIALGEBRAIC

In this section we introduce the notions from convex geometry that are used to define intersection bodies. We then consider the combinatorial types of sections of a polytope, which leads to the construction of an associated zonotope. At the end of this section, we use this construction in order to show that the intersection body of a polytope containing the origin is semialgebraic.

A set $S \subseteq \mathbb{R}^d$ is a *starshaped set* if there exists a point $o \in S$ such that the line segment $\text{conv}(o, s)$ is contained in S for every point $s \in S$. In particular, every convex set is a starshaped set. A *convex body* K is a nonempty, compact convex set. A subset $F \subseteq K$ is an *exposed face* of K if it is maximized by a linear functional, i.e. there exists some vector $\ell \in (\mathbb{R}^d)^*$ such that $F = \{x \in K \mid \langle x, \ell \rangle \geq \langle y, \ell \rangle \forall y \in K\}$. In convex geometry it is common to use functions in order to describe a starshaped set or a convex body, i.e. a non-empty convex compact subset of \mathbb{R}^d . This can be done e.g. by the radial function. A more detailed introduction can be found in [[Sch13](#)].

Definition 4.1.1 (Radial function). Given a starshaped set $S \subset \mathbb{R}^d$, the *radial function* of S is

$$\rho_S : \mathbb{R}^d \rightarrow \mathbb{R}, \quad x \mapsto \max(\lambda \in \mathbb{R} \mid \lambda x \in S).$$

As a convention $\rho_K(\emptyset) = \infty$ when $\emptyset \in K$ and it is 0 otherwise. An immediate consequence of the definition is that $\rho_K(cx) = \frac{1}{c}\rho_K(x)$ for $c > 0$. Therefore, we can equivalently define the radial function on the unit sphere S^{d-1} , and then extend to the whole space using the previously mentioned relation. Throughout this chapter we will use the convention that x denotes a vector in \mathbb{R}^d whereas u denotes a vector in S^{d-1} . With the observation that we can restrict to the sphere, we define the intersection body of K by its radial function, which is given by the Euclidean volume of the intersections of K with hyperplanes through the origin.

Definition 4.1.2 (Intersection body). Let K be a convex body in \mathbb{R}^d . Its *intersection body* is defined to be the set $IK = \{x \in \mathbb{R}^d \mid \rho_{IK}(x) \geq 1\}$ where the radial function (restricted to the sphere) is

$$\rho_{IK}(u) = \text{vol}_{d-1}(K \cap u^\perp)$$

for $u \in S^{d-1}$. We denote by u^\perp the hyperplane through the origin with normal vector u , and by vol_i the i -dimensional Euclidean volume, for $i \leq d$. A set K is *centered at the origin* if $K = -K$, i.e. if it is centrally symmetric and the origin is the center of symmetry.

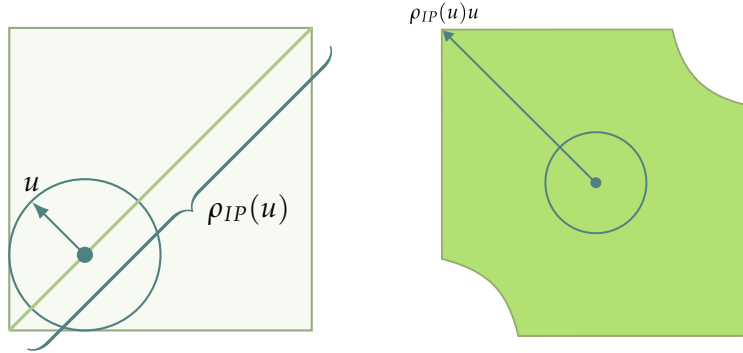


Figure 4.2: The intersection body of the shifted square from Example 4.1.3.

By construction, every intersection body is a starshaped set which is centered at the origin.

Example 4.1.3 (Intersection body of the translated square). We consider the square $P = [-2, 2]^2$. P is centered at the origin, and thus by [Gar06, Theorem 8.1.4], the intersection body is $IP = [-4, 4]^2$. However, this does not apply to the translated square

$$P + \begin{pmatrix} 1 \\ 1 \end{pmatrix} = \text{conv}\left(\begin{pmatrix} -1 \\ -1 \end{pmatrix}, \begin{pmatrix} -1 \\ 3 \end{pmatrix}, \begin{pmatrix} 3 \\ 3 \end{pmatrix}, \begin{pmatrix} 3 \\ -1 \end{pmatrix}\right).$$

For any $u \in S^2$, the distance from the origin to the boundary of IP in direction u is the length of the line segment $P \cap u^\perp$. The intersection body IP is not convex, as shown in Figure 4.2. We will continue with this in Example 4.1.7. \diamond

We begin our investigation by considering the intersection body of polytopes which contain the origin. For instance, Figure 4.1 displays the intersection body of an icosahedron centered at the origin. If the origin belongs to the interior of the polytope P , then ρ_P is continuous and hence ρ_{IP} is also continuous [Gar06]. Otherwise we may have some points of discontinuity which correspond to unit vectors u such that u^\perp contains a facet of P ; there are finitely many such directions. The intersection body is well defined, but there may arise subtleties when dealing with the boundary. However, we will see later (in Remark 4.4.1) that for our purposes everything works out.

Example 4.1.4 (Sections of the 3-cube). Let $C^{(3)} = [-1, 1]^3$ be the 3-dimensional centrally symmetric cube. The intersection body $IC^{(3)}$ is shown in Figure 4.6(a). Since the cube is centered at the origin, the intersection body is convex. We now discuss the possible polytopes that can be obtained when intersecting the cube with a hyperplane through the origin.

If we intersect $C^{(3)}$ with hyperplanes u^\perp , for $u \in S^2$, we can observe that there are two possible combinatorial types for $C^{(3)} \cap u^\perp$. All sections are either a parallelogram (Figure 4.3(a)) or a hexagon (Figure 4.3(b)). There are finitely many regions of the sphere for which the combinatorial type stays the same (cf. Lemma 4.1.5). We will see in the proof of Theorem 4.1.8 that within such a region, we can parameterize the area

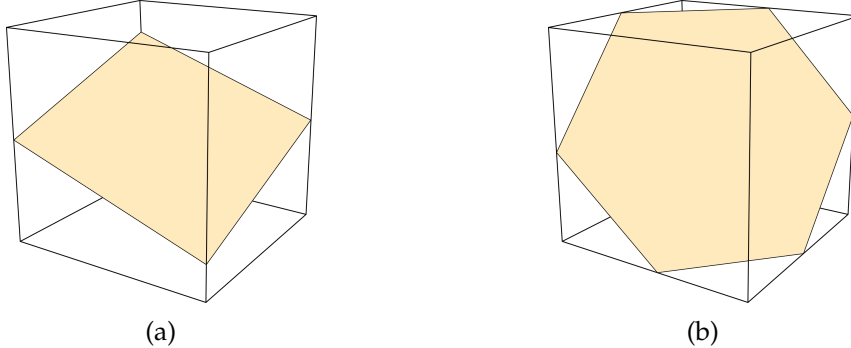


Figure 4.3: The two combinatorial types of hyperplane sections of the 3-cube.

of the parallelogram or hexagon with respect to the vector u to construct the radial function of IP . In fact, this will provide a semialgebraic description of the intersection body. If the intersection $C^{(3)} \cap u^\perp$ is a parallelogram, then the radial function in an open neighborhood of u will be a constant term over a coordinate variable, e.g. $\frac{4}{z}$. On the other hand, when the intersection is a hexagon, the radial function is a degree two polynomial over xyz . We continue with this in [Example 4.4.2](#). \diamond

LEMMA 4.1.5. Let P be a full-dimensional polytope in \mathbb{R}^d , and consider the central hyperplane arrangement

$$\mathcal{H}(P) = \left\{ v^\perp \mid v \text{ is a vertex of } P \text{ and } v \text{ is not the origin} \right\}.$$

The maximal open chambers C of $\mathcal{H}(P)$ satisfy the following property. For all $x \in C$, the hyperplane x^\perp intersects a fixed set of edges of P and the polytopes $Q = P \cap x^\perp$ are of the same combinatorial type.

Proof. Let $x \in \mathbb{R}^d \setminus \{0\}$ be generic and consider $Q = P \cap x^\perp$. The vertices of Q are the points of intersection of x^\perp with the edges of P . Perturbing x continuously, the intersecting edges (and thus the combinatorial type) remain the same, unless the hyperplane x^\perp passes through a vertex v of P . This happens if and only if $\langle x, v \rangle = 0$ and thus the set of normal vectors of such hyperplanes is given by $v^\perp = \{x \in \mathbb{R}^d \mid \langle x, v \rangle = 0\}$. Taking the union over all vertices yields the central hyperplane arrangement $\mathcal{H}(P)$. By construction, each open chamber C in the complement of $\mathcal{H}(P)$ is an open convex polyhedral cone, and consists of those points x such that x^\perp intersects a fixed set of edges of P . \square

In order to describe the radial function of the intersection body of a polytope, we are thus interested in the open chambers of hyperplane arrangement $\mathcal{H}(P)$ from [Lemma 4.1.5](#). The complexity of the explicit computation ([Algorithm 4.3.2](#)) will depend on the number of these chambers. Let $m = |\{v \text{ is a vertex of } P\}/\sim|$ where $v \sim w$ if

$v = \pm \lambda w$ for some $\lambda > 0$. Then the number of chambers is bounded from above by

$$\sum_{j=0}^d \binom{m}{j},$$

which is the number of chambers of a generic central hyperplane arrangement [Stao7, Proposition 2.4]. We note that there are several ways to view the hyperplane arrangement $\mathcal{H}(P)$ in Lemma 4.1.5. For example, since the vertices of P are the normal vectors of the facets of the polar polytope P° , we can describe $\mathcal{H}(P)$ as the collection of linear hyperplanes which are parallel to facets of P° . Furthermore, any hyperplane arrangement is the codim 1-skeleton of the normal fan of a zonotope whose edge directions are orthogonal to the hyperplanes of the arrangement. This motivates the following definition.

Definition 4.1.6 (Associated zonotope). The *zonotope associated to P* is the Minkowski sum of line segments

$$Z(P) = \sum_{v \in \text{vert}(P)} \text{conv}(-v, v).$$

The fan Σ induced by the hyperplane arrangement $\mathcal{H}(P)$ is the normal fan of the zonotope $Z(P)$. As we will see in Remark 4.4.8, the polar polytope of $Z(P)$ plays an important role in the visualization and the combinatorics of the intersection body IP . It serves as a “polyhedral approximation” of the intersection body, whose facial structure suggests a lot of intuition for the structure of the intersection body itself.

Example 4.1.7 (The associated zonotope of the translated square). We continue the study of the translated square from Example 4.1.3. The hyperplane arrangement $\mathcal{H}(P)$ consists of three hyperplanes $v_1^\perp = v_4^\perp, v_2^\perp, v_3^\perp$, where

$$v_1 = \begin{pmatrix} 3 \\ 3 \end{pmatrix}, \quad v_2 = \begin{pmatrix} 2 \\ -1 \end{pmatrix}, \quad v_3 = \begin{pmatrix} -1 \\ 2 \end{pmatrix}, \quad v_4 = \begin{pmatrix} -1 \\ -1 \end{pmatrix}.$$

This is the 1-skeleton of the normal fan of the zonotope

$$Z(P) = \text{conv}\left(\begin{pmatrix} -8 \\ 0 \end{pmatrix}, \begin{pmatrix} -6 \\ -6 \end{pmatrix}, \begin{pmatrix} 8 \\ 0 \end{pmatrix}, \begin{pmatrix} 6 \\ 6 \end{pmatrix}, \begin{pmatrix} 0 \\ -8 \end{pmatrix}, \begin{pmatrix} 0 \\ 8 \end{pmatrix}\right)$$

and its polar is

$$Z(P)^\circ = \frac{1}{24} \text{conv}\left(\begin{pmatrix} -3 \\ -1 \end{pmatrix}, \begin{pmatrix} -3 \\ 3 \end{pmatrix}, \begin{pmatrix} -1 \\ -3 \end{pmatrix}, \begin{pmatrix} 1 \\ 3 \end{pmatrix}, \begin{pmatrix} 3 \\ -3 \end{pmatrix}, \begin{pmatrix} 3 \\ 1 \end{pmatrix}\right).$$

Figure 4.4 shows the hyperplane arrangement $\mathcal{H}(P)$ and the two polytopes $Z(P)$ and $Z(P)^\circ$. Note that the pieces of the boundary of IP correspond to facets of $Z(P)^\circ$. \diamond

We now show that the intersection body of a polytope is semialgebraic, provided that the origin lies in the interior of P . In Section 4.2 we extend this statement to all convex polytopes.

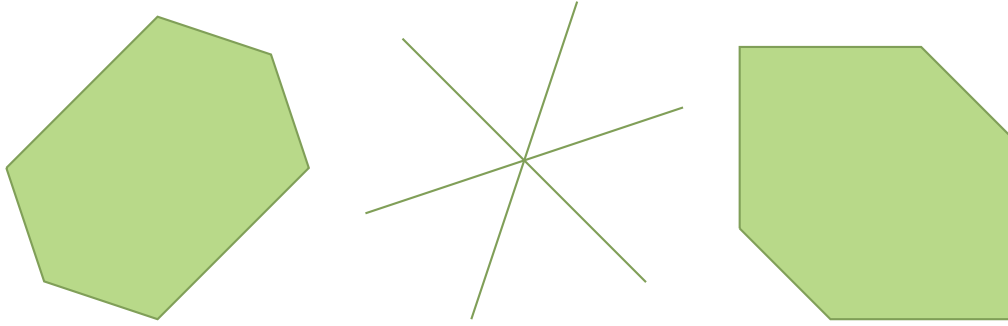


Figure 4.4: The zonotope $Z(P)$ (left), the hyperplane arrangement $\mathcal{H}(P)$ (center) and the polar $Z(P)^\circ$ of the shifted square in Examples 4.1.3 and 4.1.7.

Before we begin, we explain a key fact which is used in the following proof. Let $\Delta \subseteq \mathbb{R}^d$ be a $(d-1)$ -dimensional simplex where one of the vertices is the origin, and let $u \in S^{d-1}$ be a vector which is orthogonal to the $(d-1)$ -dimensional linear space containing Δ . Since u is a unit vector, the normalized volume of Δ agrees with the normalized volume of the d -dimensional simplex $\Delta^u = \text{conv}(\Delta, u)$. If $M_\Delta(u)$ is the matrix whose rows are the vertices of Δ^u , then the normalized volume is the determinant $\text{Vol}_d(\Delta^u) = |\det(M_\Delta(u))|$. For the Euclidean volumes this implies

$$\text{vol}_{d-1}(\Delta) = \frac{1}{(d-1)!} \text{Vol}_{d-1}(\Delta) = \frac{1}{(d-1)!} \text{Vol}_d(\Delta^u) = \frac{1}{(d-1)!} |\det(M_\Delta(u))|.$$

We will make use of this fact for computing the volume of sections of the polytope P .

THEOREM 4.1.8. Let $P \subseteq \mathbb{R}^d$ be a full-dimensional polytope containing the origin. Then IP , the intersection body of P , is semialgebraic.

Proof. Let $\mathcal{H}(P)$ be the hyperplane arrangement from Lemma 4.1.5, and fix a region $U = C \cap S^{d-1}$ for an open chamber C of $\mathcal{H}(P)$. For every $u \in U$ the hyperplane u^\perp intersects P in the same set of edges. Let v be a vertex of $Q = P \cap u^\perp$. Then there is an edge $\text{conv}(a, b)$ of P such that $v = \text{conv}(a, b) \cap u^\perp$. This implies that $v = \lambda a + (1 - \lambda)b$ for some $\lambda \in (0, 1)$ and $\langle v, u \rangle = 0$. From this we get that

$$\lambda = \frac{\langle b, u \rangle}{\langle b - a, u \rangle},$$

which implies that

$$v = \frac{\langle b, u \rangle}{\langle b - a, u \rangle} (a - b) + b = \frac{\langle b, u \rangle a - \langle a, u \rangle b}{\langle b - a, u \rangle}.$$

In this way we express v as a function of u (for fixed a and b). Let v_1, \dots, v_n be the vertices of Q and let $\text{conv}(a_i, b_i)$ be the corresponding edges of P .

We now consider the following triangulation of Q : first, triangulate each facet of Q that does not contain the origin, without adding new vertices (this can always be done e.g. by a regular subdivision using a generic lifting function [DLRS10, Proposition 2.2.4]). For each $(d-2)$ -dimensional simplex Δ in this triangulation, consider the $(d-1)$ -dimensional simplex $\text{conv}(\Delta, \mathbb{O})$ with the origin. This constitutes a triangulation \mathcal{T} of Q , in which the origin is a vertex of every maximal simplex.

Restricting to U , the radial function of the intersection body IP in direction u is the volume of Q , and hence given by

$$\rho_{IP}(u) = \text{vol}_{d-1}(Q) = \sum_{\Delta \in \mathcal{T}} \text{vol}_{d-1}(\Delta).$$

We can thus compute $\rho_{IP}(u)$ as

$$\rho_{IP}(u) = \sum_{\Delta \in \mathcal{T}} \frac{1}{(d-1)!} |\det(M_{\Delta}(u))|,$$

where

$$M_{\Delta}(u) = \begin{bmatrix} v_{i_1}(u) \\ v_{i_2}(u) \\ \vdots \\ v_{i_{d-1}}(u) \\ u \end{bmatrix} = \begin{bmatrix} \frac{\langle b_{i_1}, u \rangle a_{i_1} - \langle a_{i_1}, u \rangle b_{i_1}}{\langle b_{i_1} - a_{i_1}, u \rangle} \\ \vdots \\ \frac{\langle b_{i_{d-1}}, u \rangle a_{i_{d-1}} - \langle a_{i_{d-1}}, u \rangle b_{i_{d-1}}}{\langle b_{i_{d-1}} - a_{i_{d-1}}, u \rangle} \\ u \end{bmatrix}$$

and the row vectors $\{v_{i_1}, v_{i_2}, \dots, v_{i_{d-1}}\}$ (along with the origin) are vertices of the simplex Δ of the triangulation. Therefore, for $u \in U$ we obtain an expression $\rho_{IP}(u) = \frac{p(u)}{q(u)}$ for some polynomials $p, q \in \mathbb{R}[u_1, \dots, u_d]$ without common factors. With the same procedure applied to all regions $U_C = C \cap S^{d-1}$, where C is a chamber of $\mathcal{H}(P)$, we obtain an expression for $\rho|_{S^{d-1}}$ that is continuous and piecewise a quotient of two polynomials p_C, q_C . It follows from the definition of the radial function that

$$IP = \left\{ x \in \mathbb{R}^d \mid \rho_{IP}(x) \geq 1 \right\} = \left\{ x \in \mathbb{R}^d \mid \frac{1}{\|x\|} \rho_{IP}\left(\frac{x}{\|x\|}\right) \geq 1 \right\}.$$

Notice that for every $\Delta \in \mathcal{T}$ we have the following equality:

$$\det\left(M_{\Delta}\left(\frac{x}{\|x\|}\right)\right) = \det\begin{bmatrix} v_{i_1}\left(\frac{x}{\|x\|}\right) \\ \vdots \\ v_{i_{d-1}}\left(\frac{x}{\|x\|}\right) \\ \frac{x}{\|x\|} \end{bmatrix} = \det\begin{bmatrix} v_{i_1}(x) \\ \vdots \\ v_{i_{d-1}}(x) \\ \frac{x}{\|x\|} \end{bmatrix} = \frac{1}{\|x\|} \det(M_{\Delta}(x))$$

and therefore, if $\frac{x}{\|x\|} \in U_C$,

$$\begin{aligned}\rho_{IP}\left(\frac{x}{\|x\|}\right) &= \sum_{\Delta \in \mathcal{T}} \frac{1}{(d-1)!} \left| \det\left(M_{\Delta}\left(\frac{x}{\|x\|}\right)\right) \right| \\ &= \frac{1}{\|x\|} \sum_{\Delta \in \mathcal{T}} \frac{1}{(d-1)!} |\det(M_{\Delta}(x))| \\ &= \frac{p_C(x)}{\|x\|q_C(x)}.\end{aligned}$$

For $x \in C$ we obtain that

$$\rho_{IP}(x) = \frac{1}{\|x\|} \rho_{IP}\left(\frac{x}{\|x\|}\right) = \frac{p_C(x)}{\|x\|^2 q_C(x)}.$$

Let \mathcal{C} be the set of open chambers of $\mathcal{H}(P)$ such that $\rho_{IP}|_C \neq 0$ for every $C \in \mathcal{C}$. We can write the intersection body as

$$\begin{aligned}IP &= \bigcup_{C \in \mathcal{C}} \left\{ x \in \text{cl}(C) \mid \frac{p_C(x)}{\|x\|^2 q_C(x)} \geq 1 \right\} \\ &= \bigcup_{C \in \mathcal{C}} \left\{ x \in \text{cl}(C) \mid \|x\|^2 q_C(x) - p_C(x) \leq 0 \right\}.\end{aligned}$$

where $\text{cl}(C)$ denotes the Euclidean closure of C . This expression gives a semialgebraic description of IP . \square

Observation 4.1.9. By construction of the polynomials p_C, q_C in the previous proof, we always have $\deg p_C = \deg q_C + 1$. This can be seen from the fact that $\det(M_{\Delta}(x))$ is a polynomial of degree d , where each summand is a rational function which is the product of a monomial with $(d-1)$ rational functions, each having a linear numerator and denominator. The polynomials p_C and q_C are obtained by dividing by the greatest common denominator. Therefore, the degrees of p_C and q_C always differ by 1.

Example 4.1.10 (The radial function of the translated square). We continue with Examples 4.1.3 and 4.1.7 of the translated square P and compute its radial function restricted to the cone $C = \text{cone}((\begin{smallmatrix} 1 \\ 1 \end{smallmatrix}), (\begin{smallmatrix} 1 \\ 3 \end{smallmatrix}))$ from the hyperplane arrangement $\mathcal{H}(P)$. For any $x \in \text{int}(C)$ the intersection $Q = P \cap x^{\perp}$ is a line segment. The hyperplane x^{\perp} intersects the interior of the two adjacent edges $\text{conv}(a_1, b_1), \text{conv}(a_2, b_2)$ of P with vertices

$$a_1 = \begin{pmatrix} -1 \\ 3 \end{pmatrix}, \quad b_1 = a_2 = \begin{pmatrix} -1 \\ -1 \end{pmatrix}, \quad b_2 = \begin{pmatrix} 3 \\ -1 \end{pmatrix}.$$

Since $\dim(Q) = 1$, no further triangulation of the facets of Q is needed. Following the proof of [Theorem 4.2.4](#), we obtain the matrices

$$M_{\Delta_1}(x) = \begin{bmatrix} \frac{\langle b_{1,x} \rangle a_1 - \langle a_{1,x} \rangle b_1}{\langle b_1 - a_{1,x} \rangle} \\ x \end{bmatrix} = \begin{bmatrix} -1 & \frac{x_1}{x_2} \\ x_1 & x_2 \end{bmatrix}, \quad M_{\Delta_2}(x) = \begin{bmatrix} \frac{\langle b_{2,x} \rangle a_2 - \langle a_{2,x} \rangle b_2}{\langle b_2 - a_{2,x} \rangle} \\ x \end{bmatrix} = \begin{bmatrix} \frac{x_2}{x_1} & -1 \\ x_1 & x_2 \end{bmatrix}$$

with determinants

$$\det(M_{\Delta_1}(x)) = -x_2 - \frac{x_1^2}{x_2}, \quad \det(M_{\Delta_2}(x)) = \frac{x_2^2}{x_1} + x_1.$$

For any $x \in C$ the evaluation of the rational function $\det(M_{\Delta_1}(x))$ is negative and the evaluation of $\det(M_{\Delta_2}(x))$ is positive. Thus,

$$\begin{aligned} \frac{p_C(x)}{q_C(x)} &= |\det(M_{\Delta_1}(x))| + |\det(M_{\Delta_2}(x))| \\ &= -\left(-x_2 - \frac{x_1^2}{x_2}\right) + \left(\frac{x_2^2}{x_1} + x_1\right) \\ &= \frac{(x_1^2 + x_2^2)(x_1 + x_2)}{x_1 x_2} \end{aligned}$$

and the radial function is

$$\rho_C(x) = \frac{p_C(x)}{\|x\|^2 q_C(x)} = \frac{(x_1^2 + x_2^2)(x_1 + x_2)}{(x_1^2 + x_2^2)(x_1 x_2)} = \frac{x_1 + x_2}{x_1 x_2}.$$

The boundary of IP restricted to C is the zero set of the polynomial

$$q_C(x) - \frac{p_C(x)}{(x_1^2 + x_2^2)} = x_1 x_2 - x_1 - x_2.$$

◇

Example 4.1.11 (The intersection body of the icosahedron). Let $P \subseteq \mathbb{R}^3$ be the regular icosahedron, whose 12 vertices are all the even permutations of $(0, \pm \frac{1}{2}, \pm (\frac{1}{4}\sqrt{5} + \frac{1}{4}))$. The associated hyperplane arrangement has $32 = 12 + 20$ chambers. The first type of chambers is spanned by five rays and the radial function of IP is given by a quotient of a quartic and a quintic, defined over $\mathbb{Q}(\sqrt{5})$. In the remaining twenty chambers ρ_{IP} is a quintic over a sextic, again with coefficients in $\mathbb{Q}(\sqrt{5})$. This intersection body is the convex set shown in [Figure 4.1](#). We will continue the analysis of IP in [Example 4.4.9](#). ◇

4.2 NON-CONVEX INTERSECTION BODIES

The theory of intersection bodies assures that the intersection body of a centrally symmetric convex body is again a centrally symmetric convex body, as in [Example 4.1.4](#)

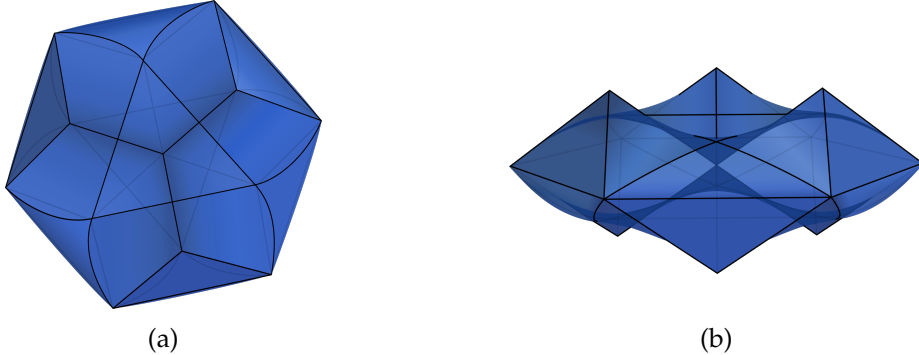


Figure 4.5: The intersection body of the cube in Example 4.2.1 from two different points of view.

and in Example 4.1.11. On the other hand, given any polytope P (indeed this holds more generally for any convex body) there exists a translation of P such that IP is not convex. In fact, this is almost always the case if the origin does not lie in the interior and holds in general when the origin lies outside of P . The main purpose of this section is to extend the result from Theorem 4.1.8 to polytopes where the origin is not contained in P , by adjusting how we compute the volume of a hyperplane section. We begin with an example of a polytope which has the origin as a vertex, yielding a non-convex intersection body.

Example 4.2.1 (A non-convex intersection body). Let P be the cube $[-1, 1]^3 + (1, 1, 1)^t$, so that the origin is a vertex of P . The hyperplane arrangement associated to P divides the space in 32 chambers. In two of them the intersection of the hyperplane with P is the origin, and thus the radial function is 0. In six regions the section of P is a quadrilateral, and the radial function has the following shape (up to permutation of the coordinates and sign):

$$\rho(x, y, z) = \frac{4}{z}.$$

There are then $18 = 6 + 12$ regions in which the radial function looks like

$$\rho(x, y, z) = \frac{2x}{yz} \quad \text{or} \quad \rho(x, y, z) = \frac{2(x+2z)}{yz}.$$

In the remaining six regions we have

$$\rho(x, y, z) = \frac{2(x^2 + 2xy + y^2 + 2xz + z^2)}{xyz}.$$

Figure 4.5 shows two different points of view of IP , which is in particular not convex. \diamond

The following lemma is a well-known result. However, as this is the key idea in the proof of Theorem 4.2.4, we provide a proof of the statement here for completeness.

LEMMA 4.2.2. Let $P \subset \mathbb{R}^d$ be a full-dimensional polytope, and let \mathcal{F} be the set of its facets. Let p be a point outside of P . For each face $F \in \mathcal{F}$, let \hat{F} denote the set $\text{conv}(F \cup \{p\})$. Then the following equality holds:

$$\text{vol}(P) = \sum_{F \in \mathcal{F}} \text{sgn}(F) \text{vol}(\hat{F})$$

where $\text{sgn}(F) = 1$ if P and p belong to the same halfspace defined by F , and -1 otherwise.

Proof. Let $\hat{P} = \text{conv}(P \cup \{p\})$ and denote by \mathcal{F}_p^+ the set of facets F of P for which the closed halfspace defined by F containing P also contains p , possibly on its boundary. Let $\mathcal{F}_p^- = \mathcal{F} \setminus \mathcal{F}_p^+$.

First we will show that $\hat{P} = \bigcup_{F \in \mathcal{F}_p^+} \hat{F}$. The inclusion $\bigcup_{F \in \mathcal{F}_p^+} \hat{F} \subseteq \hat{P}$ follows immediately from convexity. To see the opposite direction, let $q \in \hat{P}$ and consider r to be the ray starting at p and going through q . Either r intersects P only along its boundary, or there are some intersection points also in the interior of P . In the first case $r \cap P \subseteq F$ and so $q \in \hat{F}$ for some face F , which, by convexity, must be in \mathcal{F}_p^+ . On the other hand, if the ray r intersects the interior of the polytope P , denote by a the farthest among the intersection points, i.e. $a \in P$ such that

$$\|a - p\| = \max(\|\alpha - p\| \mid \alpha \in P \cap r).$$

Let F_a be a facet containing a . Then, q is contained in the convex hull of $F_a \cup \{p\}$, i.e. \hat{F}_a . From the definition of a it follows that the halfspace defined by F_a containing p must also contain P , so $F_a \in \mathcal{F}_p^+$ and our statement holds.

Next, we will show that $\bigcup_{F \in \mathcal{F}_p^-} \hat{F} = \text{cl}(\hat{P} \setminus P)$. The pyramid \hat{F} is contained in the closed halfspace defined by F which contains p . By the definition of \mathcal{F}_p^- , this halfspace does not contain P thus $\hat{F} \cap P = F$. Also, $\hat{F} \subseteq \hat{P}$ so we have that $\hat{F} \subseteq \text{cl}(\hat{P} \setminus P)$ and hence $\bigcup_{F \in \mathcal{F}_p^-} \hat{F} \subseteq \text{cl}(\hat{P} \setminus P)$. Conversely, let $q \in \text{cl}(\hat{P} \setminus P)$. If $q = p$ we are done, so assume $q \neq p$. Then, $q = \lambda p + (1 - \lambda)b$ for some $b \in P$, $\lambda \in [0, 1]$. Let a be the point at which the segment from p to b first intersects the boundary of P , i.e.

$$\|a - p\| = \min(\|\alpha - p\| \mid \alpha \in P, \alpha = tp + (1 - t)b \text{ for } t \in [0, 1]).$$

Then by construction there exists a facet $F_a \in \mathcal{F}_p^-$ containing a , such that $q \in \hat{F}_a$, which proves the reverse inclusion.

Thus, we have that

$$\text{vol}_d \left(\bigcup_{F \in \mathcal{F}_p^+} \hat{F} \right) = \text{vol}_d(\hat{P}) = \text{vol}_d(\hat{P} \setminus P) + \text{vol}_d(P) = \text{vol}_d \left(\bigcup_{F \in \mathcal{F}_p^-} \hat{F} \right) + \text{vol}_d(P).$$

If $F_1 \neq F_2$ and $F_1, F_2 \in \mathcal{F}_p^+$ or $F_1, F_2 \in \mathcal{F}_p^-$, then the d -dimensional volume of $\hat{F}_1 \cap \hat{F}_2$ is zero, therefore

$$\sum_{F \in \mathcal{F}_p^+} \text{vol}(\hat{F}) = \sum_{F \in \mathcal{F}_p^-} \text{vol}_d(\hat{F}) + \text{vol}_d(P)$$

and the claim follows. \square

Remark 4.2.3. We note that the proof of [Lemma 4.2.2](#) above solely uses the fact that the volume is a valuation on the polytope, and can thus be adapted to any such valuation. More precisely, let \mathcal{P} be a family of polytopes in \mathbb{R}^d containing the empty set, and G an abelian group. A *valuation* is a map $\varphi : \mathcal{P} \rightarrow G$ such that $\varphi(\emptyset) = 0$ and $\varphi(P \cup Q) = \varphi(P) + \varphi(Q) - \varphi(P \cap Q)$ for all $P, Q \in \mathcal{P}$ for which $P \cup Q, P \cap Q \in \mathcal{P}$ [[McM9](#)]. Since the properties of the volume which are used in the proof of [Lemma 4.2.2](#) are properties of a valuation, this proof can be adapted to hold for any such valuation. Another example of such a valuation is the lattice point count in lattice polytopes from [Section 1.1.4](#).

THEOREM 4.2.4. Let $P \subseteq \mathbb{R}^d$ be a full-dimensional polytope. Then IP , the intersection body of P , is semialgebraic.

Proof. What remains to be shown is that IP is semialgebraic in the case when the origin is not contained in P , and hence it is not contained in any of its sections $Q = P \cap u^\perp$ for $u \in \mathbb{S}^{d-1}$. From [Lemma 4.2.2](#), with $p = \mathbf{0} \in \mathbb{R}^d$ we have that

$$\text{vol}_{d-1}(Q) = \sum_{F \text{ facet of } Q} \text{sgn}(F) \text{vol}_{d-1}(\hat{F})$$

where \hat{F} is the convex hull of F and the origin. Let \mathcal{T}_F be a triangulation of F . As in the proof of [Theorem 4.1.8](#) we calculate

$$\text{vol}_{d-1}(\hat{F}) = \sum_{\Delta \in \mathcal{T}_F} \frac{1}{(d-1)!} |\det(M_\Delta(u))|$$

where $M_\Delta(u)$ is the matrix whose rows are the vertices of the simplex $\Delta \in \mathcal{T}_F$ and u . We then follow the remainder of the proof of [Theorem 4.1.8](#) to see that the intersection body is semialgebraic. \square

4.3 THE ALGORITHM

The proofs of [Theorems 4.1.8](#) and [4.2.4](#) lead to an algorithm to compute the radial function of the intersection body of a polytope. We use this section to describe this algorithm. By [Lemma 4.1.5](#) the regions C in which $\rho(x)|_C = \frac{p(x)}{\|x\|^2 q(x)}$ for fixed polynomials $p(x)$ and $q(x)$ are the closures of the open chambers of the hyperplane arrangement $\mathcal{H}(P)$. Equivalently, these are the maximal cones of the normal fan of the zonotope $Z(P)$ from [Definition 4.1.6](#). [Algorithm 4.3.1](#) computes the radial function for each of

these maximal cones individually. The radial function for the entire intersection body is computed by [Algorithm 4.3.2](#), which contains [Algorithm 4.3.1](#) as a subroutine.

Algorithm 4.3.1 (Computing the radial function for a fixed maximal cone C).

INPUT: A full-dimensional polytope $P \subseteq \mathbb{R}^d$ and a maximal cone C of the normal fan of $Z(P)$.

OUTPUT: The radial function $\rho(x)$ of the intersection body IP restricted to C .

```

1: Let  $\mathcal{F}$  be the collection of facets of  $P$  such that for all  $u \in U = \text{int}(C) \cap S^{d-1}$  and
    $F \in \mathcal{F}$  holds:  $\dim(F \cap u^\perp) = \dim(P) - 2$  and  $\emptyset \notin F$ .
2: Let  $Q = P \cap u^\perp$  for some fixed  $u \in U$ . Triangulate  $F \cap u^\perp$  for  $F \in \mathcal{F}$ , i.e. all facets
   of  $Q$  not containing the origin. Let  $\mathcal{T}$  be the collection of all maximal cells of these
   triangulations.
3: for each cell  $\Delta \in \mathcal{T}$  do
4:   Let  $v_1, \dots, v_{d-1}$  be the vertices of  $\Delta$ , ordered such that  $\det((v_1 \dots v_{d-1})) > 0$ .
5:   For  $i = 1, \dots, d-1$ , let  $e_i = \text{conv}(a_i, b_i)$  be the edge of  $P$  such that  $e_i \cap u^\perp = v_i$ .
6:   Let  $x = (x_1, \dots, x_d)$  be a vector with indeterminates  $x_1, \dots, x_d$ . Let  $M_\Delta(u)$  be
      the  $(d \times d)$ -matrix with  $i$ th row  $\frac{\langle b_i, x \rangle a_i - \langle a_i, x \rangle b_i}{\langle b_i - a_i, x \rangle}$  and last row  $x$ .
7:   if  $\text{conv}(\emptyset, \Delta)$  intersects the interior of  $P$  then
8:     Define  $\text{sgn}(\Delta) = 1$ 
9:   else
10:    Define  $\text{sgn}(\Delta) = -1$ 
11:   end if
12: end for
13: return  $\frac{1}{\|x\|^2(d-1)!} \sum_{\Delta \in \mathcal{T}} \text{sgn}(\Delta) \det(M_\Delta)$ 
```

This algorithm has as output the rational function $\rho(x)|_C = \frac{p(x)}{\|x\|^2 q(x)}$. Iterating over all regions yields the final [Algorithm 4.3.2](#).

Algorithm 4.3.2 (Computing the radial function of IP).

INPUT: A full-dimensional polytope P in \mathbb{R}^d .

OUTPUT: The radial function $\rho(x)$ of the intersection body IP .

```

1: Let  $\Sigma$  be the normal fan of the zonotope  $Z(P)$  (as in Definition 4.1.6).
2: for each maximal cone  $C$  of  $\Sigma$  do
3:   Compute  $\rho|_C$  via Algorithm 4.3.1.
4: end for
5: return  $\left( \frac{1}{\|x\|^2(d-1)!} \sum_{\Delta \in \mathcal{T}} \text{sgn}(\Delta) \det(M_\Delta), C \right)$  for  $C \in \Sigma$ 
```

An implementation of these algorithms both for SageMath 9.2 [[Sag](#)] and Oscar 0.7.1-DEV [[Osc](#)] can be found in [[BBMS21](#)].

4.4 ALGEBRAIC BOUNDARY AND DEGREE BOUND

Knowing the radial function of a star body S implies knowing its boundary. In fact, when $\emptyset \in \text{int}(S)$ then $x \in \partial S$ if and only if $\rho_S(x) = 1$ (see [Remark 4.4.1](#) for the other cases). In this section we describe the algebraic boundary (as defined in [Section 1.8](#)) of intersection bodies of polytopes, i.e. the Zariski closure of the Euclidean boundary ∂P over \mathbb{C} . Using the same notation as in the proof of [Theorem 4.1.8](#), we can observe that the algebraic boundary of the intersection body of a polytope is contained in the union of the varieties $\mathcal{V}(\|x\|^2 q_C(x) - p_C(x))$. Indeed, we actually know more: as we will prove in [Proposition 4.4.3](#), the p_C 's are divisible by the polynomial $\|x\|^2$, and hence

$$\partial_a IP = \bigcup_{C \in \mathcal{C}} \mathcal{V}\left(q_C(x) - \frac{p_C(x)}{\|x\|^2}\right),$$

where \mathcal{C} is the set of open chambers of $\mathcal{H}(P)$ such that $\rho_{IP}|_C \neq 0$. This is due to the assumption made in the proof of [Theorem 4.1.8](#) that p_C, q_C do not have common components. In other words, these are exactly the irreducible components of $\partial_a IP$.

Remark 4.4.1. As already mentioned in [Section 4.1](#), there may be difficulties when computing the boundary of IP in the case where the origin is not in the interior of the polytope P . More precisely, x is a discontinuity point of the radial function of IP if and only if x^\perp contains a facet of P . Therefore ρ_{IP} has discontinuity points if and only if the origin lies in the union of the affine linear spans of the facets of P . In this case, there are finitely many rays on which the radial function is discontinuous and these rays of discontinuity are contained in the hyperplane arrangement $\mathcal{H}(P)$. If $d = 2$, these rays disconnect the space, and this implies that we loose part of the (algebraic) boundary of IP . To fix this, we need to add segments from the origin to the boundary points in the direction of these rays to the set $\{x \in \mathbb{R}^2 \mid \rho_{IP}(x) = 1\}$. However, in higher dimensions the discontinuity rays do not disconnect \mathbb{R}^d so $\{x \in \mathbb{R}^d \mid \rho_{IP}(x) = 1\}$ approaches the region where the radial function is zero continuously except for these finitely many directions. Therefore there are no extra components of the boundary of $\partial_a IP$ for $d \geq 3$.

Example 4.4.2 (The algebraic boundary for the 3-cube). We continue [Example 4.1.4](#) by computing the intersection body of the 3-dimensional cube $C^{(3)}$ and its algebraic boundary. The intersection body $IC^{(3)}$ is displayed in [Figure 4.6\(a\)](#). The normal fan Σ of the zonotope $Z(P)$ has 14 maximal cones, dividing the Euclidean boundary of $IC^{(3)}$ into 14 regions. Among them, 6 of the regions of $\partial IC^{(3)}$ arise as the intersection of a convex cone spanned by 4 rays with a hyperplane; they constitute “facets” of IP , i.e. flat faces of dimension 2. For example the facet exposed by the vector $(1, 0, 0)^t$ is the intersection of $z = 4$ with the convex cone

$$C_1 = \text{cone}\left(\left(\begin{array}{c} 1 \\ 0 \\ 1 \end{array}\right), \left(\begin{array}{c} -1 \\ 0 \\ 1 \end{array}\right), \left(\begin{array}{c} 0 \\ 1 \\ 1 \end{array}\right), \left(\begin{array}{c} 0 \\ -1 \\ 1 \end{array}\right)\right).$$

In other words, the variety $\mathcal{V}(z - 4)$ is one of the irreducible components of $\partial_a IP$. The remaining 8 regions are spanned by 3 rays each, and the polynomial that defines the

boundary of IP is a cubic, such as

$$2xyz - 2x^2 - 4xy - 2y^2 - 4xz + 4yz - 2z^2$$

in the region

$$C_2 = \text{cone} \left(\left(\begin{smallmatrix} 0 \\ 1 \\ 1 \end{smallmatrix} \right), \left(\begin{smallmatrix} -1 \\ 1 \\ 0 \end{smallmatrix} \right), \left(\begin{smallmatrix} -1 \\ 0 \\ 1 \end{smallmatrix} \right) \right).$$

Hence $\partial_a IP$ is the union of 14 irreducible components, six of degree 1 and eight of degree 3. \diamond

PROPOSITION 4.4.3. Let $P \subseteq \mathbb{R}^d$ be a full-dimensional polytope, and $\mathcal{H}(P)$ the hyperplane arrangement from [Lemma 4.1.5](#). Fix an open chamber C of $\mathcal{H}(P)$, and let $p_C, q_C \in \mathbb{R}[x_1, \dots, x_d]$ such that $\rho_{IP}|_C = \frac{p_C(x)}{\|x\|^2 q_C(x)}$ (as in the proof of [Theorem 4.2.4](#)). Let $Q = P \cap u^\perp$ for some $u \in U = C \cap S^{d-1}$. Then the polynomial $\|x\|^2 = x_1^2 + \dots + x_d^2$ divides $p_C(x)$ and

$$\deg \left(q_C(x) - \frac{p_C(x)}{\|x\|^2} \right) \leq f_0(Q).$$

Proof. Let \mathcal{T} be a collection of simplices containing the origin, which are induced by triangulations of the facets of Q , as in the proof of [Theorem 4.2.4](#). Then the volume of Q is given by

$$\frac{p_C(x)}{q_C(x)} = \frac{1}{(d-1)!} \sum_{\Delta \in \mathcal{T}} \text{sgn}(\Delta) |\det(M_\Delta(x))|,$$

where $\text{sgn}(\Delta) \in \{1, -1\}$ depending on its position relative to the origin, and $M_\Delta(x)$ is the matrix as in the proof of [Theorem 4.1.8](#). Notice that for each $M = M_\Delta(x)$, we can rewrite the determinant to factor out a denominator:

$$\begin{aligned} \det(M(x)) &= \sum_{\sigma \in S_d} \text{sgn}(\sigma) \prod_{i=1}^d M_{i\sigma(i)} \\ &= \sum_{\sigma \in S_d} \text{sgn}(\sigma) x_{\sigma(d)} \prod_{i=1}^{d-1} \frac{\langle b_i, x \rangle a_{i\sigma(i)} - \langle a_i, x \rangle b_{i\sigma(i)}}{\langle b_i - a_i, x \rangle} \\ &= \prod_{i=1}^{d-1} \frac{1}{\langle b_i - a_i, x \rangle} \sum_{\sigma \in S_d} \text{sgn}(\sigma) x_{\sigma(d)} \prod_{i=1}^{d-1} \left(\langle b_i, x \rangle a_{i\sigma(i)} - \langle a_i, x \rangle b_{i\sigma(i)} \right) \\ &= \left(\prod_{v_i \in \text{vert}(\Delta)} \frac{1}{\langle b_i - a_i, x \rangle} \right) \cdot \det(\widehat{M}(x)) \end{aligned}$$

where

$$\widehat{M}(x) = \begin{bmatrix} & & \vdots \\ & \langle b_i, x \rangle a_i - \langle a_i, x \rangle b_i \\ & & \vdots \\ & & x \end{bmatrix}$$

and the determinant of $\widehat{M}(x)$ is a polynomial of degree d in the x_i 's. Note that if we multiply $\widehat{M}(x) \cdot x$ we obtain the vector $(0, \dots, 0, x_1^2 + \dots + x_d^2)$. Hence if $x_1^2 + \dots + x_d^2 = 0$, then $\widehat{M}(x) \cdot x = 0$, i.e. the kernel of $\widehat{M}(x)$ is non-trivial and thus $\det(\widehat{M}(x)) = 0$. This implies the containment of the complex varieties $\mathcal{V}(\|x\|^2) \subseteq \mathcal{V}(\det(\widehat{M}(x)))$ and therefore the polynomial $x_1^2 + \dots + x_d^2$ divides the polynomial $\det(\widehat{M}(x))$.

In each summand $\text{sgn}(\Delta) |\det(M_\Delta(x))|$ of $\frac{p_C}{q_C}$, every vertex of Q appears at most once, and all vertices of Q are contained in at least one simplex $\Delta \in \mathcal{T}$. Thus, the greatest common multiple of all summands is

$$\begin{aligned} q_C(x) &= (d-1)! \prod_{v_i \in \text{vert}(Q)} \langle b_i - a_i, x \rangle \\ &= (d-1)! \left(\prod_{v_i \in \text{vert}(\Delta)} \langle b_i - a_i, x \rangle \right) \left(\prod_{v_i \in \text{vert}(Q) \setminus \text{vert}(\Delta)} \langle b_i - a_i, x \rangle \right) \end{aligned}$$

for any $\Delta \in \mathcal{T}$, and

$$p_C(x) = \sum_{\Delta \in \mathcal{T}} \left(|\det(\widehat{M}(x))| \cdot \prod_{v_i \in \text{vert}(Q) \setminus \text{vert}(\Delta)} \langle b_i - a_i, x \rangle \right).$$

Hence $\deg q_C \leq f_0(Q)$. The degree bound for p then follows from [Observation 4.1.9](#). Alternatively, note that for each $\Delta \in \mathcal{T}$ the determinant $\det(\widehat{M}(x))$ is a polynomial of degree d , and $\prod_{v_i \in \text{vert}(Q) \setminus \text{vert}(\Delta)} \langle b_i - a_i, x \rangle$ has degree $f_0(Q) - (d-1)$. Thus,

$$\deg p_C \leq d + f_0(Q) - (d-1) = f_0(Q) + 1,$$

so the claim follows. \square

COROLLARY 4.4.4. In the hypotheses of [Proposition 4.4.3](#), if P is centered at the origin, then we can improve the bound to

$$\deg \left(q_C(x) - \frac{p_C(x)}{\|x\|^2} \right) \leq \frac{f_0(Q)}{2}.$$

Proof. If P is centered at the origin, then so is $Q = P \cap x^\perp$ and hence we can choose the triangulation \mathcal{T} to be centrally symmetric, i.e. $\mathcal{T} = \mathcal{T}^+ \cup (-\mathcal{T}^+)$ and $\mathcal{T}^+ \cap (-\mathcal{T}^+)$ only intersect along lower-dimensional faces. Since Q is centered at the origin, we have

$\text{sgn}(\Delta) = 1$ for all $\Delta \in \mathcal{T}$. Thus,

$$\begin{aligned}\frac{p_C}{q_C} &= \frac{1}{(d-1)!} \sum_{\Delta \in \mathcal{T}} |\det(M_{\Delta}(x))| \\ &= \frac{2}{(d-1)!} \sum_{\Delta \in \mathcal{T}^+} |\det(M_{\Delta}(x))|\end{aligned}$$

Let $\text{vert}(Q^+)$ denote the vertices of Q contained in \mathcal{T}^+ . Then in the proof of [Proposition 4.4.3](#) we obtain

$$q_C(x) = (d-1)! \prod_{v_i \in \text{vert}(Q^+)} \langle b_i - a_i, x \rangle$$

and so $\deg q_C \leq \frac{f_0}{2}$. Recall from [Observation 4.1.9](#) that $\deg p_C = \deg q_C + 1$. Thus, $\deg \frac{p_C}{q_C} < \deg q_C$. \square

Notice that generically, meaning for the generic choice of the vertices of P , the bound in [Proposition 4.4.3](#) is attained, because p and q will not have common factors. An example of such a polytope is the simplex in [Example 4.4.7](#).

THEOREM 4.4.5. Let $P \subseteq \mathbb{R}^d$ be a full-dimensional polytope with $f_1(P)$ edges. Then the degrees of the irreducible components of the algebraic boundary $\partial_a IP$ are bounded from above by

$$f_1(P) - (d-1).$$

Proof. We want to prove that $f_0(Q) \leq f_1(P) - (d-1)$, for every $Q = P \cap u^\perp$, $u \in S^{d-1} \setminus \mathcal{H}(P)$. By definition, every vertex of Q is a point lying on an edge of P , so trivially $f_0(Q) \leq f_1(P)$. We want to argue now that it is impossible to intersect more than $f_1(P) - (d-1)$ edges of P with the hyperplane $H = u^\perp$. If the origin is one of the vertices of P , then all edges that have the origin as a vertex give rise to a single vertex of Q : the origin itself. There are at least d such edges, because P is full-dimensional, and so $f_0(Q) \leq f_1(P) - (d-1)$.

Suppose now that the origin is not a vertex of P . Then H does not contain vertices of P . The hyperplane H divides \mathbb{R}^d in two half spaces H^+ and H^- , and so it divides the vertices of P in two families of k vertices in H^+ and ℓ vertices in H^- . Either k or ℓ are equal to 1, or they are both greater than one. In the first case let us assume without loss of generality that $k = 1$, i.e. there is only one vertex v^+ in H^+ . Pick one vector v^- in H^- . Since P is a full-dimensional polytope, there are at least d edges of P with v^- as a vertex. Only one of them may connect v^- to v^+ and therefore the other $d-1$ edges must lie in H^- . This gives $f_0(Q) \leq f_1(P) - (d-1)$.

On the other hand, let us assume that $k, \ell \geq 2$. Then there is at least one edge in H^+ and one edge in H^- . If $d = 3$ these are the $d-1$ edges that do not intersect the hyperplane. For $d > 3$ we reason as follows. Suppose that H intersects a facet F of P .

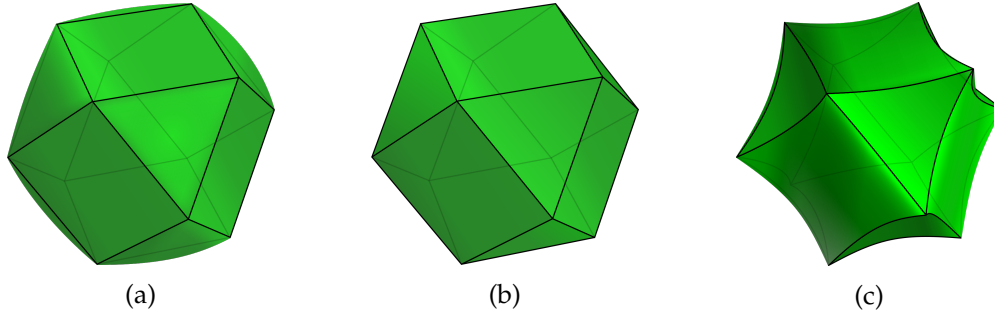


Figure 4.6: Left: the intersection body of the cube in Example 4.4.2. Right: the intersection body of the tetrahedron in Example 4.4.7. Center: the dual body of the zonotope $Z(P)$ associated to both the cube and the tetrahedron (up to dilation). Such a polytope reveals the structure of the boundary divided into regions of these two intersection bodies.

Then it cannot intersect all facets of F (i.e. a ridge of P), otherwise we would get $F \subseteq H$ which contradicts the fact that H does not intersect vertices of P . So there exists a ridge F' of P that does not intersect the hyperplane; it has dimension $d - 2 \geq 2$ and therefore it has at least $d - 1$ edges. Hence, $f_0(Q) \leq f_1(P) - (d - 1)$. By Proposition 4.4.3, the degree of each irreducible component of the algebraic boundary is bounded by $f_0(Q)$, and so the claim follows. \square

COROLLARY 4.4.6. In the hypotheses of Theorem 4.4.5, if P is centrally symmetric and centered at the origin, then we can improve the bound to

$$\frac{1}{2} (f_1(P) - (d - 1)).$$

Proof. Combining the results of Corollary 4.4.4 and Theorem 4.4.5, if P is centrally symmetric, then the degree of each irreducible component is bounded by $\frac{f_0(Q)}{2} \leq \frac{1}{2} (f_1(P) - (d - 1))$. \square

Example 4.4.7 (Different polytopes can have the same associated zonotope). Let P be the 3-dimensional tetrahedron

$$P = \text{conv} \left(\begin{pmatrix} -1 \\ -1 \\ -1 \end{pmatrix}, \begin{pmatrix} -1 \\ 1 \\ 1 \end{pmatrix}, \begin{pmatrix} 1 \\ -1 \\ 1 \end{pmatrix}, \begin{pmatrix} 1 \\ 1 \\ -1 \end{pmatrix} \right).$$

The intersection body IP is displayed in Figure 4.6(c). The associated hyperplane arrangement coincides with the one associated to the cube in Example 4.4.2, so it has 14 chambers that come in two families. The first one consists of cones spanned by four rays, such as C_1 (see Example 4.4.2). The polynomial that defines the boundary of IP

in this region is a quartic, namely

$$q_2(x, y, z) - \frac{p_2(x, y, z)}{\|(x, y, z)\|^2} = (x + z)(x - z)(y + z)(y - z) - 2(x^2 + y^2 - z^2)z.$$

On the other hand the cones of the second family are spanned by three rays: here the section of P is a triangle and the equation of the boundary if IP is a cubic. An example is the cone C_2 with the polynomial

$$q_1(x, y, z) - \frac{p_1(x, y, z)}{\|(x, y, z)\|^2} = (x - y)(x - z)(y + z) + (x - y - z)^2.$$

Note that this region furnishes an example in which the bounds given in [Proposition 4.4.3](#) and [Theorem 4.4.5](#) are attained. \diamond

Remark 4.4.8. [Definition 4.1.6](#) together with [Proposition 4.4.3](#) implies that the structure of the irreducible components of the algebraic boundary of IP is related to the face lattice of the dual of the zonotope $Z(P)$. More precisely, in the generic case, the lattice of intersection of the irreducible components restricted to the chambers of $\mathcal{H}(P)$ is a sublattice of the face lattice of the dual polytope $Z(P)^\circ$. Thus, a classification of “combinatorial types” of such intersection bodies can be approached by the classification of zonotopes, or equivalently hyperplane arrangements, and their associated oriented matroids (cf. [Section 1.2](#)). Such a classification depends on the choice of a definition of “combinatorial type of an intersection body” and is subject to future research. If IP is convex, then a possible candidate is to consider the notion of patches as introduced in [\[PSW22\]](#), which attempts to generalize the notion of faces of polytopes to more general convex semialgebraic sets. For establishing such a study, it is however worth noting that the same zonotope can be associated to two polytopes P_1 and P_2 which are not combinatorially equivalent. One example of this instance is a pair of polytopes such that $P_1 = \text{conv}(v_1, \dots, v_n)$ and $P_2 = \text{conv}(\pm v_1, \dots, \pm v_n)$, as can be seen in [Figure 4.6](#) for the cube and the tetrahedron.

To have a better overview over the structure of the boundary of IP , one strategy is to use the Schlegel diagram of $Z(P)^\circ$ [[Zie95](#), Chapter 5]. We label each maximal cell by the degree of the polynomial that defines the corresponding irreducible component of $\partial_a IP$, as can be seen in [Figures 4.7](#) and [4.8](#).

Example 4.4.9 (The algebraic boundary for the icosahedron). We continue with the regular icosahedron from [Example 4.1.11](#), which is shown in [Figure 4.1](#). In the 12 regions which are spanned by five rays, the polynomial that defines the boundary of IP has degree 5 and it looks like

$$\begin{aligned} & ((\sqrt{5}x + \sqrt{5}y - x + y)^2 - 4z^2)((\sqrt{5}x + x + 2y)^2 - (\sqrt{5}z - z)^2)y + \\ & 8\sqrt{5}x^3y + 68\sqrt{5}x^2y^2 + 72\sqrt{5}xy^3 + 20\sqrt{5}y^4 - 40\sqrt{5}xyz^2 - 20\sqrt{5}y^2z^2 + 4\sqrt{5}z^4 + \\ & 8x^3y + 164x^2y^2 + 168xy^3 + 44y^4 - 8x^2z^2 - 72xyz^2 - 44y^2z^2 + 12z^4. \end{aligned}$$

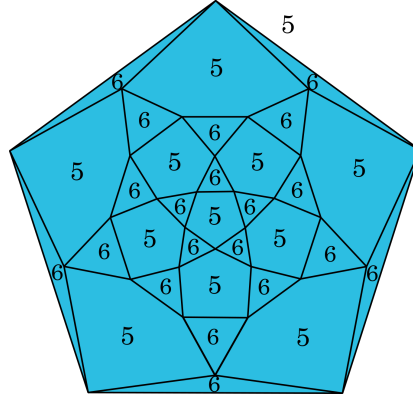


Figure 4.7: The Schlegel diagram of $Z(P)^\circ$, in the case where P is the icosahedron from Example 4.4.9. The labels represent the degrees of the polynomials of $\partial_a IP$.

In the other 20 regions spanned by three rays, ∂IP is the zero set of a sextic polynomial with the following shape

$$\begin{aligned} & ((\sqrt{5}x + x + 2y)^2 - (\sqrt{5}z - z)^2)((\sqrt{5}y - 2x - y)^2 - (\sqrt{5}z - z)^2)xy \\ & + 20\sqrt{5}x^4y - 20\sqrt{5}x^2y^3 - 4\sqrt{5}xy^4 + 4\sqrt{5}y^5 - 4\sqrt{5}x^3z^2 \\ & - 60\sqrt{5}x^2yz^2 - 12\sqrt{5}xy^2z^2 + 12\sqrt{5}xz^4 + 44x^4y - 8x^3y^2 - 44x^2y^3 \\ & + 12xy^4 + 12y^5 - 12x^3z^2 - 156x^2yz^2 - 60xy^2z^2 - 8y^3z^2 + 28xz^4. \end{aligned}$$

We visualize the structure of these pieces using the Schlegel diagram in Figure 4.7, where the numbers correspond to the degree of the polynomials, as explained in Remark 4.4.8. \diamond

Using this technique we are then able to visualize the boundary of intersection bodies of 4-dimensional polytopes via the Schlegel diagram of $Z(P)^\circ$.

Example 4.4.10 (The labeled Schlegel diagram for a 4-dimensional intersection body). We consider the 4-dimensional polytope

$$P = \text{conv}\left(\left(\begin{array}{c} 1 \\ 0 \\ 0 \end{array}\right), \left(\begin{array}{c} 0 \\ 1 \\ 0 \end{array}\right), \left(\begin{array}{c} 0 \\ 0 \\ 1 \end{array}\right), \left(\begin{array}{c} 0 \\ -1 \\ 0 \end{array}\right), \left(\begin{array}{c} 0 \\ 0 \\ -1 \end{array}\right)\right).$$

The boundary of its intersection body IP is subdivided in 16 regions. In four of them the equation is given by a polynomial of degree 3, whereas in the remaining twelve regions the polynomial has degree 5. In Figure 4.8 we show the Schlegel diagram of

$$Z(P)^\circ = \text{conv}\left(\pm\left(\begin{array}{c} 1/2 \\ -1/2 \\ 0 \end{array}\right), \pm\left(\begin{array}{c} 1 \\ 0 \\ 0 \end{array}\right), \pm\left(\begin{array}{c} 0 \\ 1 \\ 0 \end{array}\right), \pm\left(\begin{array}{c} 0 \\ 0 \\ 1 \end{array}\right)\right)$$

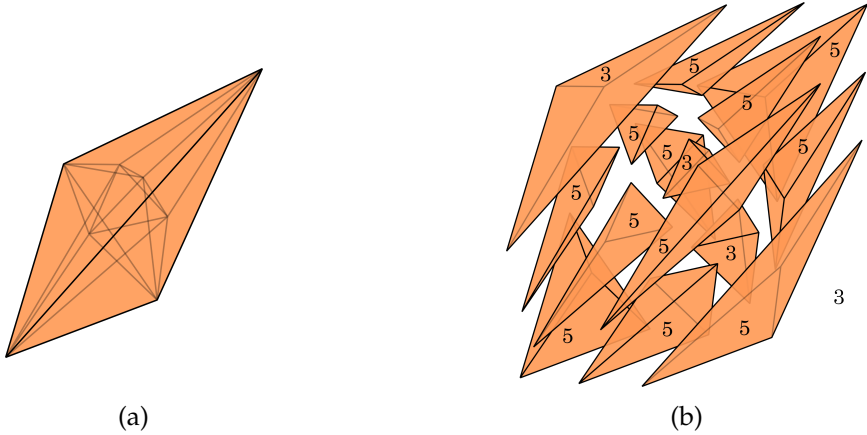


Figure 4.8: The Schlegel diagram of $Z(P)^\circ$ from Example 4.4.10. There are four cells whose corresponding polynomial in ∂IP has degree 3, including the outer facet; the others correspond to degree 5 polynomials.

with a number associated to each maximal cell which represents the degree of the polynomial in the corresponding region of ∂IP . \diamond

4.5 THE CUBE

In this section we investigate the intersection body of the d -dimensional cube $C^{(d)} = [-1, 1]^d$, with a special emphasis on the linear components of its algebraic boundary.

PROPOSITION 4.5.1. The algebraic boundary of the intersection body of the d -dimensional cube $C^{(d)}$ has at least $2d$ linear components. These components are in bijection with those $2d$ open regions of the hyperplane arrangement $\mathcal{H}(P)$ which contain the standard basis vectors or their negatives.

Proof. We show the claim for the first standard basis vector e_1 . The argument for the other vectors $\pm e_i, i = 1, \dots, d$ is analogous.

Let C be the region from Lemma 4.1.5 which contains e_1 and consider $U = C \cap S^{d-1}$. For any $u \in U$, the polytope $C^{(d)} \cap u^\perp$ is combinatorially equivalent to $C^{(d-1)}$. Hence we can compute the (signed) volume,

$$\text{vol}_{d-1}(C^{(d)} \cap u^\perp) = \det \begin{bmatrix} v^{(1)} - v^{(0)} \\ \vdots \\ v^{(d-1)} - v^{(0)} \\ u \end{bmatrix}$$

where $v^{(0)}$ is an arbitrarily chosen vertex of $C^{(d)} \cap u^\perp$ and the remaining $v^{(i)}$ are vertices of $C^{(d)} \cap u^\perp$ adjacent to $v^{(0)}$. Next, we observe that for any vertex v of $C^{(d)} \cap u^\perp$ which

lies on the edge $\text{conv}(a, b)$ of $C^{(d)}$, v is the vector

$$v = \left(-\frac{1}{u_1} \sum_{j=2}^d a_j u_j, a_2, \dots, a_d \right).$$

This follows from the formulation of v in the proof of [Theorem 4.1.8](#) and the fact that $b_1 = -a_1$ and $b_i = a_i$ for $i = 2, \dots, d$. Combining this with the determinant above gives us the following expression for the radial function restricted to U :

$$\rho_{IC^{(d)}}(u) = \frac{1}{u_1} \det \begin{bmatrix} -\sum_{j=2}^d (a_j^{(1)} - a_j^{(0)}) u_j & a_2^{(1)} - a_2^{(0)} & \dots & a_d^{(1)} - a_d^{(0)} \\ -\sum_{j=2}^d (a_j^{(2)} - a_j^{(0)}) u_j & a_2^{(2)} - a_2^{(0)} & \dots & a_d^{(2)} - a_d^{(0)} \\ \vdots & \vdots & & \vdots \\ -\sum_{j=2}^d (a_j^{(d)} - a_j^{(0)}) u_j & a_2^{(d)} - a_2^{(0)} & \dots & a_d^{(d)} - a_d^{(0)} \\ u_1^2 & u_2 & \dots & u_d \end{bmatrix}$$

where we assume the determinant is nonnegative, otherwise we multiply by -1 . Expanding the determinant along the bottom row of the matrix yields

$$\rho_{IC^{(d)}}(u) = \frac{1}{u_1} \left(u_1^2 \det \begin{bmatrix} a_2^{(1)} - a_2^{(0)} & \dots & a_d^{(1)} - a_d^{(0)} \\ a_2^{(2)} - a_2^{(0)} & \dots & a_d^{(2)} - a_d^{(0)} \\ \vdots & & \\ a_2^{(d)} - a_2^{(0)} & \dots & a_d^{(d)} - a_d^{(0)} \end{bmatrix} + \gamma(u_2, \dots, u_d) \right).$$

where $\gamma(u_2, \dots, u_d)$ is a polynomial consisting of the quadratic terms in the remaining u_i 's. Note that since γ does not contain the variable u_1 and ρ is divisible by the quadric $u_1^2 + \dots + u_d^2$ by [Proposition 4.4.3](#), it follows that

$$\rho_{IC^{(d)}}(u) = \frac{u_1^2 + \dots + u_d^2}{u_1} \det \begin{bmatrix} a_2^{(1)} - a_2^{(0)} & \dots & a_d^{(1)} - a_d^{(0)} \\ a_2^{(2)} - a_2^{(0)} & \dots & a_d^{(2)} - a_d^{(0)} \\ \vdots & & \\ a_2^{(d)} - a_2^{(0)} & \dots & a_d^{(d)} - a_d^{(0)} \end{bmatrix}. \quad (4.1)$$

Let A be the $(d-1) \times (d-1)$ -matrix appearing in this last expression (4.1). Then the irreducible component of the algebraic boundary on the corresponding region C is described by the linear equation $x_1 = |\det A|$. \square

Note that for an arbitrary polytope P of dimension at least 3, the irreducible components of the algebraic boundary $\partial_a IP$ cannot all be linear. This is implied by the fact that the intersection body of a convex body is not a polytope. It is thus worth noting that the intersection body of the cube has linear components at all. We now investigate the non-linear pieces of $\partial_a IC^{(d)}$.

Example 4.5.2 (The intersection body of the 4-cube). Let $C^{(4)} = [-1, 1]^4$ be the 4-dimensional cube and $IC^{(4)}$ be its intersection body. The associated hyperplane arrangement has $8 + 32 + 64 = 104$ chambers. The first 8 are spanned by 6 rays and the boundary here is linear, i.e. it is a 3-dimensional cube. For example, the linear face exposed by $(1, 0, 0, 0)$ is cut out by the hyperplane $w = 8$.

The second family of chambers is made of cones with 5 extreme rays, where the boundary is defined by a cubic equation with shape

$$3xyz - 3w^2 - 6x^2 - 12xy - 6y^2 - 12xz + 12yz - 6z^2.$$

Finally there are 64 cones spanned by 4 rays such that the boundary of the intersection body is a quartic, such as

$$\begin{aligned} & 4wxyz - w^3 - 3w^2x - 3wx^2 - x^3 - 3w^2y - 6wxy - 3x^2y - 3wy^2 - 3xy^2 \\ & - y^3 - 3w^2z - 6wxz - 3x^2z + 18wyz - 6xyz - 3y^2z - 3wz^2 - 3xz^2 - 3yz^2 - z^3. \end{aligned}$$

◊

Proposition 4.5.1 gives a lower bound on the number of linear components of the algebraic boundary of $IC^{(d)}$. We conjecture that for any $d \in \mathbb{N}$, the algebraic boundary of the intersection body of the d -dimensional cube centered at the origin has exactly $2d$ linear components. Computational results for $d \leq 5$ support this conjecture, as displayed in [Table 4.1](#). It shows the number of irreducible components of $IC^{(d)}$ sorted by the degree of the component, for $d = 2, 3, 4, 5$. The first two columns are the dimension of the polytope, and the number of chambers of the respective hyperplane arrangement $\mathcal{H}(C^{(d)})$. The third column is the degree bound from [Corollary 4.4.6](#). The remaining columns show the number of regions whose equation in the algebraic boundary have degree \deg , for $\deg = 1, \dots, 5$.

dimension	# chambers	degree bound	deg = 1	2	3	4	5
2	4	1	4	0	0	0	0
3	14	5	6	0	8	0	0
4	104	14	8	0	32	64	0
5	1882	38	10	0	80	320	1472

Table 4.1: Number of irreducible components of the algebraic boundary of the intersection body of the d -cube, listed by degree.

The highest degree attained in these examples is equal to the dimension of the respective cube. In particular, the degree bound for centrally symmetric polytopes, as given in [Corollary 4.4.6](#), is not attained in any of the cases for $d \geq 3$. Finally, note that the number of regions grows exponentially in d , and thus for $d \geq 3$, the number of non-linear components exceeds the number of linear components.

4.6 CONVEX INTERSECTION BODIES OF POLYGONS

In the previous sections we have seen that intersection bodies of polytopes are not always convex. Even more, convexity is not preserved under translation, as illustrated in [Example 4.1.3](#). In fact, even the combinatorics of the hyperplane arrangement $\mathcal{H}(P)$ may change. In this section we study the behavior of the hyperplane arrangement and the intersection body under translation in dimension 2. We introduce an affine line arrangement, which describes when the hyperplane arrangement is preserved under translation, and fully characterize the conditions under which IP is convex.

4.6.1 The Affine Line Arrangement and Ordered Types

In the following, we investigate how the intersection body of a polygon P behaves under translation of P . We will see that the space of translation vectors can be subdivided into regions induced by an affine line arrangement, and in each such region a continuous translation of P results in a continuous deformation of the intersection body. For this purpose, we introduce ordered types of hyperplane arrangements, which will correspond to regions of the affine line arrangement.

Let $P \subseteq \mathbb{R}^2$ be a fixed polygon with n vertices, and denote by $H_v = v^\perp \subseteq \mathbb{R}^2$ the hyperplane through the origin that is orthogonal to a vertex v of P . As seen in the previous sections, the collection of all such hyperplanes forms a central hyperplane arrangement $\mathcal{H}(P)$ in \mathbb{R}^2 . For each such hyperplane we define its *positive side*

$$H_v^+ = \{x \in \mathbb{R}^2 \mid \langle x, v \rangle > 0\},$$

and its *negative side*

$$H_v^- = \{x \in \mathbb{R}^2 \mid \langle x, v \rangle < 0\}.$$

We now choose a translation vector $t \in \mathbb{R}^2$ and consider the vertices $\{v + t \mid v \in \text{vert}(P)\}$ of the translated polygon $P_t = P + t$. Note that $P_0 = P$. The hyperplane arrangement $\mathcal{H}(P_t)$ is given by the hyperplanes $(v + t)^\perp$, where v ranges over the vertices of P . The hyperplane H_{v+t} can be obtained from H_v by a (orientation preserving) rotation $r_{v,t} : \mathbb{R}^2 \rightarrow \mathbb{R}^2$ such that $r_{v,t}\left(\frac{v}{\|v\|}\right) = \frac{v+t}{\|v+t\|}$, and thus $r_{v,t}(H_v) = H_{v+t}$, $r_{v,t}(H_v^+) = H_{v+t}^+$ and $r_{v,t}(H_v^-) = H_{v+t}^-$.

We label each chamber C of $\mathcal{H}(P_t)$ with a sign vector $s(C) \in \{+, -\}^{\text{vert}(P_t)}$ indexed by the vertices $w = v + t$ of P_t , where

$$\begin{aligned} s(C)_w &= + && \text{if } C \subseteq H_w^+, \\ s(C)_w &= - && \text{if } C \subseteq H_w^-. \end{aligned}$$

As described in [Section 1.2](#), the set $\{s(C) \mid C \in \mathcal{H}(P_t)\}$ the set of signed cocircuits of the underlying oriented matroid of the hyperplane arrangement. Let C_1, \dots, C_M be

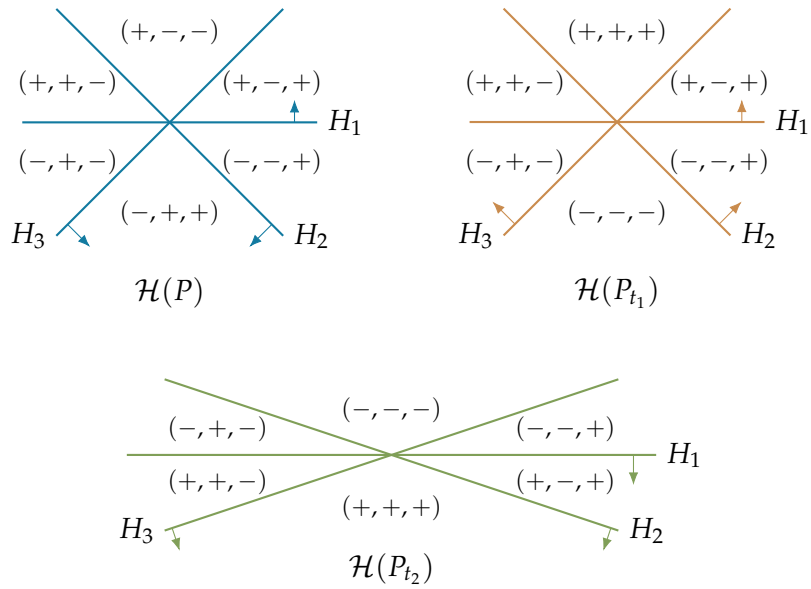


Figure 4.9: The hyperplane arrangements of P_t for the translations of the triangle from [Example 4.6.1](#).

maximal chambers of $\mathcal{H}(P_t)$ in clockwise order, where C_1 is the chamber whose signed cocircuit $s(C_1)$ is maximal with respect to reverse lexicographic order (and $+$ $>$ $-$). For the purposes of our studies, we associate to P_t the *ordered type* $\mathcal{OT}(P_t)$ of the hyperplane arrangement $\mathcal{H}(P_t)$, which is the ordered tuple of signed vectors $\mathcal{OT}(P_t) = (s(C_1), \dots, s(C_M))$.

Example 4.6.1 (Ordered types for the triangle). Let $P = \text{conv}(v_1, v_2, v_3)$ be the triangle with vertices

$$v_1 = \begin{pmatrix} 0 \\ 1 \end{pmatrix}, \quad v_2 = \begin{pmatrix} -1 \\ -1 \end{pmatrix}, \quad v_3 = \begin{pmatrix} 1 \\ -1 \end{pmatrix}.$$

[Figure 4.9](#) shows the hyperplane arrangements $\mathcal{H}(P_t)$ for

$$t_0 = \begin{pmatrix} 0 \\ 0 \end{pmatrix}, \quad t_1 = \begin{pmatrix} 0 \\ 2 \end{pmatrix}, \quad t_2 = \begin{pmatrix} 0 \\ -2 \end{pmatrix}.$$

Note that the underlying oriented matroids of $\mathcal{H}(P_t)$ for $t = t_1$ and $t = t_2$ are the same, but their ordered types differ. We continue with this in [Example 4.6.4](#). \diamond

First, we characterize the possible ordered types of hyperplane arrangements in \mathbb{R}^2 with 2 hyperplanes.

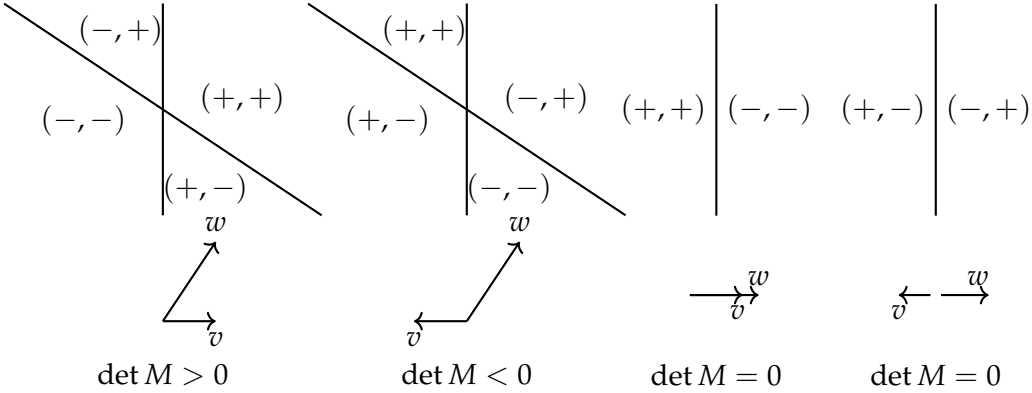


Figure 4.10: The four ordered types of arrangements with two hyperplanes as in Lemma 4.6.2.

LEMMA 4.6.2. Let $u, v \in \mathbb{R}^2$ and $\mathcal{H}(u, v) = u^\perp \cup v^\perp$. Let $M = (u \ v) \in \mathbb{R}^{2 \times 2}$ be the matrix with columns u and v . The ordered type of $\mathcal{H}(u, v)$ is uniquely determined by the sign of the determinant of M . More specifically, the ordered types are

- (i) $(++, +-, --, -+)$ if $\det M > 0$,
- (ii) $(++, -+, --, +-)$ if $\det M < 0$,
- (iii) $(++, --)$ if $\det M = 0$ and $u = \lambda v, \lambda > 0$,
- (iv) $(+-, -+)$ if $\det M = 0$ and $u = \lambda v, \lambda < 0$.

Proof. First note that $\det M \neq 0$ if and only if $u^\perp \neq v^\perp$. In this case $\mathcal{H}(u, v)$ has exactly 4 chambers. By construction, switching the order of u and v reverses the orientation of the linear space spanned by u and v . As can be seen in Figure 4.10, the labeling of the chambers (in clockwise order) solely depends on the relative orientation of u and v , i.e. the sign of the determinant of M . If $\det M = 0$ then $u^\perp = v^\perp$ and the hyperplane arrangement consists of two maximal chambers. In this case, we have that $u = \lambda v$ for some nonzero $\lambda \in \mathbb{R}$. Again, the labeling of the chambers is uniquely determined by the sign of λ , as illustrated in Figure 4.10. \square

THEOREM 4.6.3. Let $P \subseteq \mathbb{R}^2$ be a polygon. The affine hyperplane arrangement

$$\mathcal{L}(P) = \{\text{aff}(-v_1, -v_2) \mid v_1, v_2 \text{ are vertices of } P\}$$

of affine lines through pairs of vertices of $-P$ subdivides \mathbb{R}^2 into open regions. The latter are in bijection with ordered types of $\mathcal{H}(P_t)$ in the following way. For each such region R the ordered type of the hyperplane arrangement $\mathcal{H}(P_t)$ is fixed for all $t \in R$, and for any two distinct regions the ordered types are distinct.

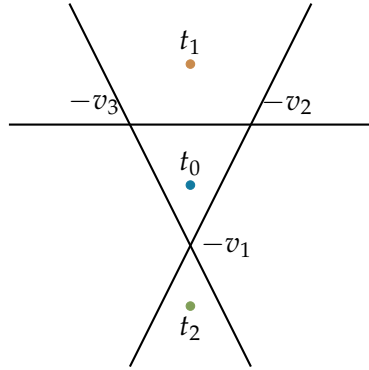


Figure 4.11: The affine line arrangement $\mathcal{L}(P)$ of the triangle from Examples 4.6.1 and 4.6.4.

Proof. Let R be a region of $\mathcal{L}(P)$ and v_1, v_2 be distinct vertices of P . Equivalently, $w_1 = v_1 + t$ and $w_2 = v_2 + t$ are distinct vertices of P_t for all $t \in \mathbb{R}^2$. By construction of $\mathcal{L}(P)$, the open region R does not intersect $\text{aff}(-v_1, -v_2)$, i.e. R lies on one side of this affine line. Consider the matrix $M_t = (w_1 \ w_2) = (v_1 + t \ v_2 + t) \in \mathbb{R}^{2 \times 2}$. Note that $\det(M_t) = 0$ if and only if $t \in \text{aff}(-v_1, -v_2)$, i.e. when w_1, w_2 lie on a common line through the origin. Furthermore, the affine line $\text{aff}(-v_1, -v_2)$ partitions the ambient space \mathbb{R}^2 into two open halfspaces, in which the determinant of M_t is nonzero and has a fixed sign. Therefore, for all $t \in R$ the matrix M_t has a fixed nonzero sign.

Let $t \in R$ and let C be a chamber of $\mathcal{H}(P_t)$ with signed cocircuit $s(C)$. We can write

$$C = \bigcap_{\substack{w_i, w_j \in \text{vert}(P_t) \setminus \{0\} \\ w_i \neq w_j}} C(w_i, w_j)$$

as the intersection of a chamber $C(w_i, w_j)$ for each subarrangement $\mathcal{H}(w_i, w_j) = w_i^\perp \cup w_j^\perp$, where (w_i, w_j) is a pair of distinct vertices of P_t which are both different from the origin. The signed cocircuit satisfies $s(C)_{w_k} = s(C(w_i, w_j))_{w_k}$ for $k = i, j$. Therefore, the ordered type of $\mathcal{H}(P_t)$ can be seen as the common refinement of ordered types of $\mathcal{H}(w_i, w_j)$, where (w_i, w_j) ranges over all pairs of vertices of P_t . By Lemma 4.6.2, the ordered type of $\mathcal{H}(w_i, w_j)$ is uniquely determined by the sign of the determinant of the matrix M_t , and thus also the sign of $s(C)_{w_k}$ is uniquely determined. Therefore, the ordered type of $\mathcal{H}(P_t)$ is uniquely determined by the position of t relative to the affine lines in $\mathcal{L}(P)$, i.e. the region $R \subseteq \mathcal{L}(P)$ containing t . \square

Example 4.6.4 (The affine line arrangement of the triangle). Let P be the triangle from Example 4.6.1. The affine line arrangement is shown in Figure 4.11. Note that the translation vectors $t = t_0, t_1, t_2$ all lie in different regions of the arrangement, and thus the ordered types of the hyperplane arrangements $\mathcal{H}(P_t)$ are distinct. \diamond

We emphasize that there are two hyperplane arrangements or line arrangements in \mathbb{R}^2 which play a main role in the study of convexity of intersection bodies of polygons.

4.6 Convex Intersection Bodies of Polygons

We have the *central* hyperplane arrangement $\mathcal{H}(P_t)$, which depends on the choice of t , and subdivides \mathbb{R}^2 into open two-dimensional cones, which we call *chambers* of $\mathcal{H}(P_t)$. On the other hand, we have the *affine* line arrangement $\mathcal{L}(P)$, which subdivides \mathbb{R}^2 into open two-dimensional components, which we call *regions* of $\mathcal{L}(P)$. Note that $\mathcal{L}(P) = \mathcal{L}(P_t) - t$ by construction.

We now describe how the regions in the affine line arrangement $\mathcal{L}(P)$ relate to the geometry of the intersection body IP_t .

LEMMA 4.6.5. Let P be a polygon and $t \in \mathbb{R}^2$. Let C be a maximal open chamber of $\mathcal{H}(P)$, and C_t be a maximal open chamber of $\mathcal{H}(P_t)$ such that $s(C) = s(C_t)$, i.e. their signed cocircuits agree. Let $u \in C$, $u_t \in C_t$ and

$$\begin{aligned}\mathcal{E} &= \{e \subseteq P \mid e \text{ is an edge of } P, u^\perp \cap e \neq \emptyset\}, \\ \mathcal{E}_t &= \{e_t \subseteq P_t \mid e_t \text{ is an edge of } P_t, u_t^\perp \cap e_t \neq \emptyset\}.\end{aligned}$$

Then $\mathcal{E}_t = \mathcal{E}$.

Proof. Let $e = \text{conv}(v_1, v_2) \in \mathcal{E}$ be an edge of P . Since $u^\perp \cap e \neq \emptyset$, we have that v_1, v_2 lie on different sides of u^\perp . Equivalently, we have $s(C)_{v_1} = -s(C)_{v_2}$, and without loss of generality $s(C)_{v_1} = +$. Thus, $u \in H_{v_1}^+ \cap H_{v_2}^-$. Since $\mathcal{H}(P_t)$ is obtained from $\mathcal{H}(P)$ by rotating the hyperplanes individually, and $s(C) = s(C_t)$ it follows that $u_t \in H_{v_1+t}^+ \cap H_{v_2+t}^-$. Since $e + t$ is an edge of P_t if and only if e is an edge of P , the claim follows. \square

THEOREM 4.6.6. Let R be a maximal open region of $\mathcal{L}(P)$ and $t \in R$. Fix a sign vector $s \in \{+, -\}^{\text{vert}(P)}$ and let C_t be an open chamber of $\mathcal{H}(P_t)$ such that $s(C_t) = s$. Then the radial function $\rho_{IP_t}|_{C_t}$ of IP_t restricted to the chamber C_t and the region R is linear and continuous in t .

Proof. By Lemma 4.6.5, for a fixed region R and fixed chamber C_t , for any vector $u_t \in C_t$ the set of edges of P_t which intersect u_t is fixed. Since P is 2-dimensional, this is a pair of edges $\text{conv}(a_1 + t, b_1 + t), \text{conv}(a_2 + t, b_2 + t)$, where a_1, a_2, b_1, b_2 are vertices of P . Let $Q_t = P_t \cap u_t^\perp$ be the one-dimensional section with vertices $v_1 = \text{conv}(a_1 + t, b_1 + t) \cap u_t^\perp$ and $v_2 = \text{conv}(a_2 + t, b_2 + t) \cap u_t^\perp$. Recall from the proof of Theorem 4.2.4 that we can compute

$$\text{vol}_1(Q_t) = \frac{1}{\|x\|^2} (\text{sgn}(v_1)|\det(M_1(x, t))| + \text{sgn}(v_2)|\det(M_1(x, t))|),$$

where $\text{sgn}(v_i) \in \{1, -1\}$ depends on the position of v_i relative to t and

$$M_i(x, t) = \left[\begin{array}{c} \frac{\langle b_i + t, x \rangle (a_i + t) - \langle a_i + t, x \rangle (b_i + t)}{\langle b_i - a_i, x \rangle} \\ x \end{array} \right] = M_i(x, \emptyset) + \left[\begin{array}{c} \frac{\langle t, x \rangle (a_i - b_i)}{\langle b_i - a_i, x \rangle} \\ x \end{array} \right].$$

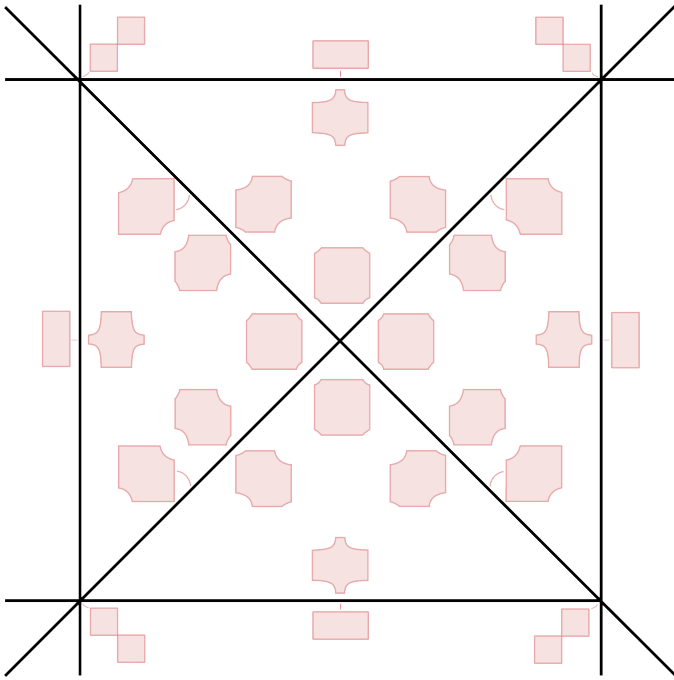


Figure 4.12: The arrangement $\mathcal{L}(P)$ of affine lines for $P = [-1, 1]^2$, together with IP_t for different choices of t .

The determinant of $M_i(x, t)$ is thus a homogeneous polynomial of degree 1 in the variable t , and so the radial function is linear and continuous in t . \square

Example 4.6.7. Figure 4.12 shows the continuous deformation of the intersection body IP_t of the unit square $P = [-1, 1]^2$ under translation by $t \in \mathbb{R}^2$ within each bounded region of the affine line arrangement. \diamond

4.6.2 Convexity

For each fixed region R of the affine line arrangement $\mathcal{L}(P)$, Theorem 4.6.6 implies that, as we move $t \in R$ continuously, the intersection body IP_t deforms continuously as well. We now characterize under which circumstances the intersection body of a polygon is convex. Recall that IP cannot be convex if the origin lies outside of P or is a vertex of P . We thus consider the distinct cases of when the origin lies in the interior of P , and when the origin is a point on the boundary. Figure 4.12 shows that in the case of the square, the intersection body of $P + t$ is convex for precisely 5 translation vectors. In Theorem 4.6.14 we show that the number of such translation vectors is always finite, and the square maximizes this number.

Definition 4.6.8 (Convexity in a chamber). Let $P \subseteq \mathbb{R}^2$ be a polygon and let C be a chamber of $\mathcal{H}(P)$. We say that $IP \subseteq \mathbb{R}^2$ is *convex in C* if $IP \cap C$ is convex. Recall from

4.6 Convex Intersection Bodies of Polygons

[Section 4.4](#) that the boundary of IP in the chamber C is defined by exactly one of the irreducible components of the algebraic boundary $\partial_a IP$. We will refer to this boundary component as *the component of $\partial_a IP$ in C* .

Remark 4.6.9. Let C be a chamber of $\mathcal{H}(P)$ such that IP is not convex in C . Then IP is not convex. However, that IP is convex in C for all C does not suffice for showing that IP is convex.

In the following [Propositions 4.6.10](#) and [4.6.11](#) we consider polygons with the origin in the interior, and characterize the geometry of the boundary of IP in terms of the geometry of the boundary of P . More precisely, we will see that the convex pieces of the boundary of IP correspond to pairs of parallel edges of P , and all convex pieces are linear. We begin by describing the linear pieces of ∂IP .

PROPOSITION 4.6.10. Let $P \subseteq \mathbb{R}^2$ be a polygon. Let C be a chamber of $\mathcal{H}(P)$, and let $x \in C$. We denote by $v_1(x), v_2(x)$ the points of intersection $x^\perp \cap \partial P = \{v_1(x), v_2(x)\}$ of the boundary of P with the line x^\perp . Let $\text{conv}(a_1, b_1), \text{conv}(a_2, b_2)$ be edges of P such that $v_1(x) \in \text{conv}(a_1, b_1)$ and $v_2(x) \in \text{conv}(a_2, b_2)$. Then the component of $\partial_a IP$ in C is linear if and only if the segments $\text{conv}(a_1, b_1)$ and $\text{conv}(a_2, b_2)$ are parallel.

Proof. We want to prove that $\{x \in C \mid \rho_{IP}|_C(x) = 1\}$ is a line segment. Assume that $v_1(x) = \lambda a_1 + (1 - \lambda)b_1$ and $v_2(x) = \mu a_2 + (1 - \mu)b_2$ for some $\lambda, \mu \in (0, 1)$. Since $v_1(x), v_2(x) \in x^\perp$, we have

$$\lambda = \frac{\langle b_1, x \rangle}{\langle b_1 - a_1, x \rangle}, \quad \mu = \frac{\langle b_2, x \rangle}{\langle b_2 - a_2, x \rangle}.$$

We want to compute the length of $\text{conv}(v_1(x), v_2(x))$, or equivalently the length of $\text{conv}(\emptyset, v_1(x) - v_2(x))$. As in the proof of [Theorem 4.1.8](#), we compute this via the area of the triangle with vertices $\emptyset, v_1(x) - v_2(x)$ and $\frac{x}{\|x\|^2}$. Hence, the radial function can be computed by the determinant

$$\rho_{IP}|_C(x) = \frac{1}{\|x\|^2} \left| \det \begin{bmatrix} v_1(x) - v_2(x) \\ x \end{bmatrix} \right|.$$

We compute the radial function explicitly. First,

$$v_1(x) - v_2(x) = \frac{(\langle b_2 - a_2, x \rangle (\langle b_1, x \rangle a_1 - \langle a_1, x \rangle b_1) - \langle b_1 - a_1, x \rangle (\langle b_2, x \rangle a_2 - \langle a_2, x \rangle b_2))}{\langle b_1 - a_1, x \rangle \langle b_2 - a_2, x \rangle}.$$

The irreducible component of $\partial_a P$ in C is given by the set of points $x \in C$ such that $\rho_{IP}|_C(x) = 1$, i.e. the points which satisfy

$$\begin{aligned} & \frac{1}{\|x\|^2} \det \left[\begin{array}{c} (\langle b_2 - a_2, x \rangle (\langle b_1, x \rangle a_1 - \langle a_1, x \rangle b_1) - \langle b_1 - a_1, x \rangle (\langle b_2, x \rangle a_2 - \langle a_2, x \rangle b_2)) \\ x \end{array} \right] \\ &= \langle b_1 - a_1, x \rangle \langle b_2 - a_2, x \rangle, \end{aligned} \tag{4.2}$$

assuming that the determinant in the left hand side is positive in C (otherwise it gets multiplied by -1). This determinant is a cubic polynomial in x , which by [Proposition 4.4.3](#) is divisible by $\|x\|^2$. Hence, the left hand side of [\(4.2\)](#) is a homogeneous linear polynomial in x . It divides the right hand side if and only if $(b_2 - a_2) = \kappa(b_1 - a_1)$ for some $\kappa \in \mathbb{R}$, i.e. if the two line segments are parallel. In this case [\(4.2\)](#) is a linear equation, and hence the curve defined by [\(4.2\)](#) is a line; otherwise it is a conic, passing through the origin. \square

PROPOSITION 4.6.11. Let $P \subseteq \mathbb{R}^2$ be polygon with the origin in its interior. If there exists a line through the origin which intersects ∂P in two non-parallel edges, then IP is not convex.

Proof. Let C be a chamber of $\mathcal{H}(P)$ such that x^\perp intersects two non-parallel edges ℓ_1, ℓ_2 of P . Consider $u_a, u_b \in C \cap S^1$. As shown in [Figure 4.13](#), we denote

$$\begin{aligned} u_a^\perp \cap \ell_1 &= a = \begin{pmatrix} a_1 \\ a_2 \end{pmatrix}, & u_b^\perp \cap \ell_1 &= b = \begin{pmatrix} b_1 \\ b_2 \end{pmatrix}, \\ u_a^\perp \cap \ell_2 &= -\alpha a, & u_b^\perp \cap \ell_2 &= -\beta b, \end{aligned}$$

for some positive real numbers $\alpha, \beta > 0$. Since ℓ_1 and ℓ_2 are not parallel, we have $\alpha \neq \beta$. We can choose a, b , such that $u_a = \frac{1}{\|a\|} \begin{pmatrix} a_2 \\ -a_1 \end{pmatrix}$ and $u_b = \frac{1}{\|b\|} \begin{pmatrix} b_2 \\ -b_1 \end{pmatrix}$. The lengths of the line segments $u_a^\perp \cap P = \text{conv}(a, -\alpha a)$ and $u_b^\perp \cap P = \text{conv}(b, -\beta b)$ are

$$\begin{aligned} \|u_a^\perp \cap P\| &= \|a - (-\alpha a)\| = (1 + \alpha)\|a\| \\ \|u_b^\perp \cap P\| &= \|b - (-\beta b)\| = (1 + \beta)\|b\|. \end{aligned}$$

Thus, the boundary points of IP in directions u_a, u_b are

$$\begin{aligned} p_a &:= \rho_{IP}(u_a) u_a = (1 + \alpha)\|a\| u_a = (1 + \alpha) \begin{pmatrix} a_2 \\ -a_1 \end{pmatrix}, \\ p_b &:= \rho_{IP}(u_b) u_b = (1 + \beta)\|b\| u_b = (1 + \beta) \begin{pmatrix} b_2 \\ -b_1 \end{pmatrix} \end{aligned}$$

respectively. Consider the midpoint $\frac{a+b}{2} \in \ell_1$ and let u_{a+b} be the unit vector in C orthogonal to $a + b$ (and thus also to $\frac{a+b}{2}$). Then $u_{a+b} = \frac{1}{\|a+b\|} \begin{pmatrix} a_2 + b_2 \\ -a_1 - b_1 \end{pmatrix}$, $u_{a+b}^\perp \cap \ell_2 = -\frac{\alpha\beta}{\alpha+\beta}(a + b)$ and the boundary point of IP in direction u_{a+b} is

$$p_{a+b} = \rho_{IP}(u_{a+b}) u_{a+b} = \left(\frac{1}{2} + \frac{\alpha\beta}{\alpha+\beta} \right) \|a + b\| u_{a+b} = \left(\frac{1}{2} + \frac{\alpha\beta}{\alpha+\beta} \right) \begin{pmatrix} a_2 + b_2 \\ -a_1 - b_1 \end{pmatrix}.$$

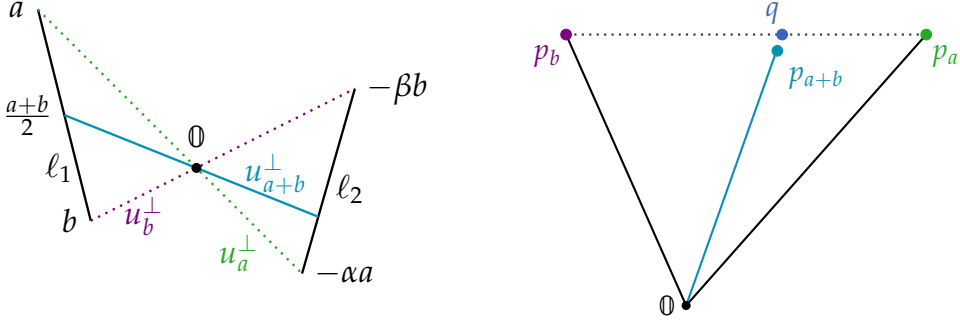


Figure 4.13: The proof of [Proposition 4.6.11](#) in a picture. Left: the lines orthogonal to u_a, u_b, u_{a+b} and their intersections with the edges ℓ_1, ℓ_2 of P . Right: the points $p_a, p_b, p_{a+b} \in \partial IP$, and the point $q \in \text{conv}(p_a, p_b)$, but $q \notin IP$.

Let $q = \text{conv}(p_a, p_b) \cap \text{cone}(u_{a+b})$, as in [Figure 4.13](#). We want to prove now that $IP \cap C$ is not convex, by showing that $\|q\| > \|p_{a+b}\|$. Indeed, we can compute that

$$q = \frac{(1+\alpha)(1+\beta)}{2+\alpha+\beta} (a_2 + b_2, -a_1 - b_1)$$

and therefore

$$\begin{aligned} \|q\| - \|p_{a+b}\| &= \frac{(1+\alpha)(1+\beta)}{2+\alpha+\beta} \|a+b\| - \left(\frac{1}{2} + \frac{\alpha\beta}{\alpha+\beta} \right) \|a+b\| \\ &= \frac{(\alpha-\beta)^2}{2(2+\alpha+\beta)(\alpha+\beta)} \|a+b\|. \end{aligned}$$

Since $\alpha \neq \beta$, this expression is strictly positive, and so $q \notin IP$. This proves that $p_a, p_b \in IP$, but the segment $\text{conv}(p_a, p_b)$ is not contained in IP . Hence, IP is not convex. \square

We are now ready to move towards a full classification of convexity of intersection bodies of polygons for any position of the origin. Note that if P is centrally symmetric, then the convexity of P follows from the following classical statement.

THEOREM 4.6.12 ([Gar06, Theorem 8.1.4]). Let $K \subseteq \mathbb{R}^2$ be a two-dimensional convex body centered at the origin. Then $IK = r_{\frac{\pi}{2}}(2K)$, where $r_{\frac{\pi}{2}}$ is a counter-clockwise rotation by $\frac{\pi}{2}$.

A key argument in the proof of the following [Theorem 4.6.12](#) is done via the chordal symmetral of P . The *chordal symmetral* $\tilde{\Delta}K$ of a star body $K \subseteq \mathbb{R}^d$ is the union of segments $\text{conv}(-c_u u, c_u u)$, where $u \in S^{d-1}$ and $c_u = \frac{1}{2} \text{vol}_{d-1}(K \cap u^\perp)$ [Gar06, Definition 5.1.3].

The chordal symmetral is starshaped set with respect to the origin. We will make use of the following statements.

PROPOSITION 4.6.13 ([Gar06, Chapter 5.1]). Let $K \subseteq \mathbb{R}^d$ be a star body. Then

- (i) K is centrally symmetric and centered at the origin if and only if $K = \tilde{\Delta}K$,
- (ii) if $K \subseteq \mathbb{R}^2$ then $IK = 2\tilde{\Delta}K$

We now prove the main result of this section.

THEOREM 4.6.14. Let $P \subseteq \mathbb{R}^2$ be a polygon. Then IP is a convex body if and only if

- (i) $P = -P$, or
- (ii) the origin is the midpoint of an edge and $P \cup -P$ is convex.

Proof. Recall that IP is not convex if the origin lies in $\mathbb{R}^2 \setminus P$, or if the origin is a vertex of P . We are left to analyze the cases in which the origin lies in the interior of P or in the interior of an edge of P .

We first consider the case in which the origin lies in the interior of P and show that IP is convex if and only if $P = -P$. If $P = -P$, then [Theorem 4.6.12](#) implies that IP is convex. Assume now that IP is convex, and the origin lies in the interior of P . Then $C \cap IP$ is convex for every chamber C of $\mathcal{H}(P)$. In particular, by [Proposition 4.6.11](#), every line u^\perp through the origin which does not intersect a vertex of P intersects ∂P in the interior of two parallel edges. Hence, the edges of P come in pairs of parallel edges. We rotate $u \in S^2$ continuously. Whenever u^\perp crosses a vertex of one edge, it must also cross a vertex in the parallel edge, since otherwise this results in a pair of non-parallel edges. This implies that for every vertex v of P , there exists a vertex w of P such that $w = -\lambda v$ for some $\lambda > 0$. Since all edges are pairwise parallel, this positive scalar λ is the same for all vertices. Therefore, we also get that $v = -\lambda w$, which implies that $\lambda = 1$. Hence, $P = -P$.

Consider now the case in which the origin lies in the interior of an edge F of P . Since the origin lies on the boundary of P , we have that $IP = \frac{1}{2}I(P \cup -P)$. Using [Proposition 4.6.13](#) we deduce the following chain of equalities:

$$IP = \frac{1}{2}I(P \cup -P) \stackrel{(i)}{=} \frac{1}{2} \cdot 2\tilde{\Delta}(P \cup -P) \stackrel{(ii)}{=} P \cup -P.$$

Therefore, IP is convex if and only if $P \cup -P$ is convex. In order for this to happen, the origin must be the midpoint of F , and additionally $P \cup -P$ must be convex. \square

Example 4.6.15. By [Corollary 4.6.16](#) for each polygon P there are only finitely many positions of the origin such that the intersection body of P is convex. [Figure 4.14](#) shows a collection of examples of polygons, together with the possible positions of the origin. \diamond

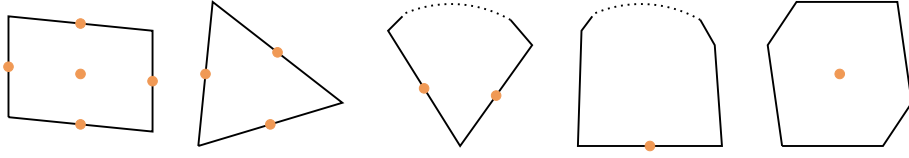


Figure 4.14: Examples in which $I(P)$ is convex; the orange points represent admissible positions of the origin. From left to right: a parallelogram ($k = 5$), an acute triangle ($k = 3$), a diamond shape ($k = 2$), a panettone shape, and a centrally symmetric polygon which is not a parallelogram ($k = 1$). The case $k = 4$ is not realizable.

COROLLARY 4.6.16. Let $P \subseteq \mathbb{R}^2$ be a polygon and let

$$k = |\{t \in \mathbb{R}^2 \mid I(P + t) \text{ is convex}\}|.$$

Then $k \leq 5$ and the equality is realized exactly when P is a parallelogram.

Proof. By [Theorem 4.6.14](#), $I(P + t)$ is convex if and only if $-t$ is the center of symmetry of P (if it exists), or a midpoint of an edge such that $(P + t) \cup -(P + t)$ is convex. Thus, the number of such $t \in \mathbb{R}^2$ is finite.

If $-t$ is the midpoint of an edge e , then $(P - t) \cup -(P - t)$ is convex if and only if the sum of the angles adjacent to e is at most π . Let v_1, \dots, v_n be the vertices of P , ordered cyclically, and let α_i be the interior angle of P at v_i (and $\alpha_{n+1} = \alpha_1$). Assume that there are m pairs of consecutive interior angles $(\alpha_i, \alpha_{i+1}), i \in [m]$ such that $\alpha_i + \alpha_{i+1} \leq \pi$. Recall that for any polygon with n vertices, the sum of all interior angles is $(n - 2)\pi$. Furthermore, for any angle in a polygon holds $\alpha_i \leq \pi$. We thus obtain that

$$\begin{aligned} 2(n-2)\pi &= 2 \sum_{i=1}^n \alpha_i = \sum_{i=1}^n (\alpha_i + \alpha_{i+1}) \\ &= \sum_{i=1}^m (\alpha_i + \alpha_{i+1}) + \sum_{i=m+1}^n (\alpha_i + \alpha_{i+1}) \\ &\leq \sum_{i=1}^m \pi + \sum_{i=m+1}^n 2\pi \\ &\leq m\pi + 2(n-m)\pi. \end{aligned}$$

This implies $m \leq 4$, hence $k \leq 5$. Note that if the pairs of interior angles with sum $\leq \pi$ are not consecutive, then this violates the convexity of P . A similar computation as above with the exterior angles of P implies that if $k = 5$ then $n = m = 4$ and all pairs of consecutive angles sum up to π . Hence, the unique maximizers of k are parallelograms. \square

4.6.3 Convexity in higher dimensions

We now discuss which of the result presented in this section may generalize to higher dimensions.

The construction of the hyperplane arrangement $\mathcal{H}(P)$ is defined for every polytope $P \subseteq \mathbb{R}^d$, and gives rise to an oriented matroid in general. The statement of [Theorem 4.6.3](#) can be generalized as follows. Let

$$\mathcal{L}(P) = \{\text{aff}(-v_1, \dots, -v_d) \mid v_1, \dots, v_d \text{ are affinely independent vertices of } P\}.$$

This yields an affine hyperplane arrangement, in which each region R gives rise to a unique oriented matroid underlying the central hyperplane arrangement $\mathcal{H}(P_t)$. However, defining the right notion of *ordered type* such that the regions R are in bijection with ordered types is more intricate for higher dimensions and is subject for further research. On the other hand, since the argument in [Theorem 4.6.6](#) solely depends on the oriented matroid, also in higher dimensions the radial function is continuous on regions of the more general version of $\mathcal{L}(P)$.

The methods used in the arguments of [Section 4.6.2](#) do not generalize to higher dimensions. For example, in contrast to [Propositions 4.6.10](#) and [4.6.11](#), in higher dimensions there exist convex pieces $IP \cap C$ which are not linear. Also the identification with the chordal symmetral body does not hold in general. These are key arguments in the proof of [Theorem 4.6.14](#) which do not generalize to higher dimensions. However, in order to obtain a convex intersection body IP , the origin must either lie in the interior of P , or in the interior of a facet of P . Otherwise there exists a hyperplane u^\perp intersecting P at most in a lower-dimensional face, and thus the radial function in direction u has value 0. This yields the following conjecture.

CONJECTURE 4.6.17. Let $P \subset \mathbb{R}^d$ be a full-dimensional polytope. Then IP is a convex body if and only if

- (i) $P = -P$, or
- (ii) the origin is the center of a symmetric facet F of P , and $P \cup -P$ is convex.

COMBINATORICS OF CORRELATED EQUILIBRIA

In 1950, Nash published a two-page article proving the existence of a Nash equilibrium for any finite game [Nas50]. This opened many new fronts, not only in game theory, but also in areas such as economics, computer science, evolutionary biology and quantum mechanics [PPV05; SP73; BL13]. To study Nash equilibria one assumes that the actions of the players are independent and completely separated from any exterior influence. Moreover, these can be described as a system of multilinear equations [Stuo2, Section 6]. However, there exist cases where a Nash equilibrium fails to predict the most beneficial outcome (e.g. Pareto optimality) for all players. There are several approaches, rooted in the concept of a *dependency equilibrium*, which generalize Nash equilibria by imposing dependencies between the actions of players. This class of equilibria has been studied from the point of view of algebraic statistics and computational algebraic geometry [Spoon03; PS22; PSA22]. On the other hand, Aumann introduced the concept of a *correlated equilibrium*, which assumes that there is an external correlation device such as a mediator or some other physical source. The resulting correlated equilibria are probability distributions of recommended joint strategies [Aum74; Aum87]. In contrast to Nash equilibria and dependency equilibria, correlated equilibria are significantly less computationally expensive, since they only require solving a linear program [PRo8]. In other words, the set of such equilibria can be described by linear inequalities in the probability simplex and thus form a convex polytope called the *correlated equilibrium polytope*. In this chapter, we study combinatorial properties of correlated equilibrium polytopes with methods from discrete geometry and real algebraic geometry.

We illustrate the concept of correlated equilibrium in an example: Two cars meet at a crossing. Both drivers would like to continue to drive, but, even more importantly, would also like to avoid a car crash. Thus, each of the drivers prefers not to drive in

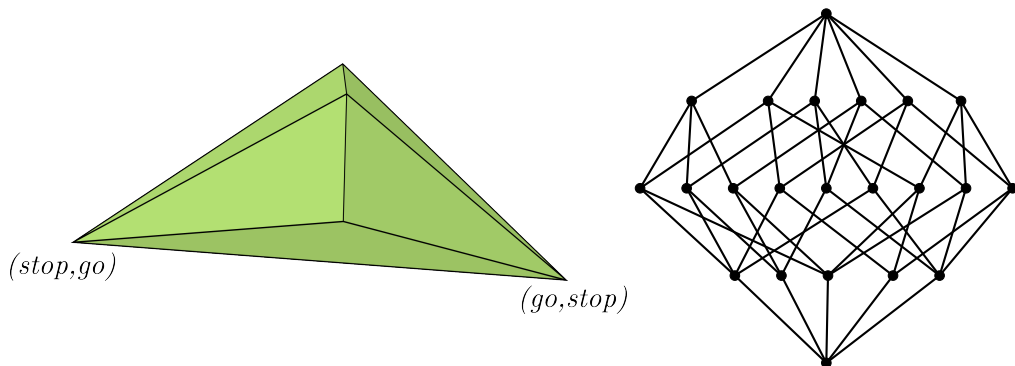


Figure 5.1: The correlated equilibrium polytope of a (2×3) -game and its face lattice.

case the other chooses to drive. We make the assumptions that both drivers are unable to communicate with each other. This is a classic game in game theory known as Chicken game or Hawk-Dove game, and we formalize this in Examples 5.1.1, 5.4.1, 5.1.3 and 5.1.6. However, this situation changes drastically if there is a traffic light installed at this crossing. We can view the traffic light as a neutral exterior party, that gives a recommendation to each player in showing green or red lights; here we assume that each driver only knows their own given recommendation. If a fixed driver is given such a recommendation (for example a red light), the driver now ponders about deviating from this recommendation in benefit of their own (selfish) good, assuming that the other player adheres to their own given recommendation. If both drivers decide not to deviate from the recommendation given by the traffic lights, a correlated equilibrium is achieved.

To our knowledge, there are no articles concerning the combinatorics of correlated equilibrium polytopes in the language of convex or discrete geometry up to this date, despite the fact that the concept of correlated equilibria is a topic of extensive research in economics and game theory [Aum87; Rago2; Vio03; NCHo4; PRo5]. In this chapter we study this class of polytopes from combinatorial perspective. In general, the correlated equilibrium polytope can exhibit a great variety of distinct combinatorial structures. This is not surprising as it is proven that any convex polytope can be realized as the correlated equilibrium payoffs of game [LSV11], i.e. as a certain projection of a correlated equilibrium polytope. Even classifying necessary conditions under which the correlated equilibrium polytope is of maximal dimension is highly nontrivial [Vio03]. For this purpose, we introduce the *region of full-dimensionality*, a set that classifies under which conditions the correlated equilibrium polytope has maximal dimension.

THEOREM 5.3.1. The region of full-dimensionality is a semialgebraic set and can be explicitly described. The full description of this semialgebraic set as the coordinate projection of a basic semialgebraic set can be found on page 176.

We continue the study of the combinatorial structure of correlated equilibrium polytopes by introducing a linear space called the the *correlated equilibrium space*, and consider an oriented matroid strata inside this space. This is a stratification of the linear space, in which regions correspond to oriented matroids, and give rise to the different combinatorial types of correlated equilibrium polytopes. We study the algebraic boundary of the strata for $(2 \times n)$ -games, which turns out to be generated by binomials corresponding to (2×2) -minors of a certain matrix (Theorem 5.4.7). These investigations yield novel insights into the possible combinatorial types of (2×3) -games.

THEOREM 5.4.8. Let G be a (2×3) -game and P_G be the associated correlated equilibrium polytope. Then one of the following holds.

- (i) P_G is a point.
- (ii) P_G is of maximal dimensional 5 and of a unique combinatorial type.

5.1 The Correlated Equilibrium Polytope

- (iii) There exists a (2×2) -game G' such that $P_{G'}$ has maximal dimensional 3 and is combinatorially equivalent to P_G .

The unique combinatorial type of dimension 5 of (2×3) -games has f -vector $(1, 11, 32, 40, 25, 8, 1)$ and its edge graph is shown in [Figure 5.4](#). A full description of this polytope can be found on MathRepo [[BHP22b](#)]. Supported by the above theorem and our computations for $(2 \times n)$ -games G (where $n \leq 5$), we conjecture that if P_G is not of maximal dimension, then there exists a smaller $(2 \times k)$ -game G' with $k < n$ such that $P_{G'}$ is a full-dimensional polytope and P_G is combinatorially equivalent to $P_{G'}$ ([Conjecture 5.4.10](#)).

This chapter is based on [[BHP22a](#)], which is joint work with Benjamin Hollering and Irem Portakal. All supplementary material, including all referenced code and the resulting computations are publicly available on a MathRepo page [[BHP22b](#)].

Overview

We study correlated equilibrium polytopes from a discrete geometric and real algebraic geometric point of view. The background is given in [Sections 1.1, 1.2, 1.4](#) and [1.8](#). We first provide a short introduction for the necessary concepts from game theory in [Section 5.1](#), including correlated equilibria and Nash equilibria. In [Section 5.2](#) we describe the correlated equilibrium cone, a convex polyhedral cone which captures the geometry of the correlated equilibrium polytope, and describe the correlated equilibrium space. We study the region of full-dimensionality in [Section 5.3](#). Finally, we consider the possible combinatorial types through the oriented matroid strata in [Section 5.4](#). All results are illustrated with examples for games of types (2×2) , (2×3) and, whenever possible, games of type $(2 \times 2 \times 2)$.

5.1 THE CORRELATED EQUILIBRIUM POLYTOPE

In this section we introduce the basic concepts of game theory, such as a game itself, and different notions of strategies. We establish the concept of correlated equilibria and illustrate the relation to Nash equilibria.

Let n be the number of players. Each player $i \in [n]$ has a fixed set of *pure strategies* $s_1^{(i)}, \dots, s_{d_i}^{(i)}, d_i \in \mathbb{N}$. It is practical to think of each strategy as a single move that a player can play, and all players perform their single move simultaneously. Afterwards, the game is over, so the choices of the possible moves can be seen as outcome of the game. A *pure joint strategy* is a tuple $s_{j_1 \dots j_n} = (s_{j_1}^{(1)}, \dots, s_{j_n}^{(n)})$ of strategies, where each player $i \in [n]$ chooses to play a fixed strategy $s_{j_i}^{(i)}$ with $j_i \in [d_i], i \in [n]$. The *payoff* $X_{j_1 \dots j_n}^{(i)} \in \mathbb{R}$ of player i at $s_{j_1 \dots j_n}$ is the quantity of how beneficial player i values the combination $(s_{j_1}^{(1)}, \dots, s_{j_n}^{(n)})$ of strategies as outcome of the game. A *mixed strategy* of a single player i is an action with probability $p^{(i)} = (p_{j_1}^{(i)}, \dots, p_{j_{d_i}}^{(i)})$, i.e. $p_{j_1}^{(i)}, \dots, p_{j_{d_i}}^{(i)} \geq 0$

and $\sum_{k=1}^{d_i} p_{j_k}^{(i)} = 1$. We can view this geometrically as a point in the $(d_i - 1)$ -dimensional probability simplex Δ_{d_i-1} .

Formally, a $(d_1 \times \dots \times d_n)$ -game in normal form is a tuple $G = (n, S, X)$, where $S = (S^{(1)}, \dots, S^{(n)})$ is the collection of strategies $S^{(i)} = (s_1^{(i)}, \dots, s_{d_i}^{(i)})$ of all players, and $X = (X^{(1)}, \dots, X^{(n)})$ is the collection of all $(d_1 \times \dots \times d_n)$ -payoff tensors. In particular, if $n = 2$, then each $X^{(i)}$ is a $(d_1 \times d_2)$ -matrix and called the *payoff matrix* of player i .

Example 5.1.1 (Traffic Lights). Recall the example from the introduction, in which two cars meet at a crossing and would like to avoid a car crash. Formally, each player $i \in [2]$ has the strategies $s_1^{(i)} = \text{"go"}$ and $s_2^{(i)} = \text{"stop"}$. The bimatrix below shows the payoffs of both players simultaneously, where each entry is a tuple $(X_{j_1 j_2}^{(1)}, X_{j_1 j_2}^{(2)})$ of the payoff of each player for the tuple of strategies $(s_{j_1}^{(1)}, s_{j_2}^{(2)}), j_1, j_2 \in [2]$ as the expected outcome of the game.

		Player 2	
		go	stop
Player 1	go	(-99, -99)	(1, 0)
	stop	(0, 1)	(0, 0)

We may interpret the given payoffs such that each of the players prefers to go (with payoff $X_{12}^{(1)} = X_{21}^{(2)} = 1$) if the other driver stops. However, both drivers choosing to drive is the worst possible outcome for each of the players individually (with payoff $X_{11}^{(i)} = -99$ for both players). Since there is no interaction between the players, and the payoffs of a car crash are very negative, the players are very likely not to risk a move, although this is not optimal for either of these players ($X_{22}^{(i)} = 0$ for both players). This is the motivation for introducing the concept of correlated equilibrium, in which the assumptions allow a dependence of the moves of the players by the suggestion of an external party, e.g. a traffic light. We continue with this in Examples 5.1.3 and 5.1.6. \diamond

We now allow a third, independent party to influence the game from the outside. Let $\tilde{S} = \{s_{j_1 \dots j_n} \mid j_i \in [d_i], i \in [n]\}$ be the set of all pure joint strategies of the game. The external party draws such a pure joint strategy with probability $p_{j_1 \dots j_n} \geq 0$, called a *mixed joint strategy*. Such a joint probability distribution is a vector (or a tensor) $p = (p_{j_1 \dots j_n} \mid j_i \in [d_i], i \in [n])$, such that $\sum_{j_1=1}^{d_1} \dots \sum_{j_n=1}^{d_n} p_{j_1 \dots j_n} = 1$. The set of all joint probability distributions is the probability simplex $\Delta_{d_1 \dots d_n - 1}$.

The external party recommends the drawn joint strategy to the players. But instead of revealing the true outcome to all players, each player is only told their own part. If player i believes that all other players will adhere to their given recommendations, then the best strategy for player i is to follow the strategy which maximizes their expected

5.1 The Correlated Equilibrium Polytope

payoff. If none of the players has such an incentive to deviate, then the condition

$$\begin{aligned} & \sum_{j_1=1}^{d_1} \cdots \widehat{\sum_{j_i=1}^{d_i}} \cdots \sum_{j_n=1}^{d_n} X_{j_1 \cdots j_{i-1} k j_{i+1} \cdots j_n}^{(i)} p_{j_1 \cdots j_{i-1} k j_{i+1} \cdots j_n} \\ & \geq \sum_{j_1=1}^{d_1} \cdots \widehat{\sum_{j_i=1}^{d_i}} \cdots \sum_{j_n=1}^{d_n} X_{j_1 \cdots j_{i-1} l j_{i+1} \cdots j_n}^{(i)} p_{j_1 \cdots j_{i-1} l j_{i+1} \cdots j_n} \end{aligned}$$

is satisfied for all $k, l \in [d_i]$, and for all $i \in [n]$ [Aum87]. This motivates the following definition.

Definition 5.1.2 (Correlated Equilibrium). Let G be a game with payoff tensors $X = (X^{(1)}, \dots, X^{(n)})$. A point $p \in \Delta_{d_1 \cdots d_n - 1}$ is a *correlated equilibrium* if and only if

$$\sum_{j_1=1}^{d_1} \cdots \widehat{\sum_{j_i=1}^{d_i}} \cdots \sum_{j_n=1}^{d_n} \left(X_{j_1 \cdots j_{i-1} k j_{i+1} \cdots j_n}^{(i)} - X_{j_1 \cdots j_{i-1} l j_{i+1} \cdots j_n}^{(i)} \right) p_{j_1 \cdots j_{i-1} k j_{i+1} \cdots j_n} \geq 0. \quad (5.1)$$

for all $k, l \in [d_i]$, and for all $i \in [n]$, which are the *incentive constraints* of the game G . These linear inequalities in (5.1) together with the linear constraints

$$p_{j_1 \cdots j_n} \geq 0 \text{ for } j_i \in [d_i], i \in [n], \text{ and } \sum_{j_1=1}^{d_1} \cdots \sum_{j_n=1}^{d_n} p_{j_1 \cdots j_n} = 1$$

define the set of all correlated equilibria of the game. The set of all such equilibria is the *correlated equilibrium polytope* P_G of the game G .

The ambient space of the polytope P_G has dimension $d_1 \cdots d_n$. By definition, the maximal dimension that P_G can achieve is $d_1 \cdots d_n - 1$. In the literature, in this case P_G is often called *full-dimensional*. To avoid confusion with conventions in discrete and convex geometry, we refer to P_G as having *maximal dimension*.

Example 5.1.3 (Traffic Lights). We continue with [Example 5.1.1](#), where the third party is given by a traffic light at the crossing. The traffic light gives the recommendation “go” to a driver if it turns green, and “stop” if it turns red. The traffic light draws randomly from one of the combinations of strategies. Let $p_{j_1 j_2}$ be the probability with which the traffic light draws the pure joint strategy $s_{j_1 j_2}$. The point $p = (p_{11}, p_{12}, p_{21}, p_{22})$ is a correlated equilibrium if and only if $p_{j_1 j_2} \geq 0$, $p_{11} + p_{12} + p_{21} + p_{22} = 1$ and

$$\begin{aligned} (X_{22}^{(1)} - X_{12}^{(1)}) p_{22} + (X_{21}^{(1)} - X_{11}^{(1)}) p_{21} &\geq 0, & (X_{12}^{(1)} - X_{22}^{(1)}) p_{12} + (X_{11}^{(1)} - X_{21}^{(1)}) p_{11} &\geq 0, \\ (X_{22}^{(2)} - X_{21}^{(2)}) p_{22} + (X_{12}^{(2)} - X_{11}^{(2)}) p_{12} &\geq 0, & (X_{21}^{(2)} - X_{22}^{(2)}) p_{21} + (X_{11}^{(2)} - X_{12}^{(2)}) p_{11} &\geq 0. \end{aligned}$$

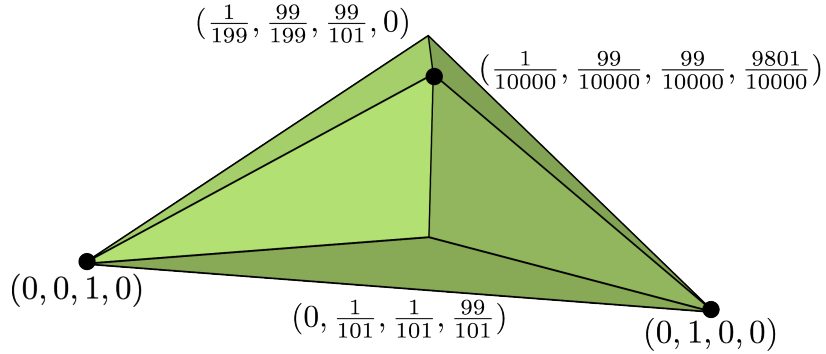


Figure 5.2: The vertices of the correlated equilibrium polytope of the [Traffic Lights example](#) ([Examples 5.1.3](#) and [5.1.6](#)). The three Nash equilibria are indicated in black.

With the payoffs as given in the bimatrix in [Example 5.1.1](#) these inequalities evaluate to

$$\begin{aligned} -p_{22} + 99p_{21} &\geq 0, & p_{12} - 99p_{11} &\geq 0, \\ -p_{22} + 99p_{12} &\geq 0, & p_{21} - 99p_{11} &\geq 0. \end{aligned}$$

The correlated equilibrium polytope, i.e. the set of points p that satisfy these inequalities, has 5 vertices with coordinates

$$\left(\begin{array}{c} 0 \\ 0 \\ 1 \\ 0 \end{array} \right), \left(\begin{array}{c} 0 \\ 1 \\ 0 \\ 0 \end{array} \right), \left(\begin{array}{c} \frac{1}{10000} \\ \frac{99}{10000} \\ \frac{99}{10000} \\ \frac{9801}{10000} \end{array} \right), \left(\begin{array}{c} 0 \\ \frac{1}{101} \\ \frac{1}{101} \\ \frac{99}{101} \end{array} \right), \left(\begin{array}{c} \frac{1}{199} \\ \frac{99}{199} \\ \frac{99}{199} \\ 0 \end{array} \right).$$

This polytope is depicted in [Figure 5.2](#). The vertices $(0,0,1,0)^t$ and $(0,1,0,0)^t$ are the probability distributions representing the pure joint strategies in which one player drives, while the other stops. The vertices $(\frac{1}{10000}, \frac{99}{10000}, \frac{99}{10000}, \frac{9801}{10000})^t$, and $(0, \frac{1}{101}, \frac{1}{101}, \frac{99}{101})^t$ are probability distributions in which it is most likely that both players stop, while the scenario in which both players drive is the least likely one. Finally, the vertex $(\frac{1}{199}, \frac{99}{199}, \frac{99}{199}, 0)^t$ is a probability distribution in which, most likely and with equal probability, one of the players drives while the other one stops. \diamond

The next proposition shows that two affinely dependent games define the same correlated equilibrium polytope.

PROPOSITION 5.1.4. Any affine linear transformation of the payoff tensors $X^{(i)}$ with positive scalars leaves the polytope P_G invariant. More precisely, let $G = (n, S, X)$ be a game. For each $i \in [n]$, fix $t_i \in \mathbb{R}$, $\lambda_i \in \mathbb{R}_{>0}$ and let $\tilde{X}_{j_1 \dots j_n}^{(i)} = \lambda_i X_{j_1 \dots j_n}^{(i)} + t_i$ for all $j_k \in [d_k], k \in [n]$. Then for the game $\tilde{G} = (n, \tilde{X}, S)$ with $\tilde{X} = (\tilde{X}^{(1)}, \dots, \tilde{X}^{(n)})$ it holds that $P_G = P_{\tilde{G}}$.

5.1 The Correlated Equilibrium Polytope

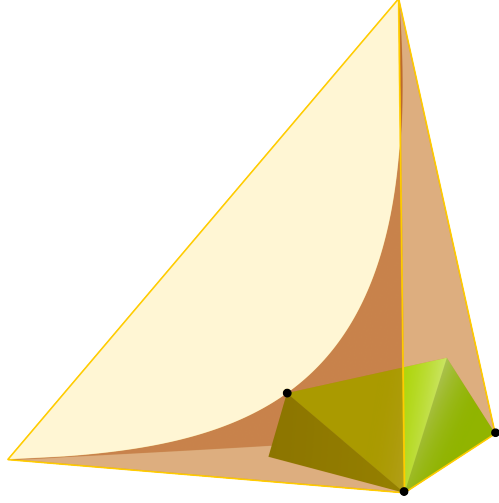


Figure 5.3: A 3-dimensional correlated equilibrium polytope (green) inside the probability simplex Δ_3 (yellow) for a (2×2) -game. Its Nash equilibria (black) are the intersection with the Segre variety (red). This picture applies to the Traffic Lights example (Examples 5.1.1, 5.1.3 and 5.1.6) as well as the Hawk-Dove game (Example 5.4.1).

Proof. For each player $i \in [n]$ let $X^{(i)}$ be their payoff tensor, fix $t_i \in \mathbb{R}$, $\lambda_i \in \mathbb{R}_{>0}$, and consider the affine transformation $\tilde{X}_{j_1 \dots j_n}^{(i)} = \lambda_i X_{j_1 \dots j_n}^{(i)} + t_i$. Then

$$\begin{aligned} & \sum_{j_1=1}^{d_1} \dots \sum_{j_i=1}^{\widehat{d_i}} \dots \sum_{j_n=1}^{d_n} \left(\tilde{X}_{j_1 \dots j_{i-1} k j_{i+1} \dots j_n}^{(i)} - \tilde{X}_{j_1 \dots j_{i-1} l j_{i+1} \dots j_n}^{(i)} \right) p_{j_1 \dots j_{i-1} k j_{i+1} \dots j_n} \\ &= \sum_{j_1=1}^{d_1} \dots \sum_{j_i=1}^{\widehat{d_i}} \dots \sum_{j_n=1}^{d_n} \left(\lambda_i X_{j_1 \dots j_{i-1} k j_{i+1} \dots j_n}^{(i)} + t_i - \lambda_i X_{j_1 \dots j_{i-1} l j_{i+1} \dots j_n}^{(i)} - t_i \right) p_{j_1 \dots j_{i-1} k j_{i+1} \dots j_n} \\ &= \lambda_i \sum_{j_1=1}^{d_1} \dots \sum_{j_i=1}^{\widehat{d_i}} \dots \sum_{j_n=1}^{d_n} \left(X_{j_1 \dots j_{i-1} k j_{i+1} \dots j_n}^{(i)} - X_{j_1 \dots j_{i-1} l j_{i+1} \dots j_n}^{(i)} \right) p_{j_1 \dots j_{i-1} k j_{i+1} \dots j_n} \geq 0. \end{aligned}$$

Since $\lambda_i > 0$, this is equivalent to (5.1) being nonnegative. \square

Definition 5.1.5 (Nash Equilibrium). Let G be a game. A *Nash equilibrium* of G is a point of the correlated equilibrium polytope that is a tensor of rank one. More specifically, the set of Nash equilibria are those points in P_G that are also contained in the image of the product map

$$\begin{aligned} \varphi : \Delta_{d_1-1} \times \dots \times \Delta_{d_n-1} &\rightarrow \Delta_{d_1 \dots d_n-1} \\ (p^{(1)}, \dots, p^{(n)}) &\mapsto p_{j_1}^{(1)} \cdot \dots \cdot p_{j_n}^{(n)} \end{aligned}$$

The image of this map is the *Segre variety* inside $\Delta_{d_1 \dots d_n-1}$.

[Figure 5.3](#) shows a 3-dimensional correlated equilibrium polytope of a (2×2) -game together with the Segre variety inside the simplex Δ_3 . We illustrate this in more details in the following example.

Example 5.1.6 (Traffic Lights). We continue with the Traffic Lights example from [Examples 5.1.1](#) and [5.1.3](#). The Nash equilibria of this game occur as vertices of the correlated equilibrium polytope P_G . More precisely, they occur as the images of the points $(p^{(1)}, p^{(2)}) \in \Delta_1 \times \Delta_1$ with coordinates $((1,0), (0,1))$, $((0,1), (1,0))$ and $((\frac{1}{100}, \frac{99}{100}), (\frac{1}{100}, \frac{99}{100}))$ under the product map φ from [Definition 5.1.5](#), which correspond to the three black vertices in [Figure 5.2](#). With indexing $p = (p_{11}, p_{12}, p_{21}, p_{22})$ the images of the first two points are $p = (0,1,0,0)$ and $(0,0,1,0)$. These are the probability distributions which correspond to the pure joint strategies in which one of the players drives, while the other one stops. The point $p = (\frac{1}{10000}, \frac{99}{10000}, \frac{99}{10000}, \frac{9801}{10000})$ is a probability distribution in which it is most likely that both players stop, independently from each other. \diamond

By [Definition 5.1.5](#), the set of Nash equilibria is a subset of the correlated equilibrium polytope, and a Nash equilibrium always exists [[Nas50](#)]. However, characterizing Nash equilibria is a computationally difficult task [[PRo5](#)]. It is thus of interest to understand where the Nash equilibria lie relative to the correlated equilibrium polytope. A game G is called *non-trivial* if $X_{j_1 \dots j_{i-1} k j_{i+1} \dots j_n}^{(i)} \neq X_{j_1 \dots j_{i-1} l j_{i+1} \dots j_n}^{(i)}$ for some player $i \in [n]$ and $k, l \in [d_i]$ with $k \neq l$. The next result states that if P_G is of maximal dimension, then any Nash equilibrium lies on a proper face of P_G .

PROPOSITION 5.1.7 ([[NCHo4](#), Proposition 1]). Let G be a non-trivial game. Then the Nash equilibria lie on a face of the correlated equilibrium polytope P_G of dimension at most $d_1 \dots d_n - 2$. In particular, if P_G has maximal dimension $d_1 \dots d_n - 1$, then the Nash equilibria lie on the relative boundary of P_G .

In order to locate the possible positions of Nash equilibria, it is thus helpful to understand the conditions under which P_G is of maximal dimension. In [Section 5.3](#) we introduce the region of full-dimensionality, which formalizes these conditions.

5.2 THE CORRELATED EQUILIBRIUM CONE

The combinatorics of the correlated equilibrium polytope is completely determined by the cone given by the incentive constraints [\(5.1\)](#), intersected with the nonnegative orthant. The *correlated equilibrium cone* $C_G \subseteq \mathbb{R}^{d_1 \dots d_n}$ is the polyhedral cone defined by inequalities

$$\begin{aligned} p_{j_1 \dots j_n} &\geq 0 \\ \sum_{j_1=1}^{d_1} \dots \widehat{\sum_{j_i=1}^{d_i}} \dots \sum_{j_n=1}^{d_n} \left(X_{j_1 \dots j_{i-1} k j_{i+1} \dots j_n}^{(i)} - X_{j_1 \dots j_{i-1} l j_{i+1} \dots j_n}^{(i)} \right) p_{j_1 \dots j_{i-1} k j_{i+1} \dots j_n} &\geq 0 \end{aligned} \tag{5.2}$$

5.2 The Correlated Equilibrium Cone

for all $k, l \in [d_i]$, and for all $i \in [n]$. For each player $i \in [n]$ this defines $d_i(d_i - 1)$ nontrivial inequalities of type (5.2). The cone C_G is a convex pointed polyhedral cone and the correlated equilibrium polytope P_G is the intersection of the cone with the hyperplane where the sum of all coordinates equals 1. Therefore, a facet of P_G is in bijection with a facet of C_G , and a vertex of P_G is in bijection with an extremal ray of C_G . We make a substitution of the coefficients in the inequality (5.2). For each $i \in [n]$, $j_1 \in [d_1], \dots, j_{i-1} \in [d_{i-1}], k, l \in [d_i], j_{i+1} \in [d_{i+1}], \dots, j_n \in [d_n]$ we define

$$Y_{j_1 \dots \hat{j}_i \dots j_n}^{(i)}(k, l) = X_{j_1 \dots j_{i-1} k j_{i+1} \dots j_n}^{(i)} - X_{j_1 \dots j_{i-1} l j_{i+1} \dots j_n}^{(i)}.$$

Note that $Y_{j_1 \dots \hat{j}_i \dots j_n}^{(i)}(k, l) = -Y_{j_1 \dots \hat{j}_i \dots j_n}^{(i)}(l, k)$. Thus, for each player $i \in [n]$ this defines $\binom{d_i}{2} \prod_{\substack{k \in [n] \\ k \neq i}} d_k$ distinct variables, so in total this defines

$$M = \sum_{i=1}^n \binom{d_i}{2} \prod_{\substack{k \in [n] \\ k \neq i}} d_k$$

many variables. Under this substitution, the above inequality becomes

$$\sum_{j_1=1}^{d_1} \dots \sum_{j_i=1}^{\widehat{d_i}} \dots \sum_{j_n=1}^{d_n} Y_{j_1 \dots \hat{j}_i \dots j_n}^{(i)}(k, l) p_{j_1 \dots j_n} \geq 0. \quad (5.3)$$

For fixed $i \in [n], k, l \in [d_i]$, let $U_{kl}^{(i)} \in \mathbb{R}^{d_1 \dots d_n}$ be the vector with entries

$$(U_{kl}^{(i)})_{j_1 \dots j_i \dots j_n} = \begin{cases} Y_{j_1 \dots \hat{j}_i \dots j_n}^{(i)}(k, l) & \text{if } j_i = k \text{ and } k < l \\ -Y_{j_1 \dots \hat{j}_i \dots j_n}^{(i)}(k, l) & \text{if } j_i = k \text{ and } k > l \\ 0 & \text{otherwise} \end{cases}$$

for each coordinate indexed by $j_1 \in [d_1], \dots, j_i \in [d_i], \dots, j_n \in [d_n]$. Using the same indexing of coordinates for $p \in \mathbb{R}^{d_1 \dots d_n}$, the inequalities (5.3) can be expressed as the inner product $\langle U_{kl}^{(i)}, p \rangle \geq 0$.

Example 5.2.1 ((2 × 2)-games). Consider a 2-player game with $d_1 = d_2 = 2$. We fix the indexing $p = (p_{11}, p_{12}, p_{21}, p_{22})$. Recall that the inequalities are

$$\begin{aligned} (X_{11}^{(1)} - X_{21}^{(1)})p_{11} + (X_{12}^{(1)} - X_{22}^{(1)})p_{12} &= Y_1^{(1)}(1, 2) p_{11} + Y_2^{(1)}(1, 2) p_{12} \geq 0 \\ (X_{21}^{(1)} - X_{11}^{(1)})p_{21} + (X_{22}^{(1)} - X_{12}^{(1)})p_{22} &= -Y_1^{(1)}(1, 2) p_{21} - Y_2^{(1)}(1, 2) p_{22} \geq 0 \\ (X_{21}^{(2)} - X_{22}^{(2)})p_{21} + (X_{11}^{(2)} - X_{12}^{(2)})p_{11} &= Y_2^{(2)}(1, 2) p_{21} + Y_1^{(2)}(1, 2) p_{11} \geq 0 \\ (X_{22}^{(2)} - X_{21}^{(2)})p_{22} + (X_{12}^{(2)} - X_{11}^{(2)})p_{12} &= -Y_2^{(2)}(1, 2) p_{22} - Y_1^{(2)}(1, 2) p_{12} \geq 0. \end{aligned}$$

The vectors $U_{kl}^{(i)}$ have entries in the 4 unknowns $Y_1^{(1)}(1,2), Y_2^{(1)}(1,2), Y_1^{(2)}(1,2), Y_2^{(2)}(1,2)$. More specifically,

$$\begin{aligned} U_{12}^{(1)} &= (Y_1^{(1)}(1,2), Y_2^{(1)}(1,2), 0, 0) \\ U_{21}^{(1)} &= -(0, 0, Y_1^{(1)}(1,2), Y_2^{(1)}(1,2)) \\ U_{12}^{(2)} &= (Y_1^{(2)}(1,2), 0, Y_2^{(2)}(1,2), 0) \\ U_{21}^{(2)} &= -(0, Y_1^{(2)}(1,2), 0, Y_2^{(2)}(1,2)). \end{aligned}$$

The cone C_G is defined by the inequalities $\langle U_{kl}^{(i)}, p \rangle \geq 0$ for $i \in [2]$, and $k, l \in [2], k \neq l$, and the inequalities $\langle e_i, p \rangle \geq 0$, where e_i denote the standard basis vectors of \mathbb{R}^4 . \diamond

Recall that the number of variables defined above is $M = \sum_{i=1}^n \binom{d_i}{2} \prod_{\substack{k \in [n] \\ k \neq i}} d_k$. The ambient dimension of the correlated equilibrium polytope and cone is $D = \prod_{i=1}^n d_i$, and the number of linear inequalities of the form (5.3) is $N = \sum_{i=1}^n d_i(d_i - 1)$. Let $U(Y) \in \mathbb{R}^{N \times D}$ be the matrix with rows $U_{kl}^{(i)}$ for $i \in [n], k, l \in [d_i], k \neq l$, and let $A(Y) \in \mathbb{R}^{(D+N) \times D}$ be the block matrix

$$A(Y) = \begin{pmatrix} U(Y) \\ Id_D \end{pmatrix}.$$

By (5.3), the cone $C_G = C(Y)$ is given by

$$C(Y) = \left\{ p \in \mathbb{R}^D \mid A(Y)p \geq 0 \right\}.$$

The matrix $A(Y)$ has full rank D , and so $C(Y)$ is a pointed cone.

For $(d_1 \times \dots \times d_n)$ -games, where $d_i \geq 3$ for some $i \in [n]$, we have additional relations

$$Y_{j_1 \dots \hat{j}_i \dots j_n}^{(i)}(k, l) + Y_{j_1 \dots \hat{j}_i \dots j_n}^{(i)}(l, t) = Y_{j_1 \dots \hat{j}_i \dots j_n}^{(i)}(k, t) \quad (5.4)$$

for $j_1 \in [d_1], \dots, j_{i-1} \in [d_{i-1}], k, l, t \in [d_i], j_{i+1} \in [d_{i+1}], \dots, j_n \in [d_n]$. A vector $Y \in \mathbb{R}^M$ corresponds to a certain game G if and only if these relations hold. Geometrically, these relations define a linear space inside \mathbb{R}^M . We thus make the following definition.

Definition 5.2.2. The *correlated equilibrium space* $\mathcal{S} \subseteq \mathbb{R}^M$ of $(d_1 \times \dots \times d_n)$ -games is the linear space defined by the equations (5.4), where $i \in [n]$ ranges over all players with at least 3 strategies. If all players have at most 2 strategies, then no such relation among the variables holds, and the correlated equilibrium space is the entire ambient space $\mathcal{S} = \mathbb{R}^M$.

Example 5.2.3 (\mathcal{S} for (2×3) -games). In a (2×3) -game, there are six variables

$$\begin{aligned} Y_1^{(1)}(1,2) &= X_{11}^{(1)} - X_{21}^{(1)}, & Y_2^{(1)}(1,2) &= X_{12}^{(1)} - X_{22}^{(1)}, & Y_3^{(1)}(1,2) &= X_{13}^{(1)} - X_{23}^{(1)}, \\ Y_1^{(2)}(1,2) &= X_{11}^{(2)} - X_{12}^{(2)}, & Y_1^{(2)}(1,3) &= X_{11}^{(2)} - X_{13}^{(2)}, & Y_1^{(2)}(2,3) &= X_{12}^{(2)} - X_{13}^{(2)}, \\ Y_2^{(2)}(1,2) &= X_{21}^{(2)} - X_{22}^{(2)}, & Y_2^{(2)}(1,3) &= X_{21}^{(2)} - X_{23}^{(2)}, & Y_2^{(2)}(2,3) &= X_{22}^{(2)} - X_{23}^{(2)}. \end{aligned}$$

The relations among these variables are

$$Y_1^{(2)}(1,2) + Y_1^{(2)}(2,3) = Y_1^{(2)}(1,3), \quad Y_2^{(2)}(1,2) + Y_2^{(2)}(2,3) = Y_2^{(2)}(1,3).$$

These relations cut out the 4-dimensional correlated equilibrium space \mathcal{S} for (2×3) -games. For any game (2×3) -games G the correlated equilibrium polytope is nonempty, a so point $Y \in \mathbb{R}^6$ defines a correlated equilibrium cone of dimension at least 1 if and only if it satisfies the above relations. \diamond

Remark 5.2.4. In the following sections we will classify correlated equilibrium polytopes and cones with respect to the variables Y instead of the payoff tensors X . We note that this is not a significant restriction, as this is a linear change of coordinates and thus does not change the geometry of the objects described in what follows, provided one restricts to the correlated equilibrium space \mathcal{S} .

5.3 THE REGION OF FULL-DIMENSIONALITY

In this section we introduce the region of full-dimensionality for a fixed type of games. For fixed $d_i \in \mathbb{N}, i \in [n]$, this region classifies for which $(d_1 \times \cdots \times d_n)$ -games the polytope P_G is of maximal dimension $D - 1 = d_1 \cdots d_n - 1$. Recall from [Proposition 5.1.7](#) that the dimension of P_G may determine the possible positions of Nash equilibria. The connections between full-dimensionality and elementary games are discussed in [\[Vio03\]](#). In general, it is not understood under which conditions P_G has maximal dimension (i.e. G is a *full game*), though there are partial results on forbidden dimensions [\[Vio10, Proposition 7\]](#).

Let $\mathcal{S} \subseteq \mathbb{R}^M$ be the correlated equilibrium space and let $A(Y)$ and $C(Y)$ be the matrix and correlated equilibrium cone as defined in [Section 5.2](#). We consider the correlated equilibrium polytope $P(Y)$ as the set of points in $C(Y)$ whose coordinates sum to 1. Recall that $P(Y)$ is of maximal dimension if and only if $C(Y)$ is full-dimensional. Thus, we are interested in the *region of full-dimensionality*

$$\mathcal{D} = \{Y \in \mathcal{S} \mid \dim(C(Y)) = D\}.$$

In [Section 1.8](#), we introduce semialgebraic sets as subsets of \mathbb{R}^M defined by a boolean combinations of finitely many polynomial inequalities. In fact, \mathcal{D} is semialgebraic.

THEOREM 5.3.1. The region \mathcal{D} of full-dimensionality is the semialgebraic set

$$\pi_Y \left(\left\{ (x, Y) \in \mathbb{R}^{D+M} \mid A(Y)x > 0 \right\} \right) \cap \mathcal{S}$$

where π_Y is the coordinate projection onto the last M coordinates.

Proof. The cone $C(Y)$ is full-dimensional if and only if it has nonempty interior, i.e. if there exists some $p \in \mathbb{R}^D$ such that $A(Y)p > 0$. Let $x = (x_{j_1 \dots j_n} \mid i \in [n], j_i \in [d_i])$ be a vector of D indeterminates. Consider the set

$$\tilde{\mathcal{D}} = \left\{ (x, Y) \in \mathbb{R}^{D+M} \mid A(Y)x > 0 \right\}.$$

The expression $A(Y)x$ defines a $(D + N)$ -dimensional vector, where each coordinate is a polynomial in variables x and Y . Hence, the set $\tilde{\mathcal{D}}$ is defined by $D + N$ polynomial inequalities, and is thus a (basic open) semialgebraic set. The region \mathcal{D} of full-dimensionality is the intersection of the correlated equilibrium space \mathcal{S} with a coordinate projection of $\tilde{\mathcal{D}}$, which can be obtained by projecting away the x -coordinates. The [Tarski–Seidenberg theorem](#) ([Theorem 1.8.2](#)) implies that the coordinate projection is semialgebraic, and hence \mathcal{D} is a semialgebraic set. \square

Example 5.3.2 (\mathcal{D} for (2×2) -games). In the case of (2×2) -games, the ambient dimension of the correlated equilibrium polytope is $D = 4$, the number of incentive constraints is $N = 4$ (so the number of inequalities that define the polytope is $D + N = 8$) and the ambient dimension of $\mathcal{D} \subseteq \mathcal{S} = \mathbb{R}^M$ is $M = 4$. The different combinatorial types in this case have been fully classified in [[CAo3](#)] and $P(Y)$ is either a point or a bipyramid over a triangle. Here, $\mathcal{D} \subseteq \mathbb{R}^4$ is the union of two open orthants:

- (i) $Y_1^{(1)}(1, 2) > 0, Y_2^{(1)}(1, 2) < 0, Y_1^{(2)}(1, 2) > 0, Y_2^{(2)}(1, 2) < 0$
- (ii) $Y_1^{(1)}(1, 2) < 0, Y_2^{(1)}(1, 2) > 0, Y_1^{(2)}(1, 2) < 0, Y_2^{(2)}(1, 2) > 0$

The file `dimensions2x2.nb` [[BHP22b](#)] contains a `Mathematica` script [[Mat](#)] which computes these inequalities. \diamond

Example 5.3.3 (\mathcal{D} for (2×3) -games). The coordinate projection of the set $\tilde{\mathcal{D}}$ onto \mathbb{R}^9 is the union of basic semialgebraic sets, where each piece is the intersection of an orthant with a binomial inequality. One of the pieces is

$$\begin{aligned} Y_1^{(1)}(1, 2) &> 0, Y_2^{(1)}(1, 2) > 0, Y_3^{(1)}(1, 2) < 0, \\ Y_1^{(2)}(1, 2) &< 0, Y_1^{(2)}(1, 3) < 0, Y_1^{(2)}(2, 3) > 0, \\ Y_2^{(2)}(1, 2) &> 0, Y_2^{(2)}(1, 3) > 0, Y_2^{(2)}(2, 3) < 0, \\ Y_2^{(2)}(1, 3) Y_1^{(2)}(2, 3) &< Y_1^{(2)}(1, 3) Y_2^{(2)}(2, 3). \end{aligned}$$

5.4 Combinatorial Types of Correlated Equilibrium Polytopes

The region \mathcal{D} of full-dimensionality for (2×3) -games consists of the intersection of the above mentioned pieces with the correlated equilibrium space \mathcal{S} . The Mathematica file `dimensions2x3.nb` [BHP22b] contains our code for computing all of the components of this semialgebraic set. \diamond

While this approach could theoretically be used to obtain inequalities for larger games, this is extremely difficult in practice since the required algebraic methods do not scale well as the number of variables involved increases. For example, we were unable to carry out this computation for $(2 \times 2 \times 2)$ -games since we must compute the coordinate projection of a semialgebraic set which lives in $D + M = 20$ -dimensional space.

5.4 COMBINATORIAL TYPES OF CORRELATED EQUILIBRIUM POLYTOPES

In this section, we consider how to systematically classify combinatorial types of polytopes arising as a correlated equilibrium polytope. First, we present a systematic approach for classifying the possible combinatorial types for arbitrary games by describing oriented matroid strata. However, even for small examples the explicit computation of the oriented matroid strata is beyond current scope and thus we introduce algebraic methods for understanding oriented matroid strata via a common algebraic boundary. We use this technique to completely classify the combinatorial types of P_G for (2×3) -games (Theorem 5.4.8). We then show that for all $(2 \times n)$ -games the irreducible components of the common algebraic boundary of the oriented matroid strata are coordinate hyperplanes and (2×2) -minors of the matrix $A(Y)$ (Theorem 5.4.7).

Example 5.4.1 (Hawk-Dove game). This game models a scenario of a competition for a shared resource. Both players can choose between conflict (hawk) or conciliation (dove) and is a generalization of the Traffic Lights example (Examples 5.1.1, 5.1.3 and 5.1.6). The inequalities for general (2×2) -games are given in Example 5.2.1. In the Hawk-Dove game, each of the two players has two strategies $s_1^{(i)} = \text{"hawk"}$ or $s_2^{(i)} = \text{"dove"}$.

		Player 2	
		Hawk	Dove
Player 1		Hawk	$(\frac{V-C}{2}, \frac{V-C}{2})$
		Dove	$(0, V)$
			$(\frac{V}{2}, \frac{V}{2})$

In this bimatrix game, V represents the value of the resource and C represents the cost of the escalated fight. It is mostly assumed that $C > V > 0$. The correlated equilibria polytope P_G is a bipyramid over a triangle. In the case $V \geq C > 0$, the game becomes an example for the famous *Prisoner's Dilemma*, in which case P_G is a single point. \diamond

As seen in the previous example, for fixed $d_1, \dots, d_n \in \mathbb{N}$, different choices of the payoffs for the players in a $(d_1 \times \dots \times d_n)$ -game can result in different combinatorial

types of correlated equilibria. We would thus like to classify the regions of the correlated equilibrium space $\mathcal{S} \subseteq \mathbb{R}^M$ such that

$$\{Y \in \mathcal{S} \mid C(Y) \text{ has a fixed combinatorial type}\}.$$

We now explain how the combinatorial type of $C(Y)$ is completely determined by the underlying oriented matroid defined by the matrix $A(Y)$. The combinatorial type of $C(Y)$ is the incidence structure of rays and facets of $C(Y)$. Equivalently, we can classify the incidence structure of facets and rays of the dual cone $C^\vee(Y)$. By definition, the (inner) facet normals of $C(Y)$ are generators of extremal rays of $C^\vee(Y)$ and vice versa. Let $h \in [D+N]$ and $A_h(Y)$ be a row of $A(Y)$. Seen as a linear functional, this row uniquely selects a face

$$F_h = \{p \in C(Y) \mid \langle A_h(Y), p \rangle = 0\}.$$

Note that this is not necessarily a facet of $C(Y)$, but all facets of $C(Y)$ arise in this way. For the dual cone $C^\vee(Y)$ this implies that $r_h = \text{cone}(A_h(Y))$ is an extremal ray of $C^\vee(Y)$ if and only if F_h is a facet of C . If $C(Y)$ is not full-dimensional, then there is some $h \in [D+N]$ such that $F_h = C(Y)$. The set of all such vectors span the lineality space

$$\mathcal{L} = C^\vee(Y) \cap (-C^\vee(Y)) = \text{span}(\{A_h \mid F_h = C(Y)\})$$

of $C^\vee(Y)$. In this case, extremal rays of $C^\vee(Y)$ are to be considered in $C^\vee(Y)/\mathcal{L}$.

We want to understand the incidence structure of extremal rays and facets of $C(Y)$. Each such ray of $C(Y)$ is contained in at least $D-1$ facets. Thus, we seek to understand which subsets of $D-1$ faces F_h of $C(Y)$ intersect in a single point. Equivalently, we want to understand which subsets of $D-1$ rays r_h of $C^\vee(Y)$ are contained in a common face. Let $H \subseteq [D+N]$ such that $|H| = D-1$, and denote by $A_H(Y)$ the submatrix of $A(Y)$ with rows indexed by H . If $\{r_h \mid h \in H\}$ lie on a common face, then these rays all lie on the hyperplane given by the rowspan of $A_H(Y)$. Note that in this case all rays $r_{h'}, h' \in [D+N] \setminus H$ lie on the same side of this hyperplane. Thus, the sign of $\det(A_{H \cup h'})$ is uniquely determined for all $h' \in [D+N] \setminus H$. In the language of [Section 1.2](#) this means that the chirotope defined by the matrix $A(Y)$ completely determines the combinatorial type.

The collections of all regions $\mathcal{R} \subseteq \mathbb{R}^M$ in which the maximal minors of $A(Y)$ satisfies a certain sign pattern are known as *oriented matroid strata* of $A(Y)$. Each cell gives rise to a fixed sign pattern of the maximal minors of $A(Y)$, i.e. the underlying chirotope and hence a fixed oriented matroid. Restricting all oriented matroid strata to the correlated equilibrium space \mathcal{S} yields a subdivision of \mathcal{S} in which distinct combinatorial types lie in distinct regions.

Let $S \subseteq \mathbb{R}^M$ be a semialgebraic set. Recall from [Section 1.8](#) that the algebraic boundary $\partial_a S$ is the Zariski closure of the topological (Euclidean) boundary ∂S , i.e. the smallest algebraic variety containing ∂S over \mathbb{C} .

5.4 Combinatorial Types of Correlated Equilibrium Polytopes

Construction 5.4.2 (Algebraic Boundary). For every $H \subseteq [D+N]$, $|H| = D$ the minor $\det(A_H)$ is a polynomial in variables Y of degree at most D , and $\text{sgn}(\det(A_H)) \in \{-1, 0, 1\}$ is a polynomial inequality. Let $s = (s_H \mid H \subseteq \binom{[D+N]}{D})$, $s_H \in \{1, -1\}$ be a sign vector. Each maximal open stratum is of the form

$$\mathcal{R}_s^\circ = \left\{ Y \in \mathbb{R}^M \mid \text{sgn}(\det(A_H(Y))) = s_H \text{ for all } H \in \binom{[D+N]}{D} \right\}.$$

Let \mathcal{R}_s denote the Euclidean closure of such an open maximal region, which is a closed basic semialgebraic set. We define the *algebraic boundary of all oriented matroid strata* $\partial_a \mathcal{R}$ as the union of the algebraic boundaries of all such closed regions, i.e.

$$\partial_a \mathcal{R} = \bigcup_s \partial_a \mathcal{R}_s = \bigcup_{H \in \binom{[D+N]}{D}} \mathcal{V}(\det(A_H(Y))),$$

where the first union ranges over all sign vectors s such that \mathcal{R}_s° is maximal, and $\mathcal{V}(\det(A_H(Y))) = \{Y \in \mathbb{R}^M \mid \det(A_H(Y)) = 0\}$. In the second union we only consider $H \in \binom{[D+N]}{D}$ such that $A_H(Y)$ contains at least one variable. Recall that $A(Y) = \begin{pmatrix} U(Y) \\ Id_N \end{pmatrix}$ where the matrix $U(Y)$ has no zero rows and all nonzero entries are variables. Thus, the only minor of $A(Y)$ that does not contain a variable is the determinant of Id_D , so the number of such minors is $\binom{D+N}{D} - 1$. We note that the minors may not be irreducible polynomials, so they do not necessarily define the irreducible components of the variety $\partial_a \mathcal{R}$. In total, this defines $\binom{D+N}{D} - 1$ hypersurfaces, whose defining polynomials are of degree at most D .

The algebraic boundary $\partial_a \mathcal{R}$ can be seen as an arrangement of hypersurfaces. Applying [BLN22] and [Baso3, Theorem 4] to this setup yields a general bound on the number of oriented matroid strata.

PROPOSITION 5.4.3. Let δ be the maximum degree of all $\beta \leq \binom{D+N}{D} - 1$ defining polynomials of the boundaries of the regions of the oriented matroid strata. Then $\delta \leq D$ and the number of maximal regions in the oriented matroid strata is at most

$$\delta(2\delta - 1)^{M-1}(1 + 3\beta).$$

The following three examples illustrate this construction for small games.

Example 5.4.4 ($\partial_a \mathcal{R}$ for (2×2) -games). In a (2×2) -game we have $D = 4$, $N = 4$ and $M = 4$. The number of irreducible components of $\partial_a \mathcal{R}$ is $\beta = 4$, and these are the 4 coordinate hyperplanes. Indeed, the classification in [CAo3] shows that in each open orthant the combinatorial type is fixed, and in the two orthants described in Example 5.3.2 there is a unique combinatorial type of maximal dimension. The file `orientedMatroidStrata2x2.m2` [BHP22b] contains a Macaulay2 script [GS22] which explicitly computes these irreducible components. \diamond

Example 5.4.5 ($\partial_a \mathcal{R}$ for (2×3) -games). In a (2×3) -game, we have $D = 6, N = 8$ and $M = 9$. The number of minors of $A_H(Y)$ that contain at least one variable is $\binom{12}{6} - 1 = 934$, but the number of irreducible components is only $\beta = 12$. All of these polynomials are homogeneous, and the maximum degree is $\delta = 2$. In fact, the irreducible components are the 9 coordinate hyperplanes, together with the 3 binomials

$$\begin{aligned} Y_2^{(2)}(1,2) Y_1^{(2)}(1,3) - Y_1^{(2)}(1,2) Y_2^{(2)}(1,3) \\ Y_2^{(2)}(1,2) Y_1^{(2)}(2,3) - Y_1^{(2)}(1,2) Y_2^{(2)}(2,3) \\ Y_2^{(2)}(1,3) Y_1^{(2)}(2,3) - Y_1^{(2)}(1,3) Y_2^{(2)}(2,3). \end{aligned}$$

Thus, [Proposition 5.4.3](#) implies that the oriented matroid strata is at most $2 \cdot 3^8(1 + 3 \cdot 12) = 485\,514$. However, as we will show in [Theorem 5.4.8](#), it turns out that there are precisely 3 distinct combinatorial types. We note that the three binomials above are precisely the binomials intersecting the the orthants in [Example 5.3.3](#). The file `orientedMatroidStrata2x3.m2` [[BHP22b](#)] contains Macaulay2 code which explicitly computes these polynomials. \diamond

Example 5.4.6 ($\partial_a \mathcal{R}$ for $(2 \times 2 \times 2)$ -games). In a $(2 \times 2 \times 2)$ -game, we have $D = 8, N = 6$ and $M = 12$. The number of minors of $A_H(Y)$ that contain at least one variable is $\binom{14}{8} - 1 = 3003$, but the number of irreducible components of $\partial_a \mathcal{R}$ is only 194. All of these polynomials are homogeneous, and the maximum degree is 6. The file `orientedMatroidStrata2x2x2.m2` [[BHP22b](#)] contains Macaulay2 code which explicitly computes these polynomials. [Proposition 5.4.3](#) implies that the number of oriented matroid strata is at most

$$6 \cdot 11^{11}(1 + 3 \cdot 194) = 998\,020\,223\,797\,278 > 10^{14}.$$

However, as in [Example 5.4.5](#), we expect the actual number to be much smaller than given by this bound. \diamond

The previous examples illustrate that the algebraic boundary of all oriented matroid strata is quite nice for (2×3) -games but becomes significantly more complicated even for $(2 \times 2 \times 2)$ -games. The following theorem shows that the nice structure we see for (2×3) -games holds for all $(2 \times n)$ -games.

THEOREM 5.4.7. Consider a $(2 \times n)$ -game, i.e. a 2-player game with strategies $d_1 = 2$ and $d_2 = n \in \mathbb{N}$. Then the irreducible components of $\partial_a \mathcal{R}$ are given by

- (i) all coordinate hyperplanes and
- (ii) certain hypersurfaces defined by quadratic binomials that are given by some (2×2) -minors of the matrix $A(Y)$.

Proof. We prove by induction on n . For $n = 2$ after reordering the rows and columns, the matrix $A(Y) = A^2(Y)$ has the following representation:

5.4 Combinatorial Types of Correlated Equilibrium Polytopes

$$\left(\begin{array}{cc|cc} Y_1^{(1)}(1,2) & & Y_2^{(1)}(1,2) & \\ & -Y_1^{(1)}(1,2) & & -Y_2^{(1)}(1,2) \\ \hline Y_1^{(2)}(1,2) & Y_2^{(2)}(1,2) & & \\ & & Y_1^{(2)}(2,1) & Y_1^{(2)}(2,1) \\ \hline & & Id_4 & \end{array} \right)$$

For $n = 3$ the columns and rows can be arranged to $A(Y) = A^3(Y)$ as follows.

$$\left(\begin{array}{cc|cc|cc} Y_1^{(1)}(1,2) & & Y_2^{(1)}(1,2) & & Y_3^{(1)}(1,2) & & \\ & -Y_1^{(1)}(1,2) & & -Y_2^{(1)}(1,2) & & -Y_3^{(1)}(1,2) & \\ \hline Y_1^{(2)}(1,2) & Y_2^{(2)}(1,2) & & & & & \\ Y_1^{(2)}(1,3) & Y_2^{(2)}(1,3) & & & & & \\ \hline & & Y_1^{(2)}(2,1) & Y_2^{(2)}(2,1) & & & \\ & & Y_1^{(2)}(2,3) & Y_2^{(2)}(2,3) & & & \\ & & & & Y_1^{(2)}(3,1) & Y_2^{(2)}(3,1) & \\ & & & & Y_1^{(2)}(3,2) & Y_2^{(2)}(3,2) & \\ \hline & & Id_6 & & & & \end{array} \right).$$

In both cases, the statement holds by Examples 5.4.4 and 5.4.5. First, we describe the general block matrix structure of $A(Y) = A^n(Y)$ for fixed $n \in \mathbb{N}$. Recall that $A^n(Y)$ is a $((D + N) \times D)$ -matrix, where $D = 2n$ and $N = 2 + n(n - 1)$. As in the case $n = 2, 3$, we can arrange the rows and columns of $A^n(Y)$ such that the first two rows consist of n blocks of size (2×2) , which are of the form $\begin{bmatrix} Y_k^{(1)}(1,2) & \\ & -Y_k^{(1)}(1,2) \end{bmatrix}$ for $k \in [n]$. The following $n(n - 1)$ rows form a block diagonal matrix, with n blocks of size $((n - 1) \times 2)$ of the form

$$\begin{bmatrix} Y_1^{(2)}(k,1) & Y_2^{(2)}(k,1) \\ \vdots & \vdots \\ Y_1^{(2)}(k,n) & Y_2^{(2)}(k,n) \end{bmatrix}$$

for each $k \in [n]$, where the row $[Y_1^{(2)}(k,k) \ Y_1^{(2)}(k,k)]$ is omitted. Finally, the last $2n$ rows consist of the identity matrix Id_{2n} .

We now assume that the statement holds for n and show it for $n + 1$. Note, that we can construct the matrix for $A^{n+1}(Y)$ by adding the following rows and columns to the

matrix for $A^n(Y)$: To the first two rows we add the block

$$\begin{bmatrix} Y_{n+1}^{(1)}(1,2) \\ -Y_{n+1}^{(1)}(1,2) \end{bmatrix}$$

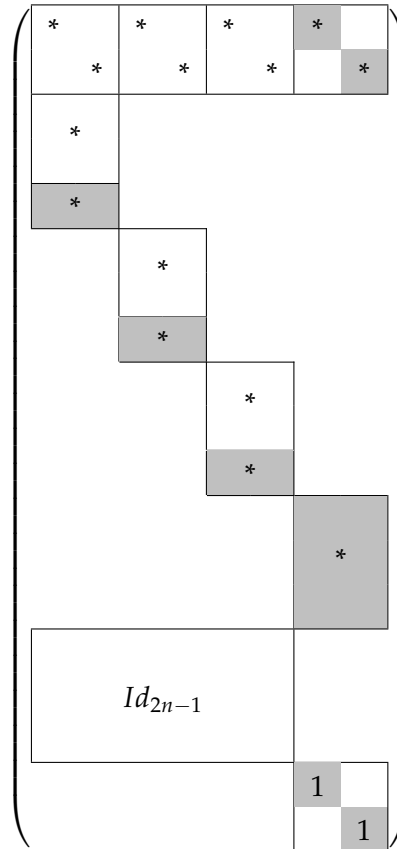
To the k th block of the block diagonal matrix we add the row

$$[Y_1^{(2)}(k, n+1) \ Y_2^{(2)}(k, n+1)],$$

and we add the entire block

$$\begin{bmatrix} Y_1^{(2)}(n+1,1) & Y_1^{(2)}(n+1,1) \\ \vdots & \vdots \\ Y_1^{(2)}(n+1,n) & Y_1^{(2)}(n+1,n) \end{bmatrix}.$$

Finally, we complete the identity matrix. Schematically, this procedure can be viewed as in the following picture, where * indicate non-zero entries, and the cells that are added when going from n to $n + 1$ are shaded in gray.



5.4 Combinatorial Types of Correlated Equilibrium Polytopes

We now consider the minors of the matrix $A^{n+1}(Y)$ for $n + 1$, and show that they are either monomials, binomials, or zero. Note that every maximal minor of $A^{n+1}(Y)$ that involves a row from the identity matrix corresponds to a smaller minor of the remaining matrix. We thus consider all minors of the submatrix of $A^{n+1}(Y)$ that consists of the first $2 + (n + 1)n$ rows. Choosing a submatrix of $A^{n+1}(Y)$ that consists of at most $n - 1$ rows from each block of the block diagonal matrix and at most n columns of even (or odd) index yields a submatrix of the matrix $A^n(Y)$, up to relabeling of variables. Thus, the statement holds by induction.

Choose any $(n \times n)$ -submatrix M of $A^{n+1}(Y)$ containing n rows from a single block of the block diagonal matrix. Then M has precisely two nonzero columns and thus has rank ≤ 2 , so the determinant of this matrix is 0. Therefore, the determinant of any square matrix containing these n rows is also 0.

Finally, consider an $((n + 1) \times (n + 1))$ -submatrix M containing the first row, and all columns of odd index (so the first row of M does not contain any 0s). We compute the determinant of M by expanding a column which has a maximum number of 0-entries. If M contains a column with only a single non-zero entry $Y_k^{(1)}(1, 2)$, then the $\det(M) = Y_k^{(1)}(1, 2) \det(\bar{M})$ for some submatrix \bar{M} of M . By induction (possibly after a relabeling of variables), $\det(\bar{M})$ is either a monomial, binomial, or 0. Suppose that no such column exists. Then for each column with first entry $Y_k^{(1)}(1, 2)$, $k \in [n + 1]$ the matrix M must contain a row from the block with entries $Y_*^{(2)}(k, *)$. However, this requires that M consists of at least $n + 2$ rows, contradicting the assumption that M is a square matrix of size $n + 1$. Thus, the determinant of every submatrix of $A^{n+1}(Y)$ containing M is zero. An analogous argument holds for any submatrix containing the second row, and all columns of even index.

Thus by induction we have that every minor of $A(Y)$ is the product of a monomial and some of the (2×2) -minors of the matrix $A(Y)$. This implies that the irreducible components of $\partial_a \mathcal{R}$ are some (2×2) -minors of $A(Y)$ and the coordinate hyperplanes. \square

We now show how the algebraic boundary of all oriented matroid strata of (2×3) -games can be used to completely determine the possible combinatorial types of the polytope.

THEOREM 5.4.8. Let G be a (2×3) -game with payoffs $Y \in \mathcal{S} \subseteq \mathbb{R}^9$ and let $P_G = P(Y)$ be its associated correlated equilibrium polytope. Then one of the following holds.

- (i) P_G is a point.
- (ii) P_G is of maximal dimensional and of a unique combinatorial type.
- (iii) There exists a (2×2) -game G' such that $P_{G'}$ is full-dimensional and combinatorially equivalent to P_G .

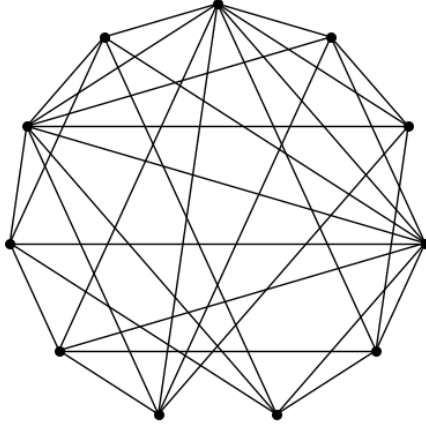


Figure 5.4: The graph of the combinatorially unique 5-dimensional polytope that arises as the correlated equilibrium polytope of a (2×3) -game, as described in [Theorem 5.4.8](#) and [Example 5.4.9](#).

Proof. First recall that the combinatorial type is fully determined by the sign patterns of the maximal minors of $A(Y)$, i.e. the oriented matroid of $A(Y)$. For (2×3) -games the matrix $A(Y)$ has 1206 nonzero maximal minors for generic Y , since 1797 of the $\binom{14}{6} = 3003$ maximal minors are identically zero. The signs of these 1206 maximal minors are completely determined by the signs of the irreducible components of $\det(A(Y)_H)$ for each $H \in \binom{[14]}{6}$. As in [Example 5.4.5](#), there are 12 such irreducible components f_1, \dots, f_{12} , which are given by the 9 coordinate hyperplanes and the 3 binomials listed in the example. This means that once we fix a sign pattern $s \in \{1, -1\}^{12}$ of the f_i the signs of all maximal minors of $A(Y)$ are uniquely determined. We note that some sign patterns are not feasible, i.e. cannot be obtained. Thus, to compute all possible combinatorial types, we compute the combinatorial type of the polytope once for each possible sign pattern s of the $f_i(Y)$ that is feasible.

We do this computationally, using the software Mathematica 13.0 and SageMath 9.6 [[Mat](#); [Sag](#)]. We first use Mathematica to find a payoff $Y \in \mathcal{S}$ such that $s_i f_i(Y) > 0$ for all $i = 1, \dots, 12$. We then compute the corresponding combinatorial type of the polytope in SageMath. These computations can be found on MathRepo [[BHP22b](#)] in the files `combinatorialTypes2x3.nb` and `combinatorialTypes2x3.ipynb` respectively. As a result we obtain 3 different possible combinatorial types, which are a single point, the unique combinatorial type of full-dimensions of (2×2) -games (a bipyramid over a triangle), and a new unique full-dimensional combinatorial type. This polytope has f -vector $(1, 11, 32, 40, 25, 8, 1)$, and the graph of this 5-dimensional polytope is depicted in [Figure 5.4](#). A full description of this polytope can be found in `combinatorialTypes2x3.ipynb` [[BHP22b](#)]. \square

Example 5.4.9 (Combinatorial types of (2×3) -games). By [Theorem 5.4.8](#), for (2×3) -games there is a unique combinatorial type of full-dimension. This is a 5-dimensional polytope with f -vector $(1, 11, 32, 40, 25, 8, 1)$ and its graph is depicted in [Figure 5.4](#). \diamond

5.4 Combinatorial Types of Correlated Equilibrium Polytopes

[Theorem 5.4.7](#) shows, that in (2×3) -games all correlated equilibrium polytopes that are not of maximal dimension appear as the maximal polytope of a smaller game. This gives rise to the following conjecture.

CONJECTURE 5.4.10. Let G be a $(2 \times n)$ -game with generic payoff matrices and let P_G be its correlated equilibrium polytope. If P_G is not of maximal dimension, then there exists a $(2 \times k)$ -game G' where $k < n$ such that $P_{G'}$ has maximal dimension and P_G and $P_{G'}$ are combinatorially equivalent.

A relevant study to this conjecture is the dual reduction process of finite games. An iterative dual reduction reduces a finite game G to a smaller elementary game G' , for which $P_{G'}$ is full-dimensional, by deleting certain pure strategies or merging several pure strategies into a single one. Any correlated equilibrium of the reduced game G' is a correlated equilibrium of the original game G , however the opposite is not always true [[Mye97](#), Section 5]. [Conjecture 5.4.10](#) is supported by our computations thus far. To test this conjecture, we sampled 100 000 random payoff matrices X for $(2 \times n)$ -games for $n = 4, 5$. The results are summarized in [Table 5.1](#), which shows the number of unique combinatorial types of a given dimension that we found for each $(2 \times n)$ -game. In all of our computations, [Conjecture 5.4.10](#) holds. The supporting code can be found on [[BHP22b](#)].

Unique Combinatorial Types by Dimension					
Dimension	0	3	5	7	9
(2×2)	1	1	0	0	0
(2×3)	1	1	1	0	0
(2×4)	1	1	1	3	0
(2×5)	1	1	1	3	4

Table 5.1: The number of unique combinatorial types of P_G of each dimension for a $(2 \times n)$ -game in a random sampling of size 100 000.

In contrast to the $(2 \times n)$ -case, $(2 \times 2 \times 2)$ -games exhibit a much wider variety of distinct combinatorial types. In a sample of 100 000 random payoff matrices for $(2 \times 2 \times 2)$ -games, we found 14 949 distinct combinatorial types which are of maximal dimension. Amongst these 7-dimensional polytopes, the number of vertices can range from 8 to 119, the number of facets from 8 to 14, and the number of total faces from 256 to 2338. Examples of f -vectors achieving these bounds are

$$\begin{aligned} f_{P_{G_1}} &= (1, 8, 28, 56, 70, 56, 28, 8, 1) \\ f_{P_{G_2}} &= (1, 119, 458, 728, 616, 302, 87, 14, 1), \\ f_{P_{G_3}} &= (1, 119, 460, 733, 620, 303, 87, 14, 1). \end{aligned}$$

BIBLIOGRAPHY

- [ABH+11] Federico Ardila, Matthias Beck, Serkan Hoşten, Julian Pfeifle, and Kim Seashore. „Root Polytopes and Growth Series of Root Lattices.“ In: *SIAM Journal on Discrete Mathematics* 25.1 (2011), pp. 360–378. doi: [10.1137/090749293](https://doi.org/10.1137/090749293).
- [AD09] Federico Ardila and Mike Develin. „Tropical Hyperplane Arrangements and Oriented Matroids.“ In: *Mathematische Zeitschrift* 262.4 (Aug. 2009), pp. 795–816. doi: [10.1007/s00209-008-0400-z](https://doi.org/10.1007/s00209-008-0400-z).
- [AGG12] Marianne Akian, Stephane Gaubert, and Alexander Guterman. „Tropical Polyhedra are Equivalent to Mean Payoff Games.“ In: *International Journal of Algebra and Computation* 22.01 (Feb. 2012), p. 1250001. doi: [10.1142/S0218196711006674](https://doi.org/10.1142/S0218196711006674).
- [AH02] Robert Aumann and Sergiu Hart, eds. *Handbook of Game Theory with Economic Applications*. Vol. 3. Handbooks in Economics. North Holland, 2002, pp. 1521–2351. ISBN: 9780444894281.
- [ALS21] Nima Arkani-Hamed, Thomas Lam, and Marcus Spradlin. „Positive Configuration Space.“ In: *Communications in Mathematical Physics* 384.2 (Apr. 2021), pp. 909–954. doi: [10.1007/s00220-021-04041-x](https://doi.org/10.1007/s00220-021-04041-x).
- [Ardo4] Federico Ardila. *A Tropical Morphism Related to the Hyperplane Arrangement of the Complete Bipartite Graph*. Apr. 2004. arXiv: [math/0404287](https://arxiv.org/abs/math/0404287).
- [Aum74] Robert J. Aumann. „Subjectivity and Correlation in Randomized Strategies.“ In: *Journal of Mathematical Economics* 1.1 (Mar. 1974), pp. 67–96. doi: [10.1016/0304-4068\(74\)90037-8](https://doi.org/10.1016/0304-4068(74)90037-8).
- [Aum87] Robert J. Aumann. „Correlated Equilibrium as an Expression of Bayesian Rationality.“ In: *Econometrica* 55.1 (Jan. 1987), pp. 1–18. doi: [10.2307/1911154](https://doi.org/10.2307/1911154).
- [Bas03] Saugata Basu. „Different Bounds on the Different Betti Numbers of Semi-Algebraic Sets.“ In: *Discrete & Computational Geometry* 30.1 (May 2003), pp. 65–85. doi: [10.1007/s00454-003-2922-9](https://doi.org/10.1007/s00454-003-2922-9).
- [BBMS21] Katalin Berlow, Marie-Charlotte Brandenburg, Chiara Meroni, and Isabelle Shankar. *MATHREPO. Mathematical Data and Software. Intersection Bodies of Polytopes*. Dec. 2021. URL: <https://mathrepo.mis.mpg.de/intersection-bodies>.

- [BBMS22] Katalin Berlow, Marie-Charlotte Brandenburg, Chiara Meroni, and Isabelle Shankar. „Intersection Bodies of Polytopes.“ In: *Beiträge zur Algebra und Geometrie (Contributions to Algebra and Geometry)* 63.2 (June 2022), pp. 419–439. DOI: [10.1007/s13366-022-00621-7](https://doi.org/10.1007/s13366-022-00621-7).
- [BPRS20] Dominik Bendle, Janko Boehm, Yue Ren, and Benjamin Schröter. *Parallel Computation of Tropical Varieties, their Positive Part, and Tropical Grassmannians*. Mar. 2020. arXiv: [2003.13752](https://arxiv.org/abs/2003.13752).
- [BCRR98] Jacek Bochnak, Michel Coste, Marie-Françoise Roy, and Marie-Françoise Roy. *Real Algebraic Geometry*. Vol. 36. Results in Mathematics and Related Areas (3). Translated from the 1987 French original, revised by the authors. Springer-Verlag, Berlin, 1998. ISBN: 3-540-64663-9. DOI: [10.1007/978-3-662-03718-8](https://doi.org/10.1007/978-3-662-03718-8).
- [BEZ20] Marie-Charlotte Brandenburg, Sophia Elia, and Leon Zhang. *GitHub repository: mariebrandenburg/polynomials-of-polytropes*. Version v1.0. July 2020. DOI: [10.5281/zenodo.3961958](https://doi.org/10.5281/zenodo.3961958). URL: <https://github.com/mariebrandenburg/polynomials-of-polytropes>.
- [BEZ23] Marie-Charlotte Brandenburg, Sophia Elia, and Leon Zhang. „Multivariate volume, Ehrhart, and h^* -polynomials of polytropes.“ In: *Journal of Symbolic Computation* 114 (Jan. 2023), pp. 209–230. DOI: [10.1016/j.jsc.2022.04.011](https://doi.org/10.1016/j.jsc.2022.04.011).
- [BF87] Imre Bárány and Zoltán Füredi. „Computing the Volume is Difficult.“ In: *Discrete & Computational Geometry* 2.4 (Dec. 1987), pp. 319–326. DOI: [10.1007/bf02187886](https://doi.org/10.1007/bf02187886).
- [BHP22a] Marie-Charlotte Brandenburg, Benjamin Hollering, and Irem Portakal. *Combinatorics of Correlated Equilibria*. Oct. 2022. DOI: [10.48550/ARXIV.2209.13938](https://doi.org/10.48550/ARXIV.2209.13938). arXiv: [2209.13938](https://arxiv.org/abs/2209.13938).
- [BHP22b] Marie-Charlotte Brandenburg, Benjamin Hollering, and Irem Portakal. *MATHREPO. Mathematical Data and Software. Combinatorics of Correlated Equilibria*. Sept. 2022. URL: <https://mathrepo.mis.mpg.de/correlated-equilibrium>.
- [BISO] Winfried Bruns, Bogdan Ichim, Christof Söger, and Ulrich von der Ohe. *Normaliz. Algorithms for rational cones and affine monoids*. URL: <https://www.normaliz.uni-osnabrueck.de>.
- [BL13] Nicolas Brunner and Noah Linden. „Connection Between Bell Nonlocality and Bayesian Game Theory.“ In: *Nature Communications* 4.1 (July 2013), Article No. 4. DOI: [10.1038/ncomms3057](https://doi.org/10.1038/ncomms3057).
- [BLN22] Saugata Basu, Antonio Lerario, and Abhiram Natarajan. „Betti Numbers of Random Hypersurface Arrangements.“ In: *Journal of the London Mathematical Society* (July 2022). DOI: [10.1112/jlms.12658](https://doi.org/10.1112/jlms.12658).

- [BLS22] Marie-Charlotte Brandenburg, Georg Loho, and Rainer Sinn. *Tropical Positivity and Determinantal Varieties*. May 2022. arXiv: [2205.14972](https://arxiv.org/abs/2205.14972).
- [BLVS+99] Anders Björner, Michel Las Vergnas, Bernd Sturmfels, Neil White, and Günter M. Ziegler. *Oriented Matroids*. 2nd ed. Vol. 46. Encyclopedia of Mathematics and its Applications. Cambridge University Press, 1999. ISBN: 0-521-77750-X. DOI: [10.1017/CBO9780511586507](https://doi.org/10.1017/CBO9780511586507).
- [Bor21] Jonathan Boretsky. *Positive Tropical Flags and the Positive Tropical Dressian*. Nov. 2021. arXiv: [2111.12587](https://arxiv.org/abs/2111.12587).
- [BPT13] Grigoriy Blekherman, Pablo A. Parrilo, and Rekha R. Thomas, eds. *Semidefinite Optimization and Convex Algebraic Geometry*. Vol. 13. MOS-SIAM Series on Optimization. Society for Industrial and Applied Mathematics, 2013. ISBN: 978-1-611972-28-3.
- [BR15] Matthias Beck and Sinai Robins. *Computing the Continuous Discretely. Integer-Point Enumeration in Polyhedra*. 2nd ed. Undergraduate Texts in Mathematics. Springer New York, 2015. ISBN: 978-1-4939-2969-6. DOI: [10.1007/978-1-4939-2969-6](https://doi.org/10.1007/978-1-4939-2969-6).
- [BS96] Louis J. Billera and Aravamuthan Sarangarajan. „The Combinatorics of Permutation Polytopes.“ In: *Formal Power Series and Algebraic Combinatorics*. Ed. by Louis J. Billera, Curtis Greene, Rodica Simion, and Richard P. Stanley. Vol. 24. Series in Discrete Mathematics and Theoretical Computer Science. American Mathematical Society, 1996, pp. 1–23. DOI: [10.1090/dimacs/024/01](https://doi.org/10.1090/dimacs/024/01).
- [BY06] Florian Block and Josephine Yu. „Tropical Convexity via Cellular Resolutions.“ In: *Journal of Algebraic Combinatorics* 24 (Aug. 2006), pp. 103–114. DOI: [10.1007/s10801-006-9104-9](https://doi.org/10.1007/s10801-006-9104-9).
- [CA03] Antoni Calvó-Armengol. *The Set of Correlated Equilibria of 2 x 2 Games*. RePEc Working Paper. Preprint. Oct. 2003. URL: <https://ideas.repec.org/p/bge/wpaper/79.html>.
- [Cam99] Stefano Campi. „Convex Intersection Bodies in Three and Four Dimensions.“ In: *Mathematika* 46.1 (June 1999), 15–27. DOI: [10.1112/S002557930000752X](https://doi.org/10.1112/S002557930000752X).
- [CHSW11] Dustin Cartwright, Mathias Häbich, Bernd Sturmfels, and Annette Werner. „Mustafin varieties.“ In: *Selecta Mathematica. New Series*. 17 (Dec. 2011), pp. 757–793. DOI: [10.1007/s00029-011-0075-x](https://doi.org/10.1007/s00029-011-0075-x).
- [CJR11] Melody Chan, Anders Jensen, and Elena Rubei. „The 4×4 Minors of a $5 \times n$ Matrix are a Tropical Basis.“ In: *Linear Algebra and its Applications* 435.7 (Oct. 2011), pp. 1598–1611. DOI: [10.1016/j.laa.2010.09.032](https://doi.org/10.1016/j.laa.2010.09.032).

- [CLO15] David A. Cox, John B. Little, and Donal O’Shea. *Ideals, Varieties, and Algorithms. An Introduction to Computational Algebraic Geometry and Commutative Algebra*. 4th ed. Undergraduate Texts in Mathematics. Springer Cham, 2015. ISBN: 978-3-319-16720-6. doi: [10.1007/978-3-319-16721-3](https://doi.org/10.1007/978-3-319-16721-3).
- [CLS11] David A. Cox, John B. Little, and Henry K. Schenck. *Toric Varieties*. Vol. 124. Graduate Studies in Mathematics. American Mathematical Society, 2011. ISBN: 978-0-8218-4819-7.
- [CR93] Joel E. Cohen and Uriel G. Rothblum. „Nonnegative Ranks, Decompositions, and Factorizations of Nonnegative Matrices.“ In: *Linear Algebra and its Applications* 190 (Sept. 1993), pp. 149–168. doi: [10.1016/0024-3795\(93\)90224-C](https://doi.org/10.1016/0024-3795(93)90224-C).
- [CT18] Robert Crowell and Ngoc Tran. *Tropical Geometry and Mechanism Design*. Nov. 2018. arXiv: [1606.04880](https://arxiv.org/abs/1606.04880).
- [Devo05] Mike Develin. „The Moduli Space of n Tropically Collinear Points in \mathbb{R}^d .“ In: *Collectanea Mathematica* 56 (2005). ISSN: 0010-0757.
- [DF88] Martin Dyer and Alan Frieze. „On the Complexity of Computing the Volume of a Polyhedron.“ In: *SIAM Journal on Computing* 17.5 (Oct. 1988), pp. 967–974. doi: [10.1137/0217060](https://doi.org/10.1137/0217060).
- [DH20] Emanuele Delucchi and Linard Hoessly. „Fundamental Polytopes of Metric Trees via Parallel Connections of Matroids.“ In: *European Journal of Combinatorics* 87 (June 2020), p. 103098. doi: [10.1016/j.ejc.2020.103098](https://doi.org/10.1016/j.ejc.2020.103098).
- [DLRS10] Jesus De Loera, Joerg Rambau, and Francisco Santos. *Triangulations*. Springer-Verlag GmbH, Aug. 2010. 535 pp. ISBN: 978-3-642-12971-1.
- [DLS03] Jesús De Loera and Bernd Sturmfels. „Algebraic unimodular counting.“ In: *Mathematical Programming, Series B* 96.2 (May 2003), pp. 183–203. doi: [10.1007/s10107-003-0383-9](https://doi.org/10.1007/s10107-003-0383-9).
- [DM88] Wolfgang Dahmen and Charles A. Micchelli. „The Number of Solutions to Linear Diophantine Equations and Multivariate Splines.“ In: *Transactions of the American Mathematical Society* 308.2 (1988), pp. 509–532. ISSN: 0002-9947. doi: [10.2307/2001089](https://doi.org/10.2307/2001089).
- [DS04] Mike Develin and Bernd Sturmfels. „Tropical Convexity.“ In: *Documenta Mathematica* 9 (2004). Erratum in *Documenta Mathematica* (9:205–206, 2004), pp. 1–27. ISSN: 1431-0643. URL: <https://www.math.uni-bielefeld.de/documenta/vol-09/vol-09.html>.
- [DSS05] Mike Develin, Francisco Santos, and Bernd Sturmfels. „On the Rank of a Tropical Matrix.“ In: *Combinatorial and Computational Geometry*. Cambridge University Press, 2005, pp. 213–242. ISBN: 0-521-84862-8. URL: www.msri.org/communications/books/Book52/.

- [Ehr62] Eugène Ehrhart. „Sur les polyèdres rationnels homothétiques à n dimensions.“ In: *Compte-rendus de l'académie des sciences, Paris* 254 (1962), pp. 616–618.
- [ES96] David Eisenbud and Bernd Sturmfels. „Binomial Ideals.“ In: *Duke Mathematical Journal* 84.1 (July 1996), pp. 1–45. DOI: [10.1215/S0012-7094-96-08401-X](https://doi.org/10.1215/S0012-7094-96-08401-X).
- [FR15] Alex Fink and Felipe Rincón. „Stiefel Tropical Linear Spaces.“ In: *Journal of Combinatorial Theory, Series A* 135 (Oct. 2015), pp. 291–331. DOI: [10.1016/j.jcta.2015.06.001](https://doi.org/10.1016/j.jcta.2015.06.001).
- [FS05] Eva Maria Feichtner and Bernd Sturmfels. „Matroid Polytopes, Nested Sets and Bergman Fans.“ In: *Portugaliae Mathematica. Nova Série* 62.4 (2005), pp. 437–468. ISSN: 0032-5155.
- [Garo6] Richard J. Gardner. *Geometric Tomography*. 2nd ed. Vol. 58. Encyclopedia of Mathematics and its Applications. Cambridge University Press, New York, 2006. ISBN: 0-521; 0-521-68493-5. DOI: [10.1017/CBO9781107341029](https://doi.org/10.1017/CBO9781107341029).
- [Gar94a] Richard J. Gardner. „A Positive Answer to the Busemann-Petty Problem in Three Dimensions.“ In: *Annals of Mathematics, Second Series* 140.2 (Sept. 1994), pp. 435–447. DOI: [10.2307/2118606](https://doi.org/10.2307/2118606).
- [Gar94b] Richard J. Gardner. „Intersection Bodies and the Busemann-Petty problem.“ In: *Transactions of the American Mathematical Society* 342 (1994), pp. 435–445. DOI: [10.2307/2154703](https://doi.org/10.2307/2154703).
- [GKS99] Richard J. Gardner, Alexander Koldobsky, and Thomas Schlumprecht. „An Analytic Solution to the Busemann-Petty Problem on Sections of Convex Bodies.“ In: *Annals of Mathematics, Second Series* 149.2 (Mar. 1999), pp. 691–703. DOI: [10.2307/120978](https://doi.org/10.2307/120978).
- [GM19] Stéphane Gaubert and Marie MacCaig. „Approximating the Volume of Tropical Polytopes is Difficult.“ In: *International Journal of Algebra and Computation* 29.2 (June 2019), pp. 357–389. DOI: [10.1142/S0218196719500061](https://doi.org/10.1142/S0218196719500061).
- [GMTW19] João Gouveia, Antonio Macchia, Rekha R. Thomas, and Amy Wiebe. „The Slack Realization Space of a Polytope.“ English. In: *SIAM Journal on Discrete Mathematics* 33.3 (2019), pp. 1637–1653. DOI: [10.1137/18M1233649](https://doi.org/10.1137/18M1233649).
- [GOT17] Jacob E. Goodman, Joseph O'Rourke, and Csaba D. Tóth, eds. *Handbook of Discrete and Computational Geometry*. 3rd ed. Discrete Mathematics and its Applications. Chapman and Hall/CRC, 2017. ISBN: 9781315119601. DOI: [10.1201/9781315119601](https://doi.org/10.1201/9781315119601).
- [GS22] Daniel R. Grayson and Michael E. Stillman. *Macaulay2 (Versions 1.15 and 1.20)*. 2022. URL: <http://www.math.uiuc.edu/Macaulay2/>.

- [HHMM20] Guillermo Hansen, Irmina Herbut, Horst Martini, and Maria Moszyńska. „Starshaped Sets.“ In: *Aequationes Mathematicae* 94.6 (Dec. 2020), pp. 1001–1092. DOI: [10.1007/s00010-020-00720-7](https://doi.org/10.1007/s00010-020-00720-7).
- [HJJSo9] Sven Herrmann, Anders Jensen, Michael Joswig, and Bernd Sturmfels. „How to Draw Tropical Planes.“ In: *The Electronic Journal of Combinatorics* 16.2 (2009), R6. DOI: [10.37236/72](https://doi.org/10.37236/72).
- [HRSoo] Birkett Huber, Jörg Rambau, and Francisco Santos. „The Cayley Trick, Lifting Subdivisions and the Bohne-Dress Theorem on Zonotopal Tilings.“ In: *Journal of the European Mathematical Society* 2.2 (June 2000), pp. 179–198. DOI: [10.1007/s100970050003](https://doi.org/10.1007/s100970050003).
- [JK10] Michael Joswig and Katja Kulas. „Tropical and Ordinary Convexity Combined.“ In: *Advances in Geometry* 10.2 (Mar. 2010), pp. 333–352. DOI: [10.1515/advgeom.2010.012](https://doi.org/10.1515/advgeom.2010.012).
- [JLS21] Dennis Jahn, Robert Löwe, and Christian Stump. „Minkowski Decompositions for Generalized Associahedra of Acyclic Type.“ In: *Algebraic Combinatorics* 4.5 (2021), pp. 757–775. DOI: [10.5802/alco.177](https://doi.org/10.5802/alco.177).
- [Jos21] Michael Joswig. *Essentials of Tropical Combinatorics*. Vol. 219. Graduate Studies in Mathematics. American Mathematical Society, 2021. ISBN: 978-1-4704-6741-8.
- [JP12] A. Jiménez and María J. De la Puente. *Six Combinatorial Classes of Maximal Convex Tropical Tetrahedra*. Oct. 2012. arXiv: [1205.4162](https://arxiv.org/abs/1205.4162).
- [JS19] Michael Joswig and Benjamin Schröter. *The Tropical Geometry of Shortest Paths*. Version 2. Oct. 2019. arXiv: [1904.01082v2](https://arxiv.org/abs/1904.01082v2).
- [JSY07] Michael Joswig, Bernd Sturmfels, and Josephine Yu. „Affine Buildings and Tropical Convexity.“ In: *Albanian Journal of Mathematics* 1.4 (2007), pp. 187–211. URL: <https://albanian-j-math.com/archives/2007-16.pdf>.
- [Kol98] Alexander Koldobsky. „Intersection Bodies, Positive Definite Distributions, and the Busemann-Petty Problem.“ In: *American Journal of Mathematics* 120.4 (Aug. 1998), pp. 827–840. DOI: [10.1353/ajm.1998.0030](https://doi.org/10.1353/ajm.1998.0030).
- [LP07] Thomas Lam and Alexander Postnikov. „Alcoved Polytopes I.“ In: *Discrete & Computational Geometry* 38 (Oct. 2007), 453–478. DOI: [10.1007/s00454-006-1294-3](https://doi.org/10.1007/s00454-006-1294-3).
- [LP18] Thomas Lam and Alexander Postnikov. „Alcoved polytopes II.“ In: *Lie Groups, Geometry, and Representation Theory*. Vol. 326. Progress in Mathematics. Dec. 2018, pp. 253–272. DOI: doi.org/10.1007/978-3-030-02191-7_10.
- [LP20] Thomas Lam and Alexander Postnikov. *Polypositroids*. Jan. 2020. DOI: [10.48550/ARXIV.2010.07120](https://doi.org/10.48550/ARXIV.2010.07120). arXiv: [2010.07120](https://arxiv.org/abs/2010.07120).

- [LS20] Georg Loho and Matthias Schymura. „Tropical Ehrhart Theory and Tropical Volume.“ In: *Research in the Mathematical Sciences* 7.4 (Sept. 2020), Article No. 30. doi: [10.1007/s40687-020-00228-1](https://doi.org/10.1007/s40687-020-00228-1).
- [LSV11] Ehud Lehrer, Eilon Solan, and Yannick Viossat. „Equilibrium Payoffs of Finite Games.“ In: *Journal of Mathematical Economics* 47.1 (Jan. 2011), pp. 48–53. doi: [10.1016/j.jmateco.2010.10.007](https://doi.org/10.1016/j.jmateco.2010.10.007).
- [Ludo06] Monika Ludwig. „Intersection Bodies and Valuations.“ In: *American Journal of Mathematics* 128.6 (Dec. 2006), pp. 1409–1428. doi: [10.1353/ajm.2006.0046](https://doi.org/10.1353/ajm.2006.0046).
- [Lut88] Erwin Lutwak. „Intersection Bodies and Dual Mixed Volumes.“ In: *Advances in Mathematics* 71.2 (Oct. 1988), pp. 232–261. doi: [10.1016/0001-8708\(88\)90077-1](https://doi.org/10.1016/0001-8708(88)90077-1).
- [Mar94] Horst Martini. „Cross-Sectional Measures.“ In: *Intuitive Geometry*. Vol. 63. Colloquia Mathematica Societatis János Bolyai. North-Holland, Amsterdam, 1994, pp. 269–310.
- [Mat] *Mathematica (Version 13.0)*. Wolfram Research, Inc. 2022. URL: <https://www.wolfram.com/mathematica>.
- [McM09] Peter McMullen. „Valuations on Lattice Polytopes.“ In: *Advances in Mathematics* 220.1 (Jan. 2009), pp. 303–323. doi: [10.1016/j.aim.2008.09.004](https://doi.org/10.1016/j.aim.2008.09.004).
- [MS05] Ezra Miller and Bernd Sturmfels. *Combinatorial Commutative Algebra*. 1st ed. Vol. 227. Graduate Texts in Mathematics. Springer New York, 2005. ISBN: 978-0-387-22356-8. doi: doi.org/10.1007/b138602.
- [MS15] Diane Maclagan and Bernd Sturmfels. *Introduction to Tropical Geometry*. Vol. 161. Graduate Studies in Mathematics. American Mathematical Society, 2015. ISBN: 978-0-8218-5198-2. doi: [10.1090/gsm/161](https://doi.org/10.1090/gsm/161).
- [MSUZ16] Mateusz Michałek, Bernd Sturmfels, Caroline Uhler, and Piotr Zwiernik. „Exponential Varieties.“ In: *Proceedings of the London Mathematical Society, Third Series* 112.1 (Jan. 2016), pp. 27–56. ISSN: 0024-6115. doi: [10.1112/plms/pdv066](https://doi.org/10.1112/plms/pdv066).
- [MY09] Hannah Markwig and Josephine Yu. „The Space of Tropically Collinear Points is Shellable.“ In: *Collectanea Mathematica* 60.1 (Feb. 2009), pp. 63–77. doi: [10.1007/BF03191216](https://doi.org/10.1007/BF03191216).
- [Mye97] Roger B. Myerson. „Dual Reduction and Elementary Games.“ In: *Games and Economic Behavior* 21.1 (1997), pp. 183–202. doi: [10.1006/game.1997.0573](https://doi.org/10.1006/game.1997.0573).
- [Nas50] John F. Nash, Jr. „Equilibrium Points in n-Person Games.“ In: *Proceedings of the National Academy of Sciences* 36.1 (Jan. 1950), pp. 48–49. doi: [10.1073/pnas.36.1.48](https://doi.org/10.1073/pnas.36.1.48).

- [NCHo4] Robert Nau, Sabrina Gomez Canovas, and Pierre Hansen. „On the Geometry of Nash equilibria and Correlated Equilibria.“ In: *International Journal of Games Theory* 32.4 (Aug. 2004). DOI: [10.1007/s001820300162](https://doi.org/10.1007/s001820300162).
- [NRTVo7] Noam Nisan, Tim Roughgarden, Eva Tardos, and Vijay V. Vazirani, eds. *Algorithmic Game Theory*. Cambridge University Press, 2007. ISBN: 9780511800481. DOI: [10.1017/cbo9780511800481](https://doi.org/10.1017/cbo9780511800481).
- [Osc] OSCAR. *Open Source Computer Algebra Research system, Version 0.8.2-DEV*. The OSCAR Team. 2022. URL: <https://oscar.computeralgebra.de>.
- [Paf15] Andreas Paffenholz. „Faces of Birkhoff Polytopes.“ In: *The Electronic Journal of Combinatorics* 22.1 (2015), P1.67. DOI: doi.org/10.37236/4499.
- [PPV05] Nicos G. Pavlidis, Konstantinos E. Parsopoulos, and Michal N. Vrahatis. „Computing Nash Equilibria Through Computational Intelligence Methods.“ In: *Journal of Computational and Applied Mathematics* 175.1 (Mar. 2005), pp. 113–136. DOI: [10.1016/j.cam.2004.06.005](https://doi.org/10.1016/j.cam.2004.06.005).
- [PRo5] Christos H. Papadimitriou and Tim Roughgarden. „Computing Equilibria in Multi-Player Games.“ In: *Proceedings of the Sixteenth Annual ACM-SIAM Symposium on Discrete Algorithms*. SODA '05. Session 1B. Society for Industrial and Applied Mathematics, 2005, pp. 82–91. ISBN: 0-89871-585-7.
- [PRo8] Christos H. Papadimitriou and Tim Roughgarden. „Computing Correlated Equilibria in Multi-Player Games.“ In: *Journal of the ACM* 55.3 (2008), Article No. 14, 1–29. DOI: [10.1145/1379759.1379762](https://doi.org/10.1145/1379759.1379762).
- [PS04] Lior Pachter and Bernd Sturmfels. „Tropical Geometry of Statistical Models.“ In: *Proceedings of the National Academy of Sciences of the United States of America* 101.46 (Nov. 2004), pp. 16132–16137. DOI: [10.1073/pnas.0406010101](https://doi.org/10.1073/pnas.0406010101).
- [PS22] Irem Portakal and Bernd Sturmfels. „Geometry of Dependency Equilibria.“ In: *Rendiconti dell'Istituto di Matematica dell'Università di Trieste* 54 (2022), Article No. 5. DOI: [10.13137/2464-8728/33881](https://doi.org/10.13137/2464-8728/33881).
- [PSA22] Irem Portakal and Javier Sendra-Arranz. *Nash Conditional Independence Curve*. June 2022. arXiv: [2206.07000](https://arxiv.org/abs/2206.07000).
- [PSW22] Daniel Plaumann, Rainer Sinn, and Jannik Lennart Wesner. „Families of Faces and the Normal Cycle of a Convex Semi-Algebraic Set.“ In: *Beiträge zur Algebra und Geometrie (Contributions to Algebra and Geometry)* (Aug. 2022). DOI: [10.1007/s13366-022-00657-9](https://doi.org/10.1007/s13366-022-00657-9).
- [Pue13] María Jesús de la Puente. „On tropical Kleene star matrices and alcoved polytopes.“ In: *Kybernetika* 49.6 (2013), pp. 897–910. URL: <http://dml.cz/dmlcz/143578>.

- [Rago02] T. E. S. Raghavan. „Non-Zero-Sum Two-Person Games.“ In: *Handbook of Game Theory with Economic Applications*. Ed. by Robert Aumann and Sergiu Hart. Vol. 3. Handbooks in Economics. North-Holland, 2002. Chap. 44, pp. 1687–1721. DOI: [10.1016/S1574-0005\(02\)03007-2](https://doi.org/10.1016/S1574-0005(02)03007-2).
- [RS10] Philipp Rostalski and Bernd Sturmfels. „Dualities in Convex Algebraic Geometry.“ In: *Rendiconti di Mathematica* 30 (2010), pp. 285–327. URL: [https://www1.mat.uniroma1.it/ricerca/rendiconti/ARCHIVIO/2010\(3-4\)/285-327.pdf](https://www1.mat.uniroma1.it/ricerca/rendiconti/ARCHIVIO/2010(3-4)/285-327.pdf).
- [RS11] Kristian Ranestad and Bernd Sturmfels. „The Convex Hull of a Variety.“ In: *Notions of Positivity and the Geometry of Polynomials*. Ed. by Petter Brändén, Mikael Passare, and Mihai Putinar. Trends in Mathematics. Springer Verlag, Aug. 2011, pp. 331–344. DOI: [10.1007/978-3-0348-0142-3_18](https://doi.org/10.1007/978-3-0348-0142-3_18).
- [RS22] Luis Crespo Ruiz and Francisco Santos. *Multitriangulations and Tropical Pfaffians*. Mar. 2022. arXiv: [2203.04633](https://arxiv.org/abs/2203.04633).
- [Sag] *SageMath, the Sage Mathematics Software System (Versions 9.0, 9.2 and 9.6)*. The Sage Developers. 2021. URL: <https://www.sagemath.org>.
- [Sano05] Francisco Santos. „The Cayley Trick and Triangulations of Products of Simplices.“ In: *Integer Points in Polyhedra—Geometry, Number Theory, Algebra, Optimization*. Ed. by Alexander Barvinok, Matthias Beck, Christian Haase, Bruce Reznick, and Volkmar Welker. Vol. 374. Contemp. Math. American Mathematical Society, 2005, pp. 151–177. DOI: [10.1090/conm/374/06904](https://doi.org/10.1090/conm/374/06904).
- [Sch03] Alexander Schrijver. *Combinatorial Optimization. Polyhedra and Efficiency*. Springer Berlin, Heidelberg, 2003. ISBN: 9783540443896.
- [Sch13] Rolf Schneider. *Convex Bodies: The Brunn–Minkowski Theory*. Encyclopedia of Mathematics and its Applications. Cambridge University Press, 2013. ISBN: 9781107601017. DOI: [10.1017/CBO9781139003858](https://doi.org/10.1017/CBO9781139003858).
- [Shi13] Yaroslav Shitov. „When do the r -by- r Minors of a Matrix Form a Tropical Basis?“ In: *Journal of Combinatorial Theory, Series A* 120.6 (Aug. 2013), pp. 1166–1201. DOI: [10.1016/j.jcta.2013.03.004](https://doi.org/10.1016/j.jcta.2013.03.004).
- [Sin15] Rainer Sinn. „Algebraic Boundaries of Convex Semi-Algebraic Sets.“ In: *Research in the Mathematical Sciences* 2.3 (Mar. 2015). DOI: [10.1186/s40687-015-0022-0](https://doi.org/10.1186/s40687-015-0022-0).
- [SP73] J. Maynard Smith and G. R. Price. „The Logic of Animal Conflict.“ In: *Nature* 246 (Nov. 1973), pp. 15–18. DOI: [10.1038/246015a0](https://doi.org/10.1038/246015a0).
- [Spo03] Wolfgang Spohn. „Dependency Equilibria and the Causal Structure of Decision and Game Situation.“ In: *Homo Oeconomicus* 20 (2003), pp. 195–255.

- [SS04] David Speyer and Bernd Sturmfels. „The Tropical Grassmannian.“ In: *Advances in Geometry* 4.3 (2004), pp. 389–411. doi: [10.1515/advg.2004.023](https://doi.org/10.1515/advg.2004.023).
- [Sta07] Richard Stanley. „An Introduction to Hyperplane Arrangements.“ In: *Geometric Combinatorics*. Ed. by Ezra Miller, Victor Reiner, and Bernd Sturmfels. Vol. 13. American Mathematical Society, Oct. 2007, pp. 389–496. doi: [10.1090/pcms/013/08](https://doi.org/10.1090/pcms/013/08).
- [Sta80] Richard P. Stanley. „Decompositions of Rational Convex Polytopes.“ In: *Annals of Discrete Mathematics* 6 (1980), pp. 333–342.
- [Stu02] Bernd Sturmfels. *Solving Systems of Polynomial Equations*. Vol. 97. CBMS Regional Conferences Series in Mathematics. American Mathematical Society, 2002. ISBN: 978-0-8218-3251-6. doi: [10.1090/cbms/097](https://doi.org/10.1090/cbms/097).
- [Stu95] Bernd Sturmfels. „On Vector Partition Functions.“ In: *Journal of Combinatorial Theory, Series A* 72.2 (Nov. 1995), pp. 302–309. doi: [10.1016/0097-3165\(95\)90067-5](https://doi.org/10.1016/0097-3165(95)90067-5).
- [Stu96] Bernd Sturmfels. *Gröbner Bases and Convex Polytopes*. Vol. 8. University Lecture Series. American Mathematical Society, 1996. ISBN: 0821804871.
- [Sul18] Seth Sullivant. *Algebraic Statistics*. Vol. 194. Graduate Studies in Mathematics. American Mathematical Society, 2018. ISBN: 9781470435172.
- [SVL13] Jan Schepers and Leen Van Langenhoven. „Unimodality Questions for Integrally Closed Lattice Polytopes.“ In: *Annals of Combinatorics* 17.3 (Sept. 2013), pp. 571–589. doi: [10.1007/s00026-013-0185-6](https://doi.org/10.1007/s00026-013-0185-6).
- [SW05] David Speyer and Lauren Williams. „The Tropical Totally Positive Grassmannian.“ In: *Journal of Algebraic Combinatorics* 22.2 (Sept. 2005), pp. 189–210. doi: [10.1007/s10801-005-2513-3](https://doi.org/10.1007/s10801-005-2513-3).
- [SW21] David Speyer and Lauren K. Williams. „The Positive Dressian Equals the Positive Tropical Grassmannian.“ In: *Transactions of the American Mathematical Society. Series B* 8 (2021), pp. 330–353. doi: [10.1090/btran/67](https://doi.org/10.1090/btran/67).
- [Tab15] Luis Felipe Tabera. „On Real Tropical Bases and Real Tropical Discriminants.“ In: *Collectanea Mathematica* 66.1 (Jan. 2015), pp. 77–92. doi: [10.1007/s13348-014-0119-6](https://doi.org/10.1007/s13348-014-0119-6).
- [Tra17] Ngoc Mai Tran. „Enumerating polytopes.“ In: *Journal of Combinatorial Theory, Series A* 151 (Oct. 2017), pp. 1–22. doi: [10.1016/j.jcta.2017.03.011](https://doi.org/10.1016/j.jcta.2017.03.011).
- [Ver15] Anatoly Vershik. „Classification of Finite Metric Spaces and Combinatorics of Convex Polytopes.“ In: *Arnold Mathematik Journal* 1 (Mar. 2015), pp. 75–81. doi: doi.org/10.1007/s40598-014-0005-z.

- [Vio03] Yannick Viossat. *Elementary Games and Games Whose Correlated Equilibrium Polytope Has Full Dimension*. HAL Working Paper. Preprint. 2003. URL: <https://hal.archives-ouvertes.fr/hal-00242991>.
- [Vio10] Yannick Viossat. „Properties and Applications of Dual Reduction.“ In: *Economic Theory* 44 (June 2010), pp. 53–68. doi: [10.1007/s00199-009-0477-6](https://doi.org/10.1007/s00199-009-0477-6).
- [Viro06] Oleg Viro. *Patchworking real algebraic varieties*. Nov. 2006. arXiv: [math/0611382](https://arxiv.org/abs/math/0611382).
- [Vir83] Oleg Viro. „Gluing algebraic hypersurfaces and constructions of curves.“ Russian. In: *Tezisy Leningradskoj Mezhdunarodnoj Topologicheskoy Konferentsii 1982*. Nauka, 1983, pp. 149–197.
- [Voh11] Rakesh Vohra. *Mechanism Design. A Linear Programming Approach*. Econometric Society Monographs. Cambridge University Press, 2011. ISBN: 9780511835216. doi: [10.1017/cbo9780511835216](https://doi.org/10.1017/cbo9780511835216).
- [Wei22] Stefan Weinzierl. *Feynman Integrals. A Comprehensive Treatment for Students and Researchers*. 1st ed. Springer International Publishing, 2022. ISBN: 978-3-030-99558-4. doi: [10.1007/978-3-030-99558-4](https://doi.org/10.1007/978-3-030-99558-4).
- [YZZ19] Ruriko Yoshida, Leon Zhang, and Xu Zhang. „Tropical Principal Component Analysis and its Application to Phylogenetics.“ In: *Bulletin of Mathematical Biology* 81 (Feb. 2019), pp. 568–597. doi: [0.1007/s11538-018-0493-4](https://doi.org/10.1007/s11538-018-0493-4).
- [Zha21] Leon Zhang. „Computing Min-Convex Hulls in the Affine Building of SL_d .“ In: *Discrete & Computational Geometry* 65.4 (June 2021), pp. 1314–1336. doi: [10.1007/s00454-020-00223-x](https://doi.org/10.1007/s00454-020-00223-x).
- [Zha99a] Gaoyong Zhang. „A Positive Solution to the Busemann-Petty Problem in \mathbb{R}^4 .“ In: *Annals of Mathematics, Second Series* 149.2 (Mar. 1999), pp. 535–543. doi: [10.2307/120974](https://doi.org/10.2307/120974).
- [Zha99b] Gaoyong Zhang. „Intersection Bodies and Polytopes.“ In: *Mathematika* 46.1 (June 1999), 29–34. doi: [10.1112/S0025579300007531](https://doi.org/10.1112/S0025579300007531).
- [Zie95] Günter M. Ziegler. *Lectures on Polytopes*. 1st ed. Vol. 152. Graduate Texts in Mathematics. Springer-Verlag, New York, 1995. ISBN: 0-387-94365-X. doi: [10.1007/978-1-4613-8431-1](https://doi.org/10.1007/978-1-4613-8431-1).

LIST OF FIGURES

Figure 1.1	The Birkhoff polytope B_3 from Chapter 2, a polytrope from Chapter 3 and the polar of a zonotope from Chapter 4.	5
Figure 1.2	A regular subdivision	8
Figure 1.3	A mixed subdivision via the Cayley trick	10
Figure 1.4	The Ehrhart polynomial of the square	11
Figure 1.5	Tropical polytopes and their dual mixed subdivisions	15
Figure 1.6	Tropical hypersurfaces and the dual subdivision of the Newton polytopes	19
Figure 1.7	Two semialgebraic sets	30
Figure 1.8	The algebraic boundary of two semialgebraic sets	30
Figure 2.1	The Birkhoff polytope B_3	35
Figure 2.2	The positive part of the tropical line	39
Figure 2.3	The positive edges of B_3	51
Figure 2.4	The 2-colorings of the graph of B_n in the proof of Proposition 2.2.4	52
Figure 2.5	The possible cartoons of maximal cones in $T_{3,3}^2$	53
Figure 2.6	The possible cartoons of maximal cones in $T_{4,4}^3$	54
Figure 2.7	The cartoon of the cone in Example 2.2.9.	55
Figure 2.8	A tropically collinear point configuration	56
Figure 2.9	The cartoon from Example 2.2.17.	58
Figure 2.10	A label of a cone in $T_{3,4}^2$ by a bipartite graph	60
Figure 2.11	A non-unique label of a two cones in $T_{4,4}^2$ by a bipartite graph	61
Figure 2.12	A collection of cartoons and a bipartite label describing the same cone	62
Figure 2.13	The construction of the bicolored phylogenetic tree	66
Figure 2.14	Three tropically collinear point configurations and the respective bicolored phylogenetic trees	68
Figure 2.15	Two bicolored phylogenetic trees differing by a split	69
Figure 2.16	The possible complements $\Gamma(C)^c$ of positive labels	72
Figure 2.17	Forbidden subgraphs in the proof of Theorem 2.4.15	73
Figure 2.18	More forbidden subgraphs in the proof of Theorem 2.4.15	73
Figure 2.19	The tree from Example 2.4.22	77
Figure 2.20	The trees from Example 2.4.24.	78
Figure 2.21	A configuration of three marked 2-faces forming a starship	84
Figure 2.22	A bicolored tree arrangement	87
Figure 3.1	A 3-dimensional polytrope.	91
Figure 3.2	The max-tropical hyperplane in \mathbb{TP}^2	94
Figure 3.3	A tropical polytope in \mathbb{TP}^2 and its canonical decomposition intro polytopes	95
Figure 3.4	Two hexagonal cells with distinct tropical types	96

Figure 3.5	The weighted digraph and polytrope associated to a Kleene star	97
Figure 3.6	The two different types of alcoved triangles.	100
Figure 3.7	The fundamental polytopes FP_3 and FP_4 .	101
Figure 3.8	A polytrope and the variables that are associated to its facets	109
Figure 3.9	A regular central triangulation of the fundamental polytope FP_4	121
Figure 4.1	The intersection body of the icosahedron.	127
Figure 4.2	The construction of the intersection body	130
Figure 4.3	The two combinatorial types of hyperplane sections of the 3-cube.	131
Figure 4.4	The zonotope $Z(P)$, the hyperplane arrangement $\mathcal{H}(P)$ and the polar $Z(P)^\circ$ of the shifted square	133
Figure 4.5	The intersection body of the translated 3-cube	137
Figure 4.6	Two intersection bodies with the same associated zonotope	145
Figure 4.7	The labeled Schlegel diagram for the icosahedron	147
Figure 4.8	The labeled Schlegel diagram for a 4-dimensional polytope	148
Figure 4.9	Hyperplane arrangements of translations of P	152
Figure 4.10	The four ordered types of arrangements with two hyperplanes	153
Figure 4.11	The affine line arrangement of the triangle	154
Figure 4.12	The intersection body of the square under translation	156
Figure 4.13	The proof of Proposition 4.6.11 in a picture	159
Figure 4.14	Examples in which IP is convex	161
Figure 5.1	The correlated equilibrium polytope of a (2×3) -game and its face lattice.	165
Figure 5.2	The correlated equilibrium polytope of the Traffic Lights example	170
Figure 5.3	The Nash equilibria as the intersection of the correlated equilibrium polytope with the Segre variety	171
Figure 5.4	The graph of the maximal correlated equilibrium polytope of a (2×3) -game	184

LIST OF TABLES

Table 2.1	When do the $(r+1) \times (r+1)$ -minors form a set of positive-tropical generators?	46
Table 3.1	Relations of coefficients of 4-dimensional volume polynomials.	122
Table 4.1	Number of irreducible components of the algebraic boundary of the intersection body of the d -cube	150
Table 5.1	The number of unique combinatorial types of P_G for a $(2 \times n)$ -game in a random sampling	185

DATEN ZUR AUTORIN

NAME: Marie-Charlotte Brandenburg
GEBURTSdatum: 23. Juni 1993
GEBURTSORT: Hamburg

Okt. 2012 - Sep. 2016 B.Sc. Mathematik
Freie Universität Berlin

Okt. 2016 - Mai 2019 M.Sc. Mathematik
Freie Universität Berlin

SEIT OKT. 2019 Doktorandin der Mathematik

BIBLIOGRAPHISCHE DATEN

Tropical Positivity and Semialgebraic Sets from Polytopes
(Tropische Positivität und Semialgebraische Mengen von Polytopen)
Brandenburg, Marie-Charlotte
Universität Leipzig, Dissertation, 2022
xvi + 201 Seiten,
57 Abbildungen,
130 Referenzen

SELBSTSTÄNDIGKEITSERKLÄRUNG

Hiermit erkläre ich, die vorliegende Dissertation selbstständig und ohne unzulässige fremde Hilfe angefertigt zu haben. Ich habe keine anderen als die angeführten Quellen und Hilfsmittel benutzt und sämtliche Textstellen, die wörtlich oder sinngemäß aus veröffentlichten oder unveröffentlichten Schriften entnommen wurden, und alle Angaben, die auf mündlichen Auskünften beruhen, als solche kenntlich gemacht. Ebenfalls sind alle von anderen Personen bereitgestellten Materialien oder erbrachten Dienstleistungen als solche gekennzeichnet.

Leipzig, den 1. Dezember 2022

.....
(Marie-Charlotte Brandenburg)